Detailed treatment of uncertainties and correlations for jet energy calibration, jet cross section measurements, for the HVP contribution to $(g\text{-}2)_\mu$ and related phenomenological studies

Bogdan MALAESCU

LPNHE, CNRS

HDR Defence

27/03/2025

Areas of interest and topics for today

$(g\text{-}2)_\mu$ & Precision QCD ⟷ Jet Physics & Performance

Statistics & Machine Learning techniques for:
Unfolding; Calibration; Anomaly detection

QCD studies @ FCC-ee

$(g\text{-}2)_\mu$

BNL → Fermilab

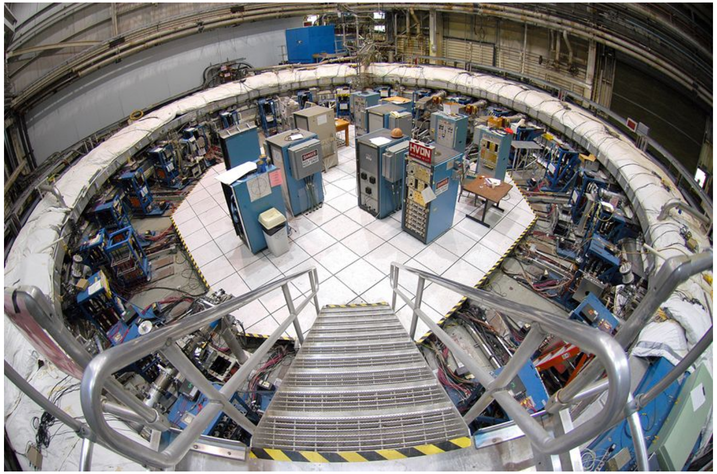

Status of a_μ before 1st / with 2nd Fermilab result

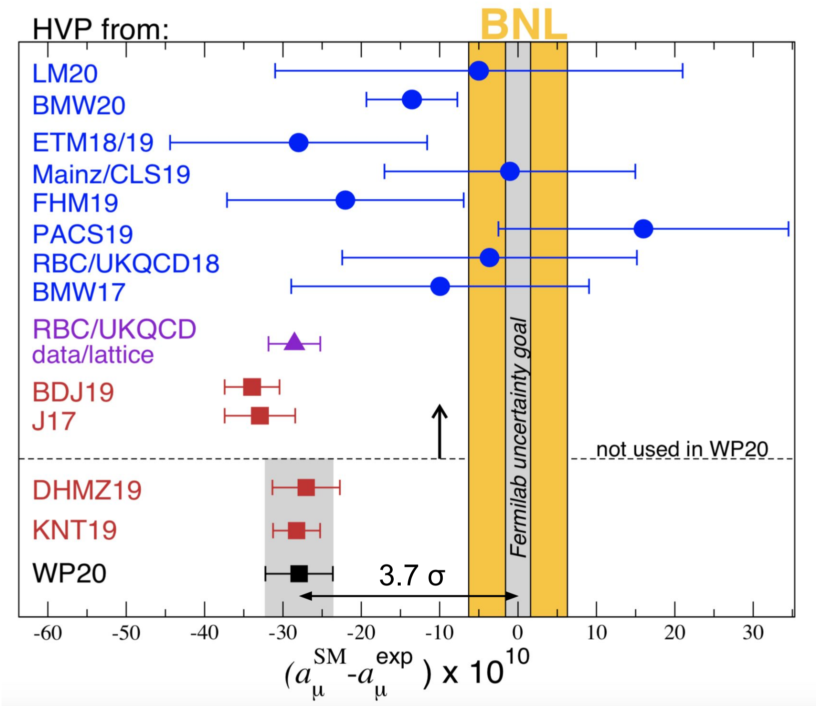

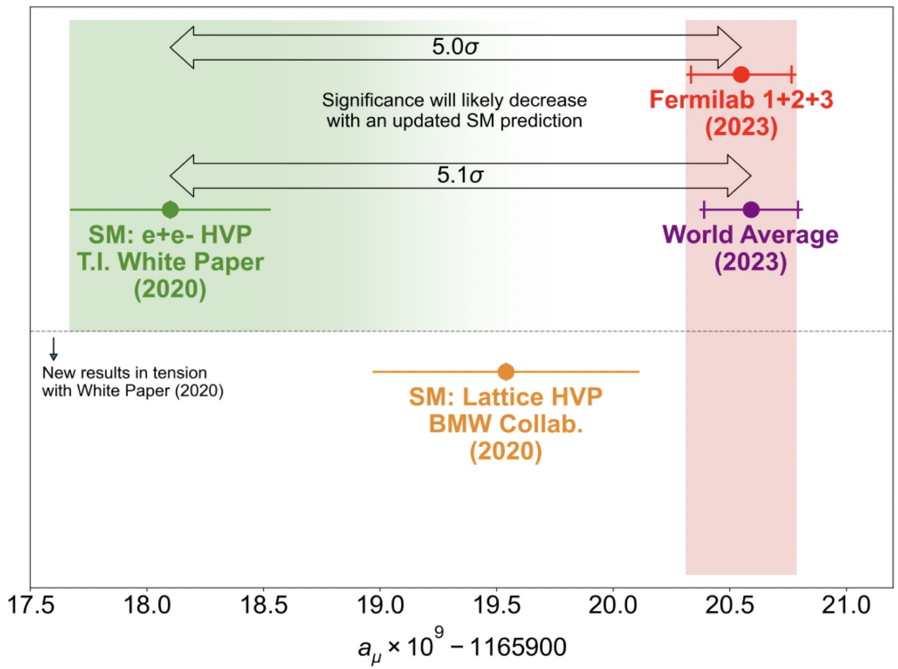

We have an interesting, long standing, multifaceted problem to solve…

Focusing here on the situation for the dispersive approach and the comparison with lattice QCD

Theoretical prediction

Why is it (so) complicated to compute one number ? (*very precisely*)

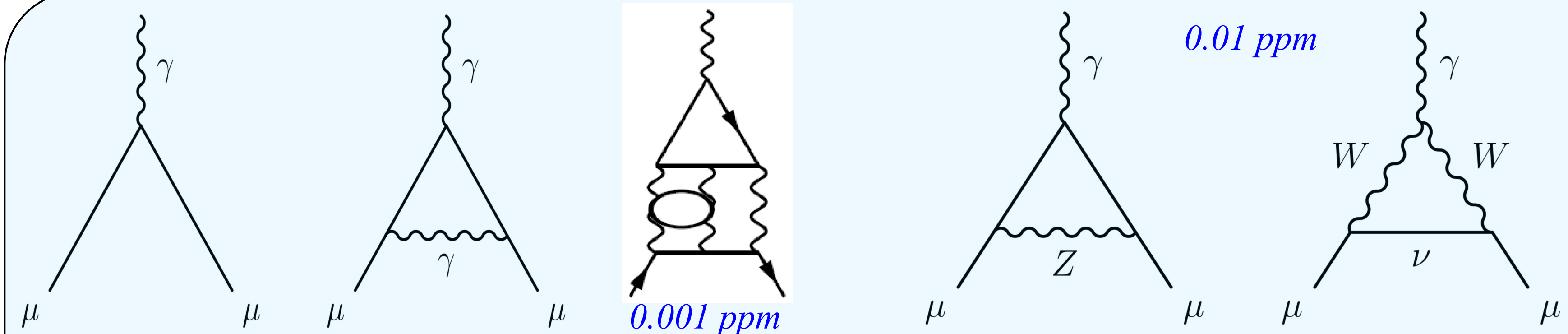

+ Many other diagrams at higher orders…

QED up to O(α^5) (Kinoshita et al.)

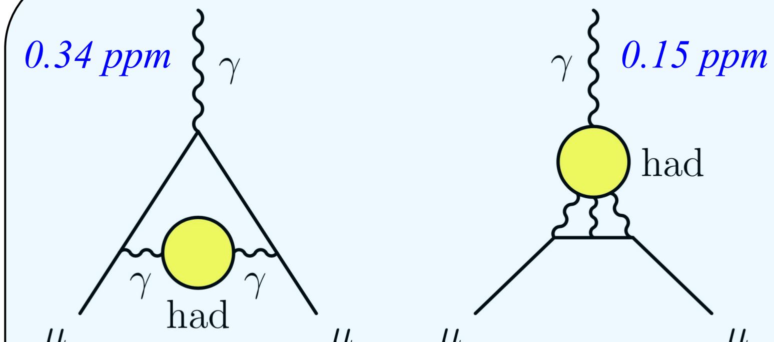

Dominant uncertainties: non-perturbative...

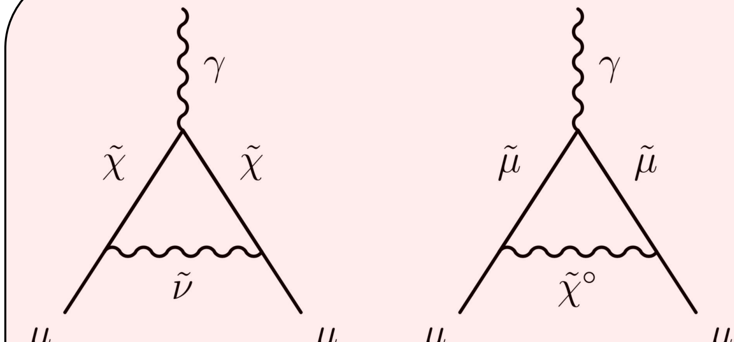

? ? ?

Hadronic Vacuum Polarization and Muon $(g\text{-}2)_\mu$

Dominant uncertainty for the theoretical prediction: from lowest-order HVP piece
Cannot be calculated from pQCD (low E-scale), but one can use experimental data on $e^+e^- \rightarrow$ hadrons cross section

Born: $\sigma^{(0)}(s) = \sigma(s)\left(\alpha/\alpha(s)\right)^2$

$$12\pi \, \mathrm{Im}\Pi_\gamma(s) = \frac{\sigma^0\,[e^+e^- \rightarrow \text{hadrons}\,(\gamma_{FSR})]}{\sigma_{pt}} \equiv R(s)$$

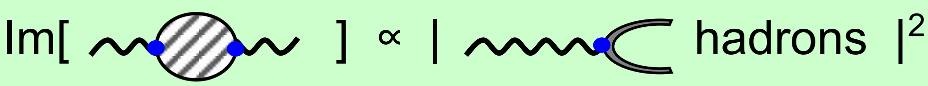

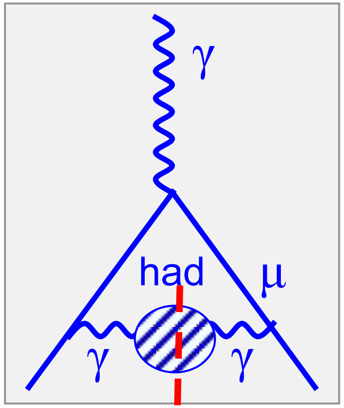

$$a_\mu^{had} = \frac{\alpha^2}{3\pi^2}\int_{4m_\pi^2}^{\infty} ds \, \frac{K(s)}{s} R(s)$$

Dispersion relation

Bouchiat and Michel, 1961

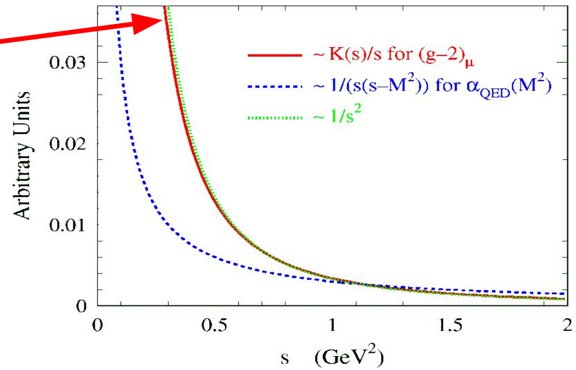

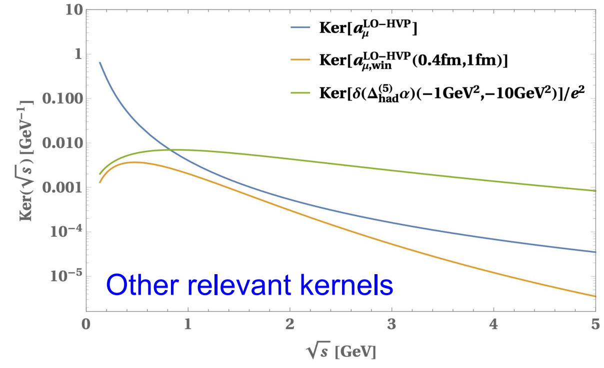

→ Precise $\sigma(e^+e^- \rightarrow \text{hadrons})$ measurements at low energy are very important
$\pi\pi$ channel: 73% (70%) of HVP contribution to a_μ (uncertainty ^{2})
→ Alternatively, one can use hadronic τ decays data + Isospin Breaking corrections

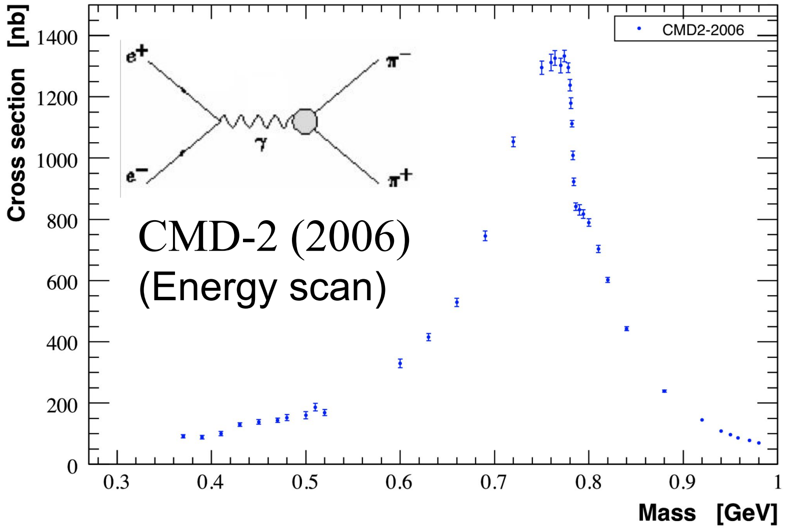

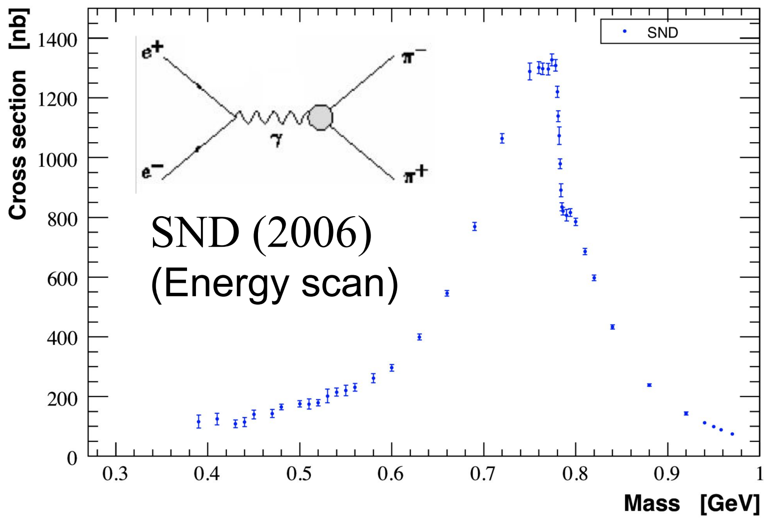

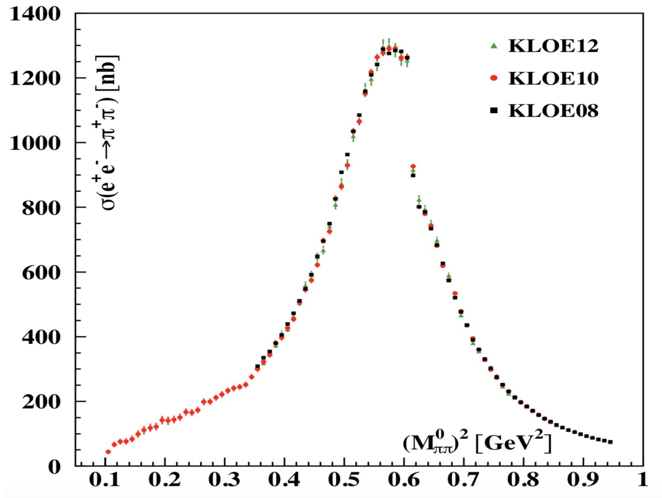

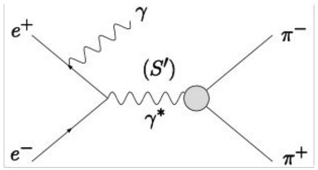

KLOE (08&10) + μμ (12) (ISR)

BaBar results: "NLO" cross-section

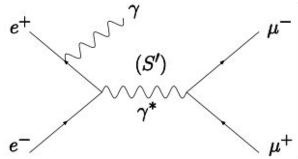

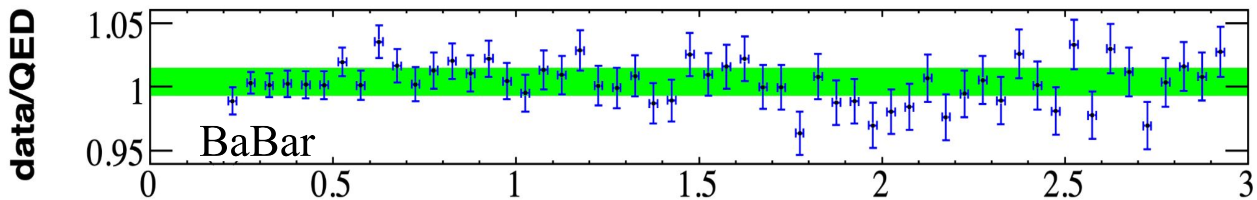

Absolute $\mu^+\mu^-$ cross section agrees with NLO QED within 1.1%

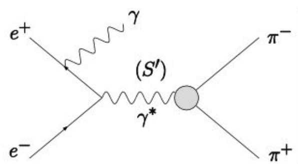

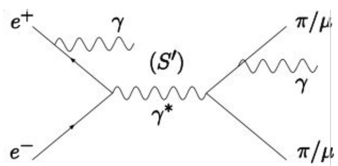

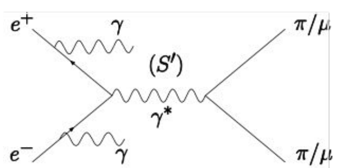

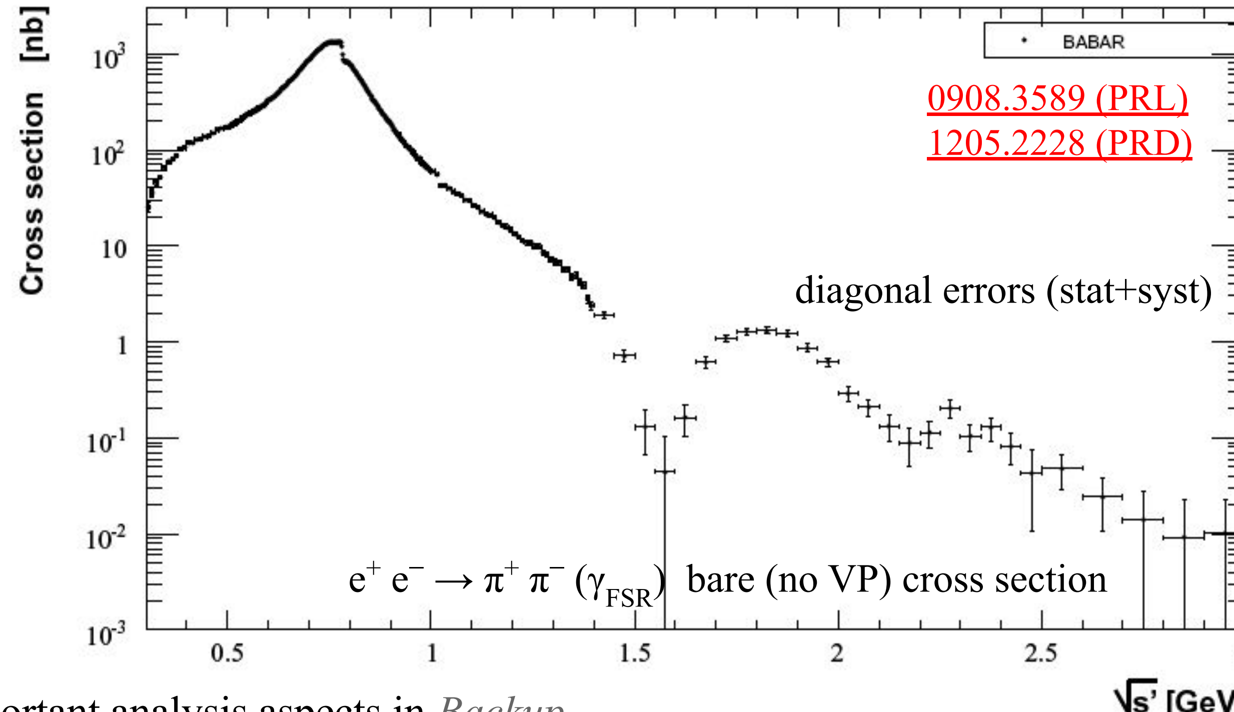

→ More details on important analysis aspects in *Backup*

Experimental data combination (Example: $e^+e^- \rightarrow \pi^+\pi^-$ channel)

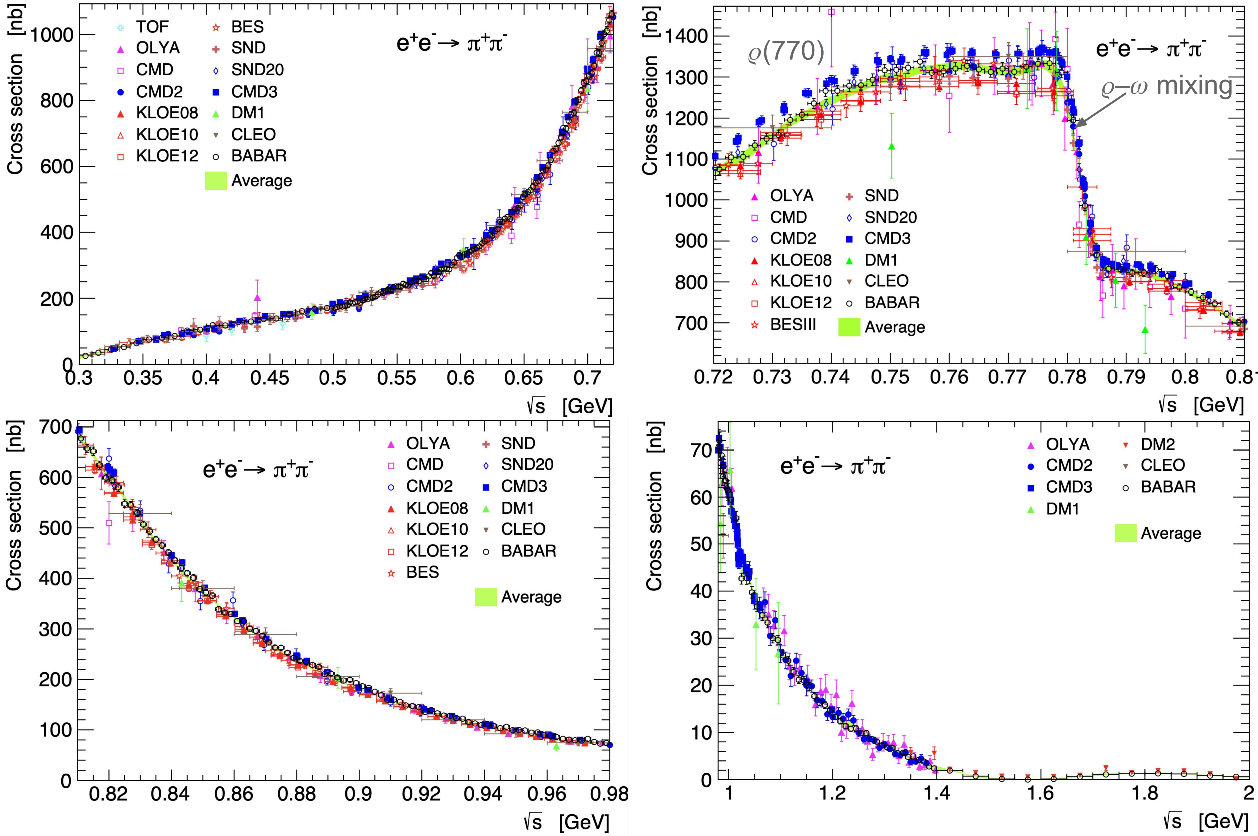

2312.02053

→ *New since g-2 Theory Initiative White Paper*: Large tensions, especially between KLOE & CMD3, which provide the smallest / largest cross-sections in the ρ region

Procedure and software (*HVPTools - Since 2009*) for combining cross section data with arbitrary point spacing/binning → Validated through closure test. Featuring full & realistic (i.e. not too optimistic) treatment of uncertainties and correlations (between measurements (data points/bins) of a given experiment, b. experiments, b. different channels), fully accounting for systematic tensions between experiments. *(1st motivation for DHMZ uncertainties = "baseline" in g-2 TI WP)*

Combination procedure implemented in HVPTools software

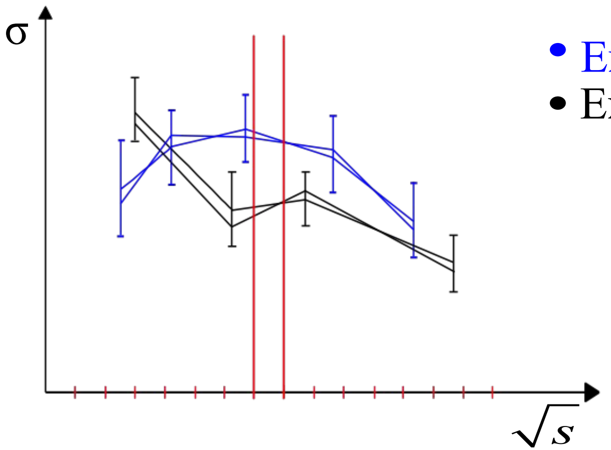

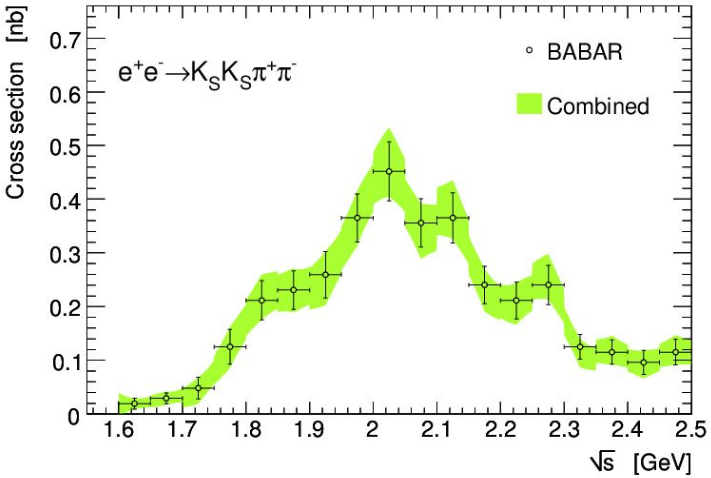

→ Define a (fine) final binning (to be filled and used for integrals etc.)

→ Linear/quadratic splines to interpolate between the points/bins of each experiment
- for binned measurements: preserve integral inside each bin
- closure test: replace nominal values of data points by Gounaris-Sakurai model and re-do the combination
  → *(non-)negligible bias for (linear)quadratic interpolation*

→ Fluctuate data points taking into account correlations & re-do the splines for each (pseudo-)experiment
- each uncertainty fluctuated coherently for all the points/bins that it impacts
- eigenvector decomposition for (statistical) covariance matrices

→ In each final bin, compute: average value for each measurement & its uncertainty;
correlation matrix between experiments

Backup

Combining the $e^+e^- \to \pi^+\pi^-$ data: relative differences

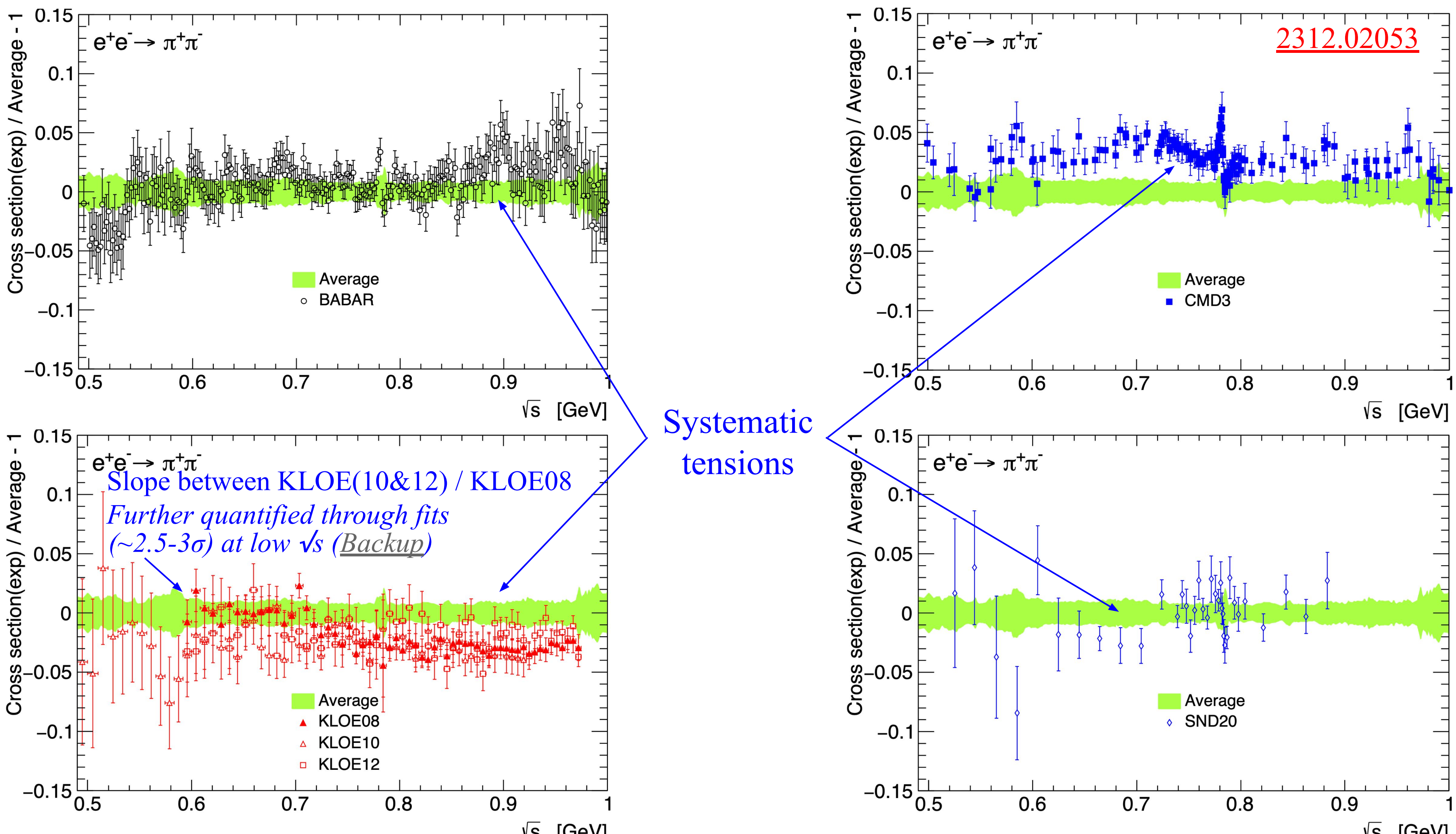

Combining the $e^+e^- \to \pi^+\pi^-$ data: relative differences

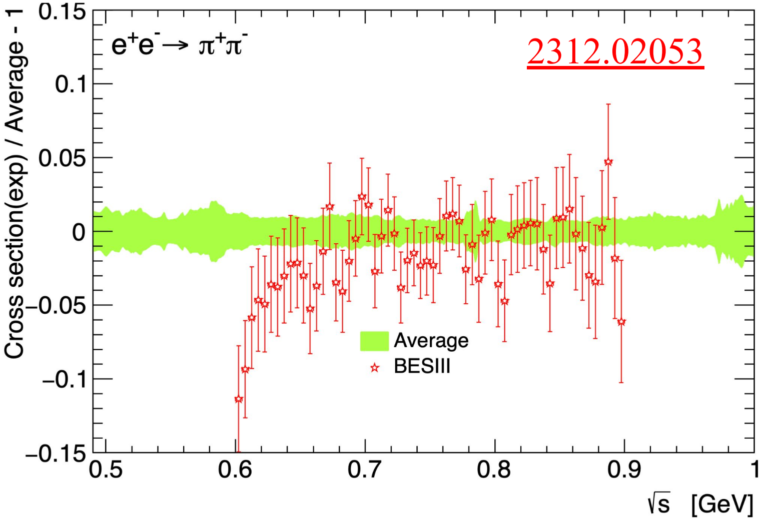

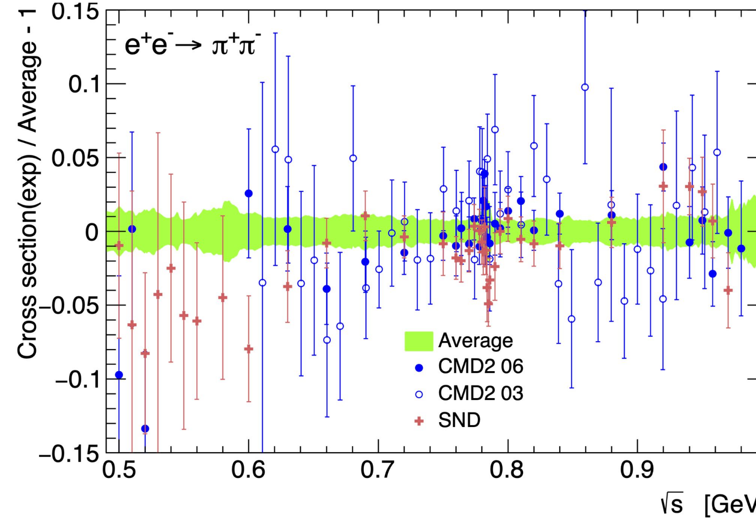

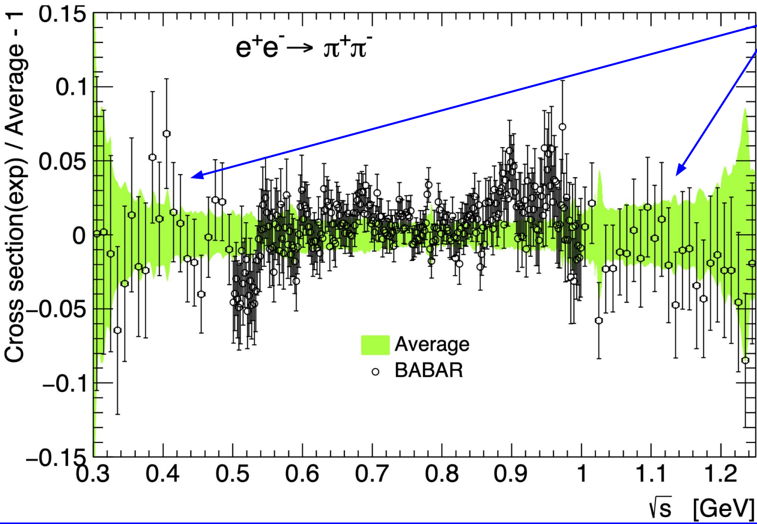

Reasonable BABAR/CMD3 agreement at low & high E

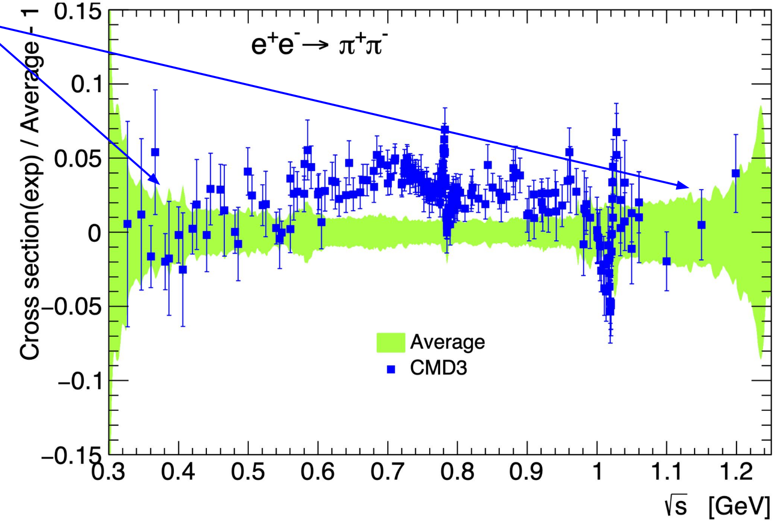

Combination procedure: weights and tension

→ For each narrow final bin minimize χ^2 to get average coefficients test locally the level of agreement

→ Average weights account for bin sizes/point-spacing of measurements: compare precisions on same footing

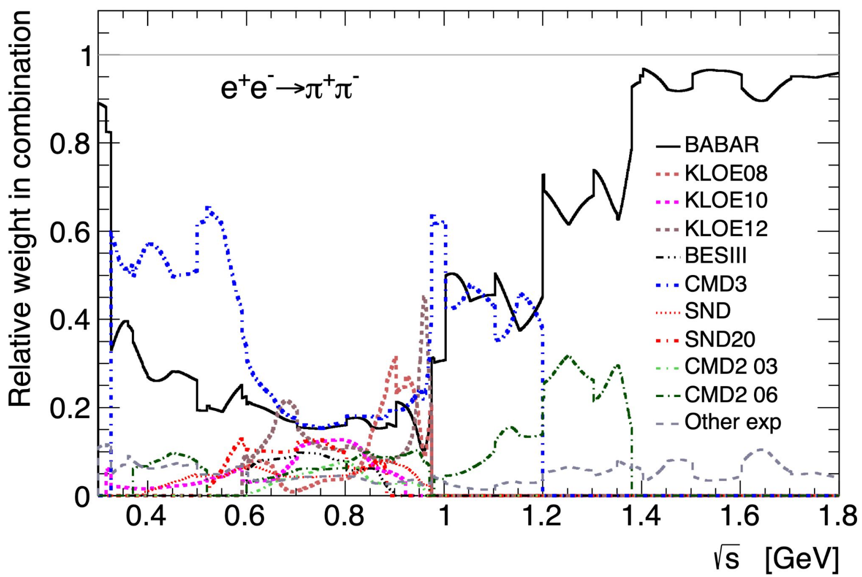

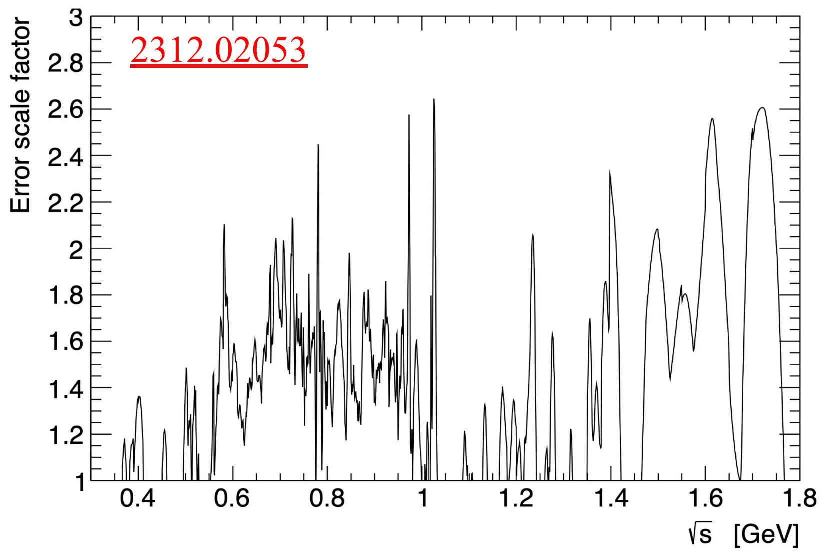

→ Average dominated by BaBar, CMD3, KLOE, SND20; BaBar covers full energy range

→ Enhanced tensions, especially between KLOE & CMD3, which provide the smallest / largest cross-sections in the ρ region: *clear indication of underestimated uncertainties*

→ *Calls for conservative uncertainty treatment* in combination fit (fits / evaluation of weights)

→ Systematic effects beyond the local χ^2 /ndof rescaling: had already motivated the inclusion of the dominant BABAR-KLOE systematic by DHMZ since 2019 *(2nd motivation for DHMZ uncertainties = "baseline" in g-2 TI White Paper)*, but *tensions are larger now*

Backup

Quantitative comparisons for a_μ^{HVP}

→ Comparison of integrals computed in various restricted energy ranges, for individual e^+e^- experiments: significance of the difference between different experiments, taking into account correlations

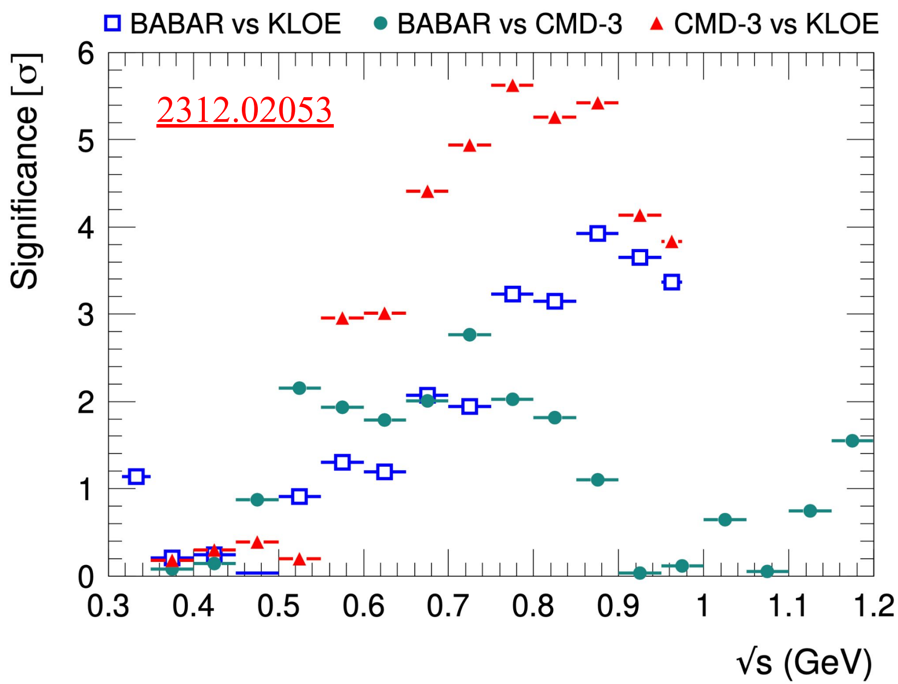

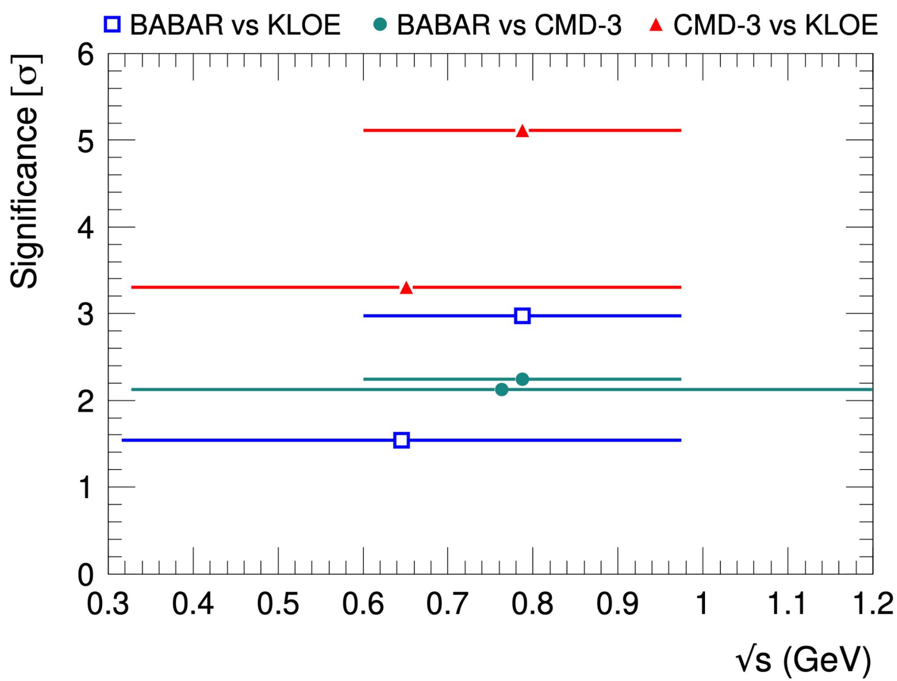

→ Largest tensions between CMD3 and KLOE

Quantitative comparisons for a_μ^{HVP}

→ Comparison of integrals computed in various restricted energy ranges, for τ / individual e^+e^- experiments: significance of the difference between different experiments, taking into account correlations

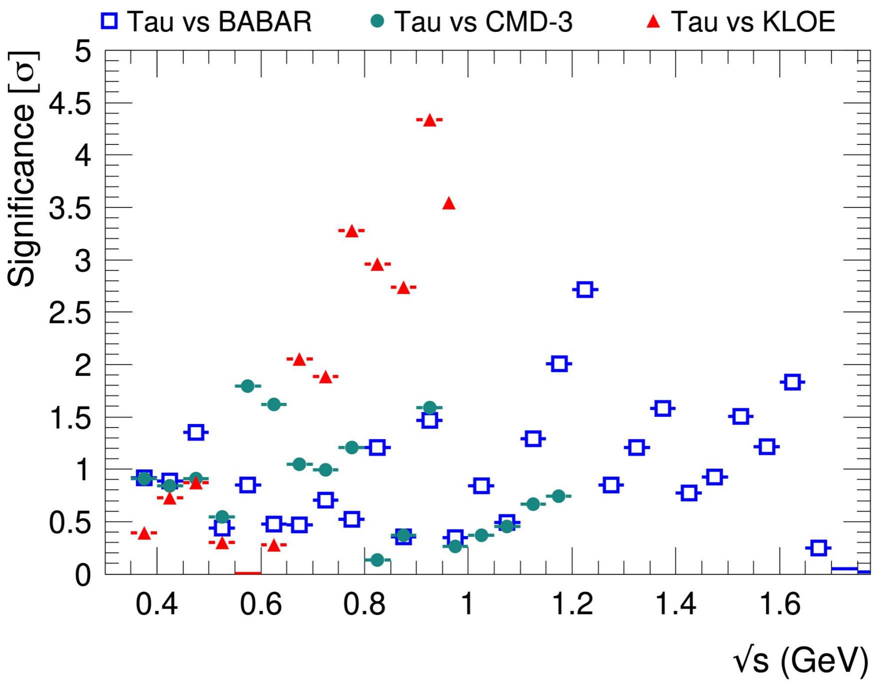

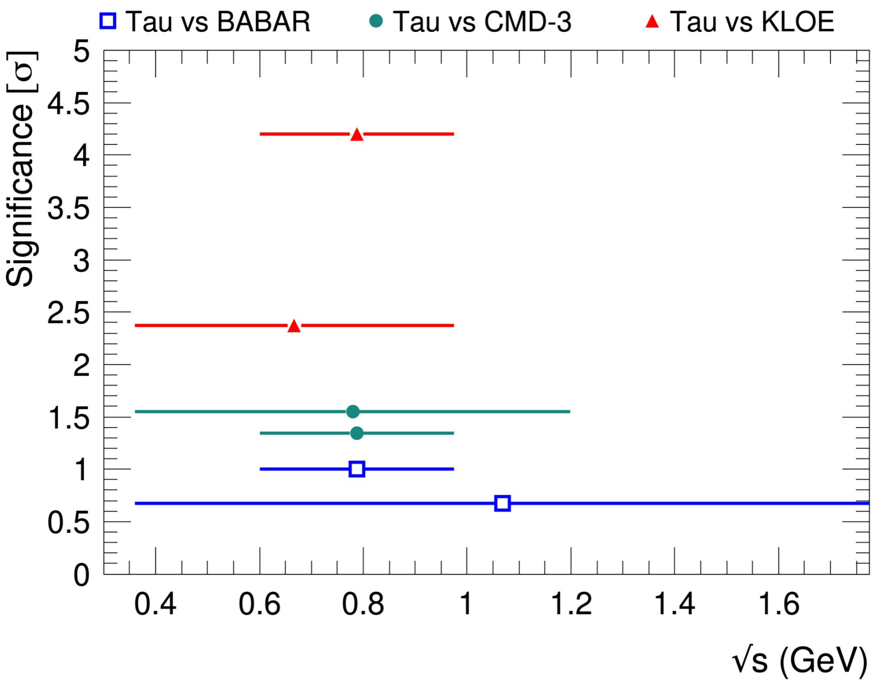

→ Largest tensions between Tau and KLOE

→ Good agreement among the Tau measurements (Backup)

Combining the $e^+e^- \to \pi^+\pi^-$ data, BaBar & CMD3 & Tau(+IB)

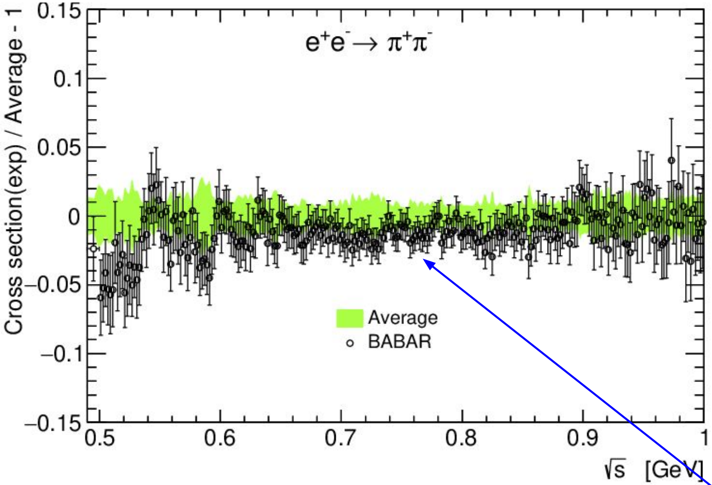

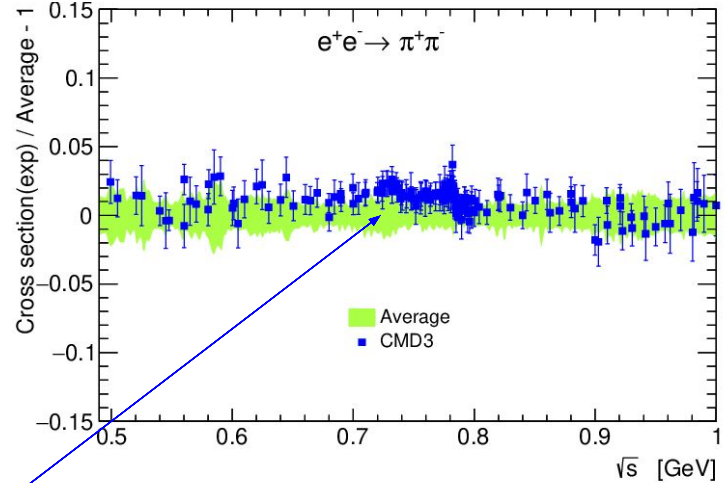

Some (reduced) systematic tensions

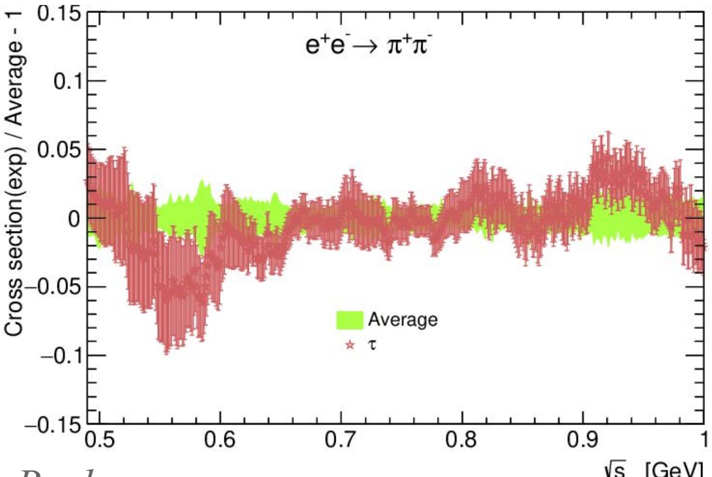

Much larger tension (slope and shift) for KLOE vs. BABAR + CMD-3 + τ combination

→ Not compatible with any realistic change of IB corrections

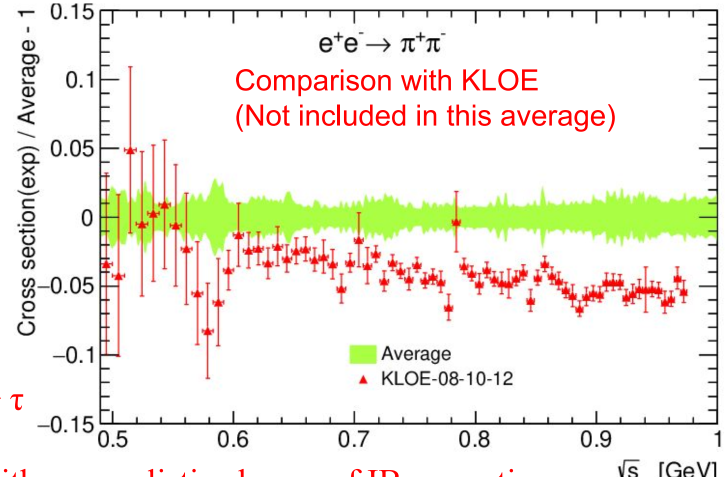

Backup

Impact of higher order photon emissions: *Unique '(N)NLO' BaBar study*

→ Studied in-situ in BaBar data, using kinematic fits: test the most frequently used Monte Carlo generators

- PHOKHARA: full NLO matrix element for ISR and FSR
- AFKQED: NLO and NNLO, with collinear approximation for additional ISR

Generic ISR diagrams

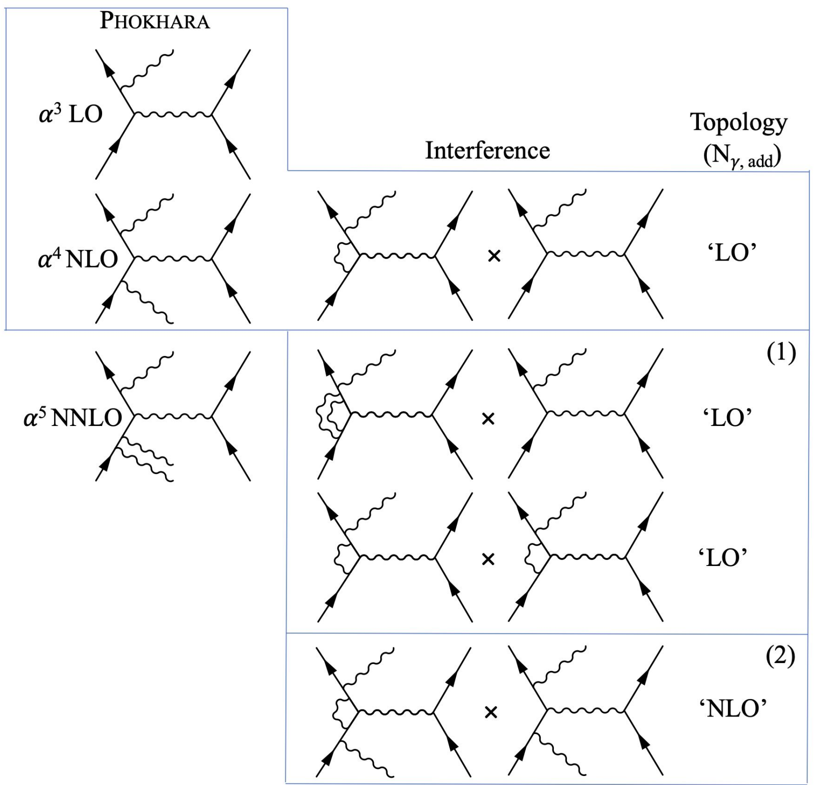

2308.05233

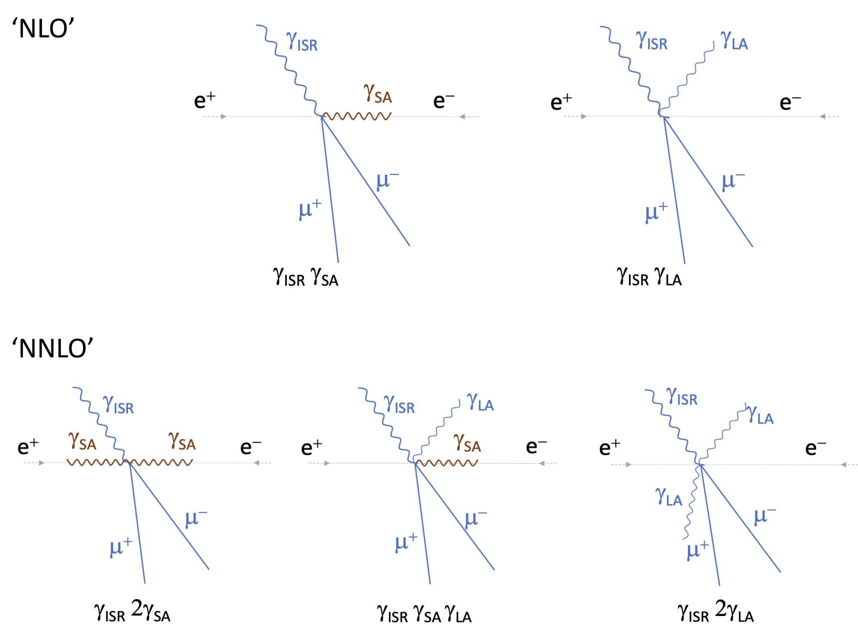

'(N)NLO': γ_{add} counting ($E_{\gamma\ add} > E_{min}$)

BaBar results on higher order photon emissions

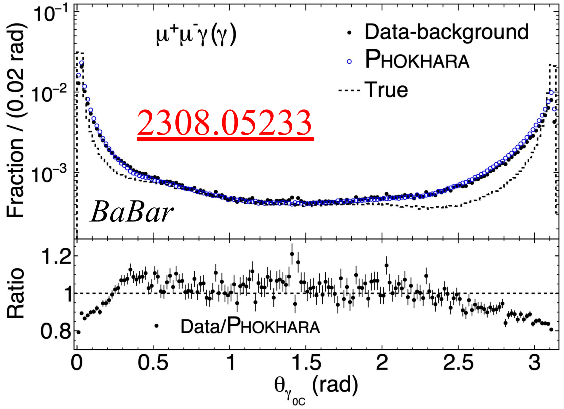

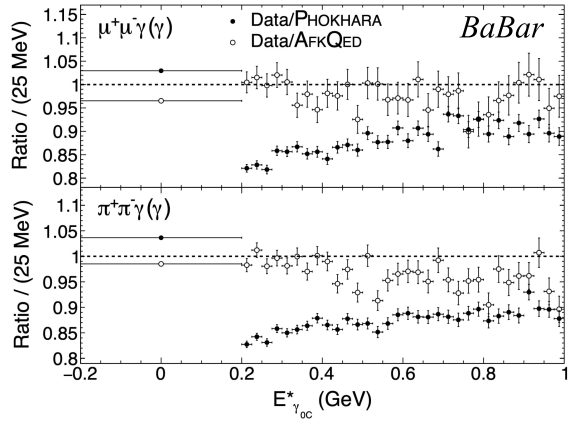

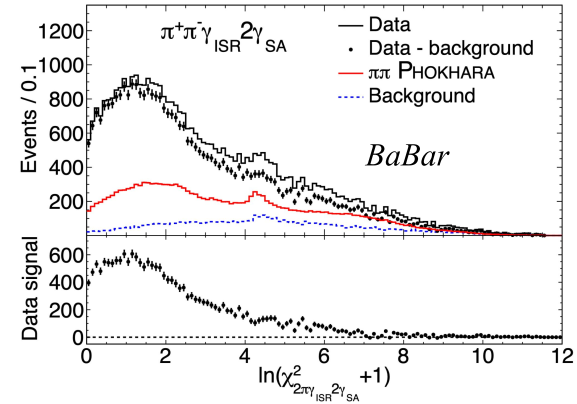

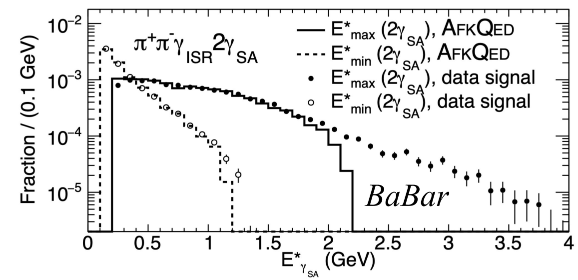

→ NLO small-angle ISR in PHOKHARA higher than in data; large-angle ratios consistent with unity

→ *Independent Belle II confirmation of PHOKHARA problem*

→ AFKQED: reasonable description of rate and energy distributions for '(N)NLO' data

→ *NNLO contributions clearly observed in data*

→ BaBar measurements: *loose selection incorporates NLO and HO radiation, minimising MC-dependence*

→ Other ISR measurements *select 'LO' topology and rely on PHOKHARA for hard NLO (but with no NNLO)*

→ Aspects further studied with fast simulation, questioning the KLOE systematic uncertainties (2312.02053)

Backup

Sum of hadronic contributions

Channel	$a_\mu^{\rm had,LO}$ $[10^{-10}]$	$\Delta\alpha_{\rm had}(m_Z^2)$ $[10^{-4}]$
$\pi^0\gamma$	$4.41 \pm 0.06 \pm 0.04 \pm 0.07$	$0.35 \pm 0.00 \pm 0.00 \pm 0.01$
$\eta\gamma$	$0.65 \pm 0.02 \pm 0.01 \pm 0.01$	$0.08 \pm 0.00 \pm 0.00 \pm 0.00$
$\pi^+\pi^-$	$507.85 \pm 0.83 \pm 3.23 \pm 0.55$	$34.50 \pm 0.06 \pm 0.20 \pm 0.04$
$\pi^+\pi^-\pi^0$	$46.21 \pm 0.40 \pm 1.10 \pm 0.86$	$4.60 \pm 0.04 \pm 0.11 \pm 0.08$
$2\pi^+2\pi^-$	$13.68 \pm 0.03 \pm 0.27 \pm 0.14$	$3.58 \pm 0.01 \pm 0.07 \pm 0.03$
$\pi^+\pi^-2\pi^0$	$18.03 \pm 0.06 \pm 0.48 \pm 0.26$	$4.45 \pm 0.02 \pm 0.12 \pm 0.07$
$2\pi^+2\pi^-\pi^0$ (η excl.)	$0.69 \pm 0.04 \pm 0.06 \pm 0.03$	$0.21 \pm 0.01 \pm 0.02 \pm 0.01$
$\pi^+\pi^-3\pi^0$ (η excl.)	$0.49 \pm 0.03 \pm 0.09 \pm 0.00$	$0.15 \pm 0.01 \pm 0.03 \pm 0.00$
$3\pi^+3\pi^-$	$0.11 \pm 0.00 \pm 0.01 \pm 0.00$	$0.04 \pm 0.00 \pm 0.00 \pm 0.00$
$2\pi^+2\pi^-2\pi^0$ (η excl.)	$0.71 \pm 0.06 \pm 0.07 \pm 0.14$	$0.25 \pm 0.02 \pm 0.02 \pm 0.05$
$\pi^+\pi^-4\pi^0$ (η excl., isospin)	$0.08 \pm 0.01 \pm 0.08 \pm 0.00$	$0.03 \pm 0.00 \pm 0.03 \pm 0.00$
$\eta\pi^+\pi^-$	$1.19 \pm 0.02 \pm 0.04 \pm 0.02$	$0.35 \pm 0.01 \pm 0.01 \pm 0.01$
$\eta\omega$	$0.35 \pm 0.01 \pm 0.02 \pm 0.01$	$0.11 \pm 0.00 \pm 0.01 \pm 0.00$
$\eta\pi^+\pi^-\pi^0$(non-ω,ϕ)	$0.34 \pm 0.03 \pm 0.03 \pm 0.04$	$0.12 \pm 0.01 \pm 0.01 \pm 0.01$
$\eta 2\pi^+2\pi^-$	$0.02 \pm 0.01 \pm 0.00 \pm 0.00$	$0.01 \pm 0.00 \pm 0.00 \pm 0.00$
$\omega\eta\pi^0$	$0.06 \pm 0.01 \pm 0.01 \pm 0.00$	$0.02 \pm 0.00 \pm 0.00 \pm 0.00$
$\omega\pi^0$ ($\omega \to \pi^0\gamma$)	$0.94 \pm 0.01 \pm 0.03 \pm 0.00$	$0.20 \pm 0.00 \pm 0.01 \pm 0.00$
$\omega 2\pi$ ($\omega \to \pi^0\gamma$)	$0.07 \pm 0.00 \pm 0.00 \pm 0.00$	$0.02 \pm 0.00 \pm 0.00 \pm 0.00$
ω (non-$3\pi,\pi\gamma,\eta\gamma$)	$0.04 \pm 0.00 \pm 0.00 \pm 0.00$	$0.00 \pm 0.00 \pm 0.00 \pm 0.00$
K^+K^-	$23.08 \pm 0.20 \pm 0.33 \pm 0.21$	$3.35 \pm 0.03 \pm 0.05 \pm 0.03$
K_SK_L	$12.82 \pm 0.06 \pm 0.18 \pm 0.15$	$1.74 \pm 0.01 \pm 0.03 \pm 0.02$
ϕ (non-$K\overline{K}, 3\pi, \pi\gamma, \eta\gamma$)	$0.05 \pm 0.00 \pm 0.00 \pm 0.00$	$0.01 \pm 0.00 \pm 0.00 \pm 0.00$
$K\overline{K}\pi$	$2.45 \pm 0.05 \pm 0.10 \pm 0.06$	$0.78 \pm 0.02 \pm 0.03 \pm 0.02$
$K\overline{K}2\pi$	$0.85 \pm 0.02 \pm 0.05 \pm 0.01$	$0.30 \pm 0.01 \pm 0.02 \pm 0.00$
$K\overline{K}\omega$	$0.00 \pm 0.00 \pm 0.00 \pm 0.00$	$0.00 \pm 0.00 \pm 0.00 \pm 0.00$
$\eta\phi$	$0.33 \pm 0.01 \pm 0.01 \pm 0.00$	$0.11 \pm 0.00 \pm 0.00 \pm 0.00$
$\eta K\overline{K}$ (non-ϕ)	$0.01 \pm 0.01 \pm 0.01 \pm 0.00$	$0.00 \pm 0.00 \pm 0.01 \pm 0.00$
$\omega 3\pi$ ($\omega \to \pi^0\gamma$)	$0.06 \pm 0.01 \pm 0.01 \pm 0.01$	$0.02 \pm 0.00 \pm 0.00 \pm 0.00$
7π ($3\pi^+3\pi^-\pi^0$ + estimate)	$0.02 \pm 0.00 \pm 0.01 \pm 0.00$	$0.01 \pm 0.00 \pm 0.00 \pm 0.00$
J/ψ (BW integral)	6.20 ± 0.11	7.00 ± 0.13
$\psi(2S)$ (BW integral)	1.56 ± 0.05	2.48 ± 0.08
R data $[3.7 - 5.0]$ GeV	$7.29 \pm 0.05 \pm 0.30 \pm 0.00$	$15.79 \pm 0.12 \pm 0.66 \pm 0.00$
$R_{\rm QCD}$ $[1.8 - 3.7$ GeV$]_{uds}$	$33.45 \pm 0.28 \pm 0.65_{\rm dual}$	$24.27 \pm 0.18 \pm 0.28_{\rm dual}$
$R_{\rm QCD}$ $[5.0 - 9.3$ GeV$]_{udsc}$	6.86 ± 0.04	34.89 ± 0.18
$R_{\rm QCD}$ $[9.3 - 12.0$ GeV$]_{udscb}$	1.20 ± 0.01	15.53 ± 0.04
$R_{\rm QCD}$ $[12.0 - 40.0$ GeV$]_{udscb}$	1.64 ± 0.00	77.94 ± 0.13
$R_{\rm QCD}$ $[> 40.0$ GeV$]_{udscb}$	0.16 ± 0.00	42.70 ± 0.05
$R_{\rm QCD}$ $[> 40.0$ GeV$]_{t}$	0.00 ± 0.00	-0.72 ± 0.01
Sum	$694.0 \pm 1.0 \pm 3.5 \pm 1.6 \pm 0.1_\psi \pm 0.7_{\rm QCD}$	$275.29 \pm 0.15 \pm 0.72 \pm 0.23 \pm 0.15_\psi \pm 0.55_{\rm QCD}$

→ 32 exclusive channels are integrated up to 1.8 GeV

Relative contributions to a_μ from missing channels (estimated based on isospin symmetry)

→ 0.87 ± 0.15 % (DEHZ 2003)
→ 0.69 ± 0.07 % (DHMZ 2010)
→ 0.09 ± 0.02 % (DHMZ 2017)
→ 0.016 ± 0.016 % (DHMZ 2019)
(*Nearly complete set of exclusive measurements from BABAR*)

Backup

R_{e+e-} → Hadrons

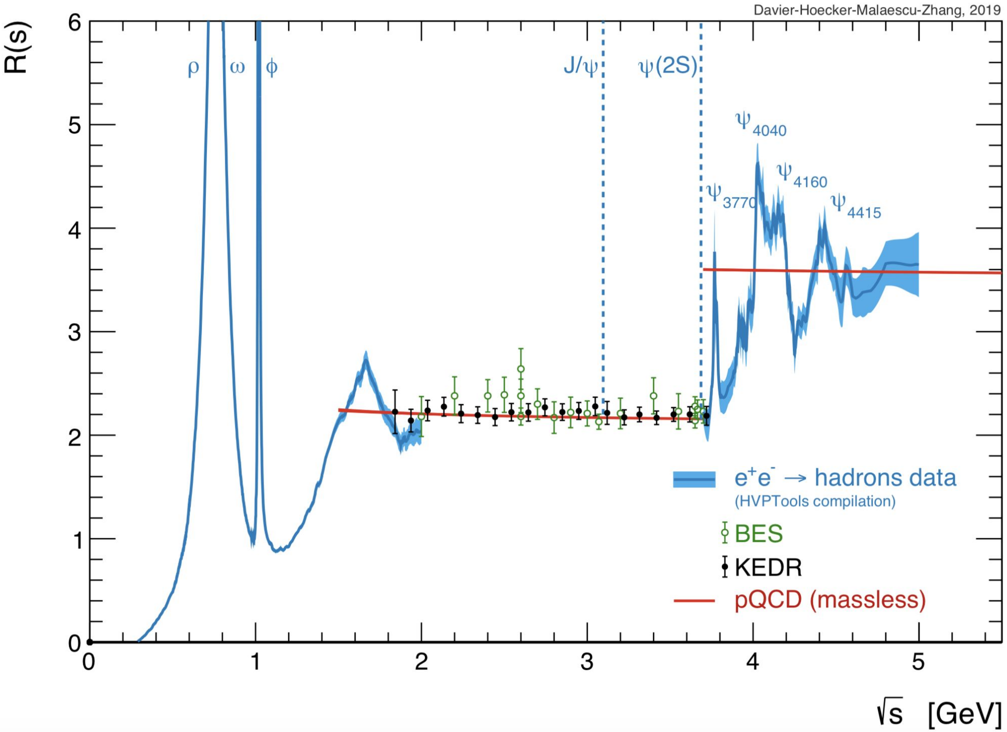

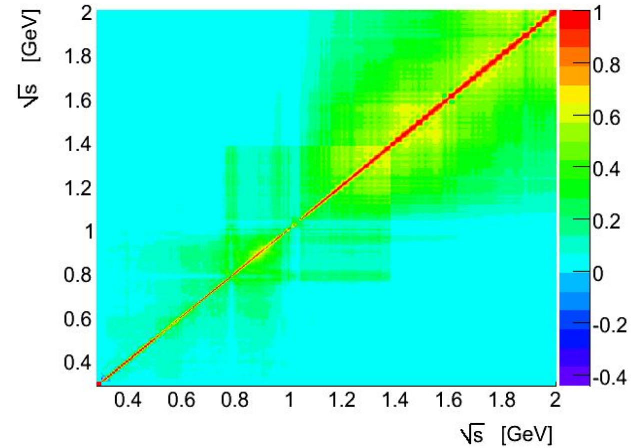

Sum of *32 exclusive channels* with *full propagation of correlations*

→ Performed non-trivial check: a_μ and $\Delta\alpha_{had}$ from sum of individual channels and from Ree integral < 1.8 GeV

→ Enables the determination of the various HVP contributions to the "running" of α_{QED} , evaluation of α_S and test of RGE with different correlation scenarios for theory uncertainties (Backup)

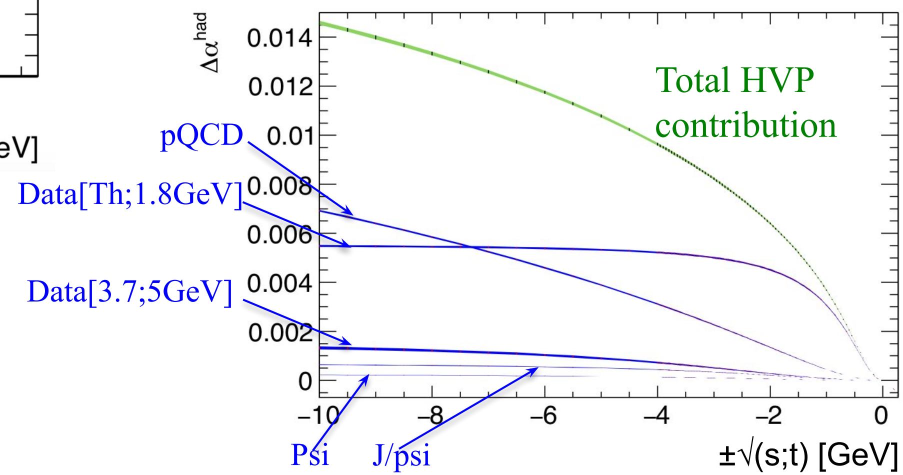

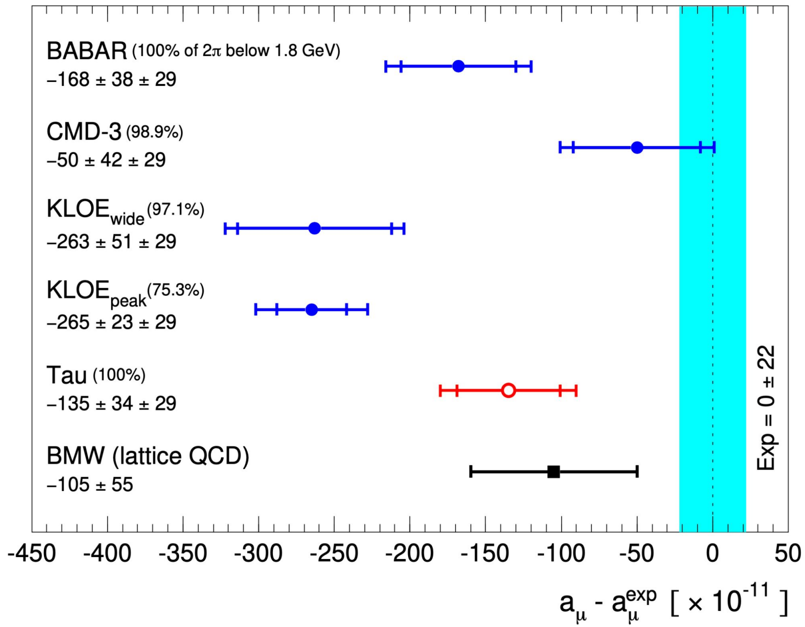

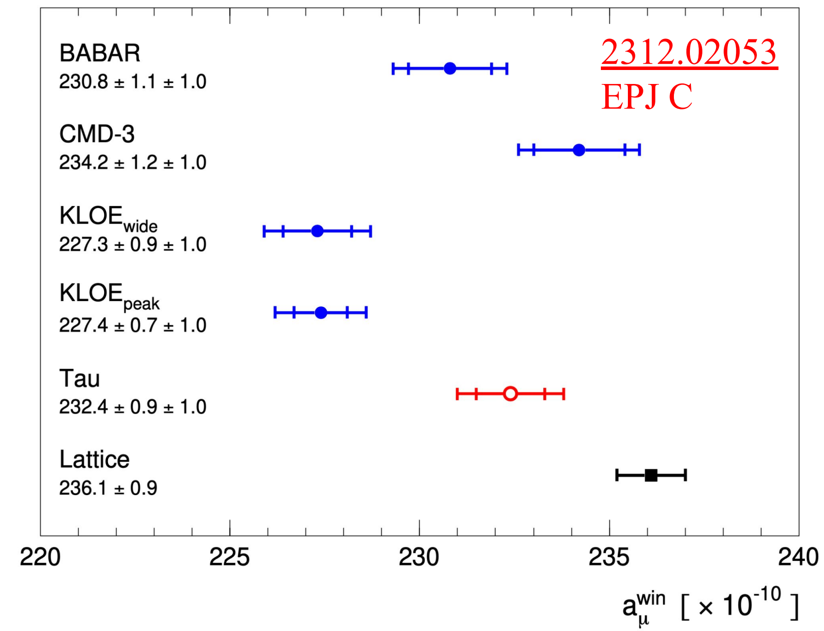

→ The τ-based HVP contribution close to the values provided by BABAR and CMD-3

→ Their combination (3.8σ > KLOEpeak) is compatible with BMW for a_μ, but a 2.9σ tension persists for a_μ^{win}

→ The BMW-based prediction is 1.8σ below the experimental value; *not* incompatible with the EW fit (Backup)

Combining BABAR, CMD-3, τ (+BMW): 2.5σ (2.8σ) difference with experiment

When including KLOE in the dispersive calculation: > 5σ w.r.t. experiment

→ *Tests of MC generators using KLOE data & in-situ studies of impact on the analysis are very much desirable*

Lattice calculations and comparisons w.r.t. dispersive

→ Lattice: employ simulations to compute electromagnetic-current two-point function

$$C(t) = \frac{1}{3e^2}\sum_{i=1}^{3}\int d^3x\,\langle J_i(\vec{x},t)J_i(0)\rangle \qquad C(t) = \frac{1}{24\pi^2}\int_0^\infty ds\,\sqrt{s}R(s)\,e^{-|t|\sqrt{s}}$$

Based on BMW'20: All contributions to C(t), with all limits taken: a→0, L→∞, $M_\pi \to M_\pi^\varphi$, ...

→ Tensions between lattice (weighted sums of $C(t)$ over t) and pre-CMD3 data-driven (DD) HVP results

$$\left[\Delta a_\mu^{\text{LO-HVP}}\right]_{\text{lat-DD}} \sim 2.1\sigma \quad \left[\Delta a_{\mu,\text{win}}^{\text{LO-HVP}}\right]_{\text{lat-DD}} \sim 4.0\sigma \quad \left[\Delta\alpha_{\text{had}}^{(5)}\left(-1 \to -10\text{GeV}^2\right)\right]_{\text{lat}-\text{DD}} \sim 1.4\sigma, \ldots$$

→ Simultaneous comparisons with correlations: ~dilution compared to $a_{\mu,\text{win}}^{\text{LO-HVP}}$ alone, but still significant tension

→ *New in this study*: Correlations among lattice HVP observables and uncertainties on these correlations

→ Differences could be explained by: a *C(t)* that is enhanced in *t* ~ [0.4, 1.5] fm

→ Lattice → R-ratio: inverse Laplace transform (ill-posed problem)

→ *Developed dedicated statistical methods, benefiting from experimental measurements*

→ Differences could be explained by enhancing measured R-ratio around (/any larger interval including) ρ-peak, but rescalings beyond the uncertainties of $R_{e^+e^-}$

2308.04221

→ Outcome of the studies stable within stat. and syst. uncertainties on lattice covariance matrices

Backup

Merging dispersive and lattice HVP calculations

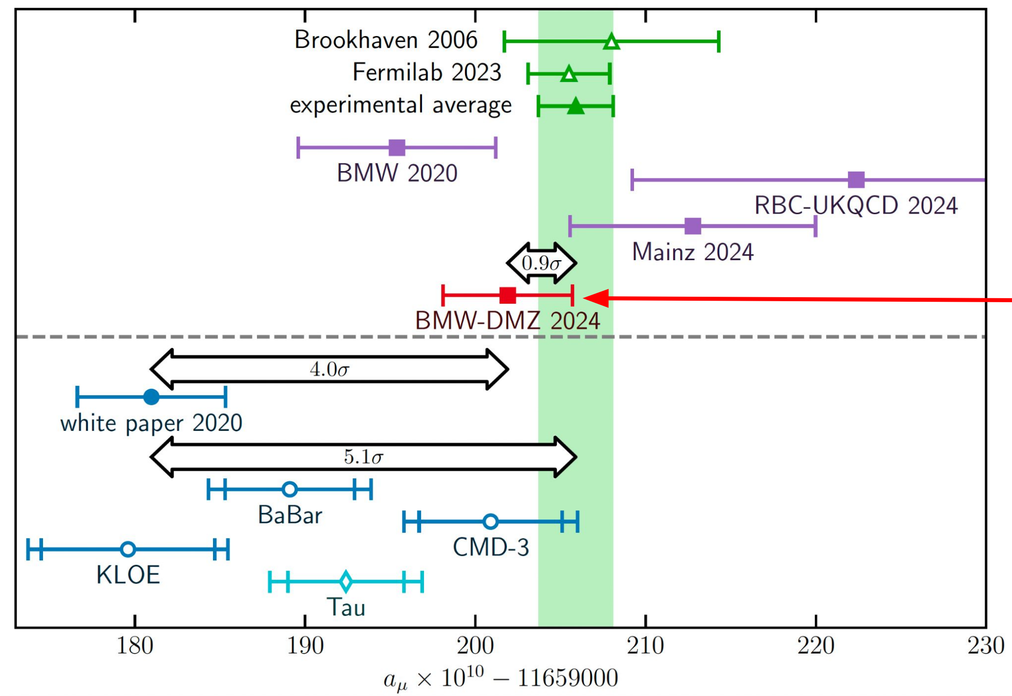

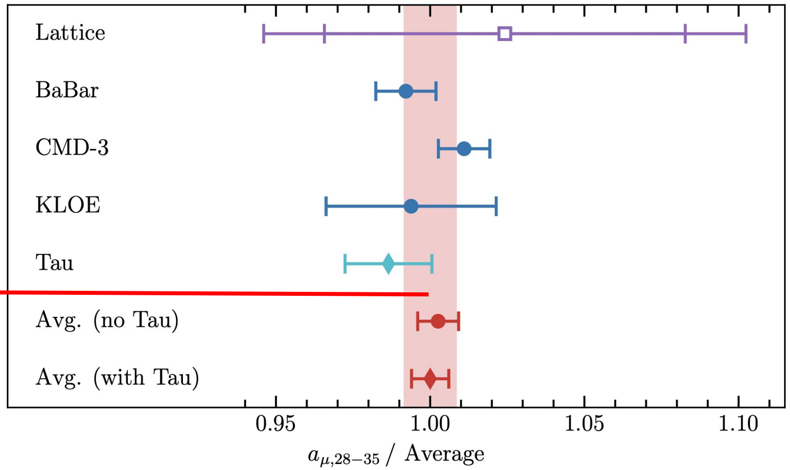

2407.10913

→ *Currently most precise prediction, based on improved lattice QCD (BMW) + data-driven inputs (DMZ) at large-t (input data in good agreement at low energy)*

Backup

Uncertainties on uncertainties and correlations

Numerous indications of uncertainties on uncertainties and on correlations, with a direct impact on combination fits

→ Shapes of systematic uncertainties *evaluated* in ~wide mass ranges with sharp transitions

→ One standard deviation is statistically not well defined for systematic uncertainties

→ Systematic uncertainties like acceptance, tracking efficiency, background etc. not necessarily fully correlated between low and high mass

→ Are all systematic uncertainty components fully independent between each-other? (e.g. tracking / trigger)

→ Y*ield uncertainties on uncertainties and on correlations*

→ Tensions between measurements (BABAR/KLOE/CMD3; 3 KLOE results etc.): *experimental indications of underestimated uncertainties*

→ *Statistical methods* (χ^2 with correlations, likelihood fits, ratios of measured quantities etc.) *should not over-exploit the information on the amplitude and correlations of uncertainties*

Topic of general interest, in other fields too (e.g. ATLAS JES and Jet Xsec studies)

Backup

Remarks and conclusions on $(g-2)_\mu$

We have an interesting, long standing, multifaceted problem…
… And very important elements to solve the puzzle started to become available !

→ Future e+e- measurements very important: independent 2π measurement from BaBar w/o PID this year
Long-term collaboration with M. Davier, A.-M. Lutz, Z. Zhang
Intense work by Leonard Polat & Andres Pinto (*PostDocs*)

Guiding ideas:

→ Need *rigorous* and *realistic* treatment of uncertainties and correlations at all levels
(Underestimated uncertainties do not bring scientific progress & can put studies on wrong path)

→ Caution about significance:
statistics-dominated measurement; prediction uncertainty limited by non-Gaussian systematic effects

→ Studies for understanding differences between data-driven and Lattice QCD approaches need to follow similar standards as the g-2 experiment: *double-blinding*

Jet studies with ATLAS @ LHC

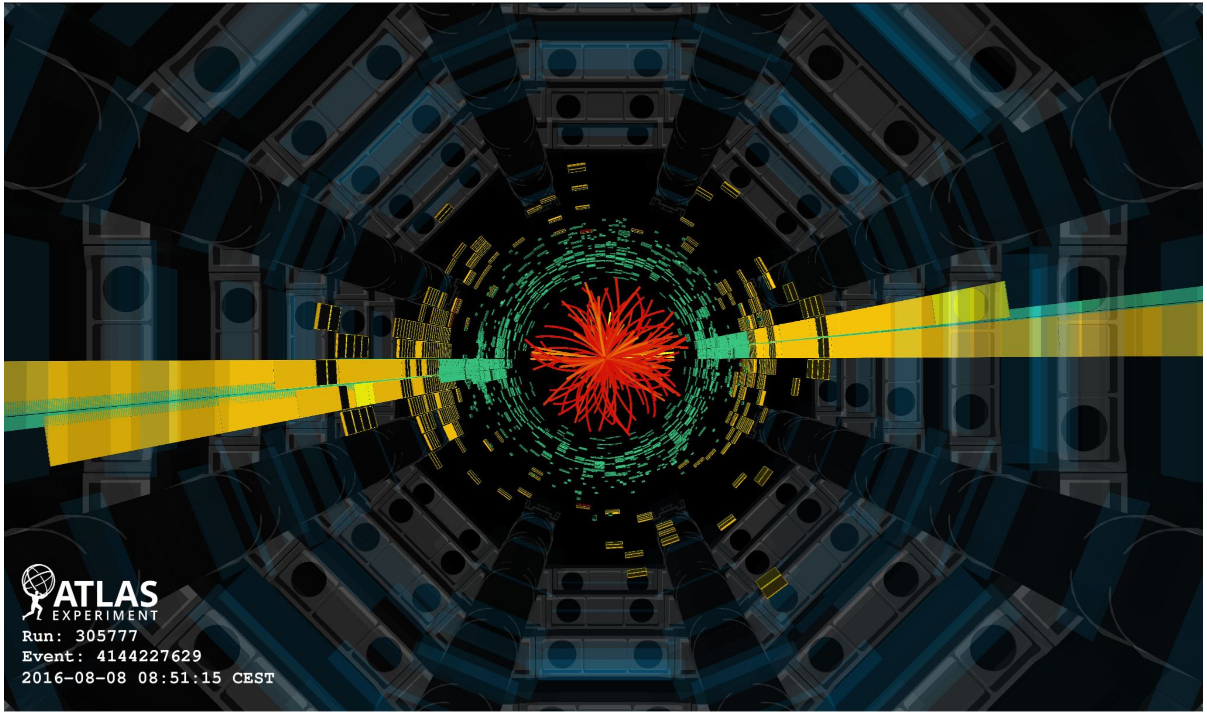

Jets @ LHC

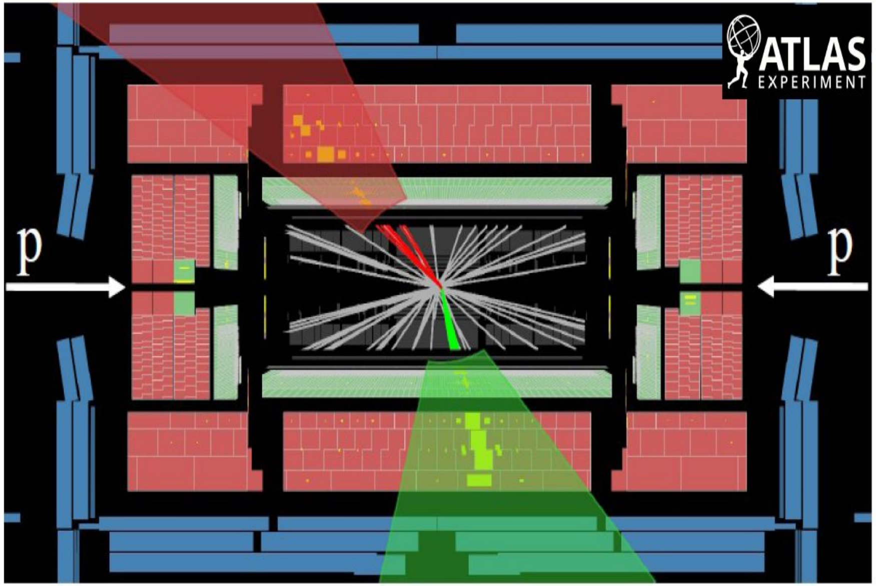

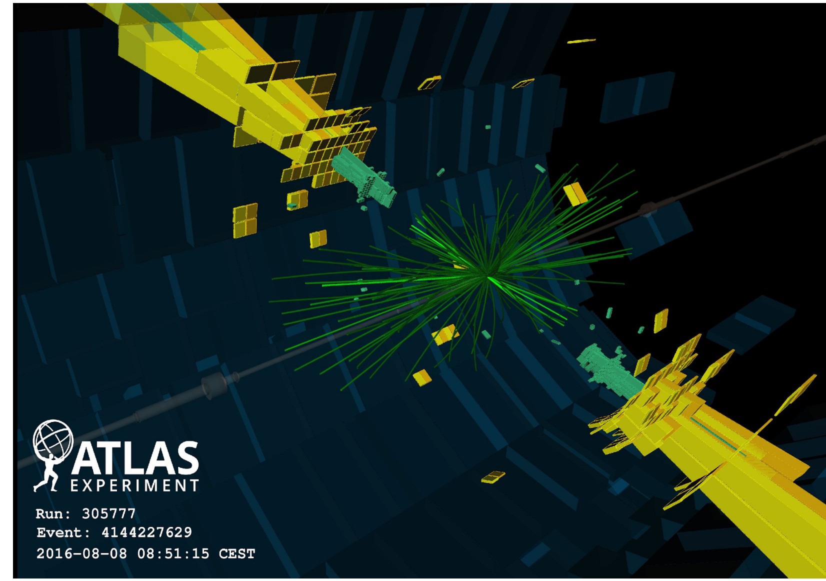

Jets: "sprays" of (quasi-)stable particles called hadrons, observed in the ATLAS detector

→ Proxy to fundamental interactions in Nature, probing the smallest scales accessible in laboratory:
Test SM on wide phase-space; important ingredients to α_s and PDF fits; sensitivity to New Physics

→ Precise and robust definition necessary for any quantitative studies:
anti-k_t - infrared and collinear safe

Backup

Example of (un)folding problem @ LHC

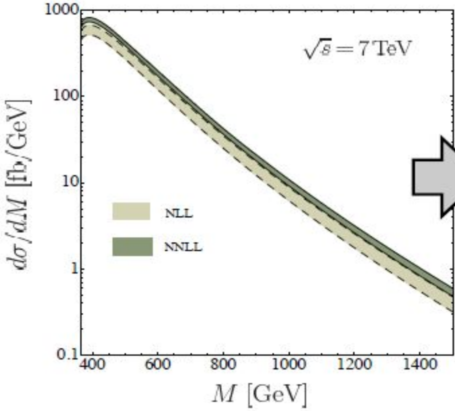

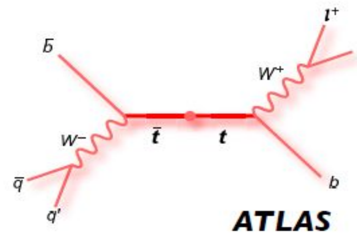

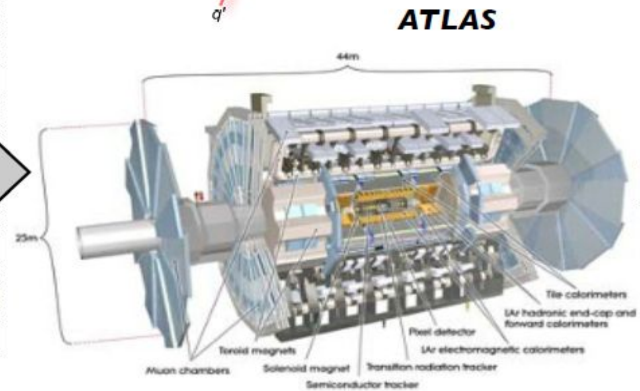

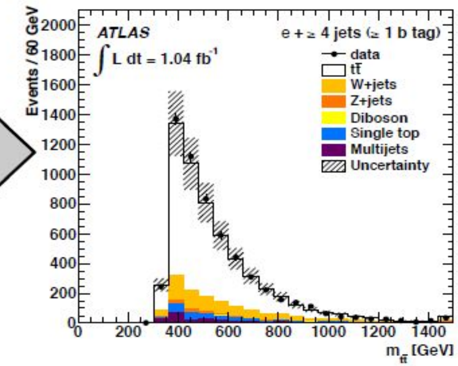

Folding

Calibration + Unfolding

Typical proton-proton collision: a complex process in a difficult environment

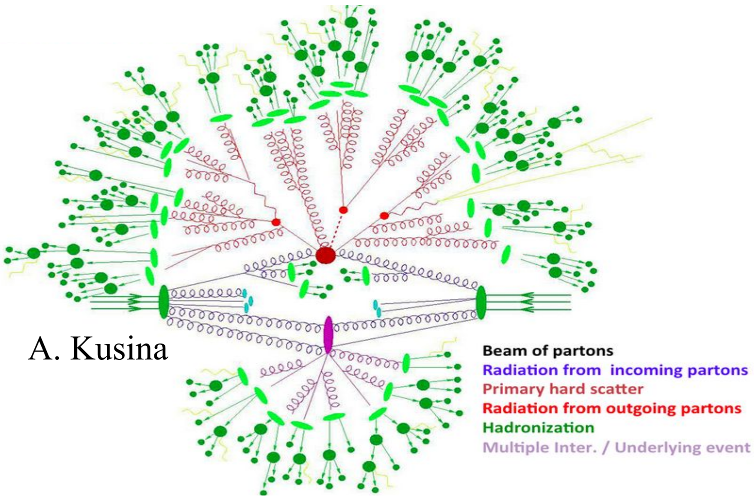

A. Kusina

Pile-up

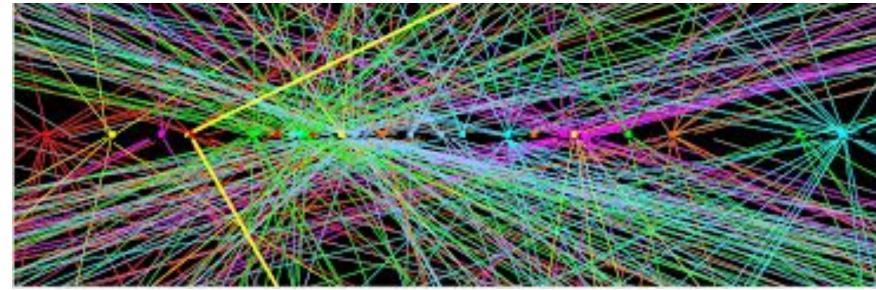

NP corrections
Hadronization & UE

Calibration+Unfolding
Jet energy response & resolution

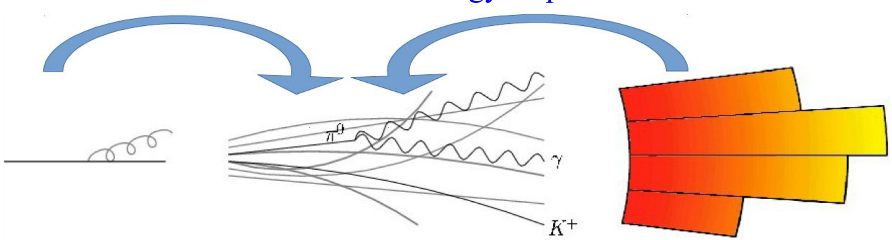

parton level jet

particle level jet

Data/theory comparison

calorimeter (reconstructed) level jet

Goal: *publish data "corrected for detector effects"* *(on average, in the sense of an estimator)*, ***with minimal bias and minimal model dependence***, *with the full information needed for comparisons with theory predictions*

→ Typically implies unfolding to hadron level although there are cases where one can unfold to parton level

Jet reconstruction and calibration procedure

Reconstructed jets → **p_T-density-based pile-up correction** → **Residual pile-up correction** → **Absolute MC-based calibration** → **Global sequential calibration** → **Residual *in situ* calibration**

- **Reconstructed jets**: Jet finding applied to tracking- and/or calorimeter-based inputs.
- **p_T-density-based pile-up correction**: Applied as a function of event pile-up p_T density and jet area.
- **Residual pile-up correction**: Removes residual pile-up dependence, as a function of μ and N_{PV}.
- **Absolute MC-based calibration**: Corrects jet 4-momentum to the particle-level energy scale. Both the energy and direction are calibrated.
- **Global sequential calibration**: Reduces flavour dependence and energy leakage effects using calorimeter, track, and muon-segment variables.
- **Residual *in situ* calibration**: A residual calibration is applied **only to data** to correct for data/MC differences.

$$c = \frac{\mathcal{R}^{\text{data}}_{in\text{-}situ}}{\mathcal{R}^{\text{MC}}_{in\text{-}situ}} \equiv \frac{\left(p_T^{jet} \middle/ p_T^{reference} \right)^{reco}_{data}}{\left(p_T^{jet} \middle/ p_T^{reference} \right)^{reco}_{MC}}$$

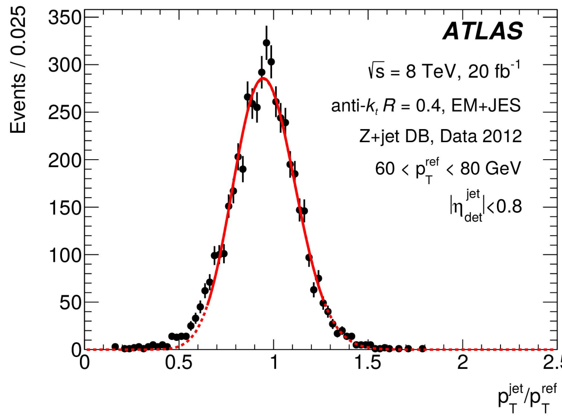

Dijet balance

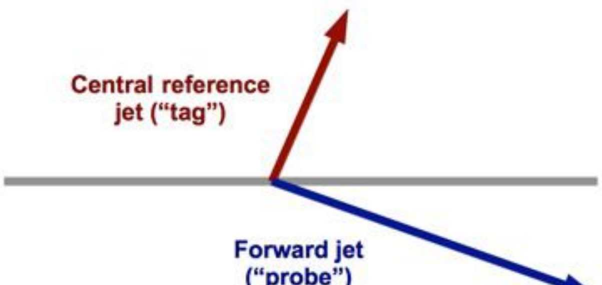

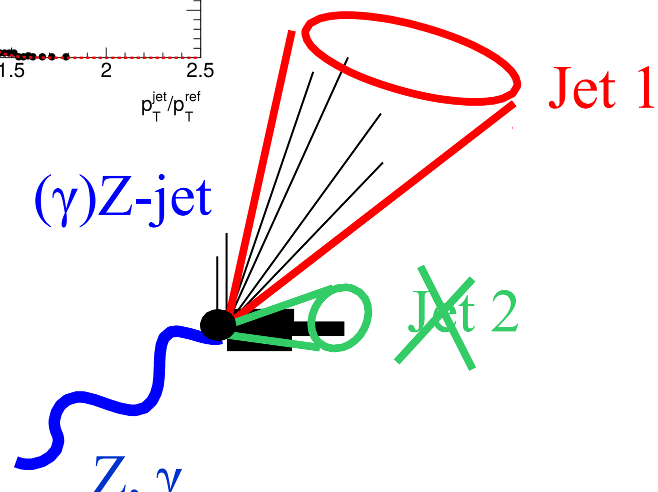

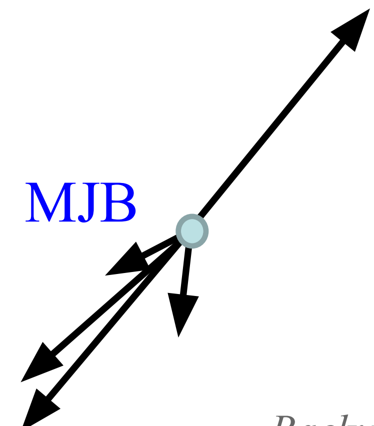

Backup

In-situ η – intercalibration calibration method

$$\mathcal{A} = \frac{p_T^{\text{left}} - p_T^{\text{right}}}{p_T^{\text{avg}}} \qquad \mathcal{R} = \frac{c^{\text{right}}}{c^{\text{left}}} = \frac{2 + \langle\mathcal{A}\rangle}{2 - \langle\mathcal{A}\rangle} \approx \frac{\langle p_T^{\text{left}}\rangle}{\langle p_T^{\text{right}}\rangle}$$

$$S(c_{1x}, \ldots, c_{Nx}) = \sum_{j=2}^{N} \sum_{i=1}^{j-1} \left(\frac{1}{\Delta\langle\mathcal{R}_{ijx}\rangle} \left(c_{ix}\langle\mathcal{R}_{ijx}\rangle - c_{jx}\right)\right)^2 + X(c_{ix})$$

→ p_T balance in dijet *in-situ* events to achieve homogeneity of the calibration in η: using multiple combinations of central-forward bins to obtain a better statistical precision

→ Over-constrained system: gained a factor ~1000 in speed by using analytic solution (*Robert Hankache - PhD*)

→ Reduced modeling uncertainty by a factor ~2, avoiding double-counting of detector effects (*Louis Ginabat - PhD*)

→ Detailed study of the compatibility of constraints, improved statistical uncertainties and correlations (*Line Delagrange - PhD*)

→ Input for ML-based calibration (*Laura Boggia - PhD*)

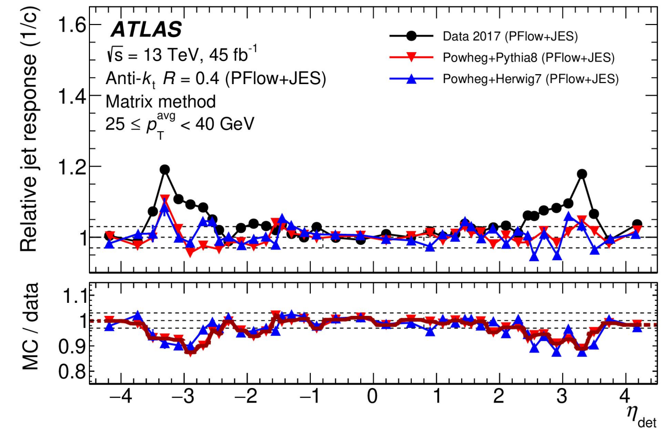

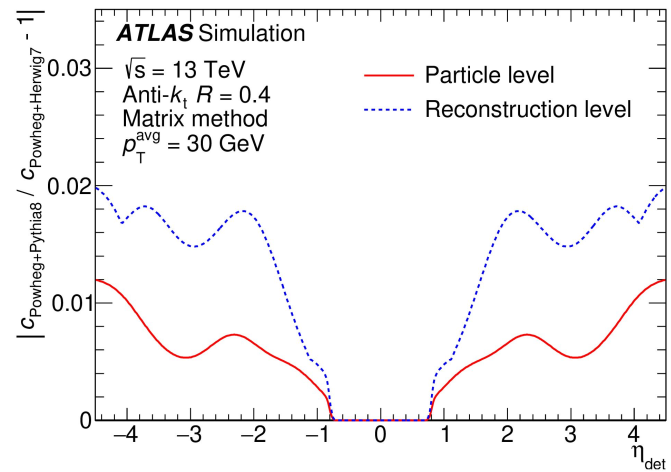

Backup

γ–jet + Z–jet + MJB combination

→ Combination of in-situ results with spline-based interpolations + weighted averages

→ Testing also compatibility of in-situ inputs

(*Inspired by methodology employed for hadronic spectra*)

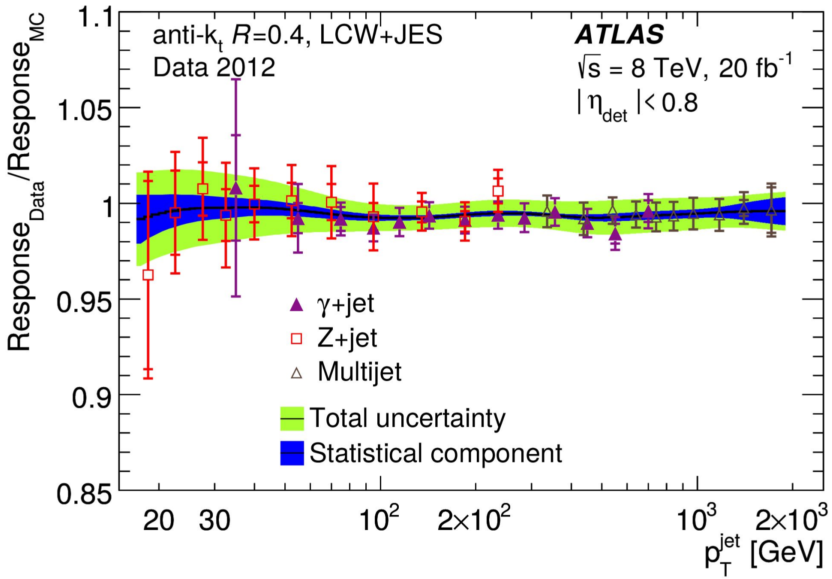

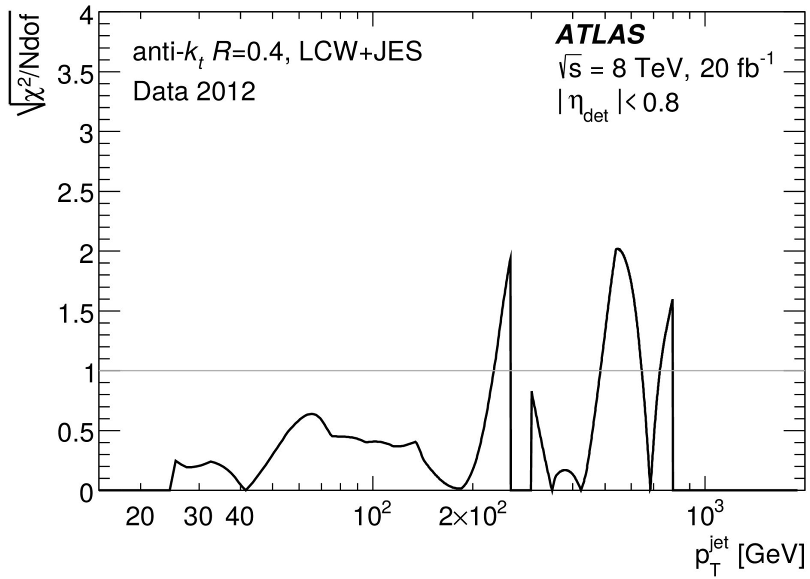

→ Includes Z+jet method for jet calibration and resolution (*Guillaume Lefebvre - PhD*)

γ–jet + Z–jet + E/p combination

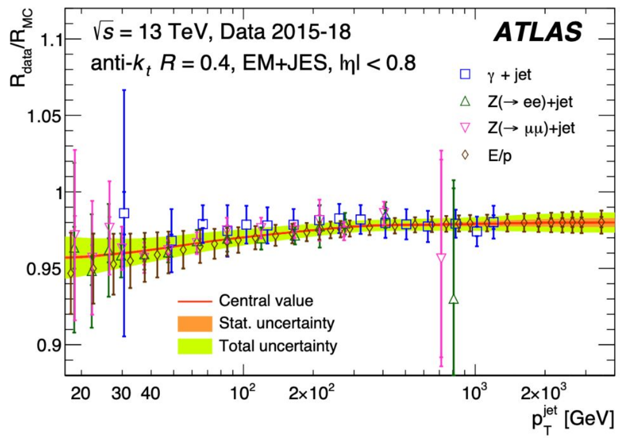

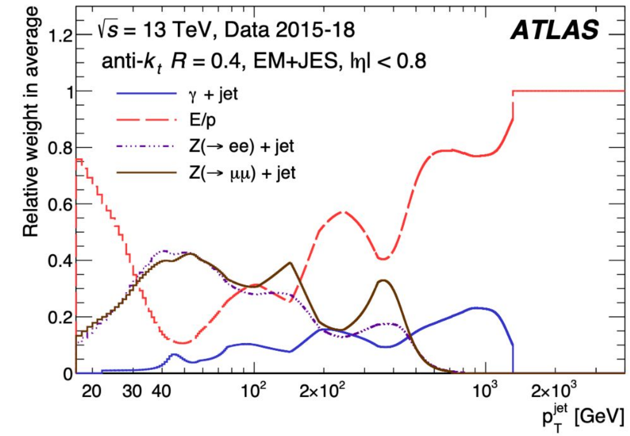

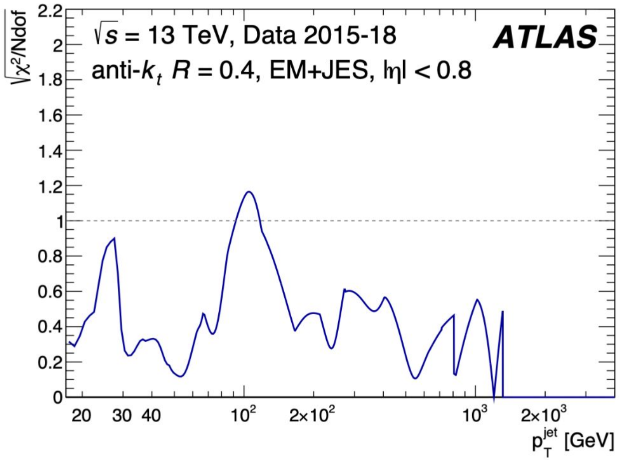

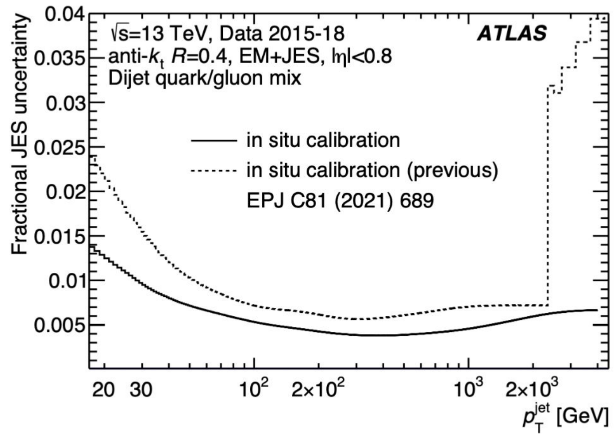

→ Important improvement due to E/p method (*Lata Panwar - PostDoc*)

Backup

In-situ uncertainties affecting the combination result

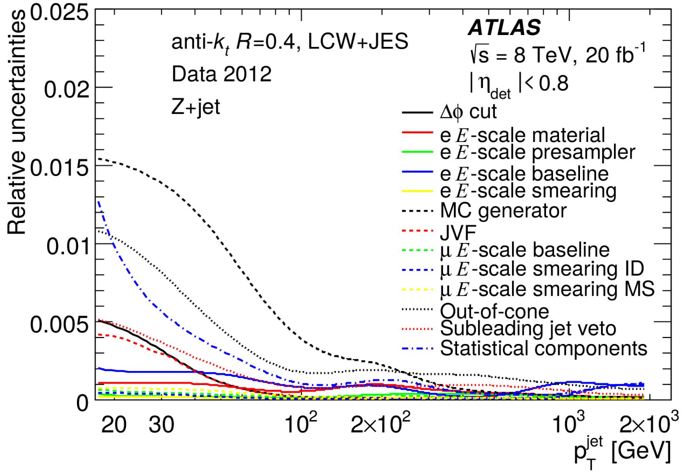

→ 47 in-situ uncertainty components (NPs) :
full propagation of information on uncertainty & correlations

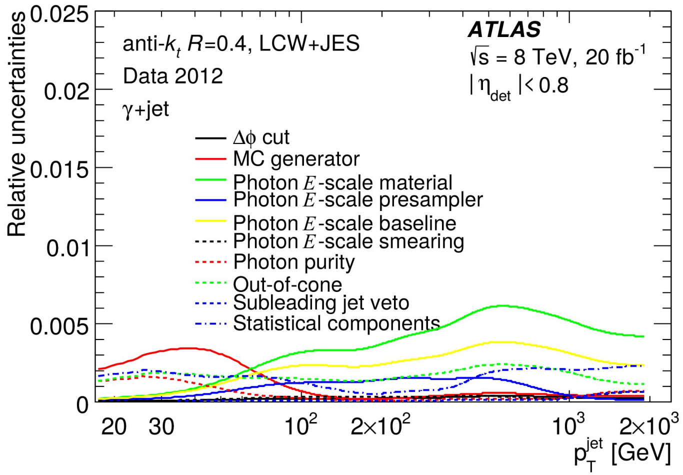

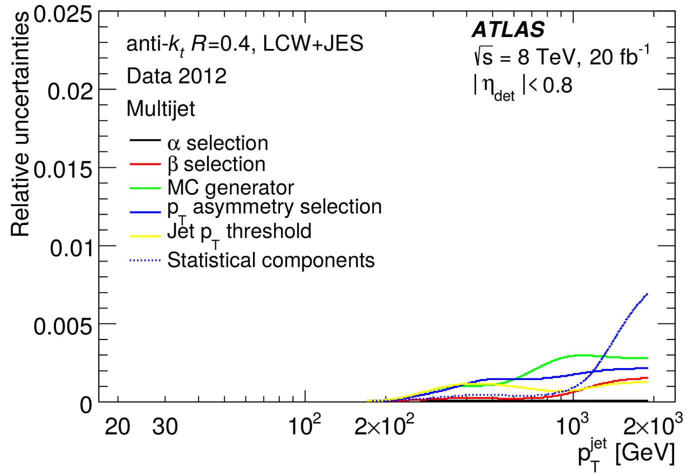

Using a diagonalization procedure to reduce the number of NPs

$$C = S \cdot D \cdot S^T$$

$$D = \begin{pmatrix} \ddots & 0 & 0 \\ 0 & \sigma_i^2 & 0 \\ 0 & 0 & \ddots \end{pmatrix}$$

$$S = \begin{pmatrix} V_1 & \cdots & V_n \\ \vdots & & \vdots \end{pmatrix}$$

- V_i = eigen vectors
- σ_i^2 = eigen values

Going from 47 in-situ NPs to 6 NPs

$$C = \sum_{i=1}^{N_{bins}} \sigma_i^2 C(V_i) \simeq \sum_{i=1}^{N_{ev}-1} \sigma_i^2 C(V_i) + C'(\text{other e.v.})$$

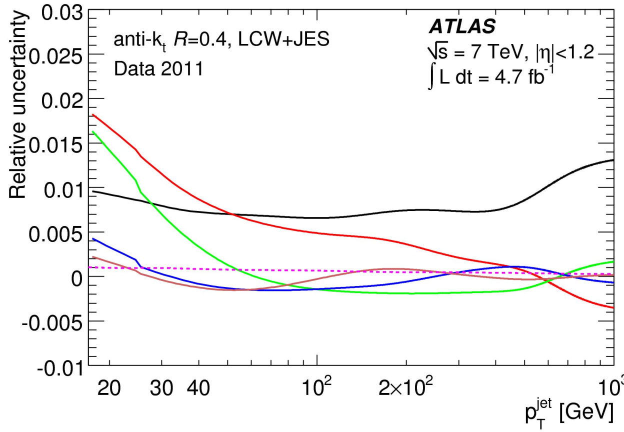

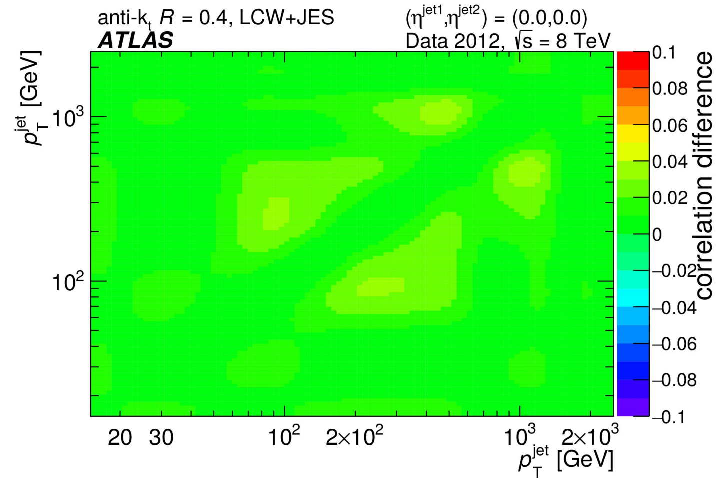

→ Use part (N_{ev} -1) of the important (large) eigenvalues, plus an effective contribution for the others (rest term), to approximate the covariance matrix: percent-level precision on correlations (difference between original and approximate matrices)

→ Keep track of uncertainty origin using a reduction by category:

"statistical", "modeling", "detector", "mixed (modeling/detector)", "special"

Uncertainties on JES correlations

→ Derived two alternative configurations with stronger/weaker correlations w.r.t. nominal

(*Inspired remarks about uncertainties on uncertainties for combinations of hadronic spectra*)

Nominal correlation matrix

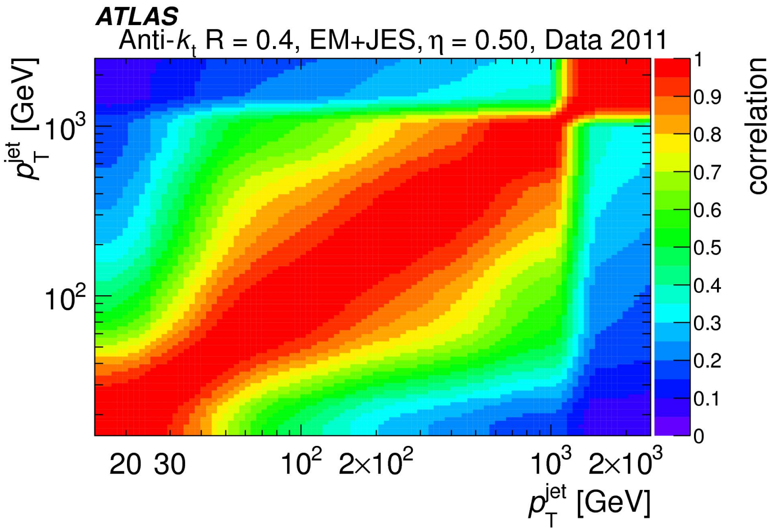

Strong - Weak correlation scenarios

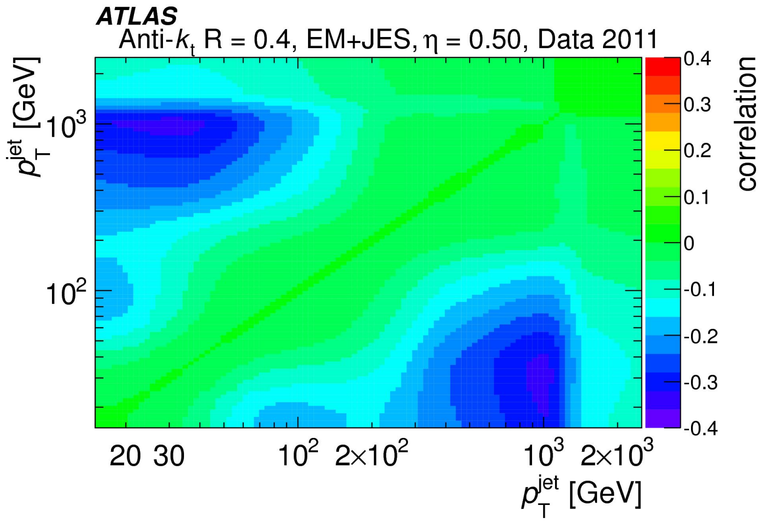

First γ-jet + Z-jet + Dijets + Zero Bias JER fit

→ Good agreement (local χ^2 with correlations) between in-situ methods

→ In-situ combination based on global fit of (N, S, C)

→ Full propagation of uncertainties & correlations:
3 eigenvectors are enough for ~10^{-3} precision on correlations

$$\frac{\sigma(p_T)}{p_T} = \frac{N}{p_T} \oplus \frac{S}{\sqrt{p_T}} \oplus C$$

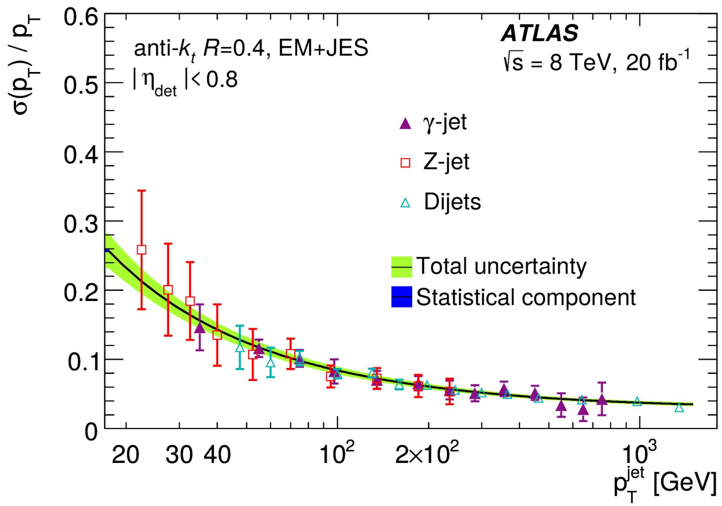

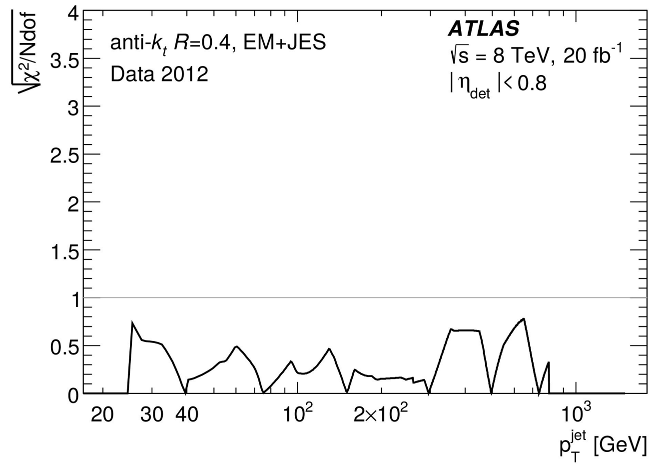

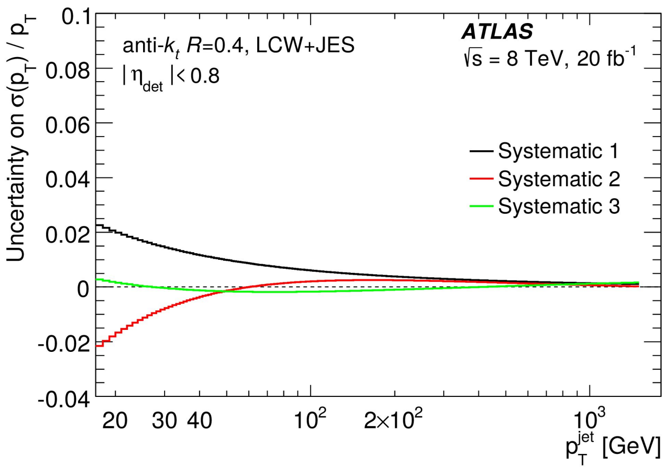

→ Coherent propagation of uncertainties & correlations
in physics analyses (*Dimitris Varouchas - PostDoc*)

Backup

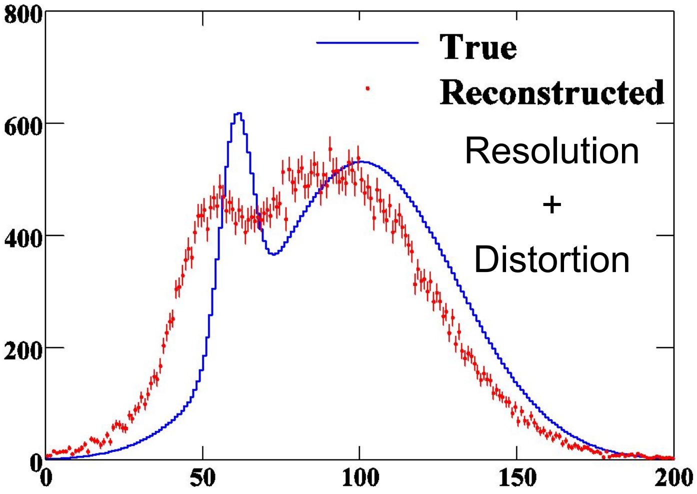

Transfer matrix: relates particle level & reconstructed observable (MC)

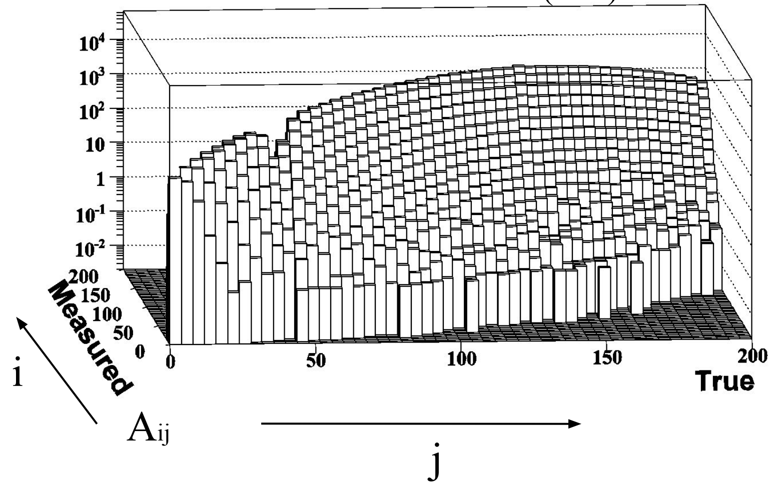

→ Folding: $$f_{\rm meas}(y) = \int R(y|x)\ f_{\rm true}(x)\ dx$$

$$P_{ij} = \frac{A_{ij}}{\sum_{k=1}^{n_d} A_{kj}}\ ;\ d = P \cdot t$$

→ Unfolding of detector smearing effects is generally not a simple numerical problem

Regularization methods are often necessary

Backup

Data unfolding: methodology & studies

→ Measurements corrected back to truth particle level using a matrix-based unfolding method
- transfer matrix relating the true & reconstructed observable (MC): matching needed
- 3 steps procedure: 1) matching (in)efficiency correction at reco level;
  2) IDS / SVD / bin-by-bin / IBU unfolding for jets with matching;
  3) matching (in)efficiency correction at true level.

→ Numerous aspects studied in this context, among which:
- choice of the phase-space
- optimization of the choice of the binning
- intrinsic unfolding uncertainties and choice of the regularization
- propagation of statistical and systematic (JES, JER etc.) uncertainties, with their correlations
- non-linear effects in the uncertainty propagation
- statistical noise in the uncertainty propagation
- modeling uncertainties and “hidden variables”

→ Developments of ML-based methods: will enable qualitative improvements of such measurements

Data-driven closure test: motivation, procedure, example

→ In-situ (i.e. *realistic*) determination of the unfolding uncertainty related to the data/MC shape difference and to the regularization (performed for several unfolding methods; choosing the most precise)

- reweight true MC by (smooth) function: improved data/recoMC agreement
  Reweighting performed within fine bins / event-by-event
- unfold the reweighted reconstructed MC
- compare with reweighted true MC

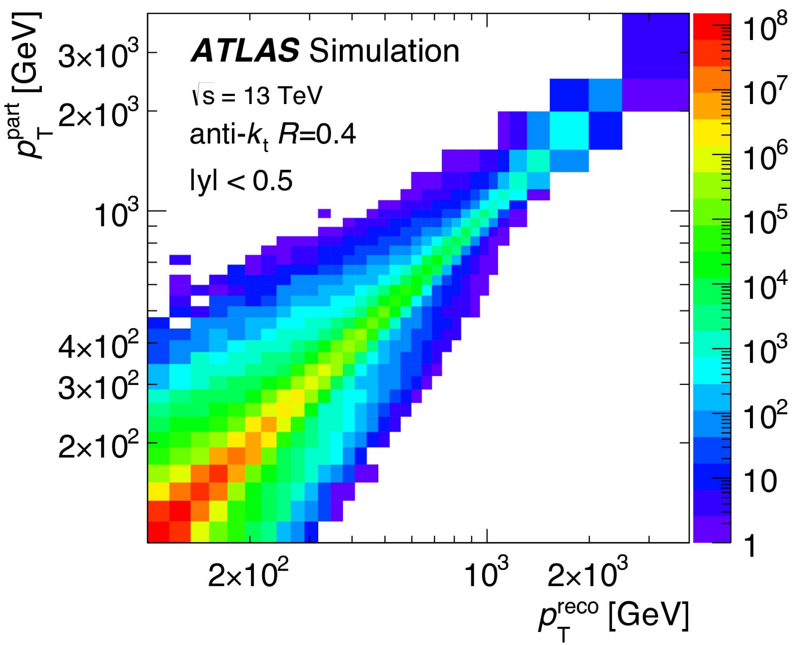

1711.02692

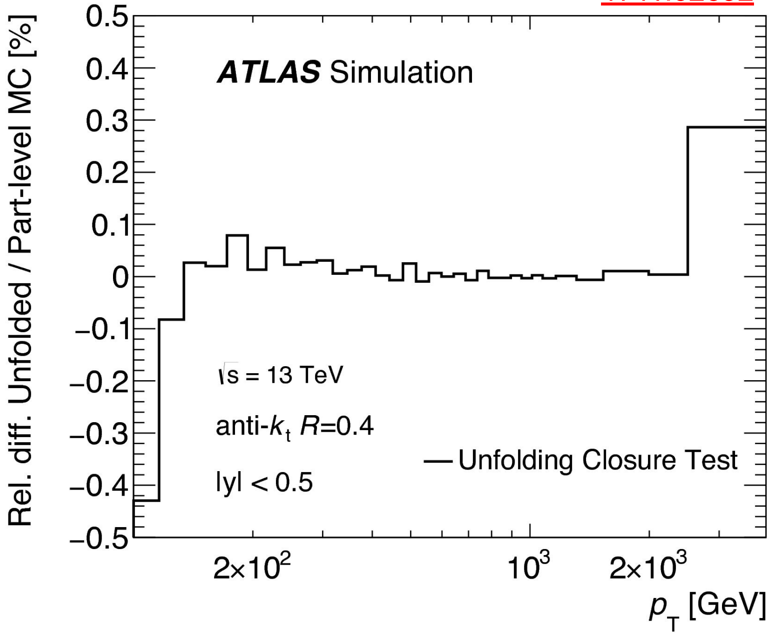

Statistical uncertainties

- Due to data and MC
- Propagated using pseudo-experiments done separately/simultaneously for data and MC

→ Bootstrap method

- multiply event weights by random number: Poisson(1)
- seed given by event number
- allows to correlate measurements with overlapping samples

ATL-PHYS-PUB-2021-011

1711.02692

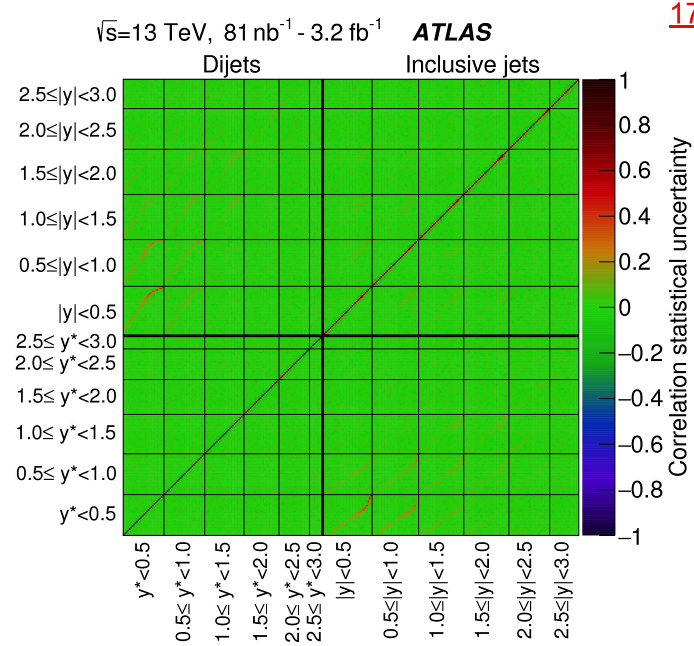

- Publish covariance matrix and/or a series of results based on each pseudo-experiment (i.e. Bootstrap replicas)

Propagation of systematic uncertainties from inputs

→ Modify input (pseudo-)data spectrum by ±1σ of the (asymmetric) uncertainty, re-do unfolding and compare with nominal result

→ Can also use 1...5σ scans or pseudo-experiments

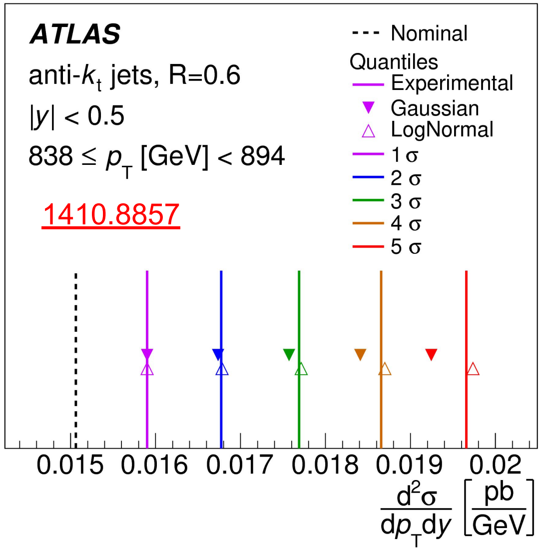

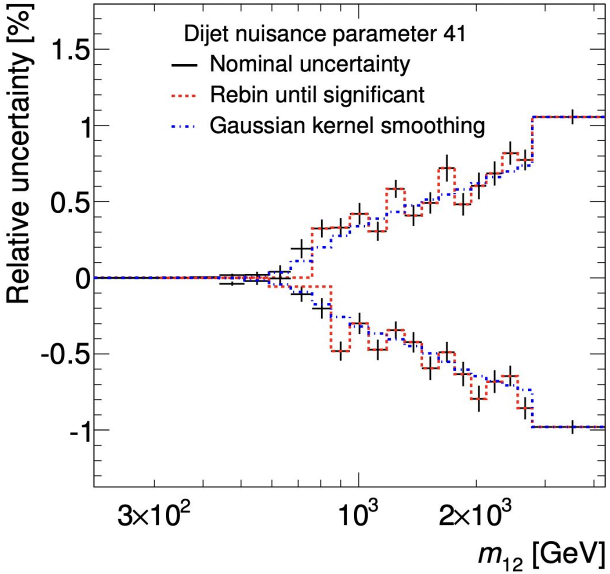

→ Bootstrap method to evaluate statistical uncertainties on the propagated systematics + rebinning/smoothing

Evaluate statistical significance to avoid multiple-counting of statistical uncertainties (1312.3524)

→ For resolution uncertainties, perform smearing of the transfer matrix: smearing factor given by quadratic difference between resolution enhanced by 1σ and nominal resolution

Propagation of systematic uncertainties from inputs

→ Split of systematics in sub-components (fully correlated in phase-space, independent between each-other) allows to evaluate correlations between different phase-space regions and between different measurements

Relevant when effectively merging uncertainty components in ML-based methods

→ Information made available in HEPData tables (http://hepdata.cedar.ac.uk/)

$$Cov_{ij} = \sum_{k=1}^{N_{syst}} s_i^k \cdot s_j^k$$

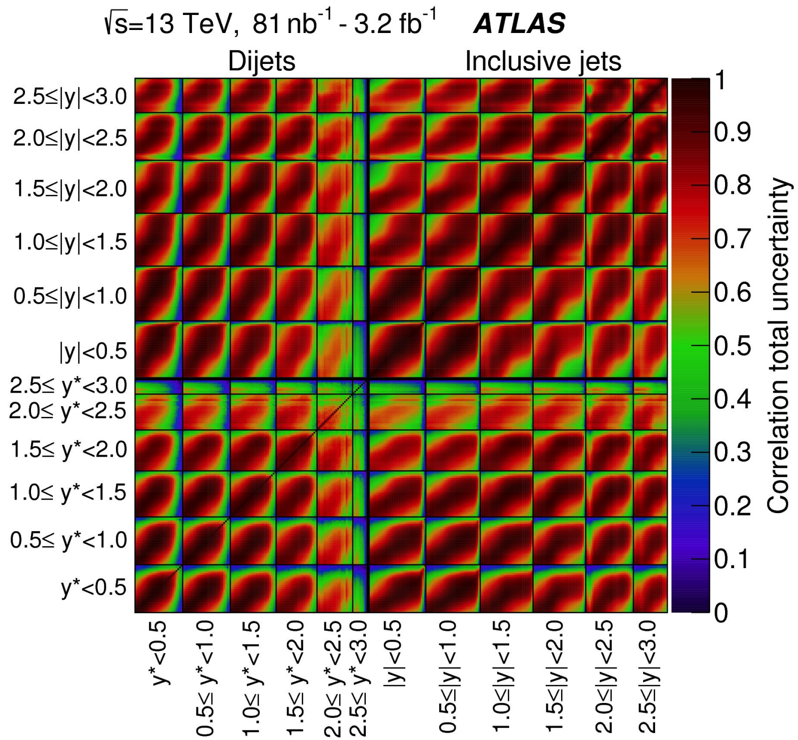

1711.02692

Inclusive jet and dijet cross sections - ATLAS

→ Double-differential measurements for anti-k_T jets with R=0.4, $\sqrt{s}$=13 TeV, L=3.2fb^{-1}
(p_T^{jet} ; |y|) (m_{jj} ; y*) compared to NLO pQCD + Non-pert. & EW corrections

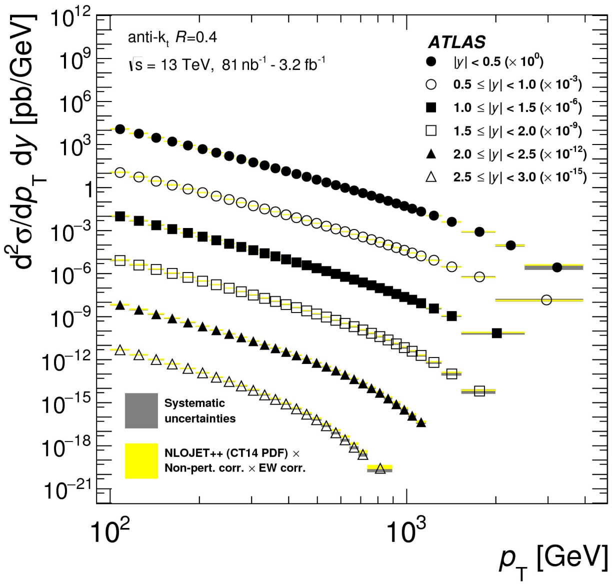

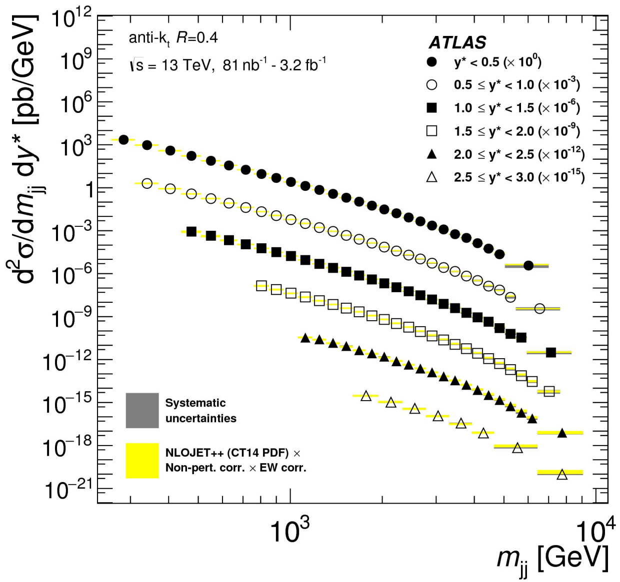

1711.02692

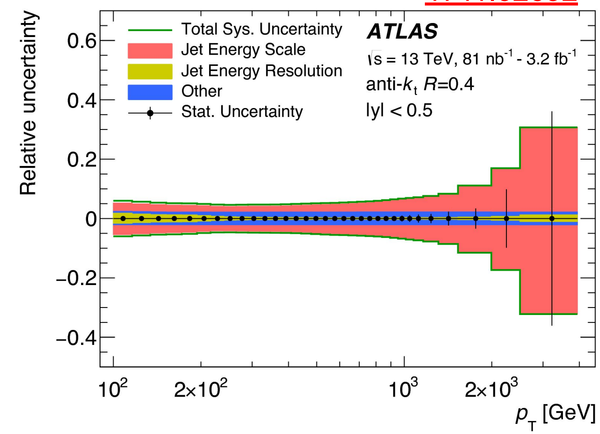

- At least 2 jets: p_T^{jet} > 75 GeV, |y| < 3
- $p_T^{jet\ 1} + p_T^{jet\ 2}$ > 200 GeV

→ Uncertainties (~5% on wide range, sub-% statistical → *precision era*)

Backup

Theoretical predictions and uncertainties

→ Perturbative QCD predictions from NLOJET++
- Uncertainties: renormalization & factorization scales (0.5 / 2 variations + p_T^{jet} vs. p_T^{max} scale choice), PDFs and α_S via APPLGRID
- NNLO prediction (APPLfast)

→ EW corrections

→ Non-perturbative corrections (accounting for hadronization and UE) and uncertainties: various Pythia tunes + different MC generators(Herwig++); strong dependence on R
- additional comparisons to Powheg (NLO ME + PS)

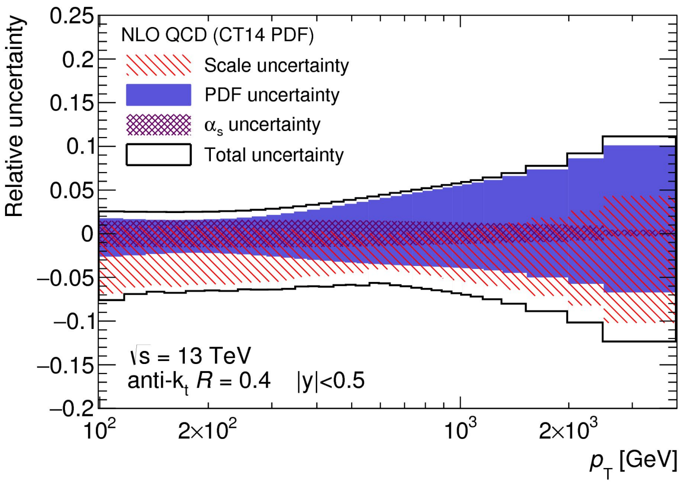

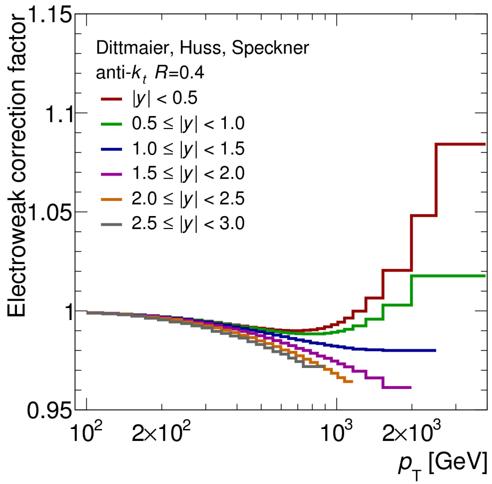

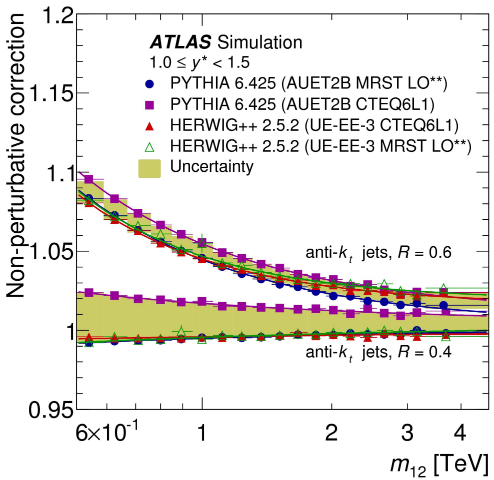

Inclusive jet cross sections at √s=8 TeV: Theory/Data

→ Good data/theory agreement within uncertainties observed for most PDF sets

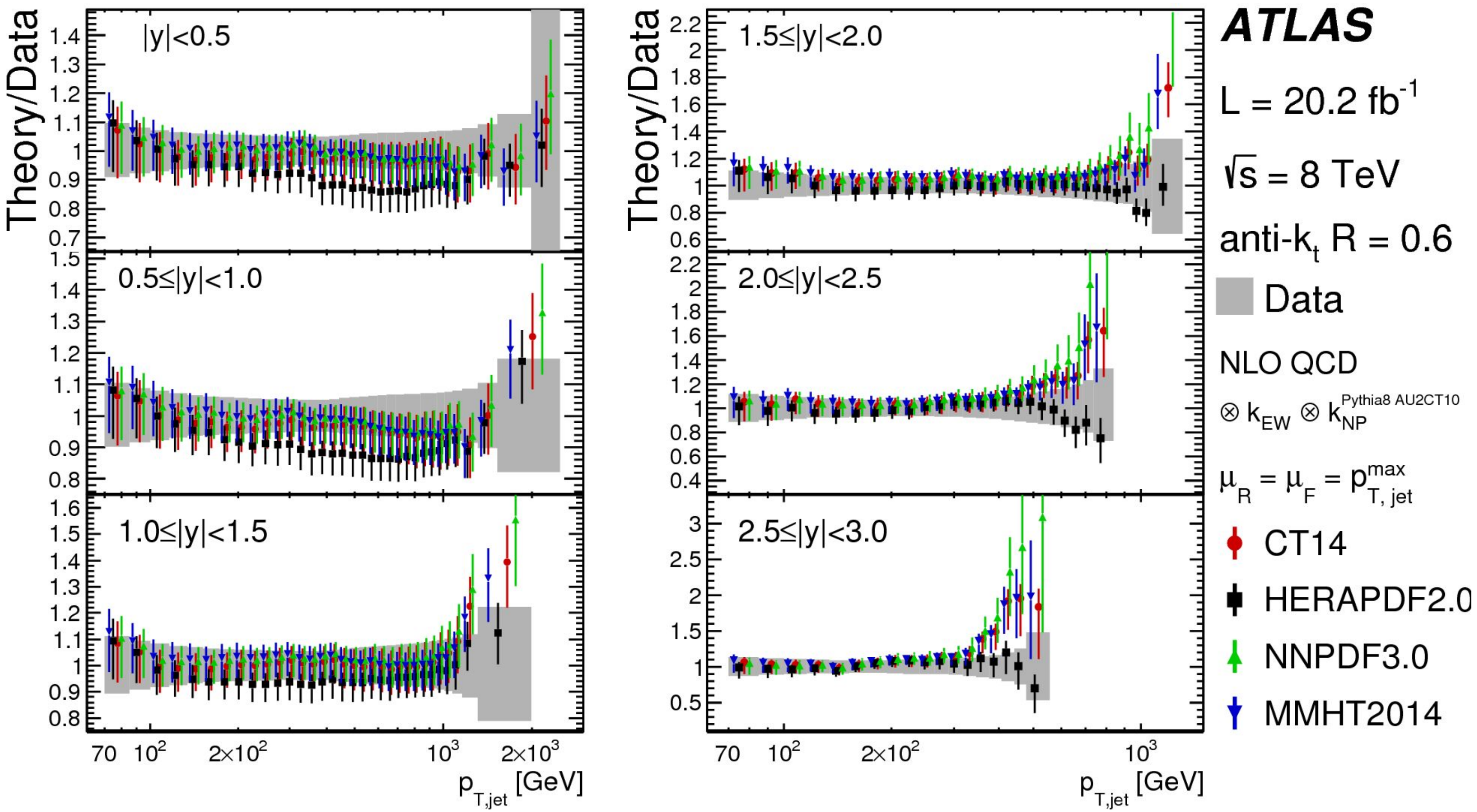

Backup

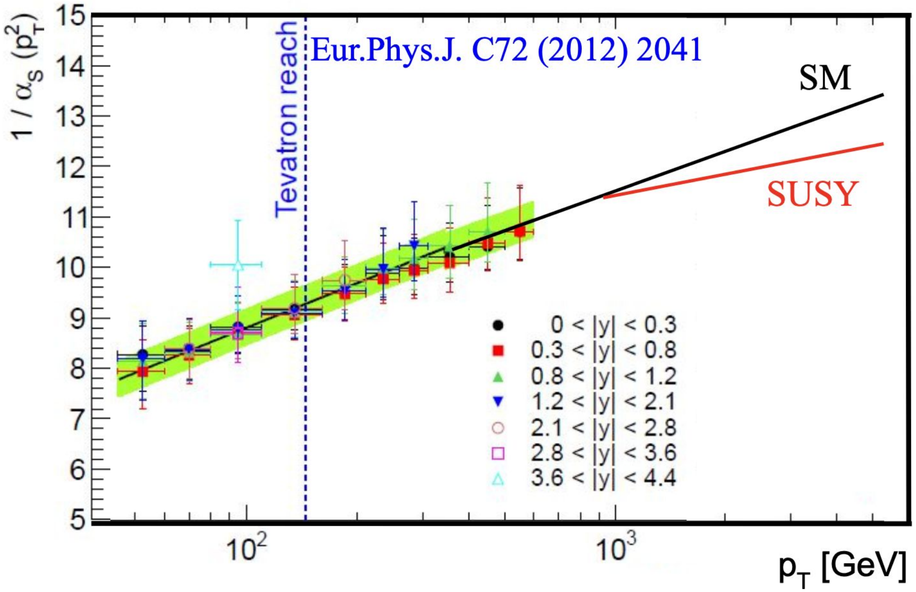

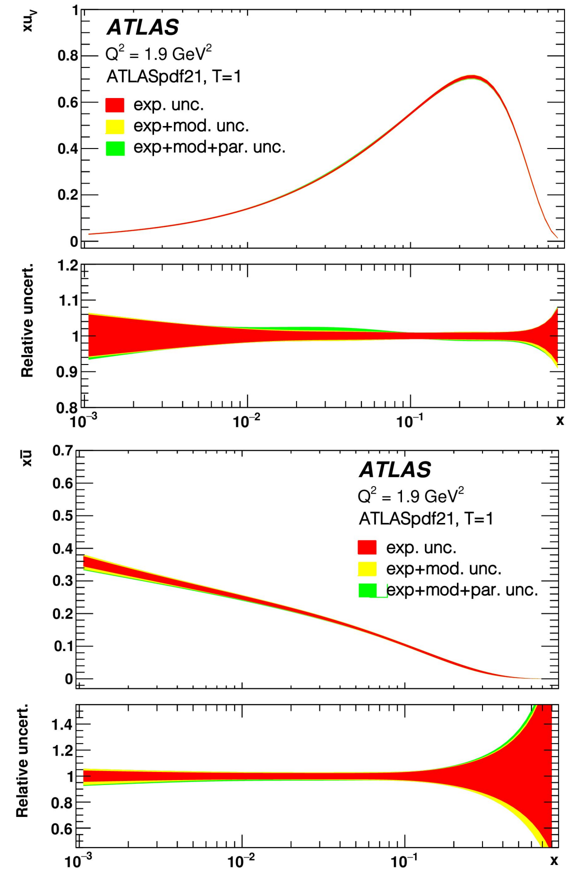

→ Involves using information on uncertainties and their correlations (between various measurement bins), keeping in mind that there are uncertainties impacting them too

Backup

α_s from jet Xsec ratios: energy range for the RGE test and PDF sensitivity

→ Observables like *$R_{3/2}$, $R_{\Delta\Phi}$ and (A)TEEC* non-trivial due to events that are *not* back-to-back dijets: *sensitivity to α_s originates from probability of emission of extra radiation (3^{rd} jet etc.)*

→ *Relevant scale for RGE test related to $p_{T,3}$ (low), not to event-level observables* (e.g. $p_T^{\text{lead. jet}}$, $p_T^{\text{(all jets)}}$, $(p_{T,1}+p_{T,2})/2$, $H_T/2$)

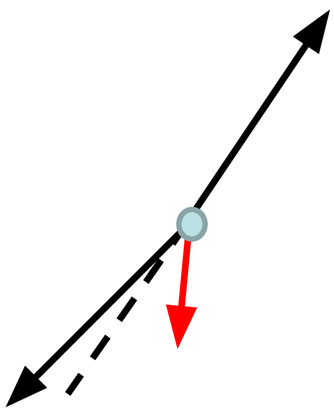

Observable [Ref.]	$\alpha_s(M_Z^2)$	Range PDF variations
R_{32} [109]	$0.111 \pm 0.006\,(\text{exp})^{+0.016}_{-0.003}\,(\text{PDF, NP, scale})$	0.109 – 0.116
R_{32} [110]	$0.1148 \pm 0.0014\,(\text{exp}) \pm 0.0018\,(\text{PDF}) \pm 0.0050\,(\text{theory})$	0.1135 – 0.1148
3-jet mass [108]	$0.1171 \pm 0.0013\,(\text{exp}) \pm 0.0024\,(\text{PDF}) \pm 0.0008\,(\text{NP})^{+0.0069}_{-0.0040}\,(\text{scale})$	0.1143 – 0.1183
2-jets [111]	$0.1159 \pm 0.0025\,(\text{exp, PDF, NP})$	0.1159 – 0.1183
3-jets [111]	$0.1161 \pm 0.0021\,(\text{exp, PDF, NP})$	0.1159 – 0.1179
2- & 3-jets [111]	$0.1161 \pm 0.0021\,(\text{exp, PDF, NP})$	0.1161 – 0.1188
R_{32} [111]	$0.1150 \pm 0.0010\,(\text{exp}) \pm 0.0013\,(\text{PDF}) \pm 0.0015\,(\text{NP})^{+0.0050}_{-0.0000}\,(\text{scale})$	0.1139 – 0.1184
TEEC [112]	$0.1162 \pm 0.0011\,(\text{exp}) \pm 0.0018\,(\text{PDF}) \pm 0.0003\,(\text{NP})^{+0.0076}_{-0.0061}\,(\text{scale})$	0.1151 – 0.1177
ATEEC [112]	$0.1196 \pm 0.0013\,(\text{exp}) \pm 0.0017\,(\text{PDF}) \pm 0.0004\,(\text{NP})^{+0.0061}_{-0.0013}\,(\text{scale})$	0.1185 – 0.1206
$R_{\Delta\phi}$ [113]	$0.1127^{+0.0019}_{-0.0018}\,(\text{exp}) \pm 0.0006\,(\text{PDF})^{+0.0003}_{-0.0001}\,(\text{NP})^{+0.0052}_{-0.0019}\,(\text{scale})$	0.1127 – 0.1156

→ *PDF uncertainties non-negligible for (α_s from) cross-section ratio measurements & (A)TEEC:*

- probability of extra radiation sensitive to the type of partons in the initial state
- both α_s & PDF sensitivities of the observables reduced for ratios: both relevant for the α_s evaluation

Backup

Quantitative data/theory comparisons

→ Generalized

$$\chi^2(\mathbf{d};\mathbf{t}) = \min_{\beta_a}\left\{\sum_{i,j}\left[d_i - \left(1+\sum_a \beta_a \cdot \left(\boldsymbol{\epsilon}_a^{\pm}(\beta_a)\right)_i\right)t_i\right]\cdot\left[C_{\rm su}^{-1}(\mathbf{t})\right]_{ij}\right.$$
$$\left.\cdot\left[d_j - \left(1+\sum_a \beta_a \cdot \left(\boldsymbol{\epsilon}_a^{\pm}(\beta_a)\right)_j\right)t_j\right] + \sum_a \beta_a^2\right\},$$

Accounts for correlations and asymmetries of experimental and theoretical uncertainties (stat. & syst.)

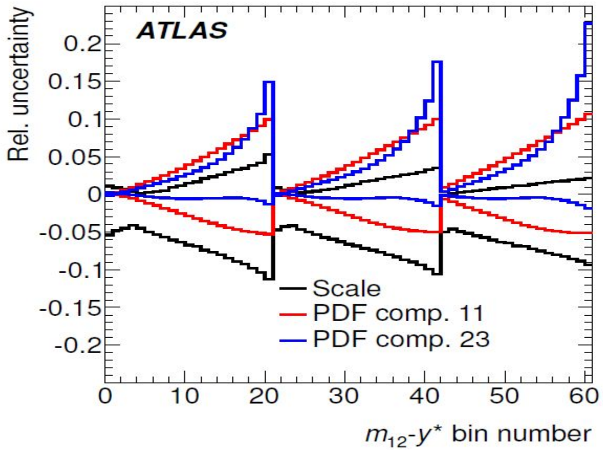

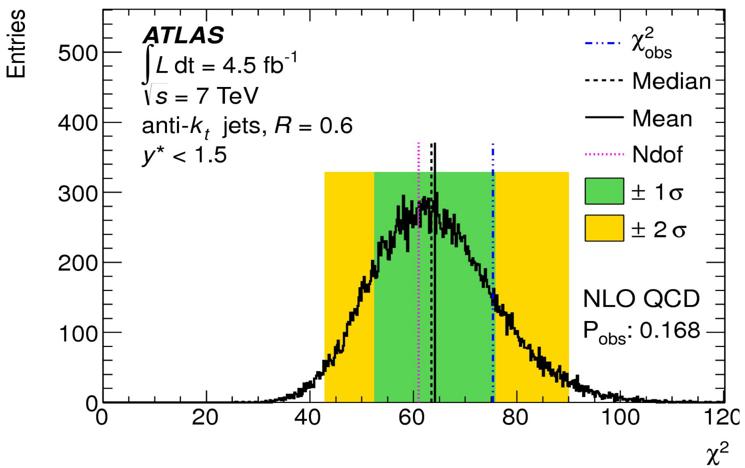

→ Using frequentist method to compute p-value:

- pseudo-experiments from theory prediction, with the full information on the uncertainties: build the generalized χ^2 distribution (no assumption needed)
- observed χ^2 from the data/theory comparison

Quantitative comparison between data and NLO QCD+NP+EW

Comparisons performed for a large number of configurations:

→ PDFs: ABM11(as for 7TeV), CT14, MMHT 2014, NNPDF 3.0, HERAPDF 2.0, ABMP16

→ Phase-space regions:

p_T ranges:
- "wide": > 70; > 100; 100 − 900; 100 − 400 GeV
- "narrow": 70 − 100; 100 − 240; 240 − 408; 408 − 642; 642 − 952; > 952 GeV

|y| ranges:
- "individual bins": |y| < 0.5; 0.5 − 1; 1 − 1.5; 1.5 − 2; 2 − 2.5; 2.5 − 3
- "full range": |y| < 3
- "pairs of consecutive bins": |y| < 1; 0.5 − 1.5; 1 − 2; 1.5 − 2.5; 2 − 3
- "central-forward pairs": |y| < 0.5 & 2.5 − 3; < 0.5 & 2 − 2.5; < 0.5 & 1.5 − 2

→ R=0.4 and R=0.6; $p_T^{\text{leading jet}}$ and p_T^{jet} scale choices

→ Generally good agreement for inclusive jets for individual & pairs of |y| bins

→ Tension when including all |y| bins for inclusive jets
→ Sensitive to treatment of correlations for "2-point" systematic uncertainties

→ Good data/theory agreement for dijets

Backup

Testing realistic alternative correlation assumptions

Inclusive jets - nominal χ^2/ndf for CT14 with $p_T^{\text{leading jet}}$ scale*:*
321 – 360/159 (8 TeV); 419/177(13 TeV)

Splitting a single systematic: some χ^2 reduction, but still small p-values.

Splitting simultaneously several uncertainties:

→ JES Flavour Response, JES MJB Fragmentation, JES Pile-up Rho Topology:
χ^2 reduction by up to 51 units (8 TeV)

→ Scale variations, alternative scale choice, non-perturbative correction:
χ^2 reduction by up to 87 units (8 TeV)
– more work needed on the correlations of theory uncertainties

→ Splitting both the experimental and theoretical uncertainties:
χ^2 reduction by up to 96 units (8 TeV); 58 units (13 TeV)

→ Possible (extra) motivation for including scale uncertainties in PDF fits - in progress

Note: there is also an uncertainty on the phase-space dependence for the size of 2-point systematics
→ may explain part of the observed tension

Limits on New Physics using unfolded distributions

→ Explore BSM physics directly at particle level

Contact Interaction Model (CI)
New force mediated by heavy particle

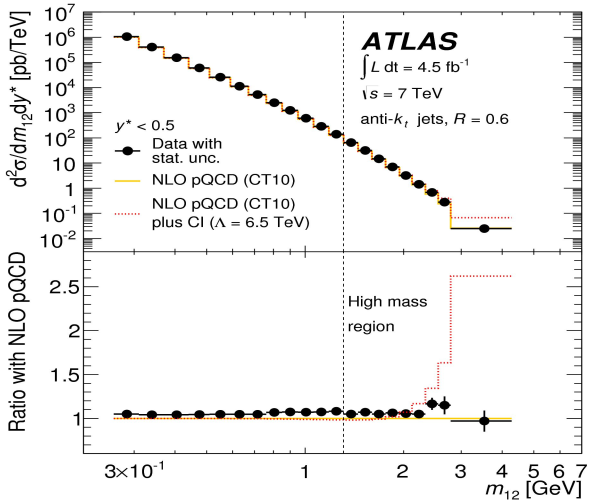

$CLs = p_{s+b}/(1-p_b)$

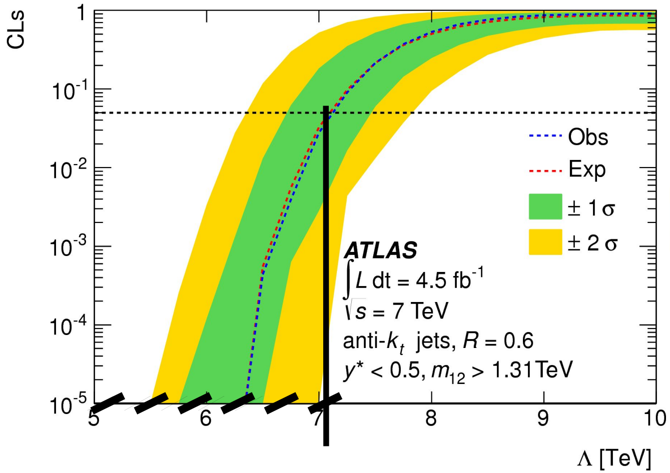

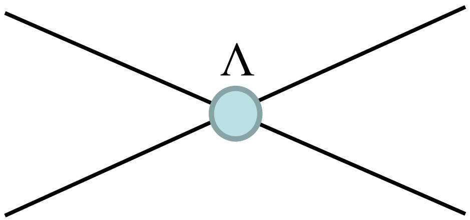

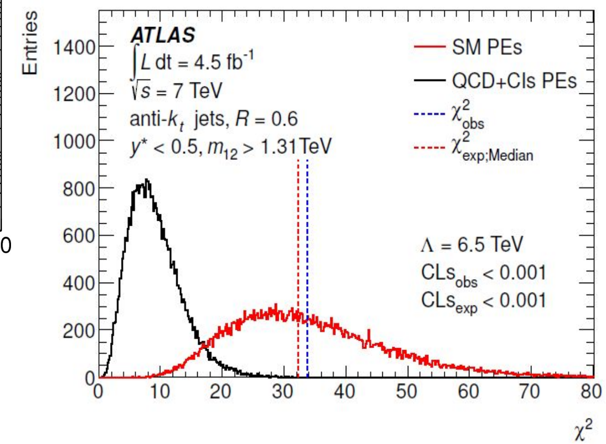

→ Full frequentist analysis (CLs), with generalized χ^2 as test statistic

→ Accounts for correlations and asymmetries of uncertainties (stat. & syst.)

→ Limits similar to the ones obtained by dedicated searches
(comparing reconstructed-level data with theory predictions folded with detector effects)

Backup

Generic Gaussian signals: folding-based method

→ Limits on generic Gaussian signals can be re-interpreted in terms of various signal models

→ Previously studied at reconstructed-level – hadron-level preferable (limits more straightforward to use)

→ Folding method using MC-based transfer matrix allows to factorize physics & detector effects

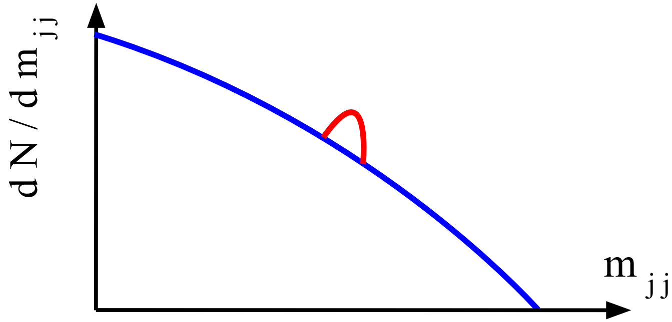

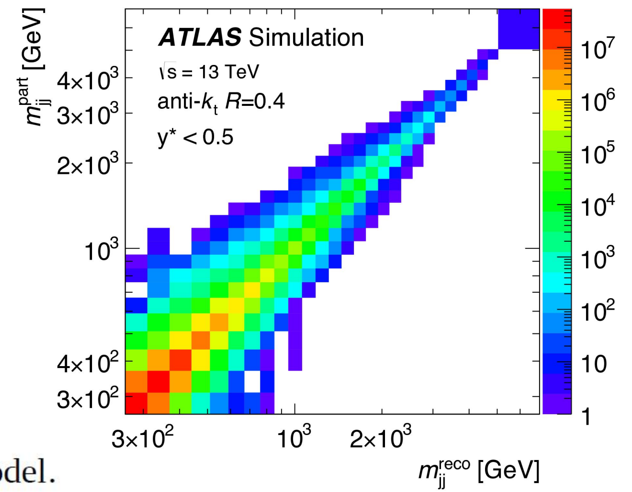

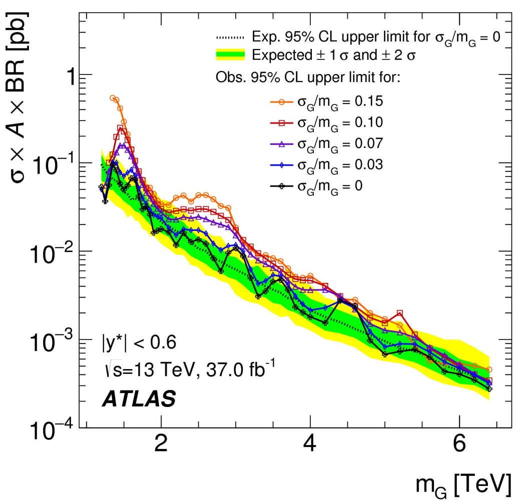

(*Robert Hankache - PhD*)

$f_y(M^{truth})$ = truth entries for a given model.

$F'_x(M^{reco})$ = the expected reco entries.

$$f_y(M^{truth}) \xrightarrow{\text{Folding}} F'_x(M^{reco}) = \sum_y f_y * \underbrace{E_y^T * A_{xy} / E_x^R}_{\widetilde{A}}$$

→ For resonance width ~ resolution: differences between folding result and reconstructed-level limits of up to 20% (different interpretation)

Backup

Conclusion

→ *Interesting QCD / New Physics-related questions to address both at the energy frontier, with jets, and in precision low-energy studies employing hadronic spectra*

→ *Developed several methodologies relevant for both areas*

→ *Potential for multiple improvements of such measurements and their phenomenological interpretation*

Thank you !!!

Backup

The $(g\text{-}2)_\mu$: definition & experimental measurement

- Magnetic dipole moment of a charged lepton: $\vec{\mu} = g\dfrac{e}{2m}\vec{s}$

- "anomaly" = deviation w.r.t. Dirac's prediction: $a = \dfrac{g-2}{2}$

- Experimental "ingredients" to measure a_μ:

→ Polarised muons from pion decays (parity violation)

spin orientation

$\bar{\nu}_\mu \longleftarrow \pi^- \longrightarrow \mu^-_{\text{polarised}}$

→ "Anomalous frequency"

(difference between spin precession and cyclotron frequency)

proportional to a_μ for the "magic γ"

$$\vec{\omega}_a = \frac{e}{m_\mu c}\left[a_\mu \vec{B} - \left(a_\mu - \frac{1}{\gamma^2 - 1}\right)\vec{\beta}\times\vec{E}\right] \approx \frac{e}{m_\mu c} a_\mu \vec{B}$$

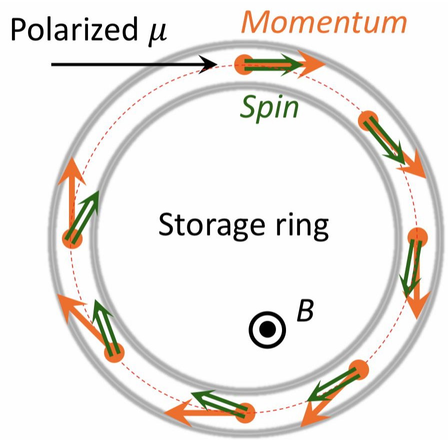

→ Parity violation in muon decays

(electron emitted in the direction opposite to the muon spin)

$\mu^-_{\text{polarised}} \longrightarrow e^- + \bar{\nu}_e + \nu_\mu$

From BNL to Fermilab

BNL → 1 month long trip for the g-2 storage ring

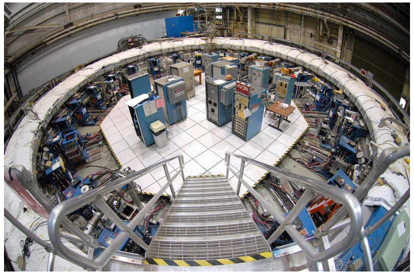

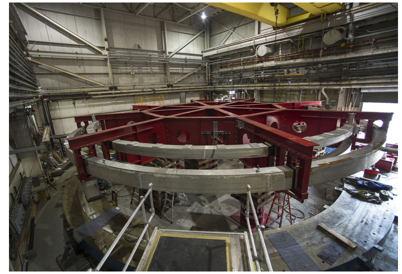

→ Fermilab
July 26, 2013

This is NOT an UFO !!!

a_μ^{Exp}(BNL): $(11\ 659\ 208.9 \pm 6.3)\ 10^{-10}$

a_μ^{Exp}(Fermilab runs 1-3 + BNL): $(11\ 659\ 205.9 \pm 2.2)\ 10^{-10}$ (0.19 ppm) → One of the most precise quantities ever measured

- Expectation for final publication: another factor 2 improvement for the statistical precision

The $(g-2)_\mu$ experiment

a_μ^{Exp}(BNL): $(11\ 659\ 208.9 \pm 6.3)\ 10^{-10}$

→ Expected uncertainty reduction by a factor 4 with the experiment at Fermilab

- improved apparatus and enhanced statistics: more intense (x20) and pure muon beam; B-field mapped every 3 days with special trolley with probes pulled through beampipe (homogeneity ~ ppm); tracking system for electron detectors etc.

- 1st publication: similar precision & good agreement with BNL (7th of April 2021) PRL 126, 141801 (2021)

a_μ^{Exp}(Fermilab): $(11\ 659\ 204.0 \pm 5.1 \pm 1.8)\ 10^{-10}$ → 6% of total data

a_μ^{Exp}(Fermilab + BNL): $(11\ 659\ 206.1 \pm 4.1)\ 10^{-10}$ (0.35 ppm)

- 2nd publication: uncertainty reduction by a factor ~2 (10th of August 2023) PRL 131, 161802 (2023) (+Run 2 & 3 data)

a_μ^{Exp}(Fermilab): $(11\ 659\ 205.5 \pm 2.4)\ 10^{-10}$ (0.20 ppm)

a_μ^{Exp}(Fermilab + BNL): $(11\ 659\ 205.9 \pm 2.2)\ 10^{-10}$ (0.19 ppm)

→ One of the most precise quantities ever measured

- Expectation for final publication: another factor 2 improvement for the statistical precision

→ Initiative for a measurement using slow muons (KEK, Japan)

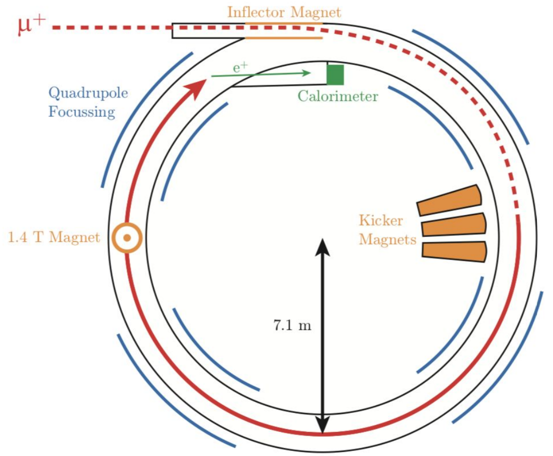

PRD 103, 072002 (2021)

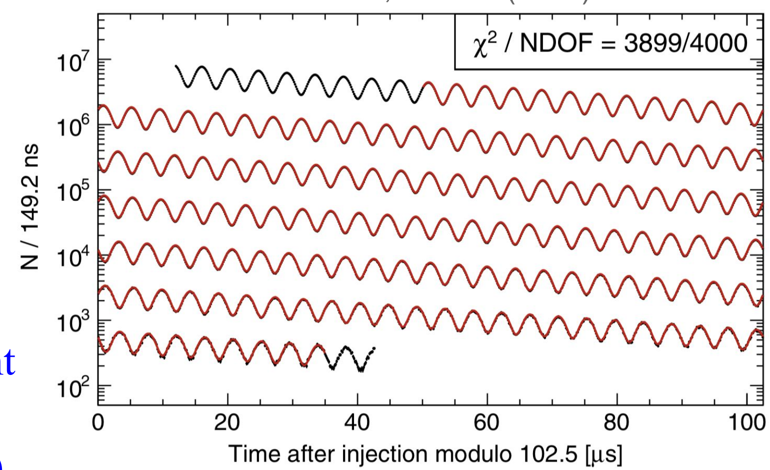

Precision of the $(g\text{-}2)_\mu$ experiments

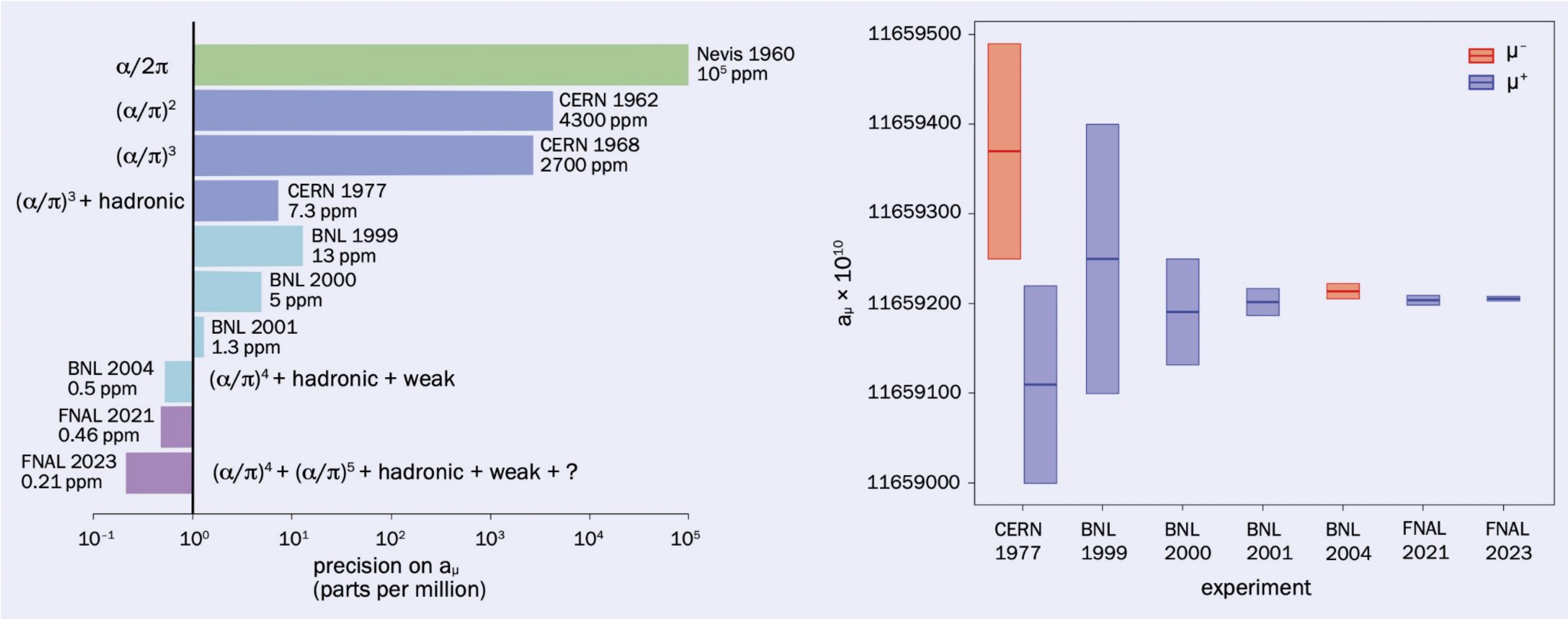

CERN Courier March-April '25

Lepton Magnetic Anomaly: from Dirac to QED

- Magnetic dipole moment of a charged lepton: $\vec{\mu} = g\frac{e}{2m}\vec{s}$

  Dirac (1928) $g_e=2$ $a_e=0$

- "anomaly" = deviation w.r.t. Dirac's prediction: $a = \frac{g-2}{2}$

anomaly discovered:

Kusch-Foley (1948) $a_e = (1.19 \pm 0.05)\ 10^{-3}$

and explained by $O(\alpha)$ QED contribution:

Schwinger (1948) $a_e = \alpha/2\pi = 1.16\ 10^{-3}$

first triumph of QED

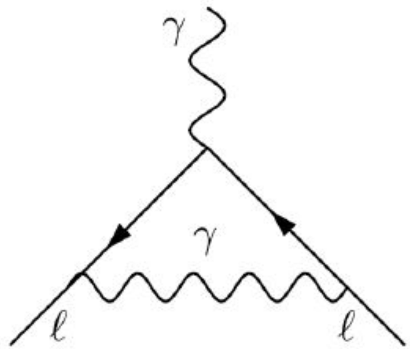

$\Rightarrow$ a_e sensitive to quantum fluctuations of fields

More Quantum Fluctuations

$$a = a^{\mathrm{QED}} + a^{\mathrm{had}} + a^{\mathrm{weak}} \quad + \text{ ? } a^{\text{new physics}} \text{ ?}$$

typical contributions:

QED up to $O(\alpha^5)$ (Kinoshita et al.)

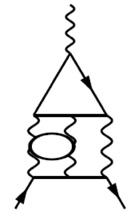

Hadrons vacuum polarization

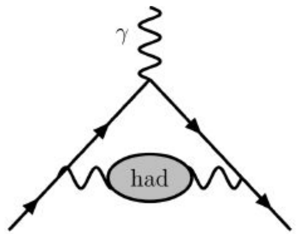

light-by-light (dispersive & lattice QCD)

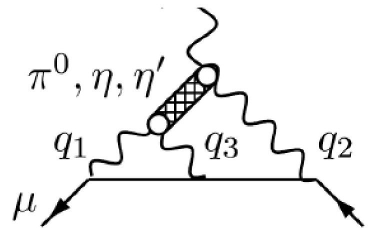

Electroweak

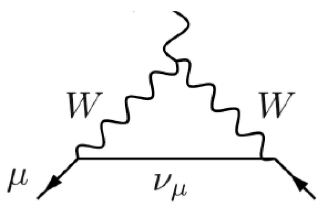

new physics at high mass scale

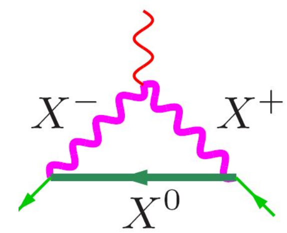

$\delta a_l \propto \dfrac{m_l^2}{M^2}$ $\Rightarrow$ a_μ much more sensitive to high scales

Theory initiative white paper executive summary & new results

Contribution	Section	Equation	Value $\times 10^{11}$	References
Experiment (E821)		Eq. (8.13)	116 592 089(63)	Ref. [1]
HVP LO (e^+e^-)	Sec. 2.3.7	Eq. (2.33)	6931(40)	Refs. [2–7]
HVP NLO (e^+e^-)	Sec. 2.3.8	Eq. (2.34)	−98.3(7)	Ref. [7]
HVP NNLO (e^+e^-)	Sec. 2.3.8	Eq. (2.35)	12.4(1)	Ref. [8]
HVP LO (lattice, $udsc$)	Sec. 3.5.1	Eq. (3.49)	7116(184)	Refs. [9–17]
HLbL (phenomenology)	Sec. 4.9.4	Eq. (4.92)	92(19)	Refs. [18–30]
HLbL NLO (phenomenology)	Sec. 4.8	Eq. (4.91)	2(1)	Ref. [31]
HLbL (lattice, uds)	Sec. 5.7	Eq. (5.49)	79(35)	Ref. [32]
HLbL (phenomenology + lattice)	Sec. 8	Eq. (8.10)	90(17)	Refs. [18–30, 32]
QED	Sec. 6.5	Eq. (6.30)	116 584 718.931(104)	Refs. [33, 34]
Electroweak	Sec. 7.4	Eq. (7.16)	153.6(1.0)	Refs. [35, 36]
HVP (e^+e^-, LO + NLO + NNLO)	Sec. 8	Eq. (8.5)	6845(40)	Refs. [2–8]
HLbL (phenomenology + lattice + NLO)	Sec. 8	Eq. (8.11)	92(18)	Refs. [18–32]
Total SM Value	Sec. 8	Eq. (8.12)	116 591 810(43)	Refs. [2–8, 18–24, 31–36]
Difference: $\Delta a_\mu := a_\mu^{\rm exp} - a_\mu^{\rm SM}$	Sec. 8	Eq. (8.14)	279(76)	

→ Dominant uncertainty: HVP LO → *Merging* of model independent results: DHMZ and KNT (and CHHKS for $\pi^+\pi^-$ & $\pi^+\pi^-\pi^0$) Central value from simple average; BABAR-KLOE tension & correlations between channels from DHMZ; Max(DHMZ & KNT uncertainties) in each channel

→ HLbL also has an important uncertainty

→ Lattice QCD (+QED) results become more and more interesting; *Precision of BMW20* (*to be cross-checked* by other lattice groups) became *similar to the one of dispersive approaches*; *Good agreement* using Euclidean time windows (related to HVP with suppression of very low and high energies) for which various groups achieved similar precision; *If BMW20 result is fully confirmed, the difference w.r.t. dispersive results* to be understood.

→ A tension between the BNL measurement and the reference SM prediction: ~ 3.7 σ (~ 4.2 σ including FNAL)

→ Tension significantly smaller when using BMW20 for the LO HVP

Status of a_μ before/with 1st Fermilab result

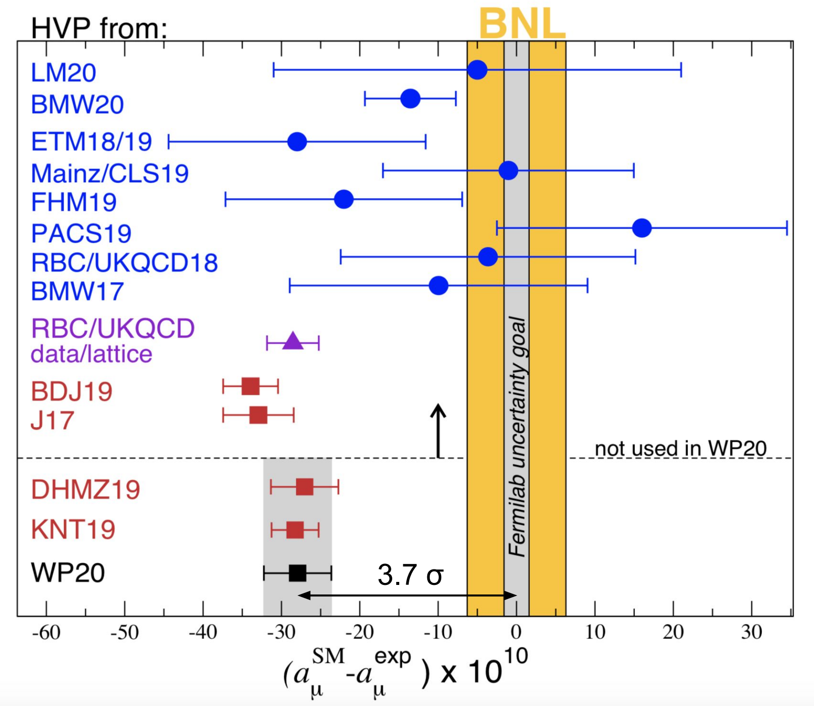

Important to account for BABAR-KLOE diff. & inter-channel correlations

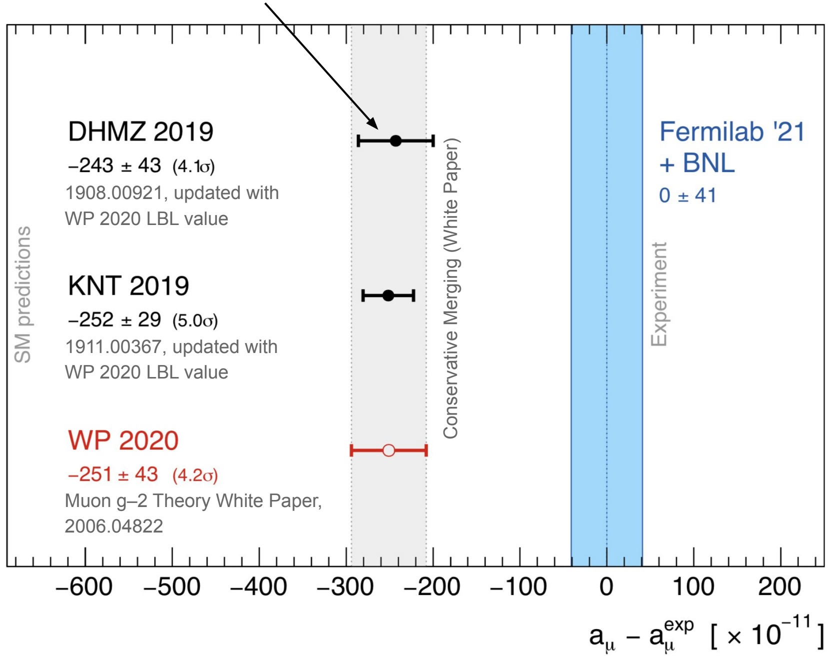

→ Caution about significance:
statistics-dominated measurement; prediction uncertainty limited by non-Gaussian systematic effects

→ Nevertheless, large discrepancy between measurement and reference SM prediction
(to be significantly improved in view of the forthcoming updates of the Fermilab measurement)

→ Tension significantly smaller when using BMW20 for the LO HVP (TBC by other lattice groups), *not* incompatible with the EW fit (*see below*)

The ISR method for the $e^+e^- \rightarrow \pi^+\pi^-$ channel at BaBar

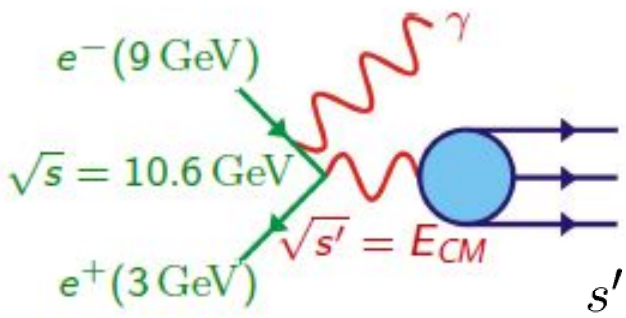

hadrons

$$x = 2E^*_\gamma/\sqrt{s}$$

$$s' = s(1-x) = M^2_{\text{hadrons}}$$

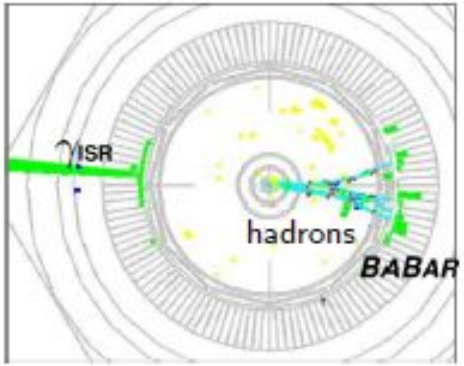

- *High energy ISR photon (E^*_γ >3 GeV) detected at large angle*, back-to-back to hadrons
  → defines √s' and provides strong background rejection
  → high acceptance, large boost to hadrons (start @ threshold; easier PID)
- Final state can be hadronic or leptonic (QED)
  → $\mu^+\mu^-\gamma_{ISR}(\gamma_{FSR})$, $\pi^+\pi^-\gamma_{ISR}(\gamma_{FSR})$ and $K^+K^-\gamma_{ISR}(\gamma_{FSR})$ measured simultaneously
  → $\mu^+\mu^-\gamma(\gamma)$ used for ISR luminosity: *add. ISR almost cancels for $\pi\pi\gamma(\gamma)/\mu\mu\gamma(\gamma)$*
- *Kinematic fit* including ISR photon (+ additional ISR/FSR)
  → removes multihadronic background
  → improves mass resolution (a few MeV)
- *Data/MC corrections* for efficiencies and acceptance
- Continuous measurement from threshold to 3-5 GeV
  → *reduced systematic uncertainties* compared to multiple data sets with different colliders and detectors

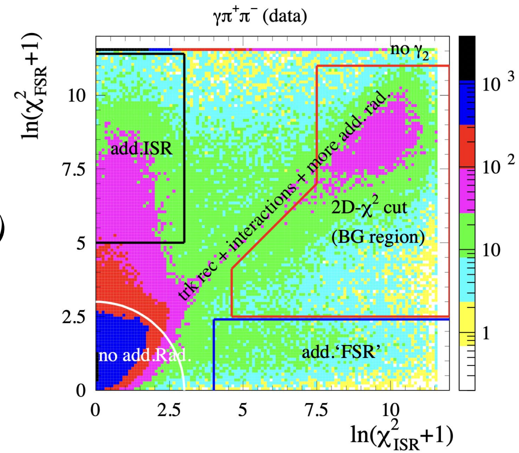

Back

Impact of higher order photon emissions studied with fast simulation

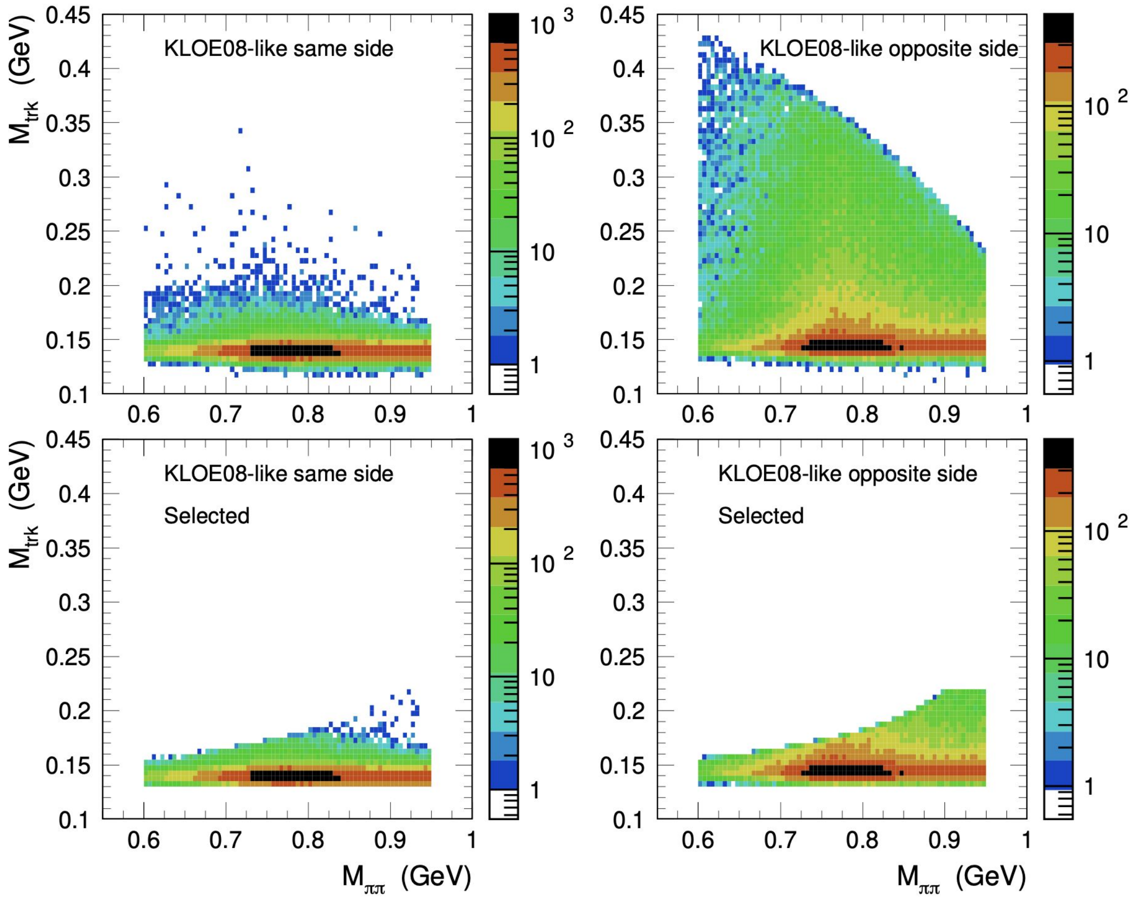

2312.02053

M_{trk} : common track mass of the two charged particles, computed under the LO assumption

→ Sensitivity of the KLOE selection to additional ‘NLO’ photon emissions (E > 5 MeV) in the same/opposite hemispheres w.r.t. the hard ISR photon

Back

Impact of higher order photon emissions studied with fast simulation

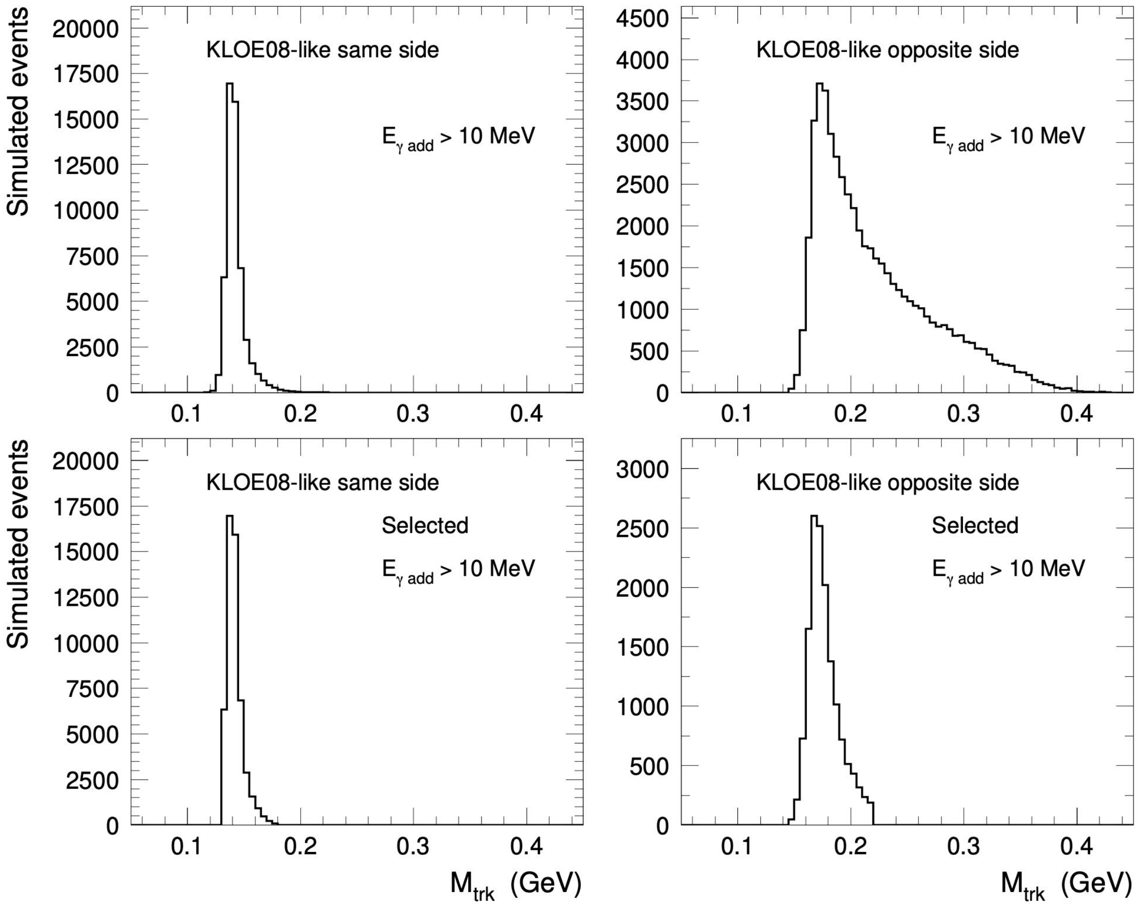

2312.02053

M_{trk} : common track mass of the two charged particles, computed under the LO assumption

→ Sensitivity of the KLOE selection to additional 'NLO' photon emissions (E > 10 MeV) in the same/opposite hemispheres w.r.t. the hard ISR photon

Impact of higher order photon emissions studied with fast simulation

2312.02053

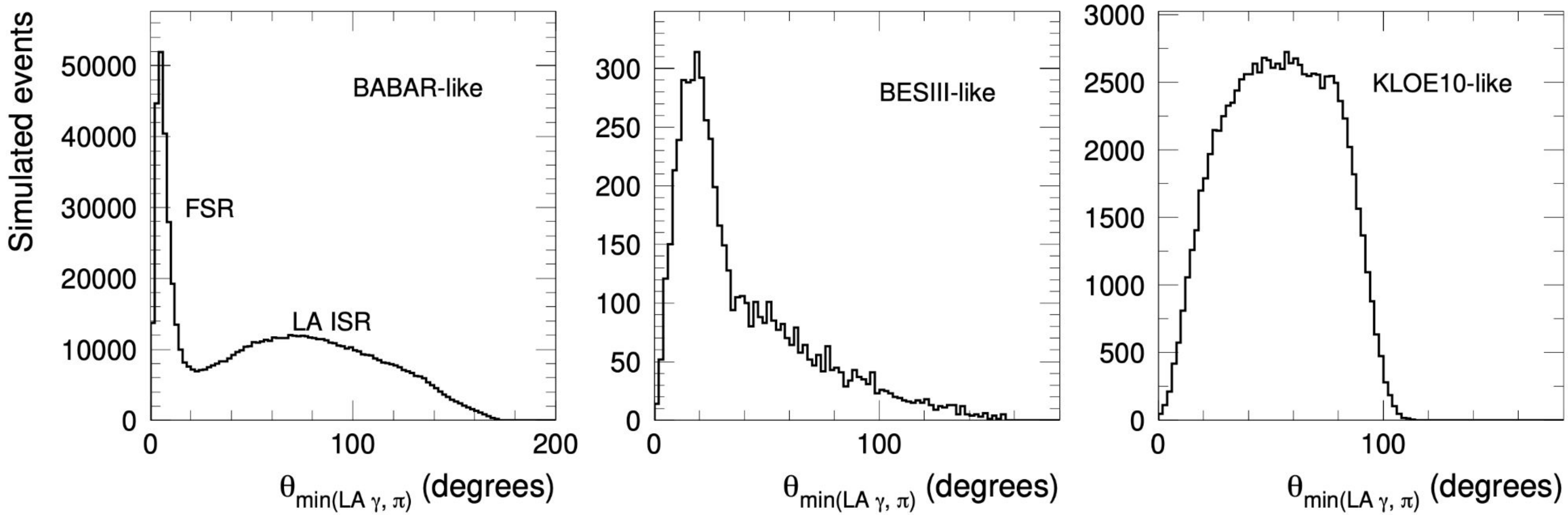

→ The angular separation between FSR and LA ISR events is pronounced at high CM energy (BABAR), still visible at intermediate CM energy (BESIII), and vanishes at low CM energy (KLOE)

The BaBar ISR program for differential hadronic Xsec measurements

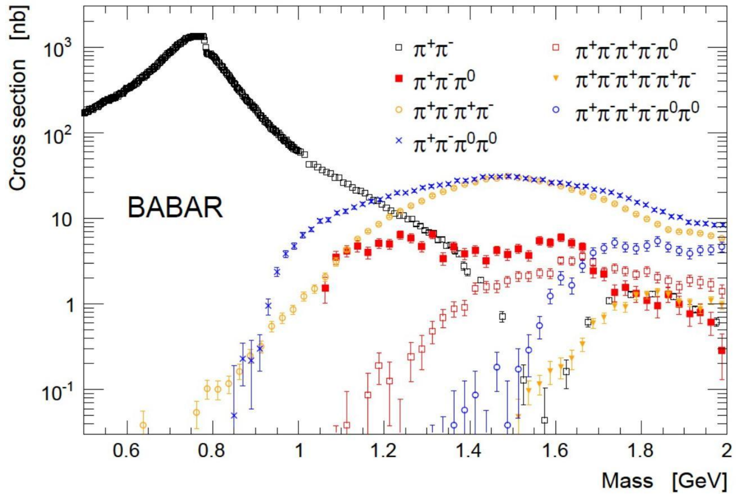

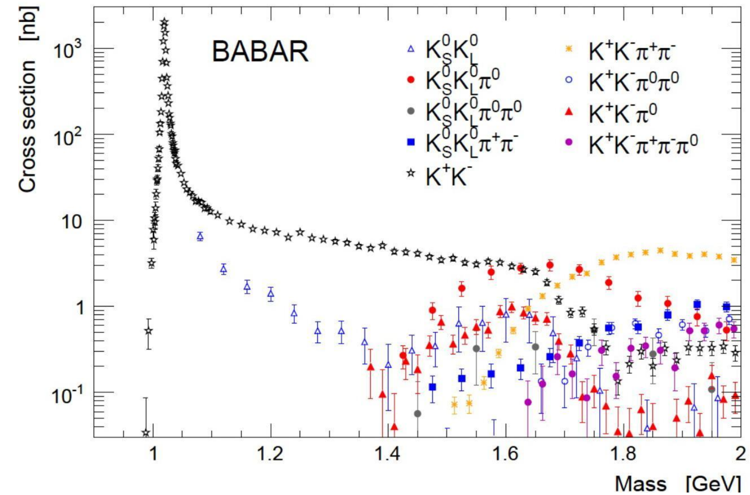

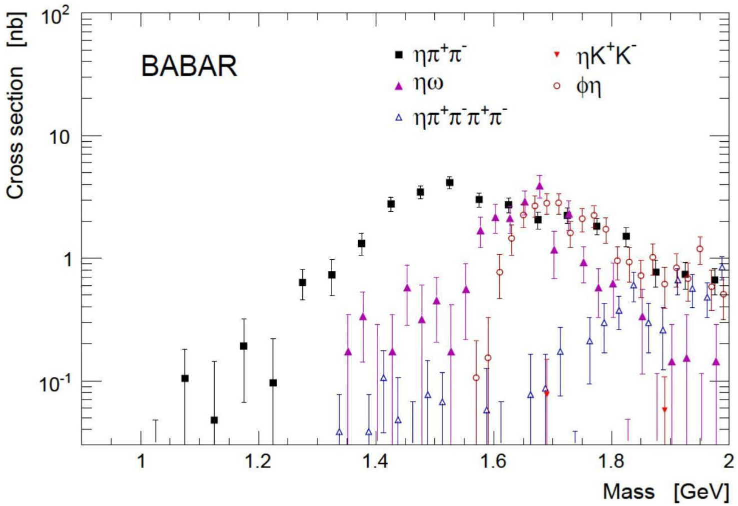

→ Large effort invested from many groups (Frascati, Mainz, Novosibirsk, Orsay - Paris, …)

→ Developed *innovative methods* allowing to obtain a large number of *robust and precise measurements*

Back

Combination for the $e^+e^- \rightarrow \pi^+\pi^-\pi^0$ channel

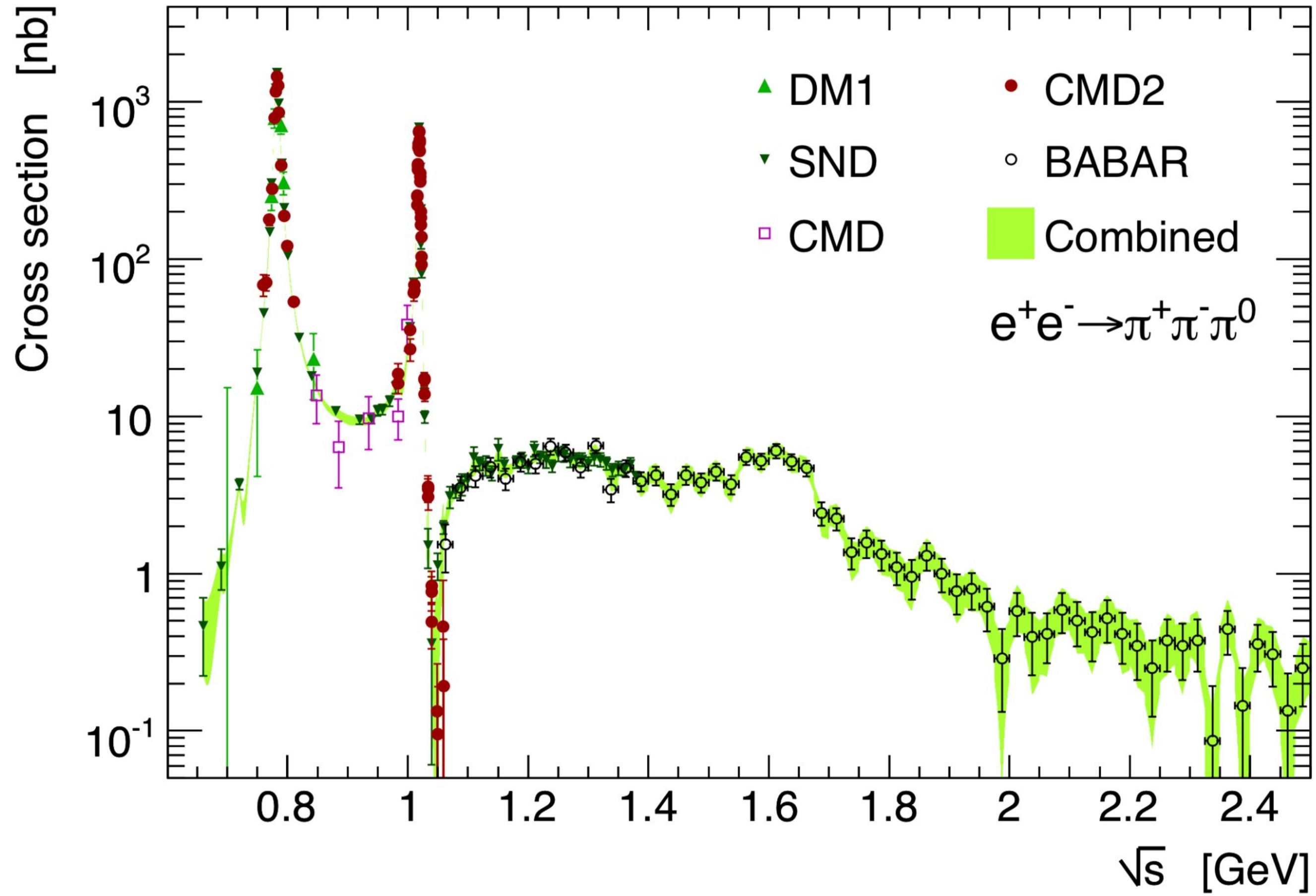

New data for the $e^+e^- \to \pi^+\pi^-\pi^0$ channel

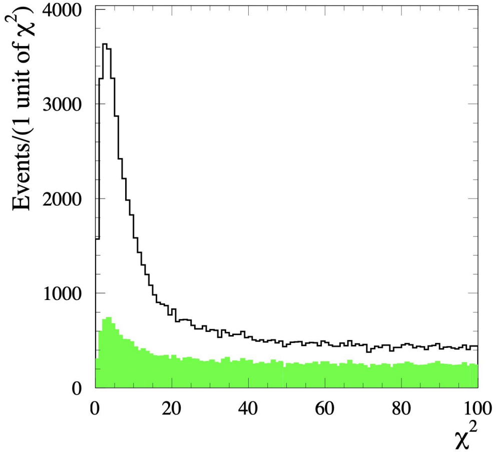

2110.00520

→ LO kinematic fits for event selection and √s' reconstruction
→ Unfolded measurement (0.62-3.5 GeV) to correct for detector resolution
→ ISR lumi' derived from total luminosity base on Bhabha (and di-muon) events

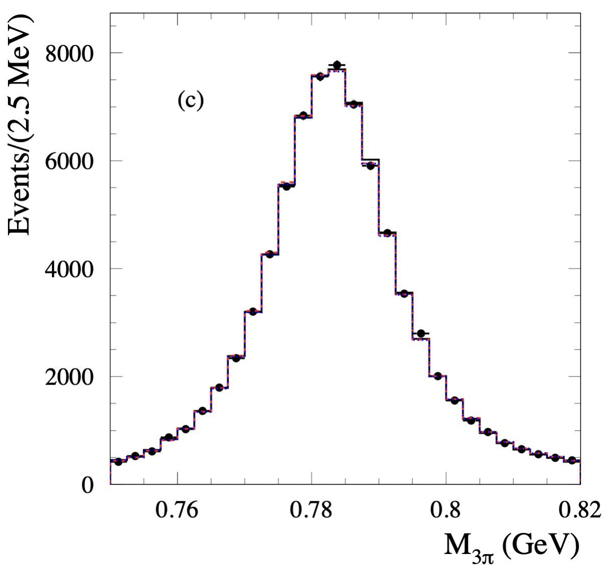

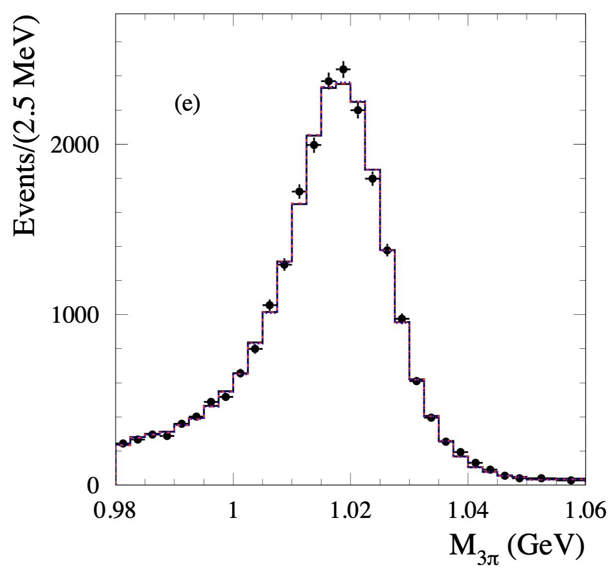

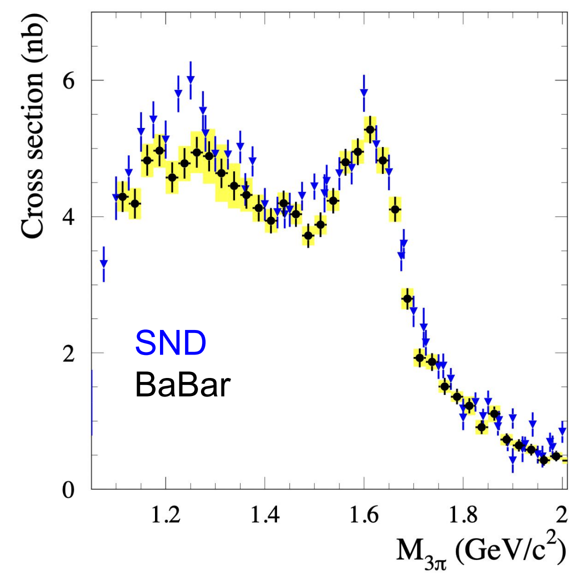

$e^+e^- \longrightarrow \pi^+\pi^-\pi^+\pi^-$, $e^+e^- \longrightarrow \pi^+\pi^-\pi^0\pi^0$

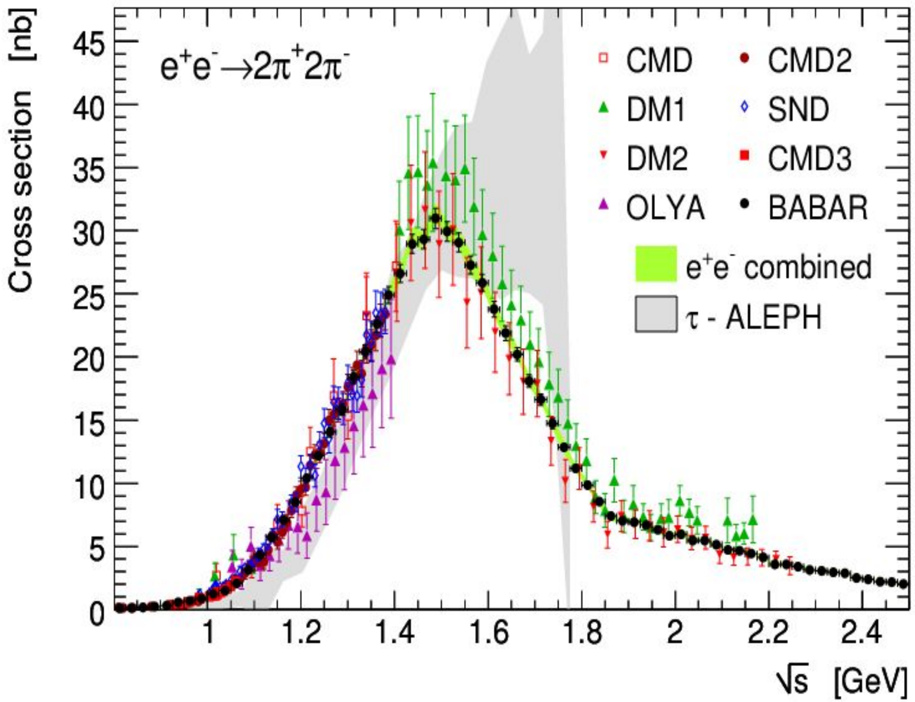

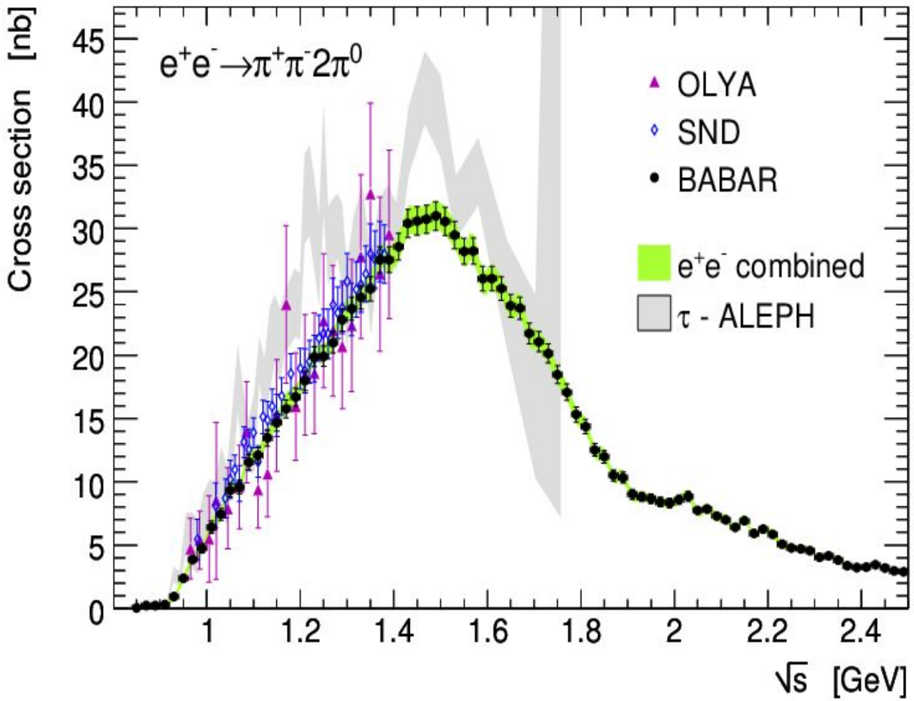

→ Essentially normalization differences w.r.t. τ data: *cross-checks very desirable*

Combination for the $e^+e^- \to K^+K^-$ channel

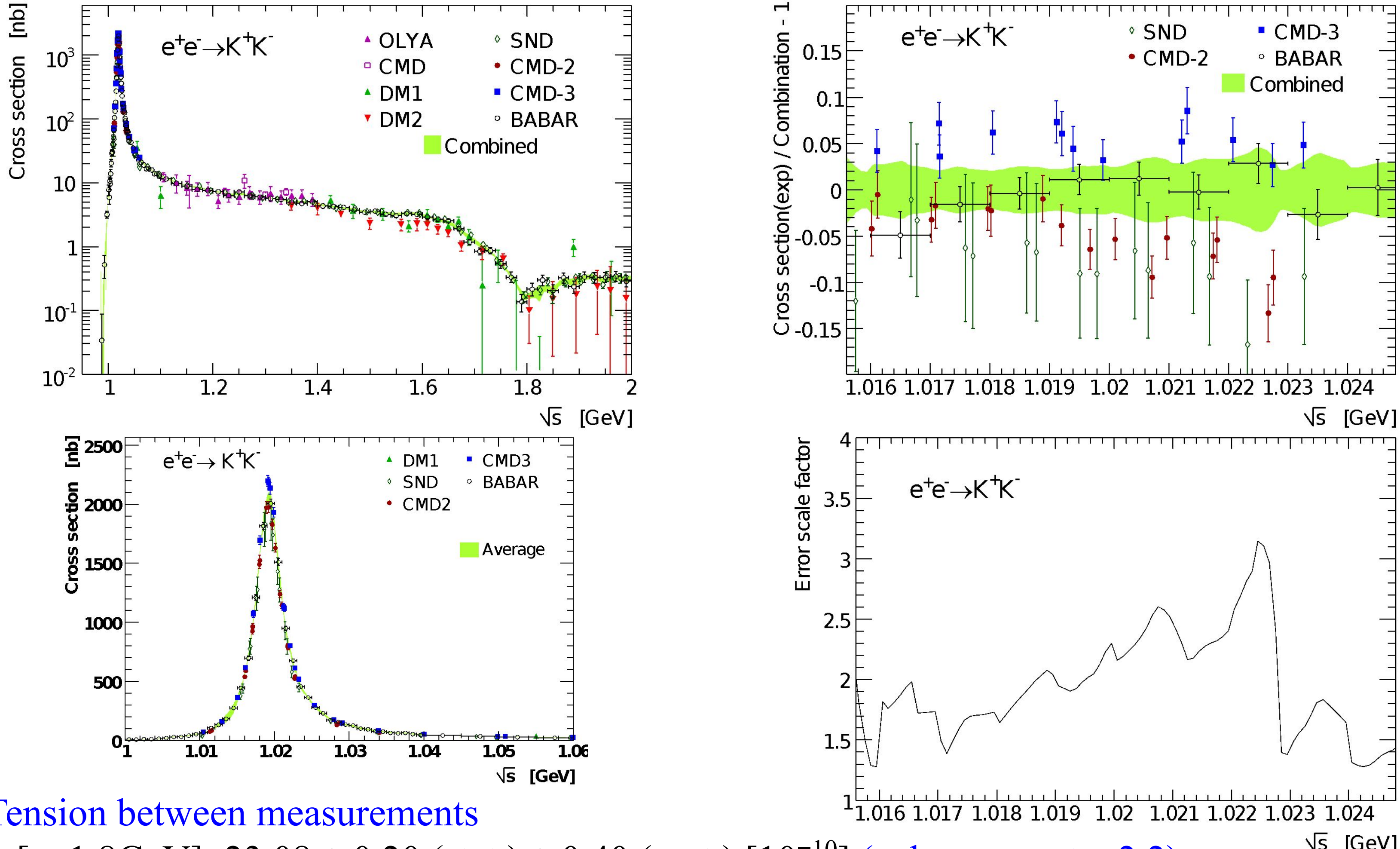

→ Tension between measurements

→ $a_\mu[\to 1.8\text{GeV}]$: 23.08 ± 0.20 (stat.) ± 0.40 (syst.) $[10^{-10}]$ (enhancement x 2.2)

Combination for the $e^+e^- \rightarrow KK\pi$ and $KK2\pi$ channels

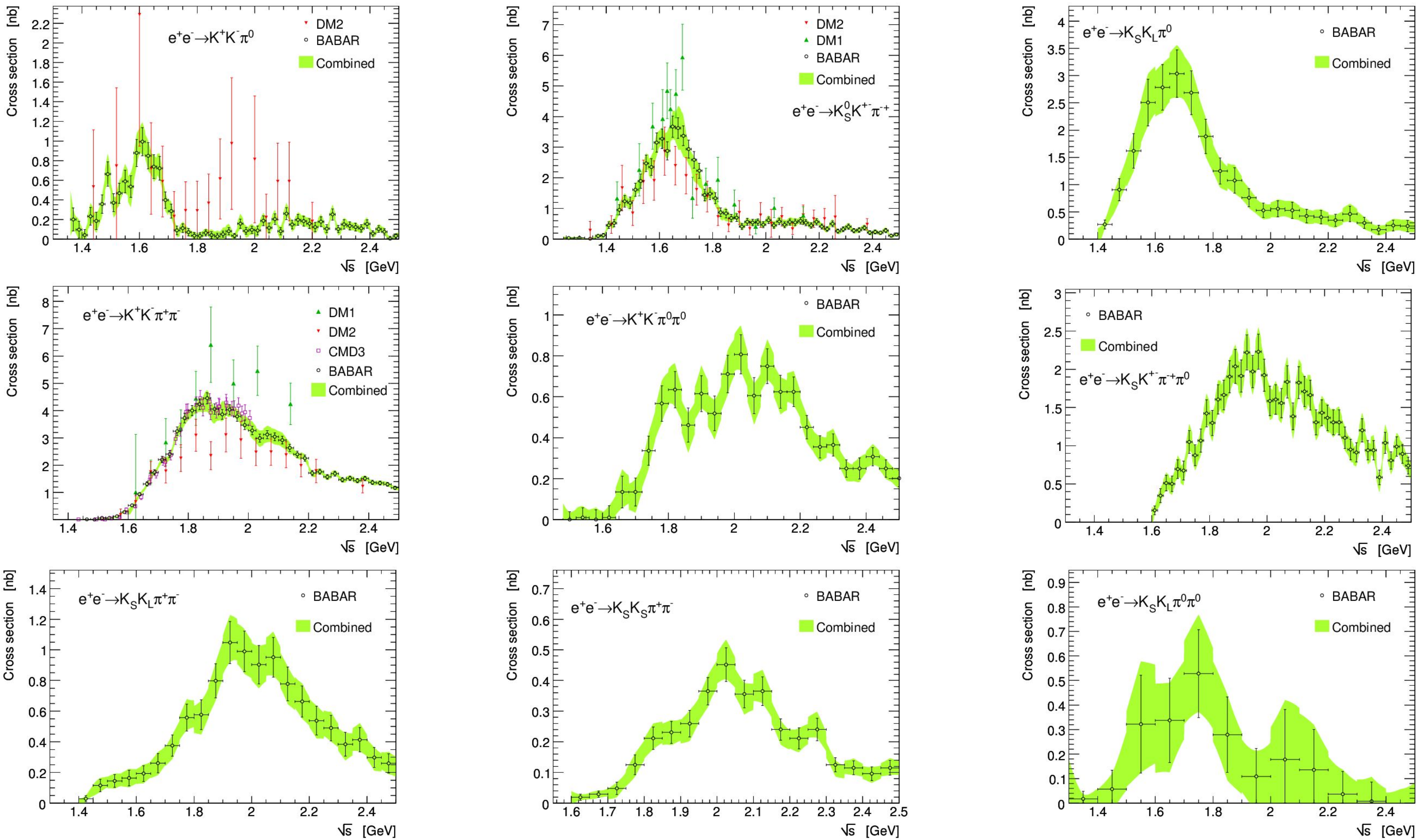

Examples of ~new high-multiplicity measurements

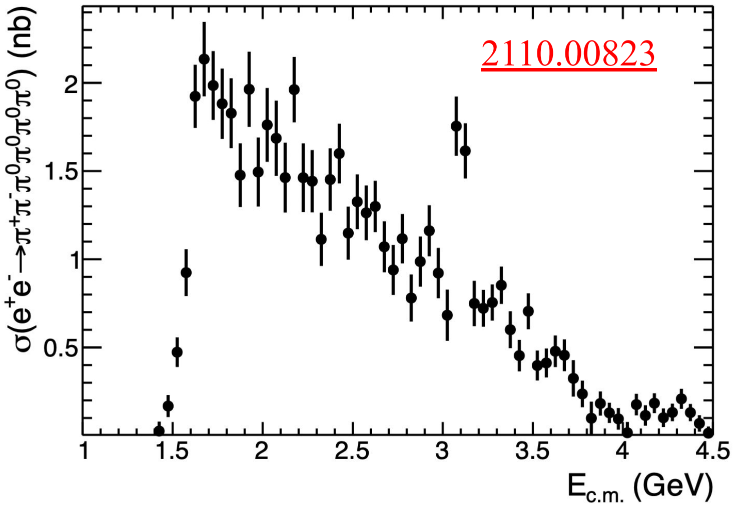

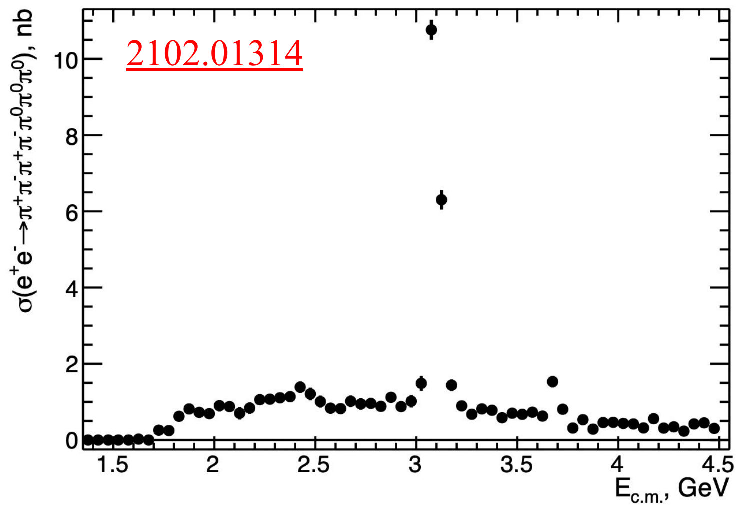

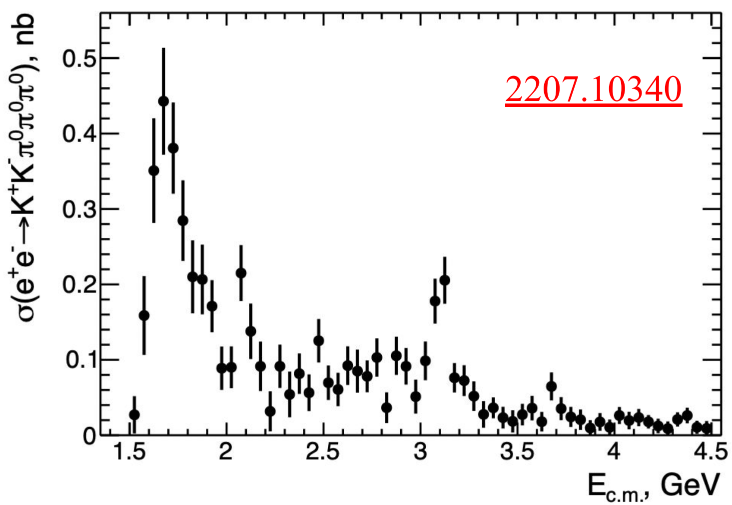

Contributions from the 1.8 – 3.7 GeV region

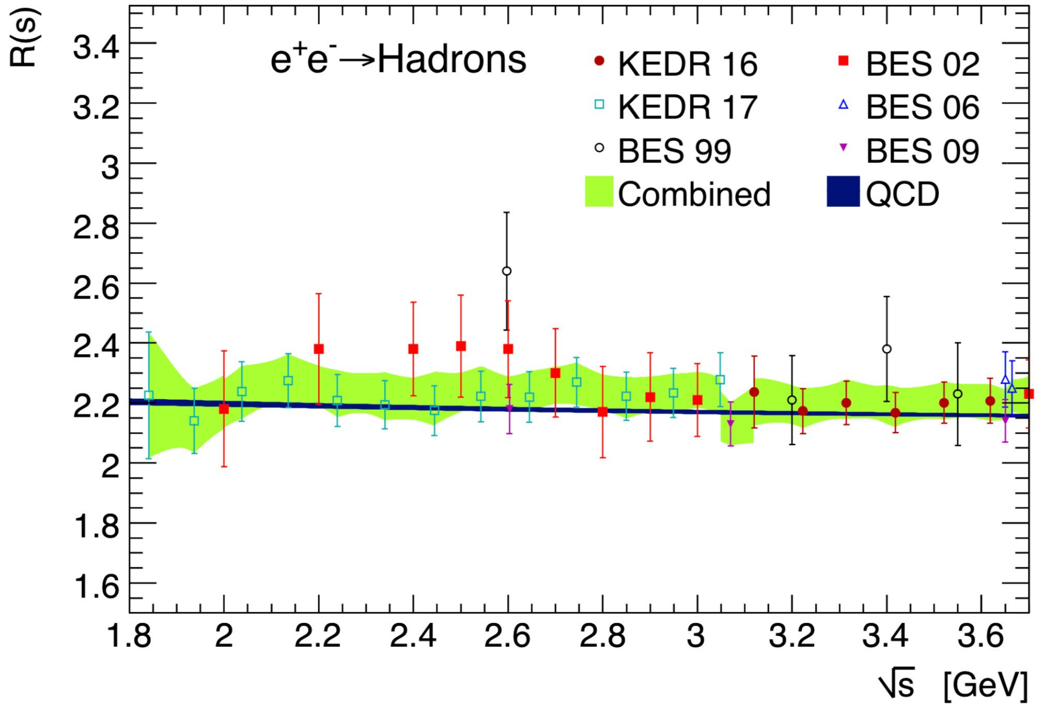

→ Contribution evaluated from pQCD (4 loops) + $O(\alpha_s^2)$ quark mass corrections

→ Uncertainties: α_s, truncation of perturbative series, CIPT/FOPT, m_q

→ 1.8-2.0 GeV: 7.65±0.31(data excl.); 8.30±0.09(QCD); added syst. 0.65 [10^{-10}]

→ 2.0-3.7 GeV: 25.82±0.61(data); 25.15 ± 0.19(QCD); agreement within 1σ

→ BES III results to be included: ~tension with pQCD and with KEDR 16 (*next slide*)

2112.11728

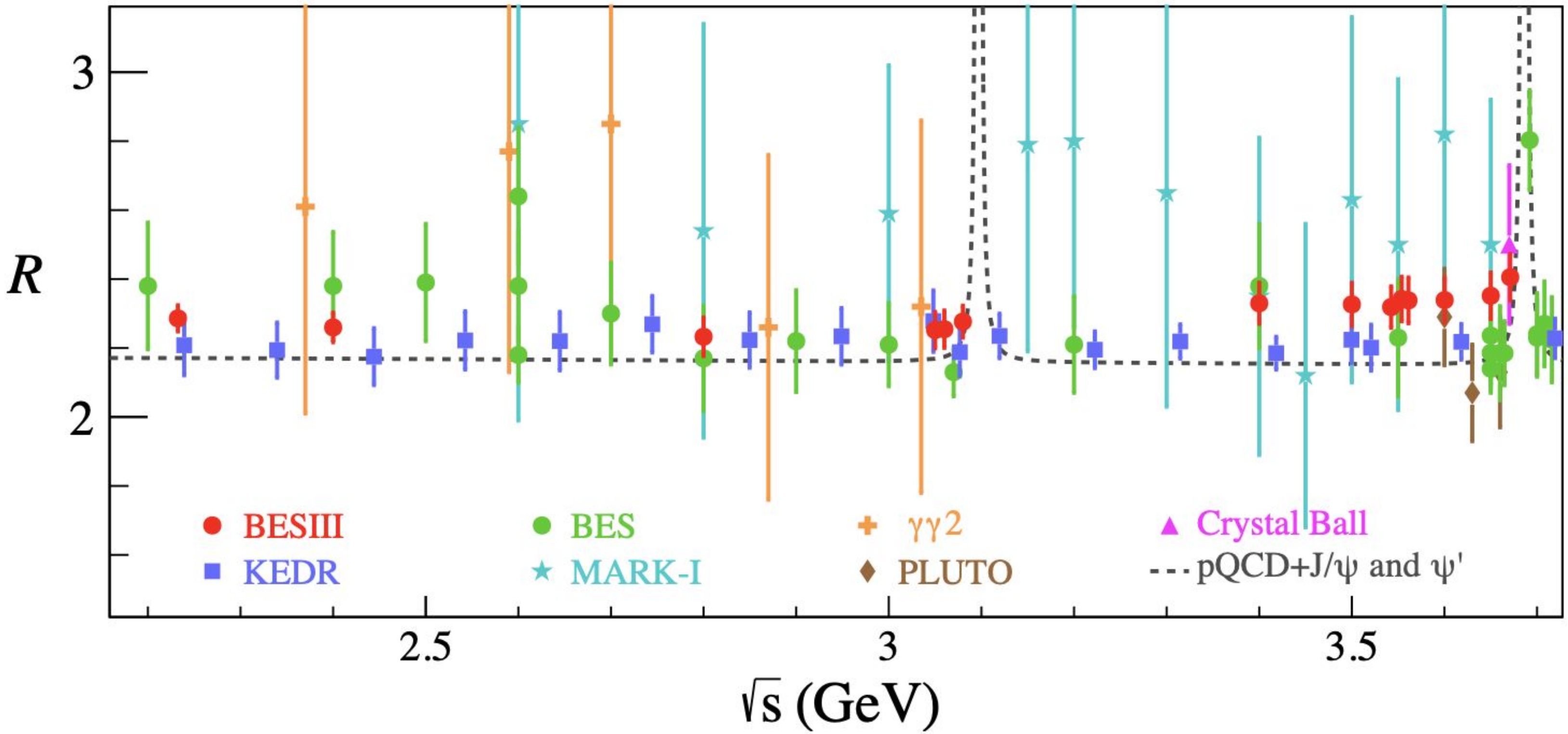

→ BES III results to be included: ~tension with pQCD and with KEDR 16

→ Another example of "*uncertainties on the uncertainties*" / *systematic effects to be understood* at the level of precision that is claimed

Contributions from the charm resonance region

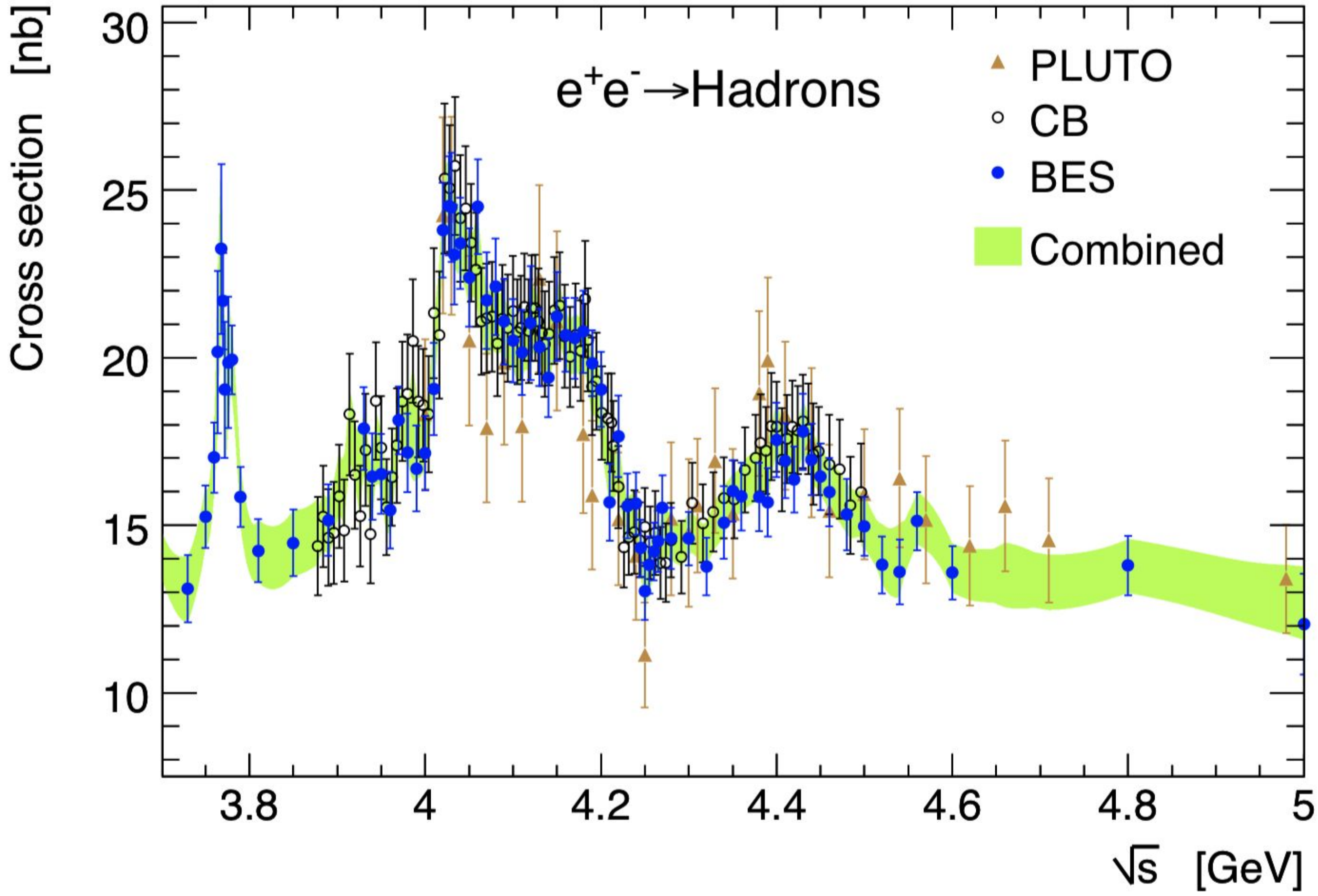

Comparison of SND measurement with BABAR and KLOE

2004.00263

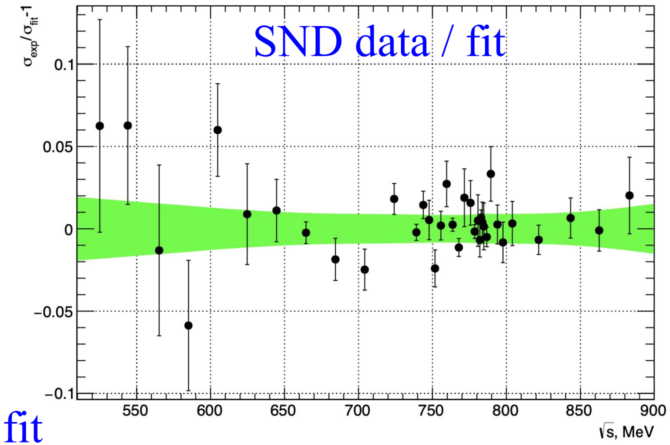

BABAR / SND fit

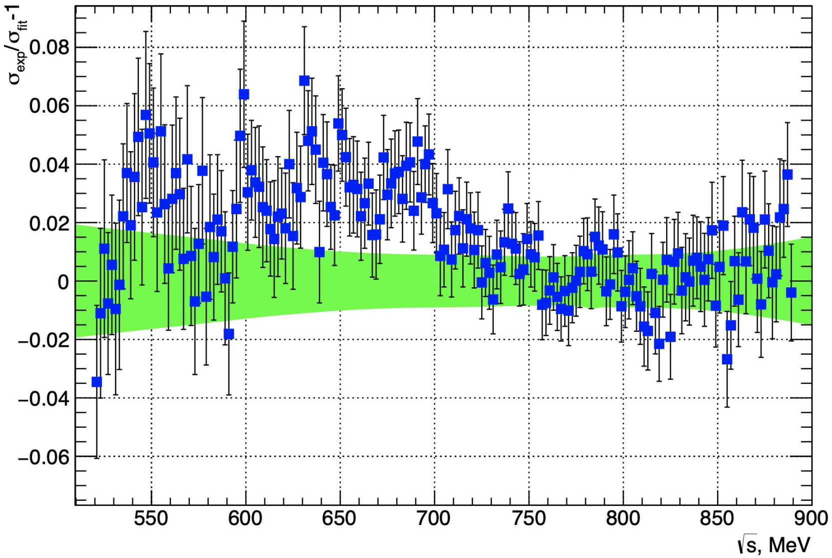

KLOE / SND fit

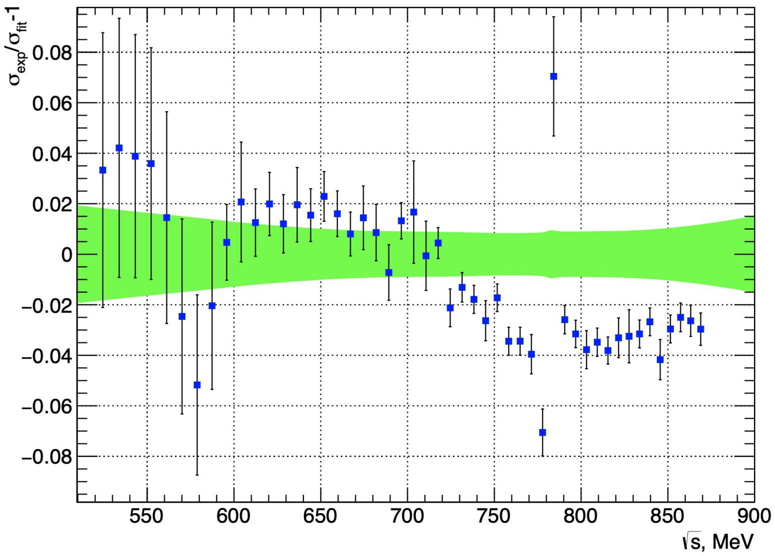

Combine cross section data: goal and requirements

→ Goal: combine experimental spectra with arbitrary point spacing / binning

→ Requirements:

- Properly propagate uncertainties and correlations

  - *Between measurements (data points/bins) of a given experiment*
    (covariance matrices and/or detailed split of uncertainties in sub-components)
  - *Between experiments* (common systematic uncertainties, e.g. VP)
    based on detailed information provided in publications
  - *Between different channels* – motivated by understanding of the meaning of systematic uncertainties and identifying the common ones

  BABAR luminosity (ISR or BhaBha), efficiencies (photon, Ks, Kl, modeling);
  BABAR radiative corrections; $4\pi 2\pi^0 - \eta\omega$
  CMD2 $\eta\gamma - \pi^0\gamma$; CMD2/3 luminosity; SND luminosity;
  FSR; hadronic VP (old experiments)
  (1st motivation for using DHMZ uncertainties as "baseline" in the g-2 TI White Paper)

- Minimize biases

- Optimize g-2 integral uncertainty
  (*without overestimating the precision with which the uncertainties of the measurements are known*)

Back

Combination procedure implemented in HVPTools software

For each final bin:

→ Compute an average value for each measurement and its uncertainty

→ Compute correlation matrix between experiments

→ Minimize χ^2 and get average coefficients (weights)

→ Compute average between experiments and its uncertainty

Evaluation of integrals and propagation of uncertainties:

→ Integral(s) evaluated for nominal result and for each set of toy pseudo-experiments; uncertainty of integrals from RMS of results for all toys

→ The pseudo-experiments also used to derive (statistical & systematic) covariance matrices of combined cross sections → Integral evaluation

→ Uncertainties also propagated through $\pm 1\sigma$ shifts of each uncertainty:
- allows to account for correlations between different channels (for integrals and spectra)

→ *Checked consistency between the different approaches*

For each final bin:
→ Minimize χ^2 and get average coefficients

Note: average weights must account for bin sizes / point spacing of measurements
(do not over-estimate the weight of experiments with large bins)
→ Weights in fine bins evaluated using a common (large) binning for measurements + interpolation
→ Compare the precisions on the same footing

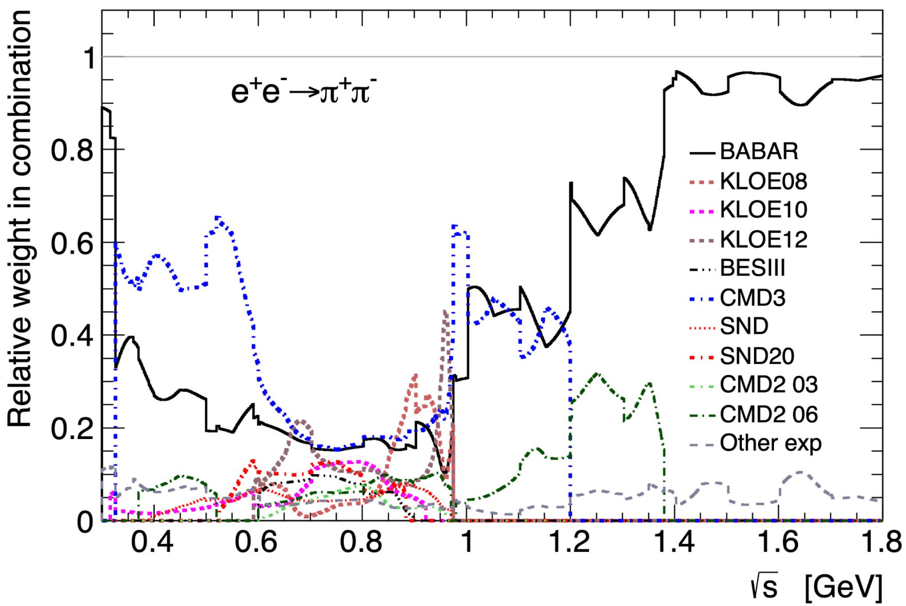

→ Bins used by KLOE larger than the ones by BABAR in ρ-ω interference region (factor ~3)

→ Average dominated by BaBar, CMD3, KLOE, SND20
BaBar covering full range

Back

Combination procedure: compatibility between measurements

For each final bin:

→ χ^2 /ndof: test locally the level of agreement between input measurements, *taking into account correlations*

→ Scale uncertainties in bins with χ^2 /ndof > 1 (PDG): *locally* conservative; Adopted by KNT since ’17

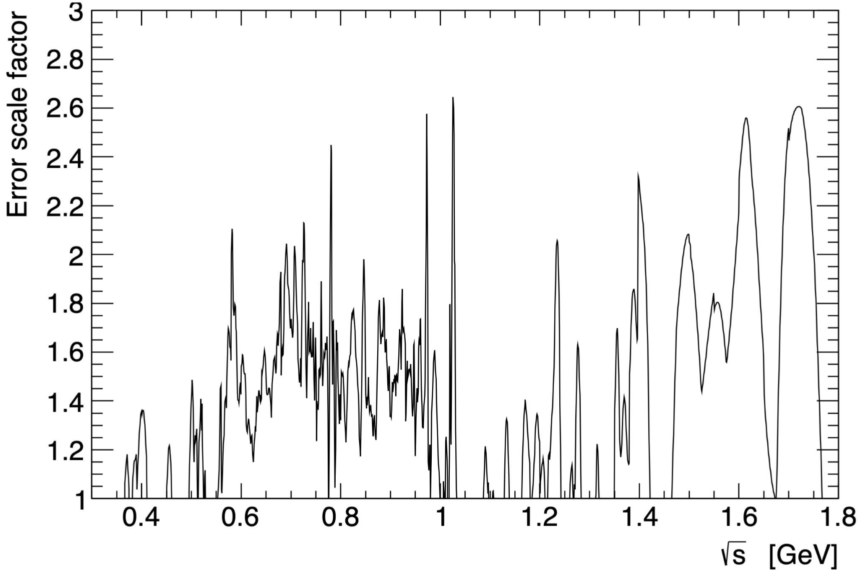

→ Tension between measurements, especially between KLOE & CMD3, which provide the smallest / largest cross-sections in the ρ region:

Indication of underestimated uncertainties

Motivates conservative uncertainty treatment

in combination fit (evaluation of weights / fits based on analyticity & unitarity to constrain uncertainties at low √s - *below*)

→ Observed (systematic) tension between measurements, beyond the local χ^2 /ndof rescaling

→ (*Since 2019*) Included extra (dominant) uncertainty: 1/2 difference between integrals w/o either BABAR or KLOE *(2^{nd} motivation for using DHMZ uncertainties as “baseline” in the TI WP)*

Extra uncertainty started to be adopted in other studies (2205.12963)

However, *tensions are larger now and we need to understand their source!*

Two panel TI discussions with 49 questions addressed to CMD3 did not allow to identify any major problem. CMD2 / CMD3 tension still open question!

Combination for the $e^+e^- \rightarrow \pi^+\pi^-$ channel (DHMZ '19)

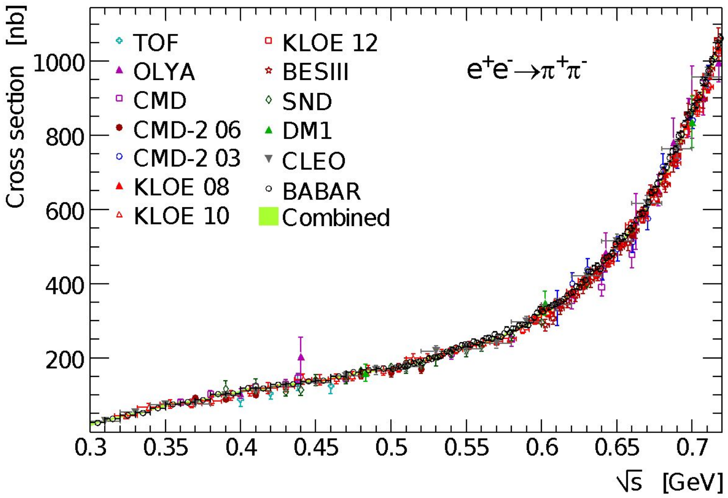

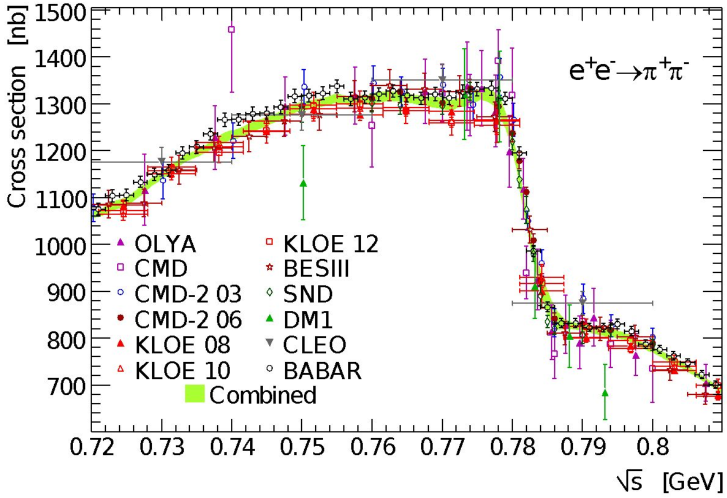

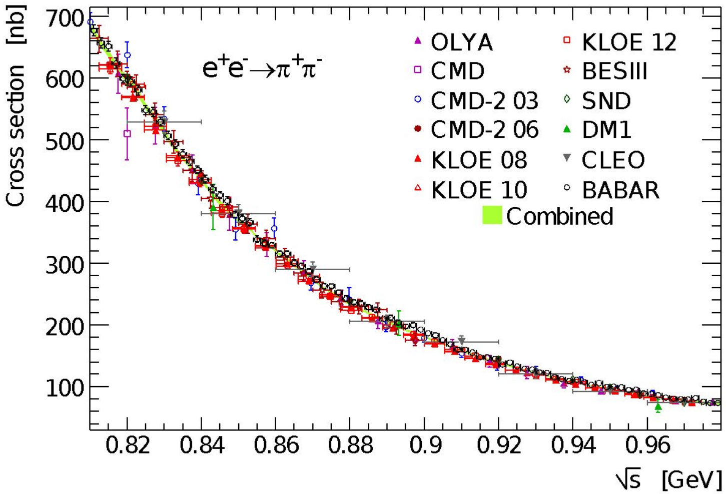

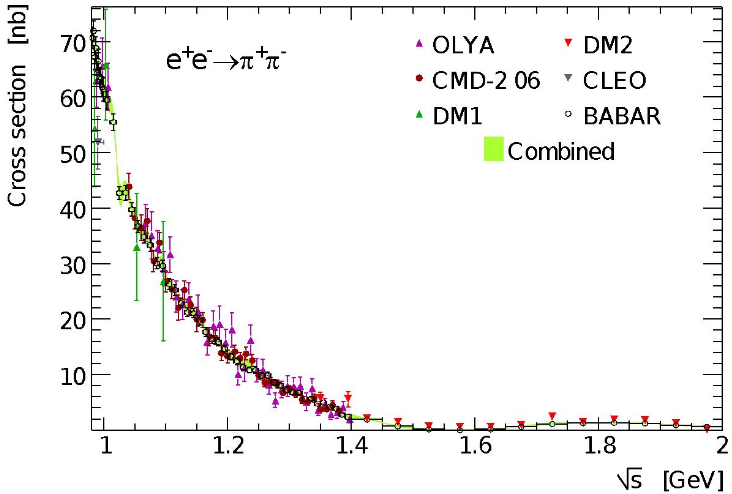

More on the combination for the $e^+e^- \rightarrow \pi^+\pi^-$ channel (DHMZ '19)

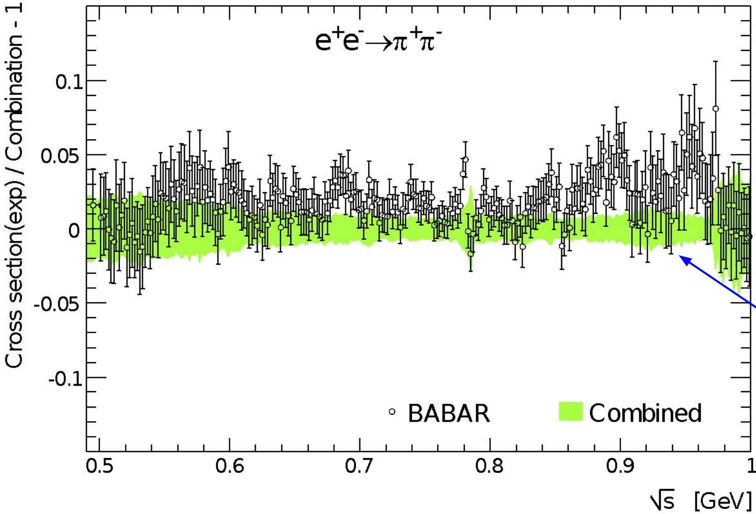

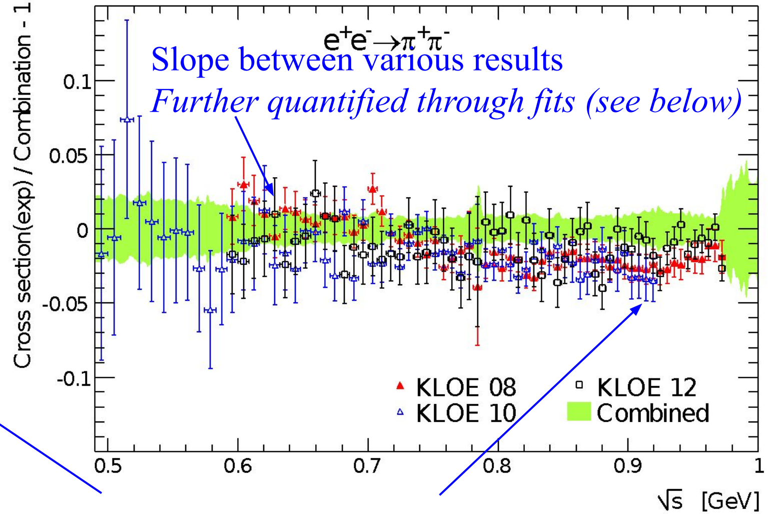

Slope between various results

Further quantified through fits (see below)

Local tension & systematic trends

Indication of "uncertainties on uncertainties" (i.e. unaccounted biases)

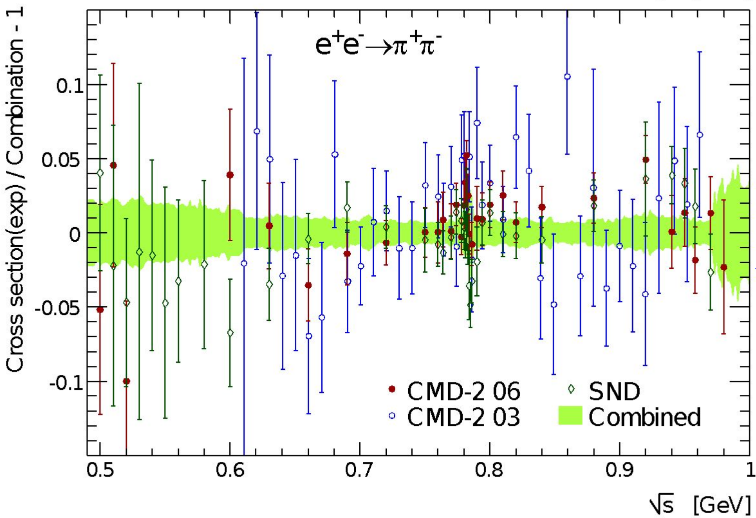

Other experiments not yet precise enough to discriminate

(see however update from SND: ~significant tension with KLOE above 720 MeV)

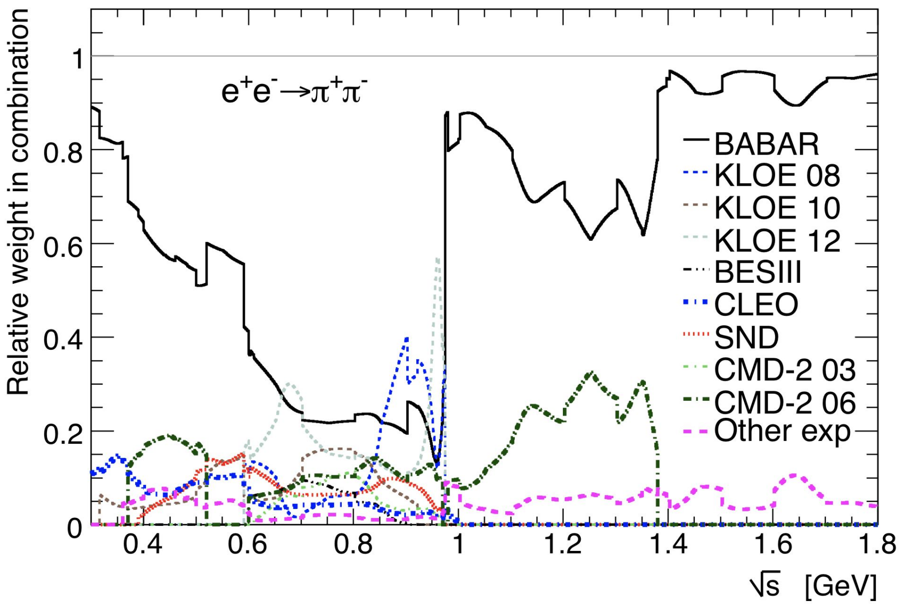
Relative weight in combination
e+e-→π+π-
BABAR
KLOE 08
KLOE 10
KLOE 12
BESIII
CLEO
SND
CMD-2 03
CMD-2 06
Other exp
0
0.2
0.4
0.6
0.8
1
0.4
0.6
0.8
1
1.2
1.4
1.6
1.8
√s [GeV]

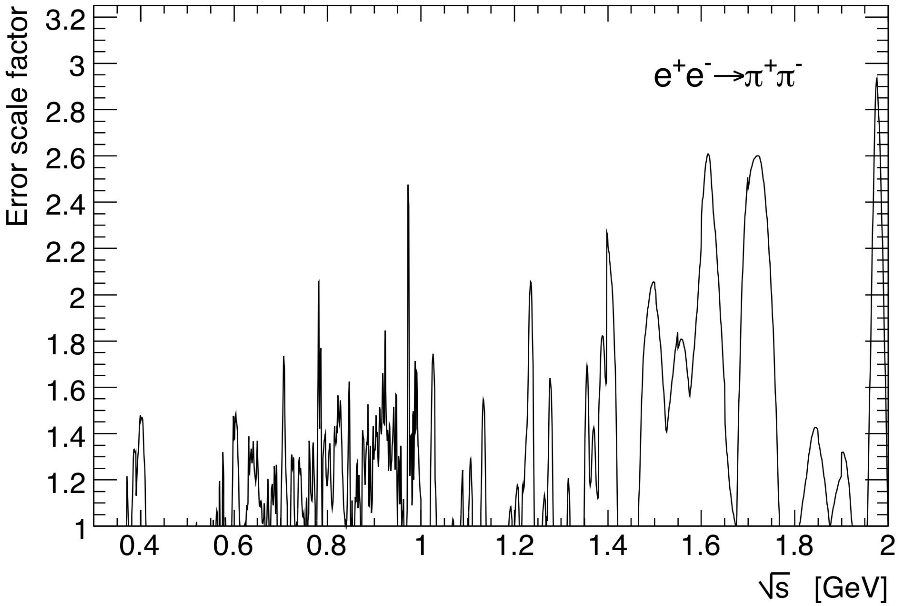
Error scale factor
e+e-→π+π-
1
1.2
1.4
1.6
1.8
2
2.2
2.4
2.6
2.8
3
3.2
0.4
0.6
0.8
1
1.2
1.4
1.6
1.8
2
√s [GeV]

Improving a_μ through fits for the $e^+e^- \to \pi^+\pi^-$ channel (*Since 2019*)

→ Fit bare form-factor using 6 param. model based on *analyticity* and *unitarity*

$$|F_\pi^0|^2 = |R(s) \times J(s)|^2$$

$$R(s) = 1 + \alpha_V s + \frac{\kappa s}{m_\omega^2 - s - i m_\omega \Gamma_\omega}$$

(1611.09359, C. Hanhart et al.)

$$J(s) = e^{1-\frac{\delta_1(s_0)}{\pi}} \left(1 - \frac{s}{s_0}\right)^{\left[1-\frac{\delta_1(s_0)}{\pi}\right]\frac{s_0}{s}} \left(1 - \frac{s}{s_0}\right)^{-1} e^{\frac{s}{\pi}\int_{4m_\pi^2}^{s_0} dt \frac{\delta_1(t)}{t(t-s)}}$$

Omnès integral

(hep-ph/0402285, F.J. Ynduraín et al.)

$$\cot\delta_1(s) = \frac{\sqrt{s}}{2k^3}\left(m_\rho^2 - s\right)\left[\frac{2m_\pi^3}{m_\rho^2\sqrt{s}} + B_0 + B_1\omega(s)\right]$$

(1102.2183, F.J. Ynduraín et al.)

$$k = \frac{\sqrt{s - 4m_\pi^2}}{2}$$

$$\omega(s) = \frac{\sqrt{s} - \sqrt{s_0 - s}}{\sqrt{s} + \sqrt{s_0 - s}} \qquad \sqrt{s_0} = 1.05 \text{ GeV}$$

→ Conservative χ^2 (diagonal matrix) & local rescaling of input uncertainties

→ Full propagation of uncertainties & correlations using pseudo-experiments

DHMZ - 1908.00921

Back

Fit parameters, uncertainties and correlations $e^+e^- \to \pi^+\pi^-$

	α_V	$\kappa[10^{-4}]$	B_0	B_1	m_ρ [MeV]	m_ω [MeV]
α_V	0.133 ± 0.020	0.52	−0.45	−0.97	0.90	−0.25
$\kappa[10^{-4}]$		21.6 ± 0.5	−0.33	−0.57	0.64	−0.08
B_0			1.040 ± 0.003	0.40	−0.40	0.29
B_1				-0.13 ± 0.11	−0.96	0.20
m_ρ [MeV]					774.5 ± 0.8	−0.17
m_ω [MeV]						782.0 ± 0.1

→ κ corresponds to a Br ($\omega \to \pi^+\pi^-$) of $(2.09 \pm 0.09) \cdot 10^{-2}$, in agreement with the result extracted from the fit of arXiv:1810.00007, $(1.95 \pm 0.08) \cdot 10^{-2}$. Both values disagree with the PDG average $(1.51 \pm 0.12) \cdot 10^{-2}$, dominated by the result of arXiv:1611.09359 which uses fits to essentially the same data.

→ The fitted ω mass is found to be lower than the PDG average obtained from 3π decays by $(0.65 \pm 0.12 \pm 0.12_{PDG})$ MeV, in agreement with previous fits of the $\rho - \omega$ interference in the 2π spectrum (see e.g. arXiv:1205.2228 and arXiv:1810.00007).

Fit performed up to 1 GeV: comparison with data

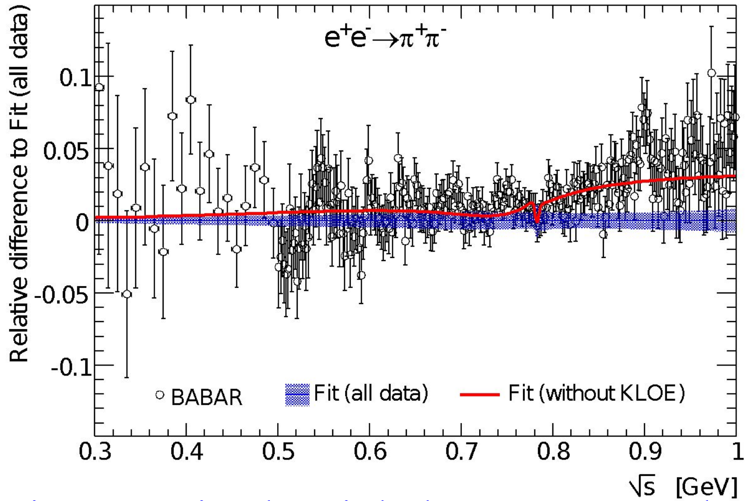

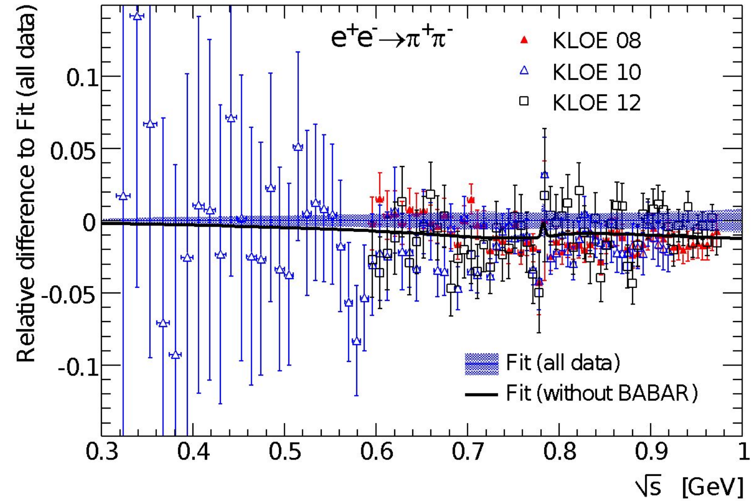

→ Fit constrained mainly by BABAR and KLOE measurements

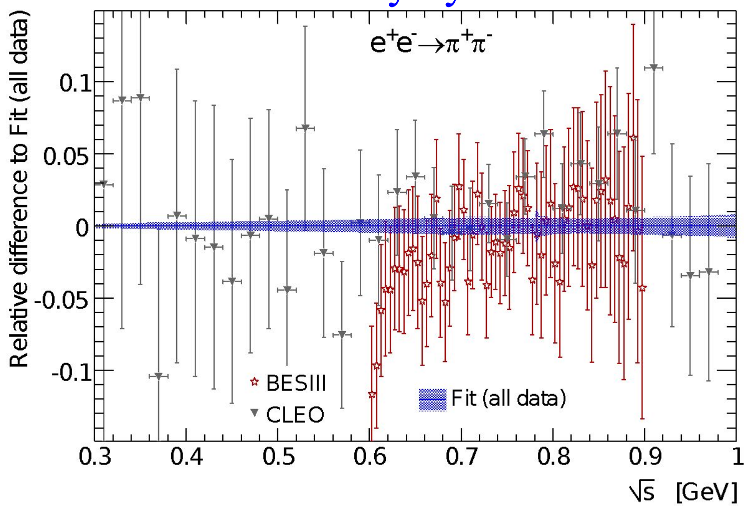

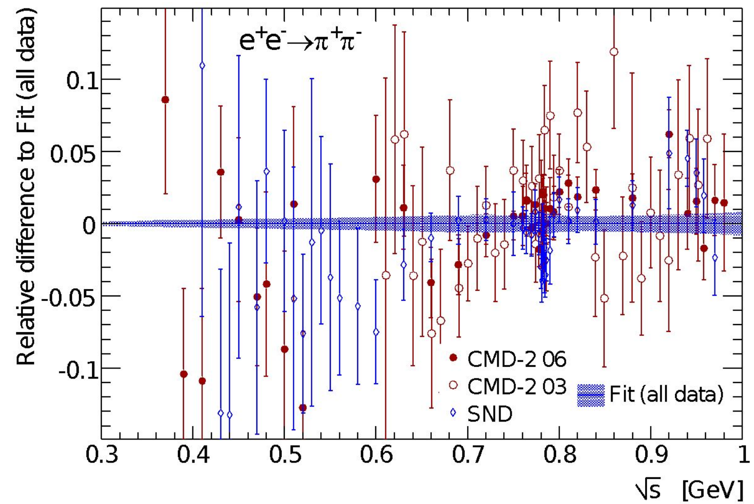

Fit performed up to 1 GeV, Result used up to 0.6 GeV

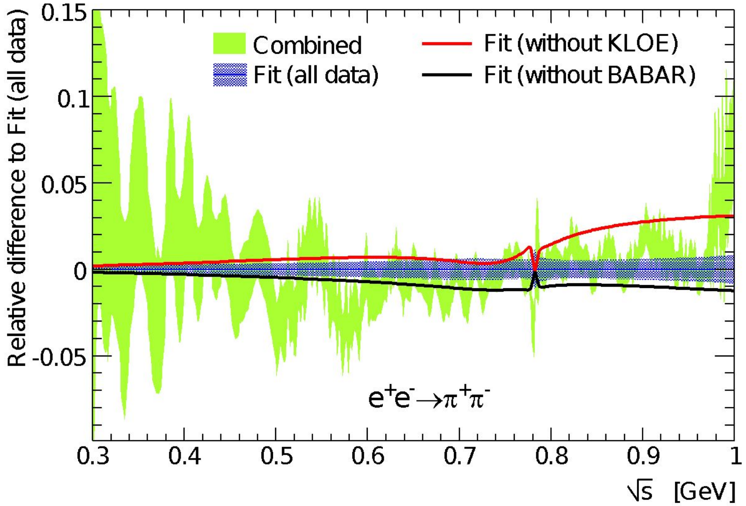

→ Use fit only below 0.6 GeV for a_μ integral:

- where data is less precise and scarce
- less impacted by potential uncertainties of inelastic effects

$\sqrt{s}$ range [GeV]	a_μ^{had} [10^{-10}] Fit	a_μ^{had} [10^{-10}] Data Integration
0.3 - 0.6	$109.80 \pm 0.37_{exp} \pm 0.36_{para*}$	$109.6 \pm 1.0_{exp}$

→ The difference 0.2 ± 0.9 (72% correlation accounted for)

→ The fit improves the precision by a factor ~2

(*) Parameter uncertainty corresponds to variations with/without the B_1 term in the phase shift formula and $\sqrt{s_0}$ varied from 1.05 GeV to 1.3 GeV (absolute values summed linearly), *checked to be statistically significant*

Combined results: Fit [<0.6GeV] + Data[0.6-1.8GeV]

→ Full uncertainty propagation using the same pseudo-experiments as for the spline-based combination: 62% correlation among the two contributions

$\sqrt{s}$ range [GeV]	a_μ^{had} $[10^{-10}]$ All data	a_μ^{had} $[10^{-10}]$ All but BABAR	a_μ^{had} $[10^{-10}]$ All but KLOE
threshold - 1.8	$506.9 \pm 1.9_{total}$	$505.0 \pm 2.1_{total}$	$510.6 \pm 2.2_{total}$

→ The difference "All but BABAR" and "All but KLOE" = 5.6, to be compared with 1.9 uncertainty with "All data"

- The local error inflation is not sufficient to amplify the uncertainty
- Global tension (normalisation/shape) not previously accounted for
- Potential underestimated uncertainty in at least one of the measurements?
- Other measurements not precise enough to discriminate BABAR / KLOE

→ Given the fact we do not know which dataset is problematic, we decide to:

- Add half of the discrepancy (2.8×10^{-10}) as an uncertainty (corrected local PDG inflation to avoid double counting)
- Take ("All but BABAR" + "All but KLOE") / 2 as central value

Channel	$a_\mu^{\mathrm{had,LO}}$ $[10^{-10}]$	$\Delta\alpha_{\mathrm{had}}(m_Z^2)$ $[10^{-4}]$
$\pi^+\pi^-$	$507.85 \pm 0.83 \pm \boxed{3.23} \pm 0.55$	$34.50 \pm 0.06 \pm \boxed{0.20} \pm 0.04$

→ *Potential precision improvement* for a_μ ; less important for $\Delta\alpha_{had}(m_Z^2)$, BABAR-KLOE syst. ~16% of total uncertainty

α_S extraction from the Adler function and test of the RGE

$$D(Q^2) \equiv \sum_{i,j} Q_i Q_j \, D_{ij}(Q^2) = 3\pi Q^2 \, \frac{d\Delta\alpha_{\rm had}(Q^2)}{\alpha \, dQ^2}$$

2302.01359

→ Experimental values with correlations; Theoretical predictions: perturbative + non-perturbative corrections (OPE)

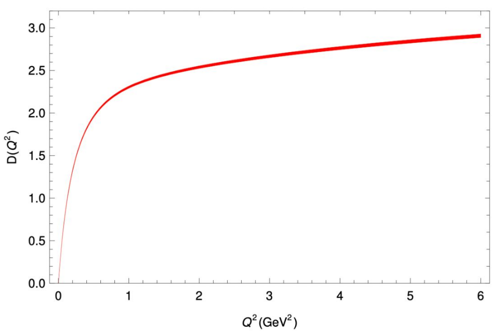

Correlation matrix

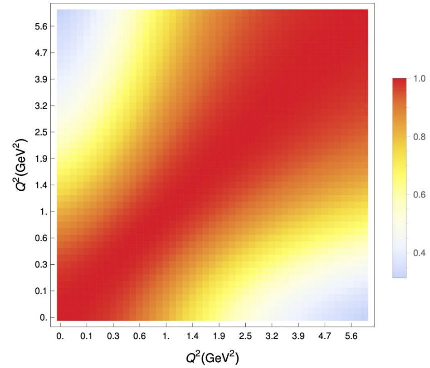

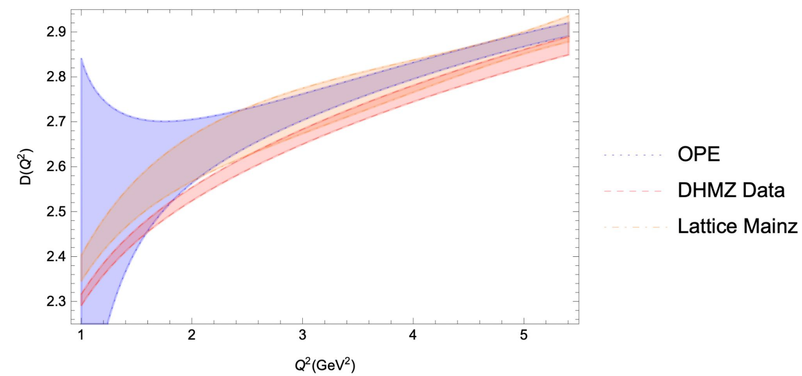

→ Using W.Av. $\alpha_S(M_Z)$ value ~0.118: OPE prediction in good agreement with Lattice QCD, above dispersive

→ Fit DHMZ data: $\alpha_s^{(n_f=5)}(M_Z^2) = 0.1136 \pm 0.0025$

→ Performing RGE test and evaluating its precision, with different correlation scenarios for theory uncertainties

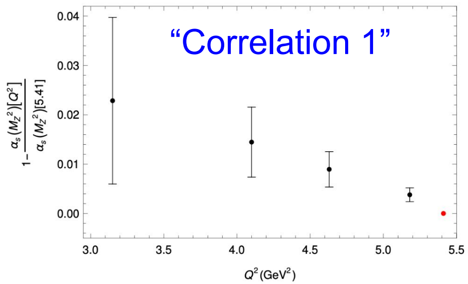

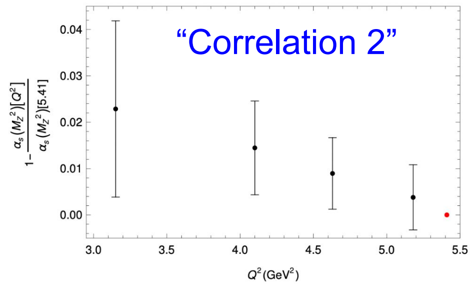

Back

Combining the τ data in the ππ channel

1312.1501

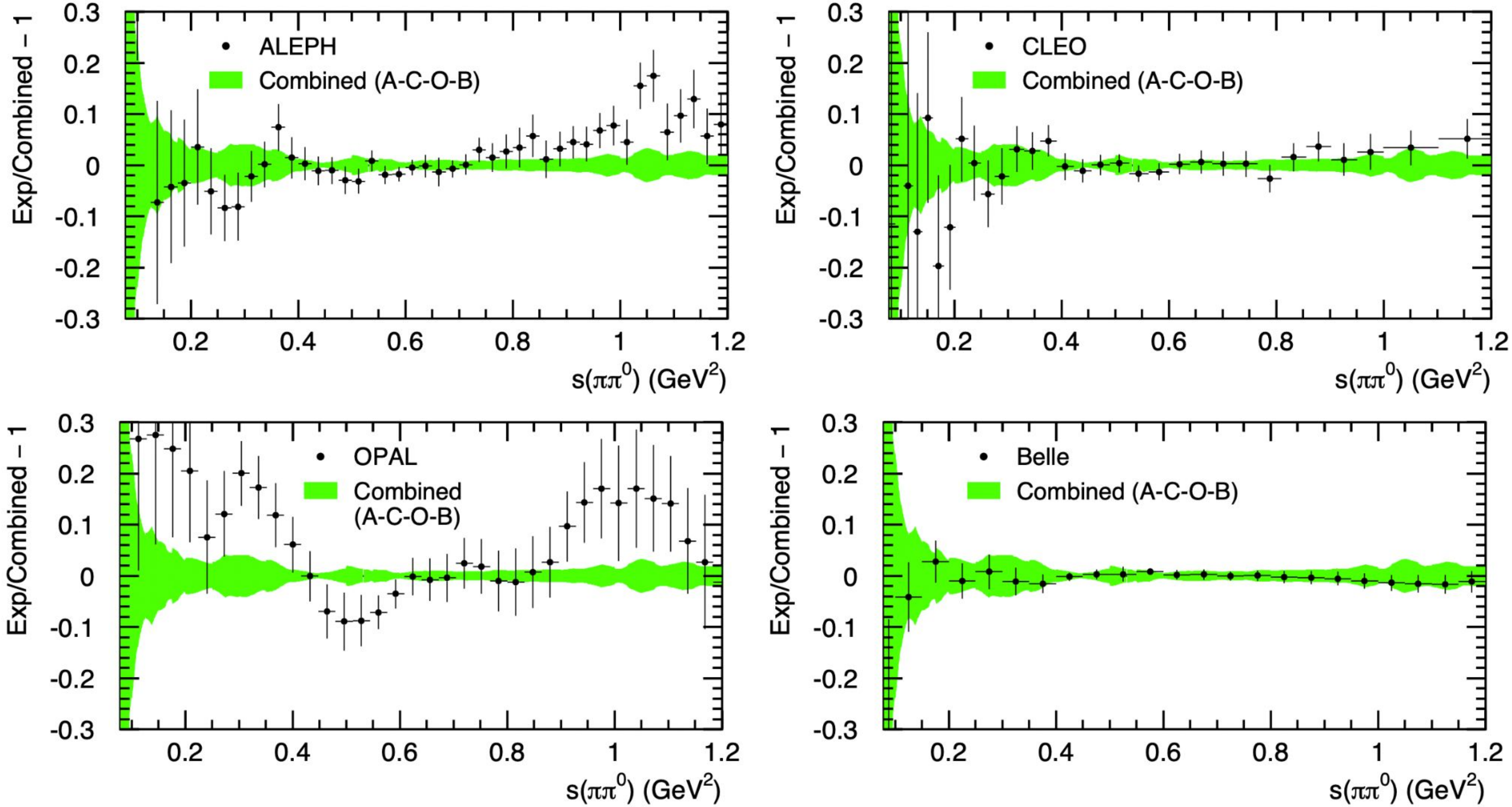

Back

Combination: compatibility between measurements

For each final bin:

→ χ^2 /ndof: test locally the level of agreement between input measurements, *taking into account correlations*

→ Scale uncertainties in bins with χ^2 /ndof > 1 (PDG)

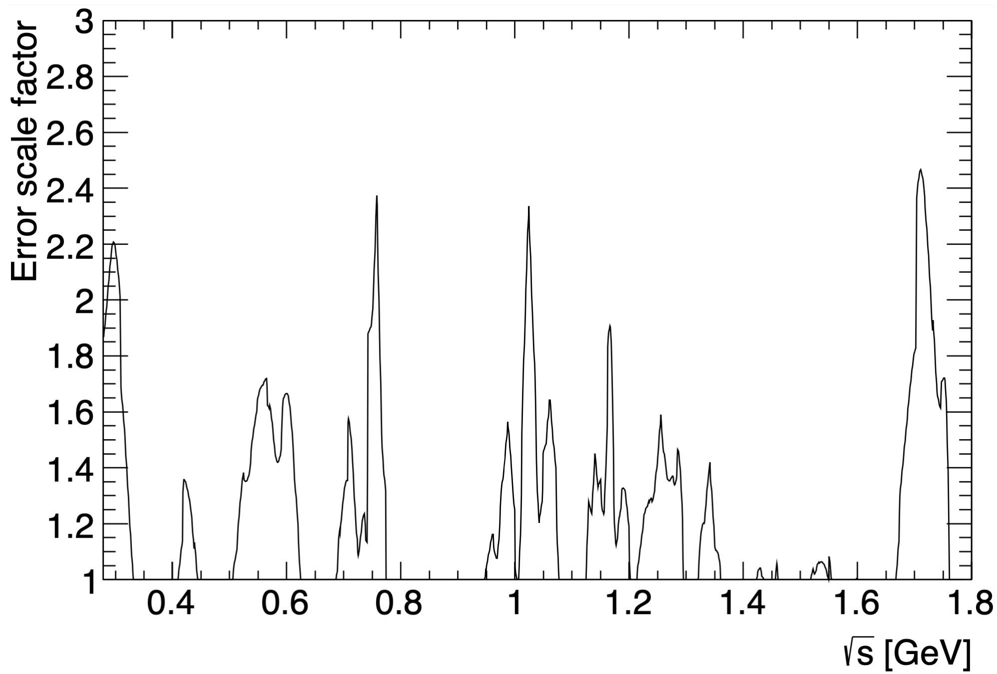

→ Level of agreement significantly better than the one observed for $e^+e^- \rightarrow \pi^+\pi^-$ data

Combination: weights of various measurements

For each final bin:

→ Minimize χ^2 and get average coefficients

Note: average weights must account for bin sizes / point spacing of measurements
(Compare the precisions on the same footing: do not over-estimate the weight of experiments with large bins)

→ Weights in fine bins evaluated using a common (large) binning for measurements + interpolation

→ Their determination also integrates bin-to-bin statistical & systematic correlations on moderate energy ranges

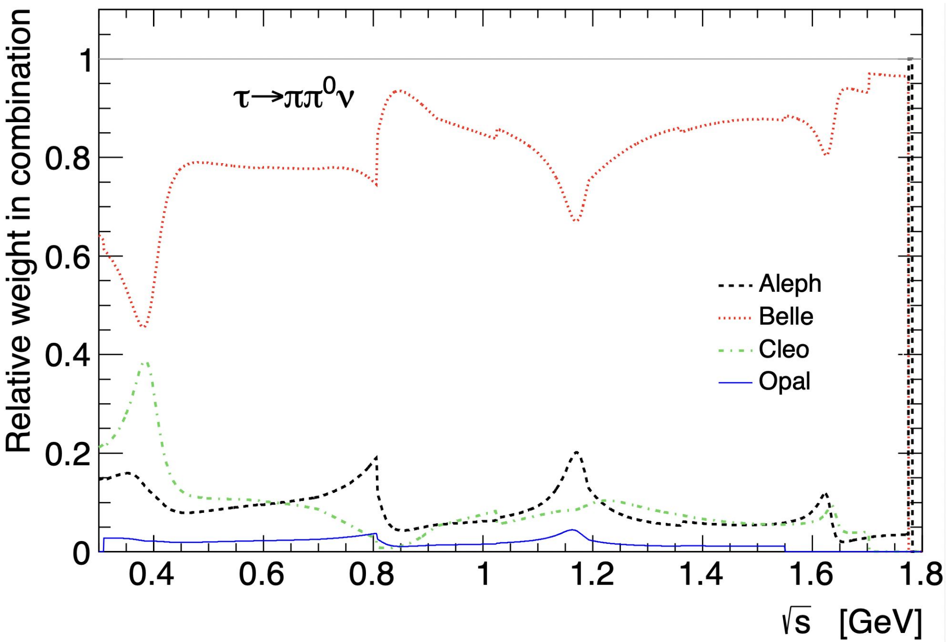

→ Shape information provided mainly by Belle (reflected by the weights from the combination of spectra)

Combining the τ data in the ππ channel

→ Normalisation dominated by ALEPH (directly impacting and very relevant for the integrals)

Experiment	$a_\mu^{\rm had,LO}[\pi\pi,\tau]$ (10^{-10}) $2m_{\pi^\pm} - 0.36$ GeV	$0.36 - 1.8$ GeV
ALEPH	$9.80 \pm 0.40 \pm 0.05 \pm 0.07$	$501.2 \pm 4.5 \pm 2.7 \pm 1.9$
CLEO	$9.65 \pm 0.42 \pm 0.17 \pm 0.07$	$504.5 \pm 5.4 \pm 8.8 \pm 1.9$
OPAL	$11.31 \pm 0.76 \pm 0.15 \pm 0.07$	$515.6 \pm 9.9 \pm 6.9 \pm 1.9$
Belle	$9.74 \pm 0.28 \pm 0.15 \pm 0.07$	$503.9 \pm 1.9 \pm 7.8 \pm 1.9$
Combined	$9.82 \pm 0.13 \pm 0.04 \pm 0.07$	$506.4 \pm 1.9 \pm 2.2 \pm 1.9$

Table 6. The isospin-breaking-corrected $a_\mu^{\rm had,LO}[\pi\pi,\tau]$ (in units of 10^{-10}) from the measured mass spectrum by ALEPH, CLEO, OPAL and Belle, and the combined spectrum using the corresponding branching fraction values. The results are shown separately in two different energy ranges. The first errors are due to the shapes of the mass spectra, which also include very small contributions from the τ-mass and $|V_{ud}|$ uncertainties. The second errors originate from $B_{\pi\pi^0}$ and B_e, and the third errors are due to the isospin-breaking corrections, which are partially anti-correlated between the two energy ranges. The last row gives the evaluations using the combined spectra.

Individual measurements with the corresponding uncertainties:

ALEPH: 511.0 ± 5.3 (±1.9 common, from IB)

CLEO: 514.2 ± 10.1

OPAL: 526.9 ± 12.3

Belle: 513.7 ± 8.0

→ Most precise determination from ALEPH, due to most precise Br

→ Uncertainty from combined spectra (±2.9) smaller than uncertainty from weighted average of integrals (±3.8):
Due to better use of the available information on the precision of the measurements (Br and mass-dependent uncertainties)

χ^2 : 1.45/3 dof, when averaging the 4 individual integrals

χ^2 : 1.88/3-4 dof, when comparing the 4 individual integrals with the integral of the combined spectrum

→ Excellent agreement among the 4 measurements

Moment integrals from τ data (2π channel) with IB corrections

$$\sigma^{I=1}_{e^+e^-\to\pi^+\pi^-} = \frac{4\pi\alpha^2}{s} v_{1,\pi^-\pi^0\nu_\tau}$$

a_μ [0.36 , 1.775 GeV] = $(507.51 \pm 1.86) \times 10^{-10}$

uncertainties from *combined spectrum*

$$v_{1,X^-}(s) = \frac{m_\tau^2}{6|V_{ud}|^2}\frac{\mathcal{B}_{X^-}}{\mathcal{B}_e}\frac{1}{N_X}\frac{dN_X}{ds}\times\left(1-\frac{s}{m_\tau^2}\right)^2\left(1+\frac{2s}{m_\tau^2}\right)^{-1}\frac{R_{\rm IB}(s)}{S_{\rm EW}}$$

$\pm\, 2.12 \times 10^{-10}$

uncertainties from *normalisation (Be & Bππ⁰)*

$\pm\, 1.9 \times 10^{-10}$

uncertainties from *IB uncertainties*

a_μ [0.36 , 1.775 GeV] = $(507.51 \pm 3.41) \times 10^{-10}$

uncertainties from *combined spectrum*, *normalisation (Be & Bππ⁰)* and *IB uncertainties*

→ Next slides:
Display of energy dependence for IB corrections and uncertainties

$$R_{\rm IB}(s) = \frac{{\rm FSR}(s)}{G_{\rm EM}(s)}\frac{\beta_0^3(s)}{\beta_-^3(s)}\left|\frac{F_0(s)}{F_-(s)}\right|^2$$

Moment integrals from IB corrections for τ data (2π channel)

a_μ [0.36 , 1.775 GeV] = $(-11.94 \pm 0.15) \times 10^{-10}$ → Corr. & unc. from *IB Sew (Short-distance EW radiative effects)*

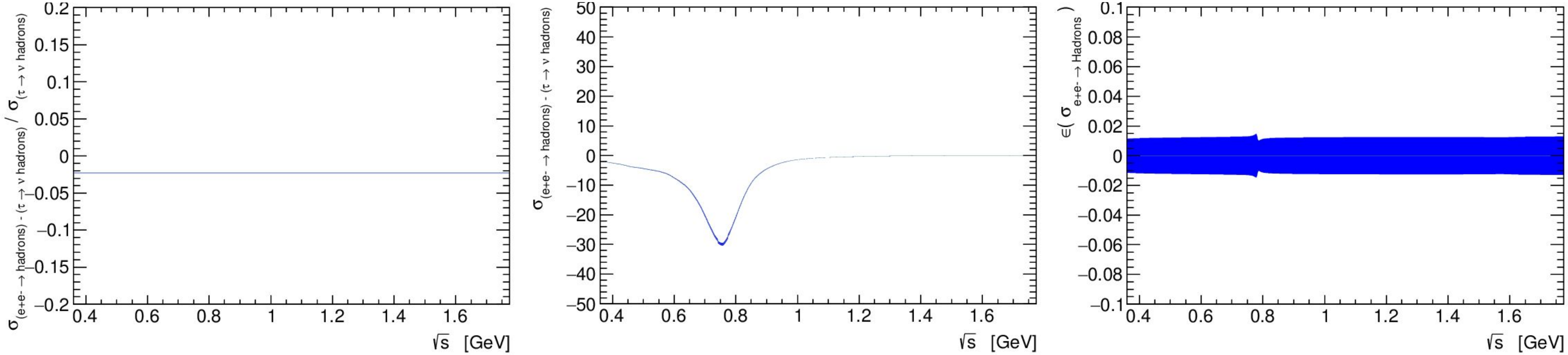

a_μ [0.36 , 1.775 GeV] = $(-1.31 \pm 0.94) \times 10^{-10}$ → Corr. & unc. from *IB Gem (long-distance radiative corrections)*

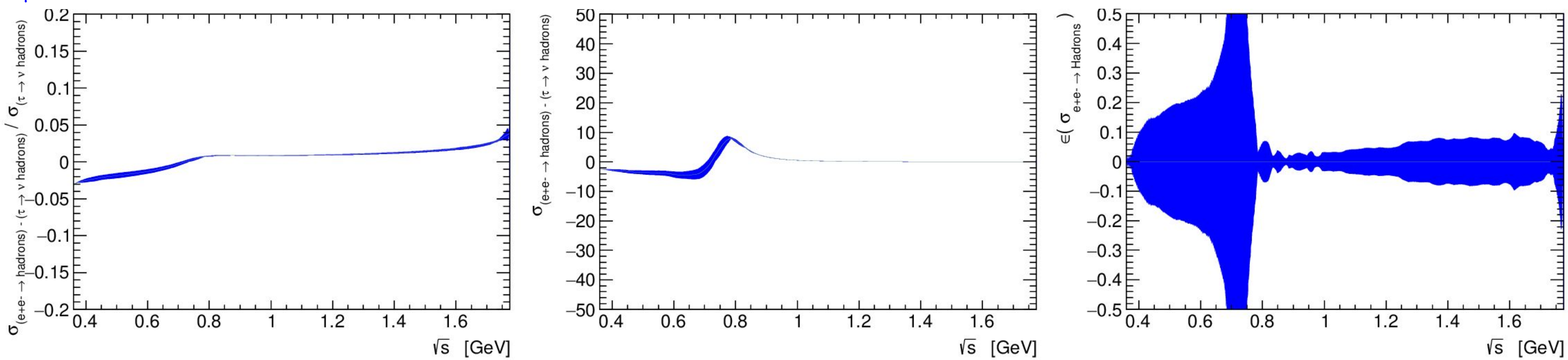

Moment integrals from IB corrections for τ data (2π channel)

a_μ [0.36 , 1.775 GeV] = $(4.41 \pm 0.43) \times 10^{-10}$ → Corrections and uncertainties from *IB FSR*

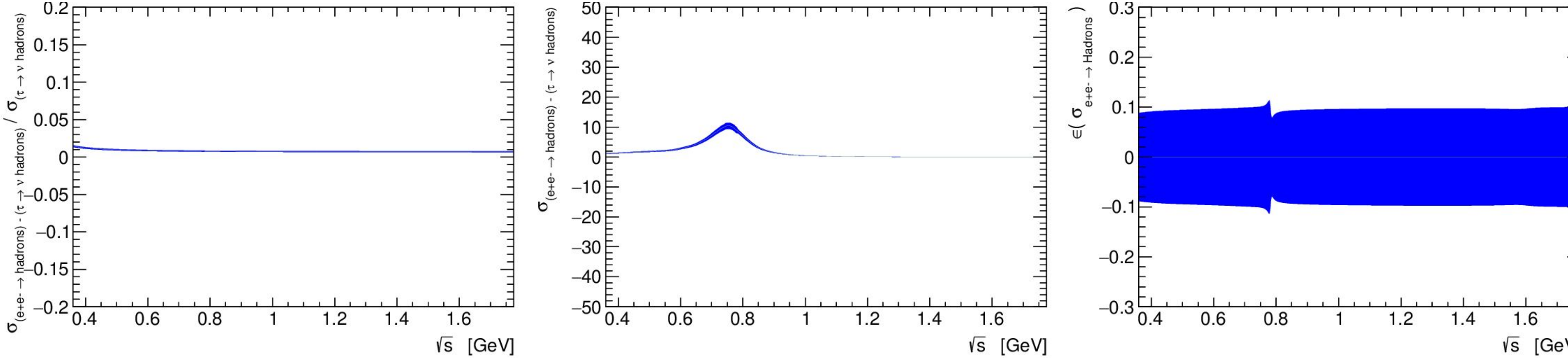

a_μ [0.36 , 1.775 GeV] = $(-6.05 \pm 0) \times 10^{-10}$ → Corrections and uncertainties from *IB beta ($\pi^\pm - \pi^0$ mass splitting)*

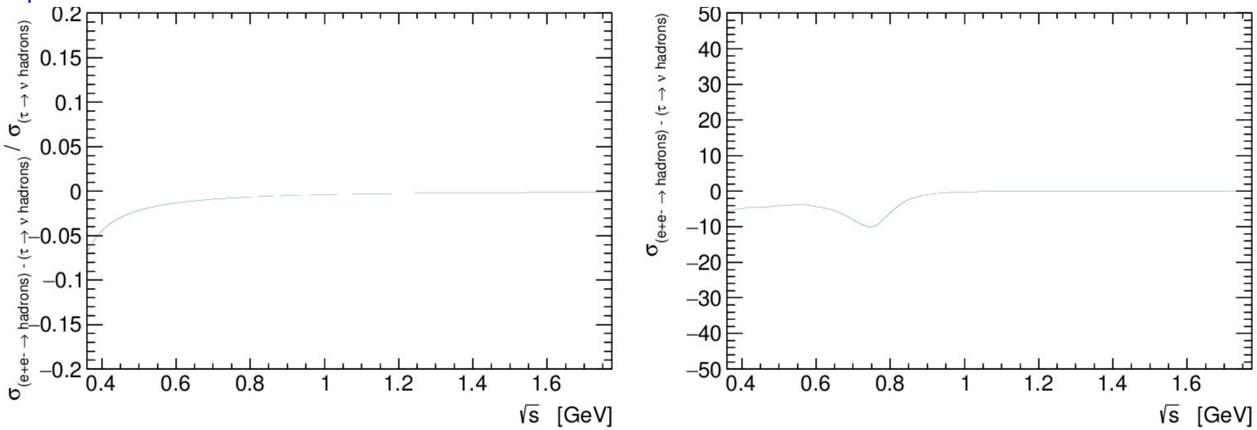

$$\frac{\beta_0^3(s)}{\beta_-^3(s)}$$

Moment integrals from IB corrections for τ data (2π channel)

a_μ [0.36 , 1.775 GeV] = $(4.11 \pm 0) \times 10^{-10}$ → Corrections and uncertainties from *IB mPi (impact on ρ width)*

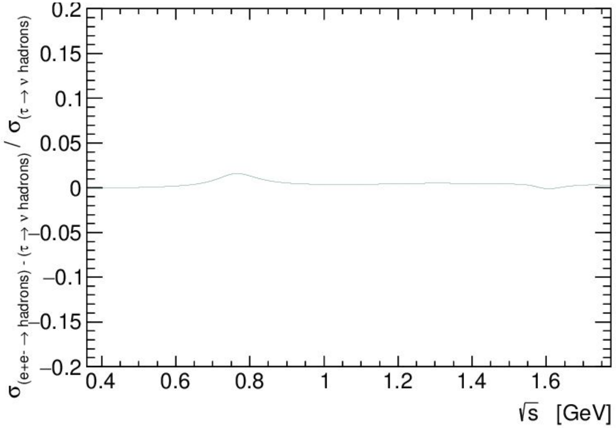

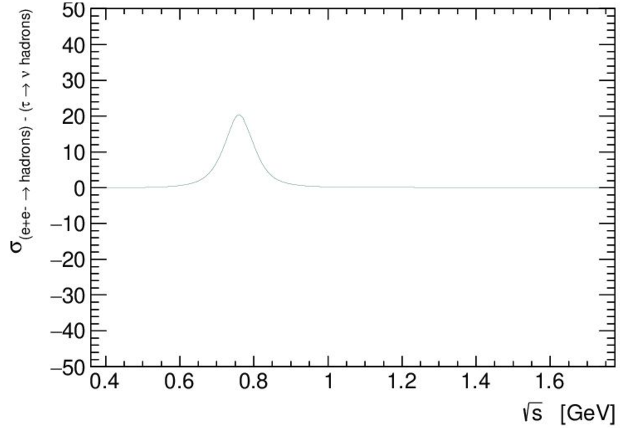

$$\left|\frac{F_0(s)}{F_-(s)}\right|^2$$

a_μ [0.36 , 1.775 GeV] = $(0.20 \pm 0.27) \times 10^{-10}$ → Corrections and uncertainties from *IB mRho*

$$\left|\frac{F_0(s)}{F_-(s)}\right|^2$$

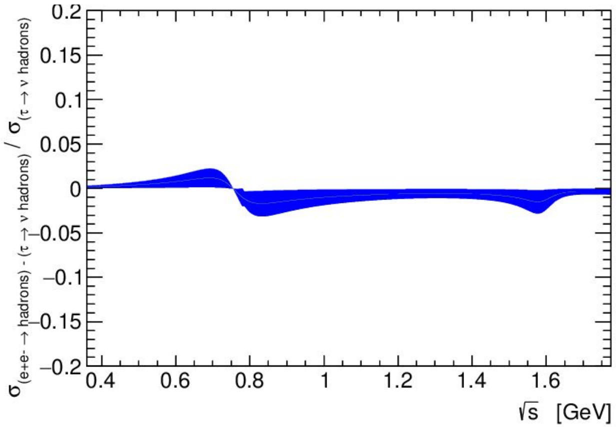

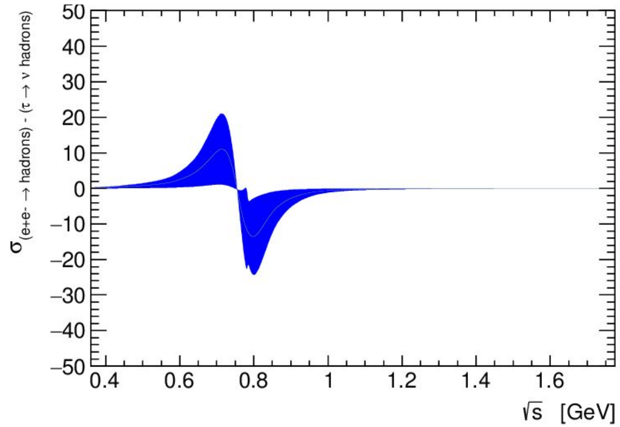

Moment integrals from IB corrections for τ data (2π channel)

a_μ [0.36 , 1.775 GeV] = $(3.99 \pm 0.98) \times 10^{-10}$ → Corrections from *IB interference* and uncertainties from *IB KS-GS*

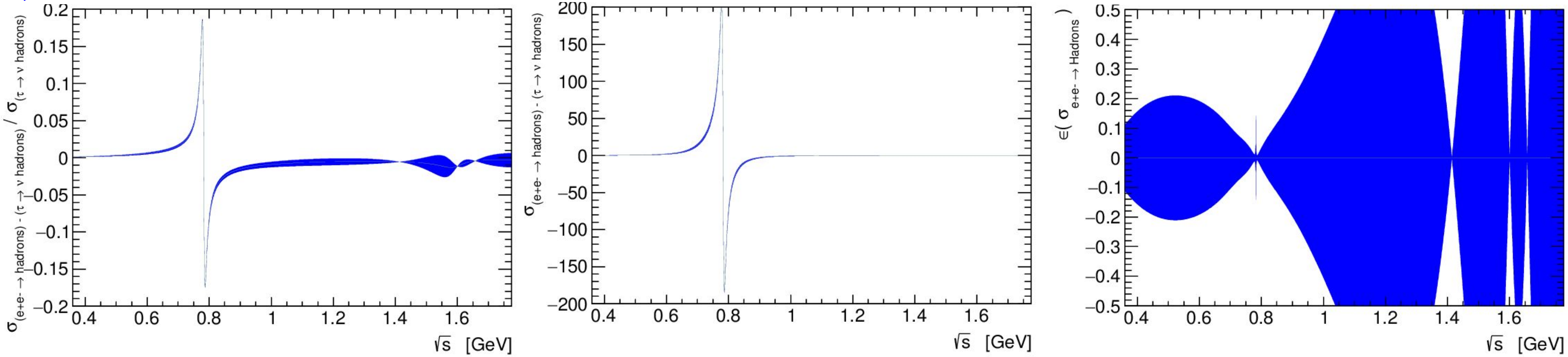

a_μ [0.36 , 1.775 GeV] = $(-5.82 \pm 0.59) \times 10^{-10}$ → *IB EM decay* corrections and uncertainties from *IB EM decay*

$$\left|\frac{F_0(s)}{F_-(s)}\right|^2$$

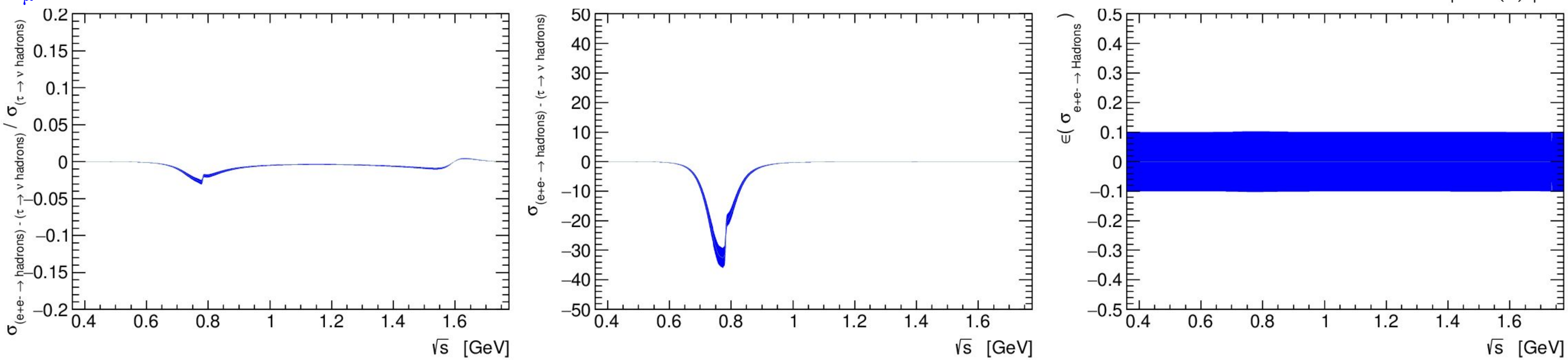

Moment integrals from IB corrections for τ data (2π channel)

a_μ [0.36 , 1.775 GeV] = $(-5.82 \pm 1.57) \times 10^{-10}$

→ *IB EM decay* corrections and uncertainties from *IB EM decay + KS-GS (conservative sum of uncertainties)*

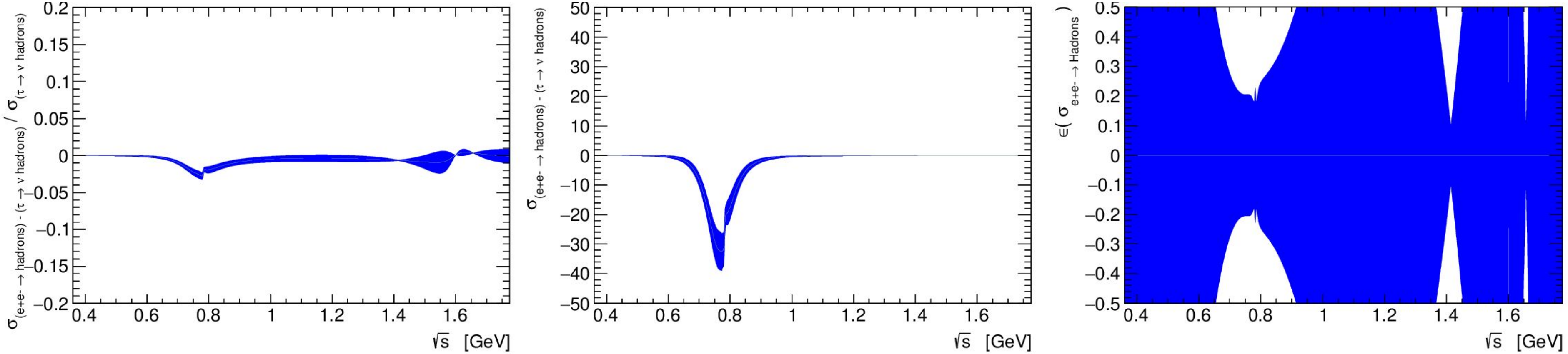

→ Note:

Various models for description of ρ-ω interference in IB corrections adjusted to the same e+e- data

KS-GS uncertainty, using external parameters, conservatively covers this effect

Comparison with IB-corrected τ data

$$\sigma^{I=1}_{e^+e^-\to\pi^+\pi^-} = \frac{4\pi\alpha^2}{s} v_{1,\pi^-\pi^0\nu_\tau}$$

$$v_{1,X^-}(s) = \frac{m_\tau^2}{6|V_{ud}|^2}\frac{\mathcal{B}_{X^-}}{\mathcal{B}_e}\frac{1}{N_X}\frac{dN_X}{ds} \times \left(1-\frac{s}{m_\tau^2}\right)^2\left(1+\frac{2s}{m_\tau^2}\right)^{-1}\frac{R_{\rm IB}(s)}{S_{\rm EW}}$$

→ Comparing corrections used by Davier et al. with the ones by F. Jegerlehner

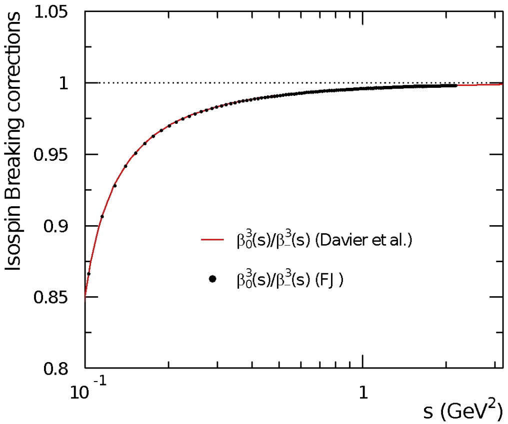

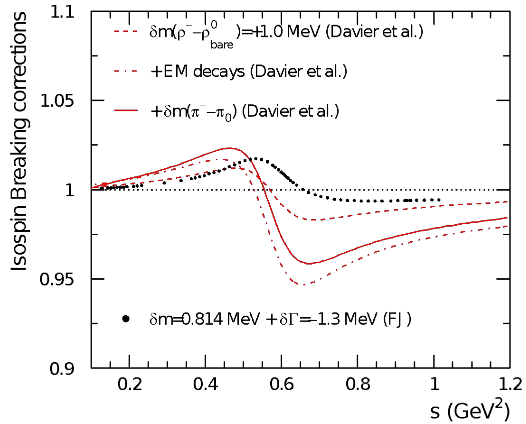

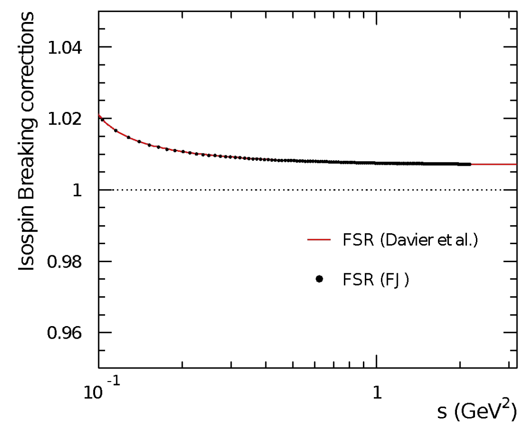

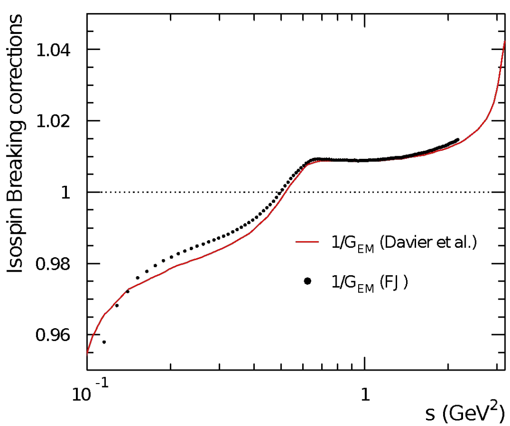

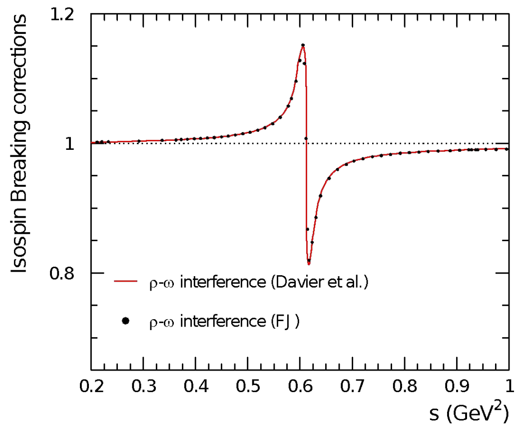

$$R_{\rm IB}(s) = \frac{{\rm FSR}(s)}{G_{\rm EM}(s)}\frac{\beta_0^3(s)}{\beta_-^3(s)}\left|\frac{F_0(s)}{F_-(s)}\right|^2$$

Comparison with IB-corrected τ data

→ for a_μ, $e^+e^- - \tau$ difference of 2.2 σ (Davier et al.)

→ the $\rho-\gamma$ mixing correction proposed in arXiv:1101.2872 (FJ) seems to over-estimate the $e^+e^- - \tau$ difference

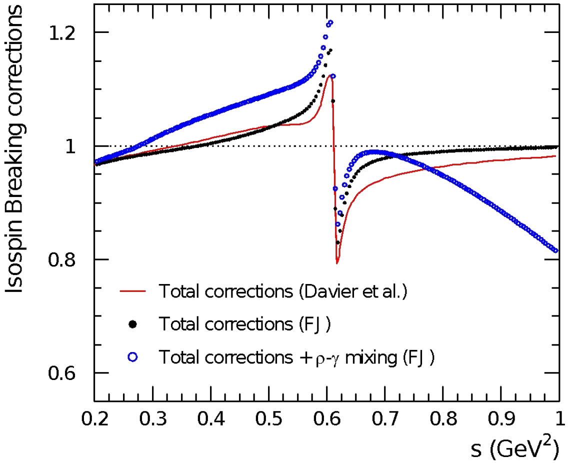

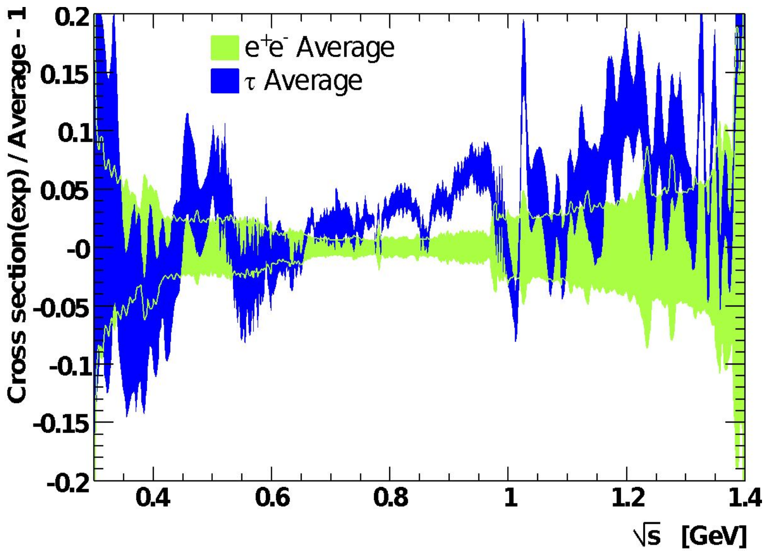

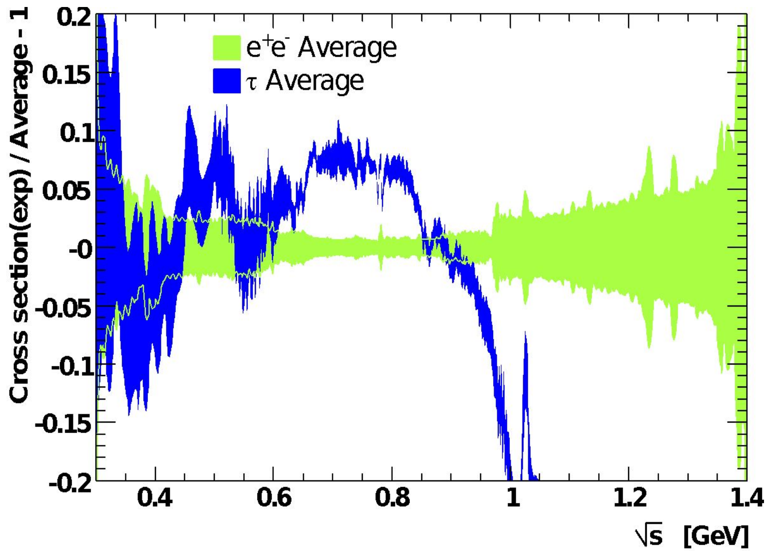

The new context for dispersive HVP since White Paper 2020 and Tau data

- At the time of WP 2020 $\Delta a_\mu^{\mathrm{HVP\ LO}}$ (10^{-10})

  KLOE$_{\mathrm{peak}}$ (0.6-0.9+comb) 2.3

  BABAR 3.8

  BABAR − KLOE difference 9.8 (5.6 found with all-KLOE/all-BABAR)

- Now

→ γ-ρ mixing not justified from theoretical point of view (discussions with several TI theorists)

  CMD-3 4.2 *result changing e+e- data landscape*

  CMD-3 − KLOE difference 21.6

  BABAR LO/NLO/NNLO study: *points to a necessary revisiting of KLOE analysis*

- Focusing on τ for 2π (competitive with best e^+e^- 2π) + e^+e^- for the rest (non-2π + I=0)

  data $1.9_{\mathrm{spectrum}} \oplus 2.2_{\mathrm{BR}} = 2.9$

  IB correction -14.9 ± 1.9 uncertainty x11 smaller than CMD3-KLOE ≠

Combining the $e^+e^- \to \pi^+\pi^-$ data, BaBar & CMD3 & Tau(+IB)

→ Motivated by the previous findings, combine τ, BABAR and CMD-3 spectra

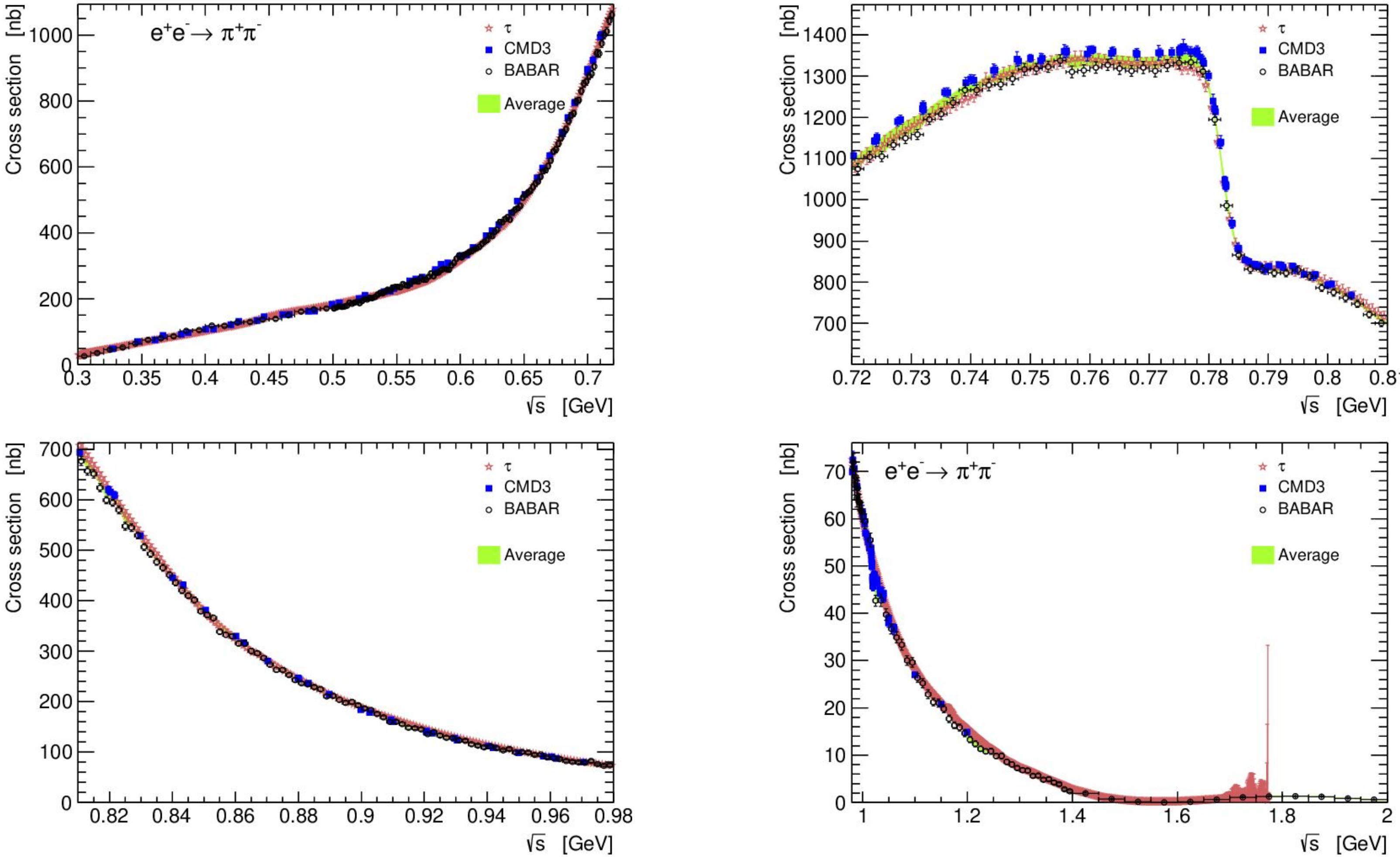

Back

Combining the $e^+e^- \to \pi^+\pi^-$ data, BaBar & CMD3 & Tau(+IB)

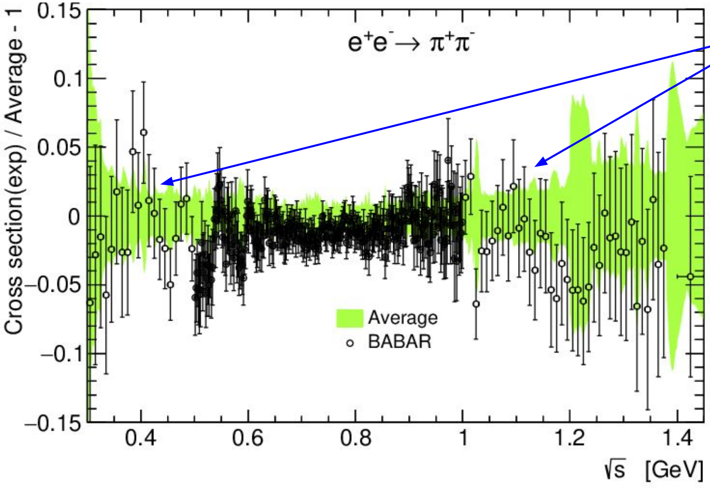

Reasonable BABAR/CMD3 agreement at low & high E

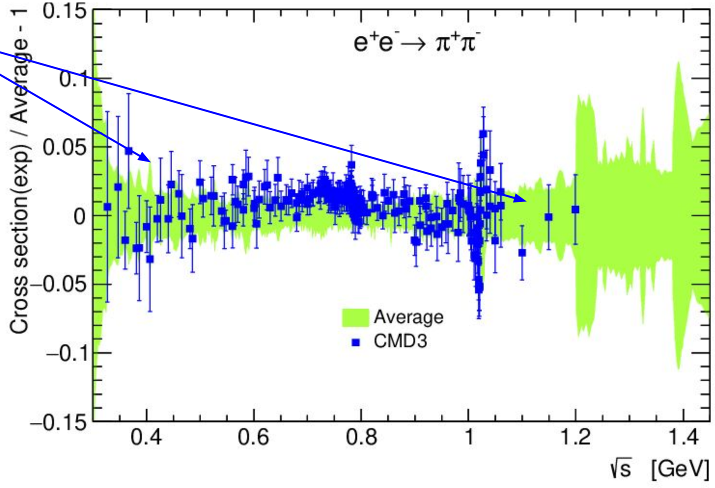

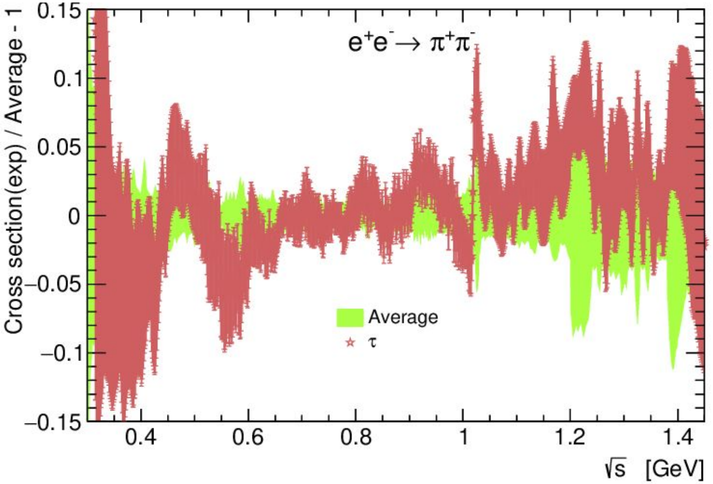

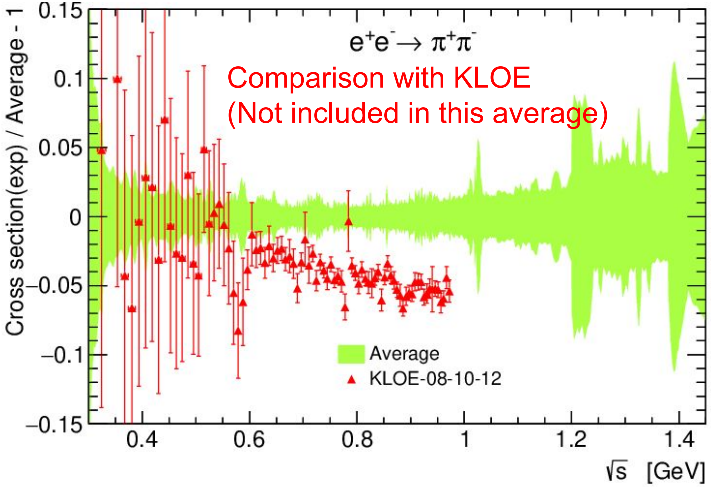

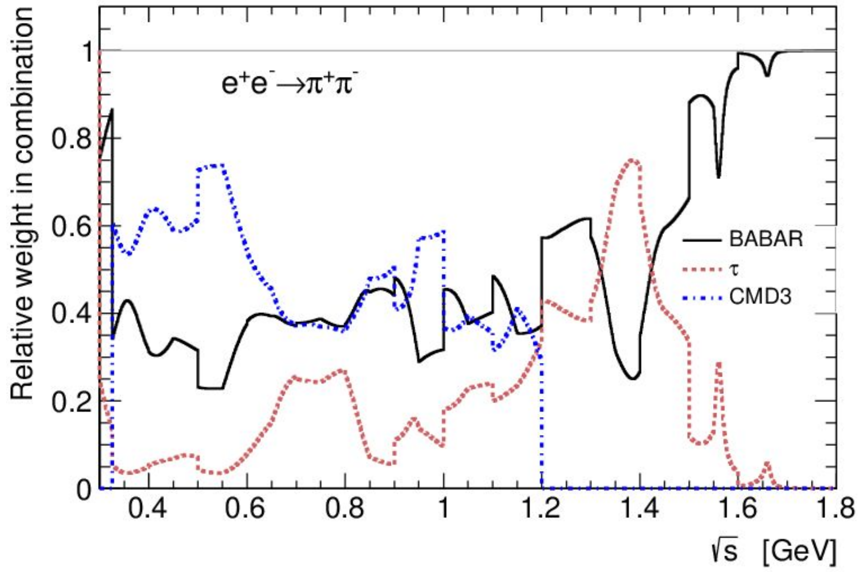

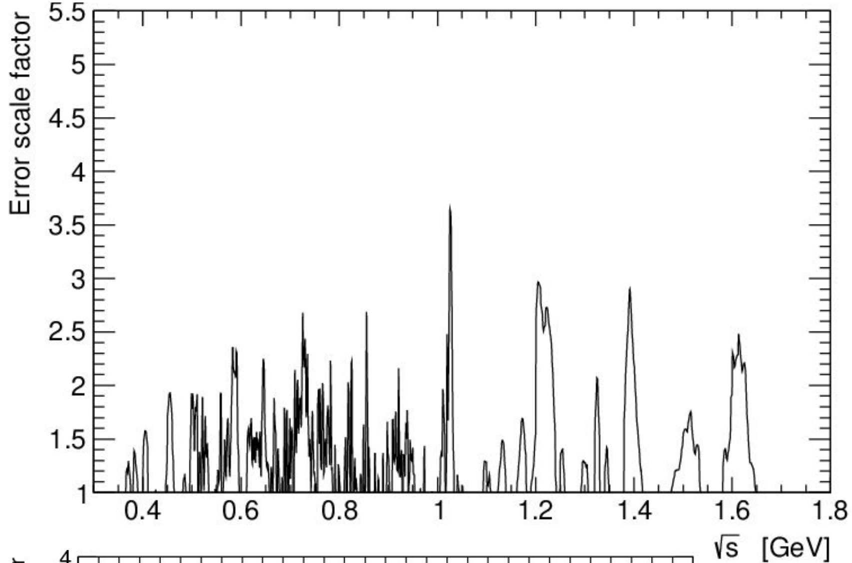

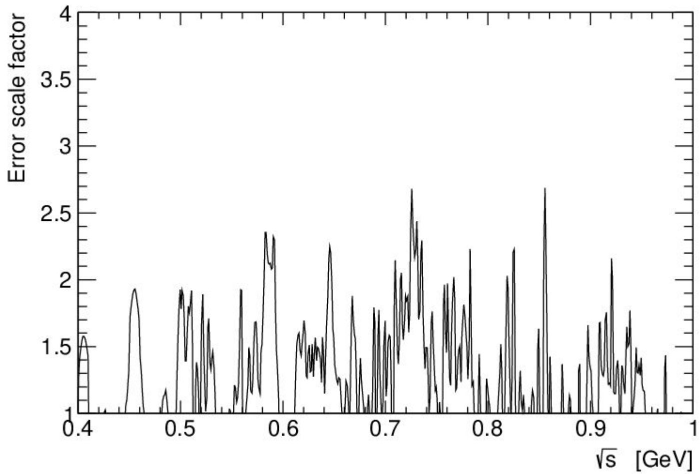

→ Average dominated by BaBar and CMD3;
BaBar and τ cover full energy range

→ Some tension between BaBar & CMD3 in the ρ region

→ Much larger tension (slope and shift) when comparing KLOE with the BABAR + CMD-3 + τ combination

Combining the $e^+e^- \to \pi^+\pi^-$ data, BaBar & CMD3 & Tau(+IB)

x 10^{-10}

a_μ [0.3 ; 1.8 GeV] = 519.8 ±3.3 (±1.3(stat) ±3.1 (syst))

Without applying the χ^2 /ndof rescaling of uncertainties:
a_μ [0.3 ; 1.8 GeV] = 519.8 ±2.5 (±1.0 (stat) ±2.3 (syst))

→ Coherent with DHLMZ value (2312.02053, EPJ C) obtained from average of BaBar, CMD3 and τ integrals:
518.0 ±3.3 (after uncertainty rescaling x1.5)
(Different e+e- combination to complete CMD3 energy range;
Using fit of τ data to complete their integral for [Thr.;0.36 GeV])

a_μ^{win} [0.3 ; 1.8 GeV] = 148.5 ±1.0 (±0.4(stat) ±0.9 (syst))

Without applying the χ^2 /ndof rescaling of uncertainties:
a_μ^{win} [0.3 ; 1.8 GeV] = 148.5 ±0.7 (±0.3 (stat) ±0.6 (syst))

a_μ [0.6 ; 0.9747 GeV] = 394.6 ±2.5 (±1.3 (stat) ±2.2 (syst))

Without applying the χ^2 /ndof rescaling of uncertainties:
a_μ [0.6 ; 0.9747 GeV] = 394.6 ±1.8 (±0.9(stat) ±1.6 (syst))

a_μ^{win} [0.6 ; 0.9747 GeV] = 127.4 ±0.8 (±0.4 (stat) ±0.7 (syst))

Without applying the χ^2 /ndof rescaling of uncertainties:
a_μ^{win} [0.6 ; 0.9747 GeV] = 127.4 ±0.6 (±0.3(stat) ±0.5 (syst))

→ Still non-negligible effect of uncertainty enhancement through the local χ^2 /ndof rescaling;
In addition, an extra uncertainty accounting for systematic deviations between measurements has to be added, as done for DHMZ'19

Treatment of the KLOE correlation matrices

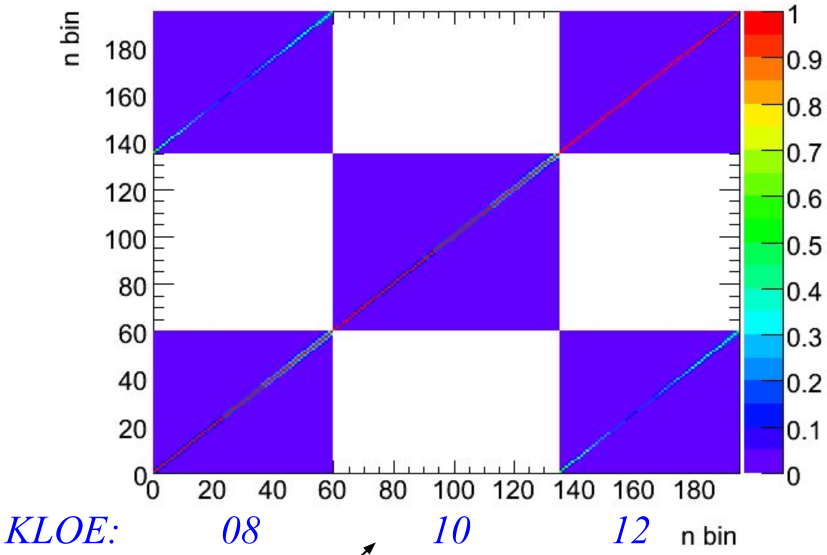

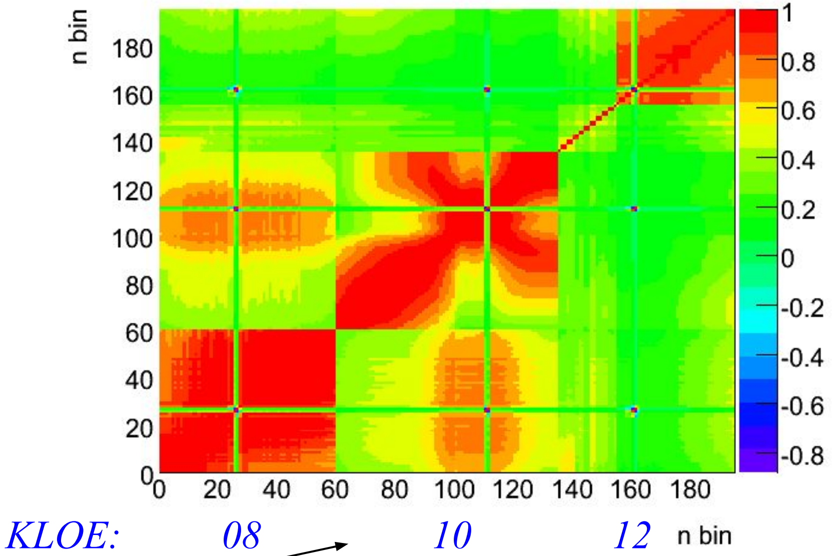

→ Statistical and systematic correlation matrices among the 3 measurements

Treatment of the KLOE data – eigenvector decomposition

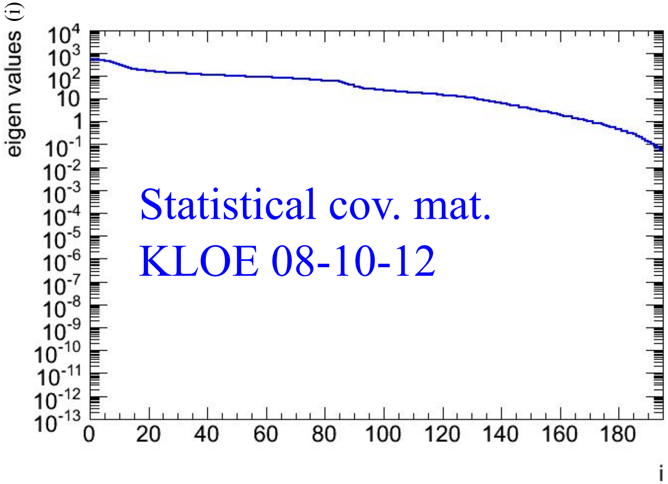

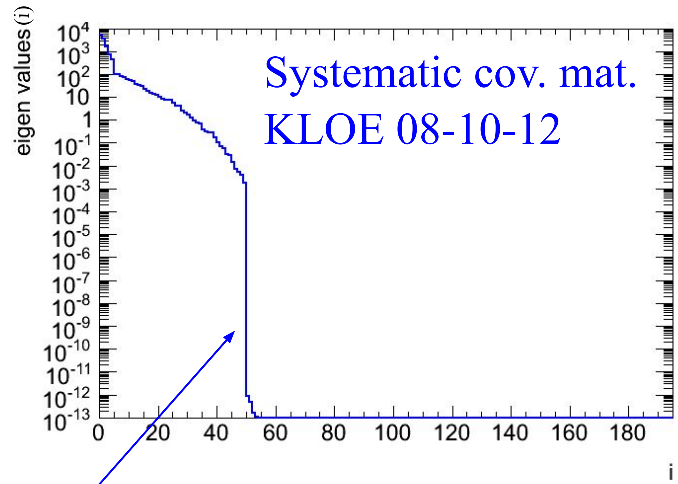

$$C = S \cdot D \cdot S^T$$

$$D = \begin{pmatrix} \ddots & 0 & 0 \\ 0 & \sigma_i^2 & 0 \\ 0 & 0 & \ddots \end{pmatrix}$$

$$S = \begin{pmatrix} V_1 & \dots & V_n \end{pmatrix}$$

→ "counting" the number of independent components (50) used to build the covariance matrix

→ Problem of negative eigenvalues for previous systematic covariance matrix solved (informed KLOE collaboration about the problem in summer 2016)

Treatment of the KLOE data – eigenvector decomposition

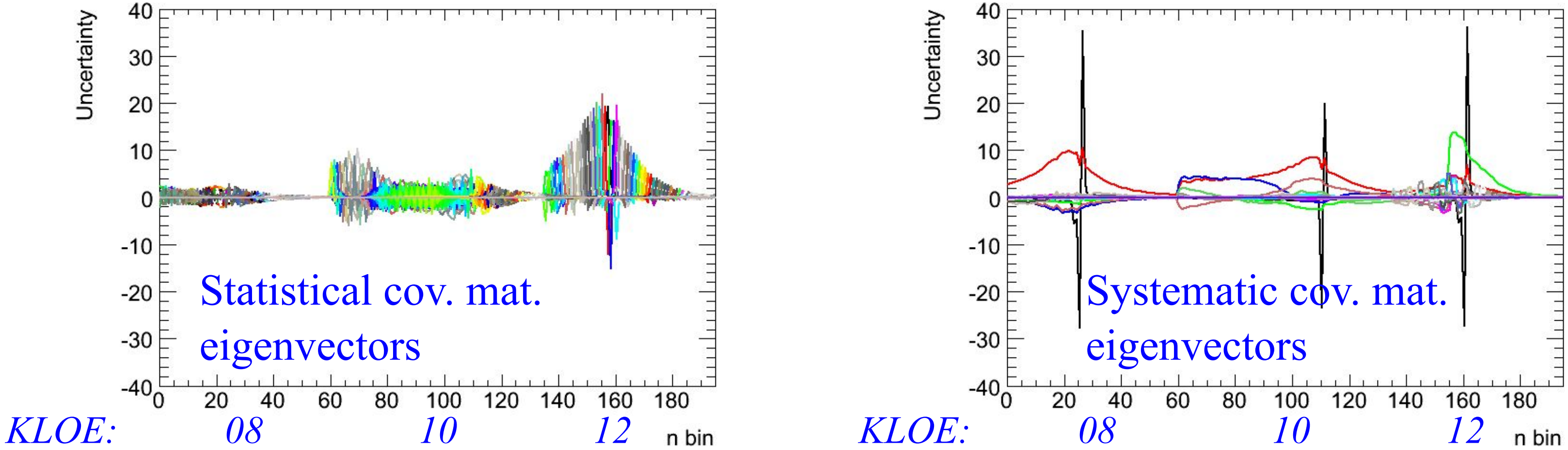

→ Each normalized eigenvector (σ_i*V_i) treated as an uncertainty fully correlated between the bins

→ All these uncertainties are independent between each-other

$$C = \sum_{i=1}^{N_{bins}} \sigma_i^2 \cdot C(V_i)$$

→ Checked exact matching with the original matrices + with all a_μ integrals and uncertainties published by KLOE

Treatment of the KLOE data – eigenvector decomposition

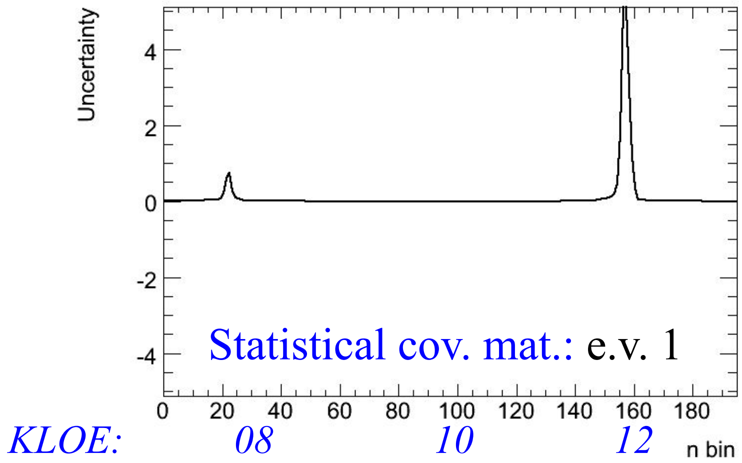

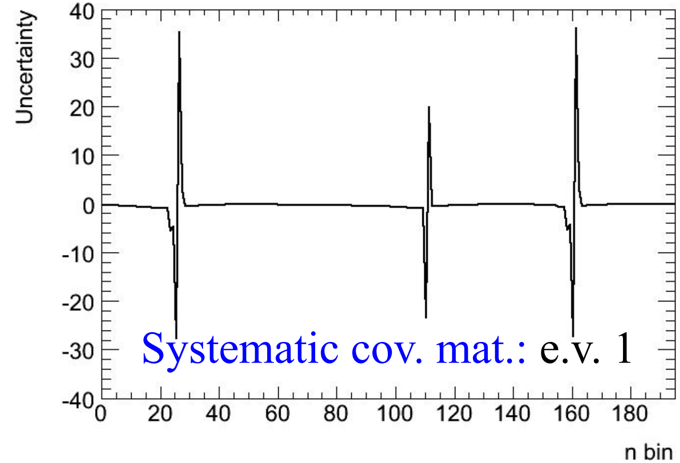

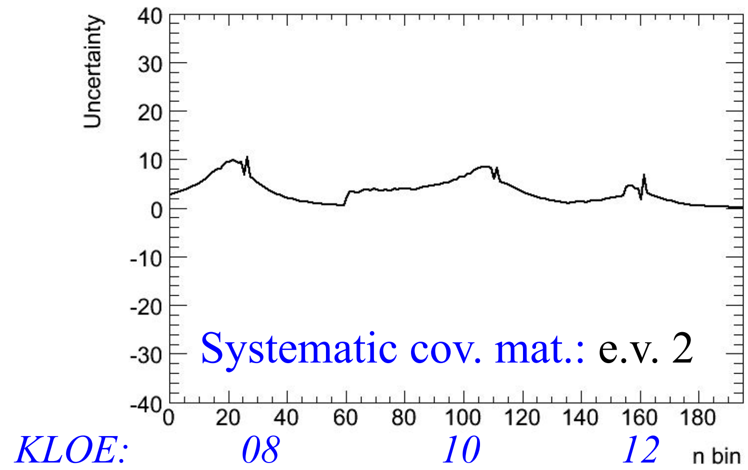

→ Eigenvectors carry the general features of the correlations:

- long-range for systematics
- ~short-range for statistical uncertainties + correlations between KLOE 08 & 12

Local comparison of the 3 KLOE measurements

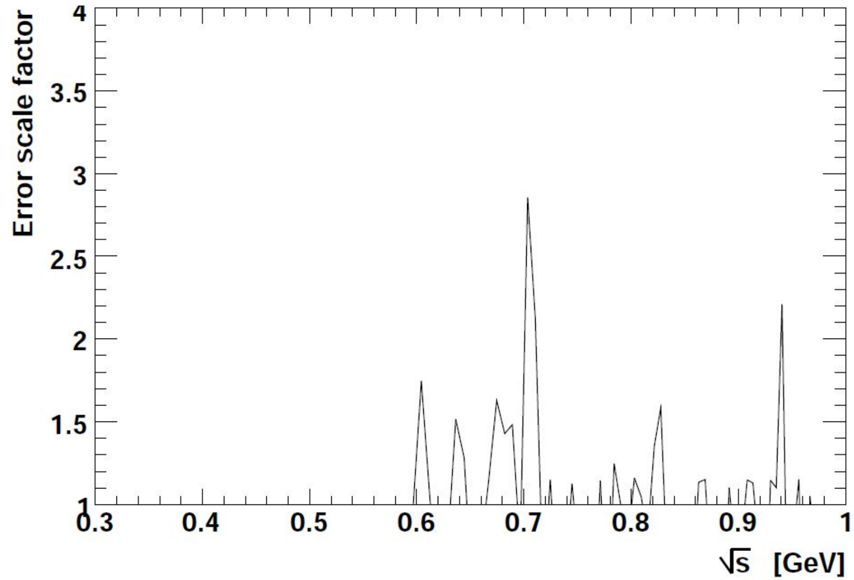

→ Local χ^2 /ndof test of the local compatibility between KLOE 08 & 10 & 12, taking into account the correlations: some tensions observed

→ Does not probe general trends of the difference between the measurements (e.g. slopes in the ratio)

→ Compute ratio between pairs of KLOE measurements

→ Full propagation of uncertainties and correlations using pseudo-experiments (agreement with analytical linear uncertainty propagation)

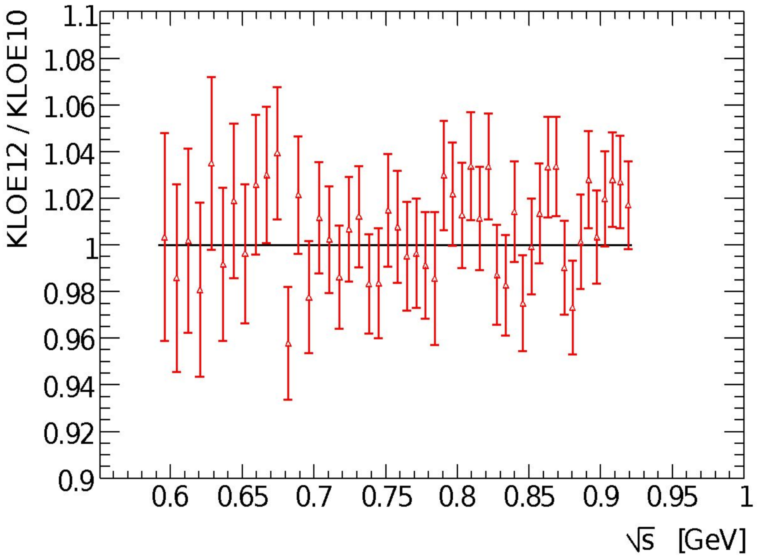

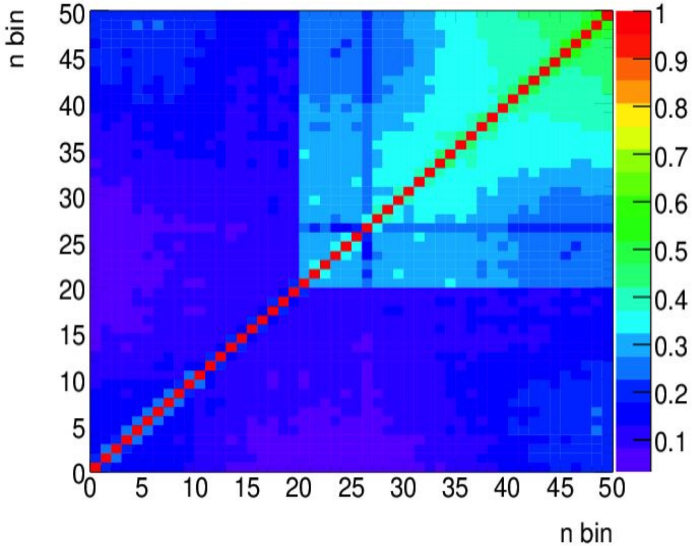

→ Good agreement between KLOE 10 and KLOE 12

Back

Ratios between measurements

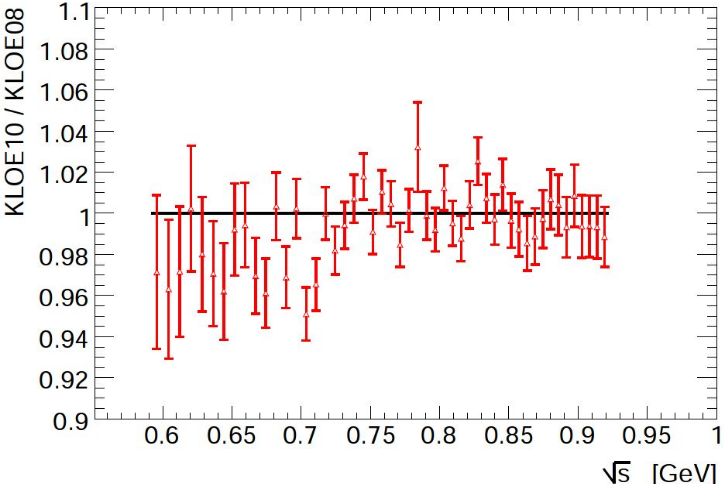

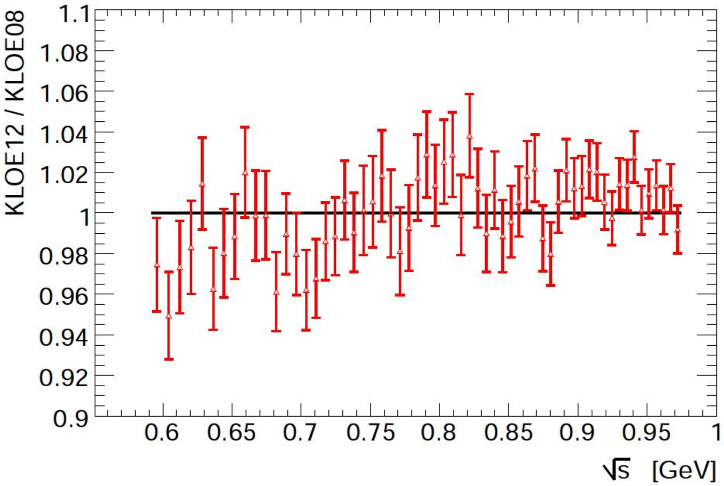

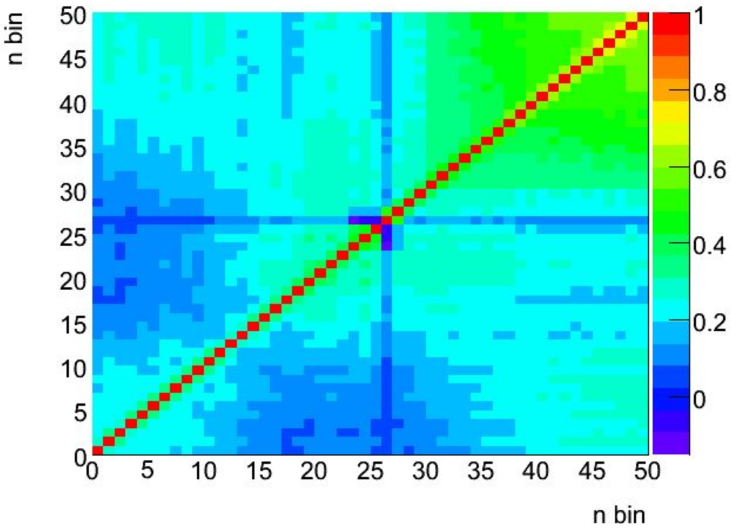

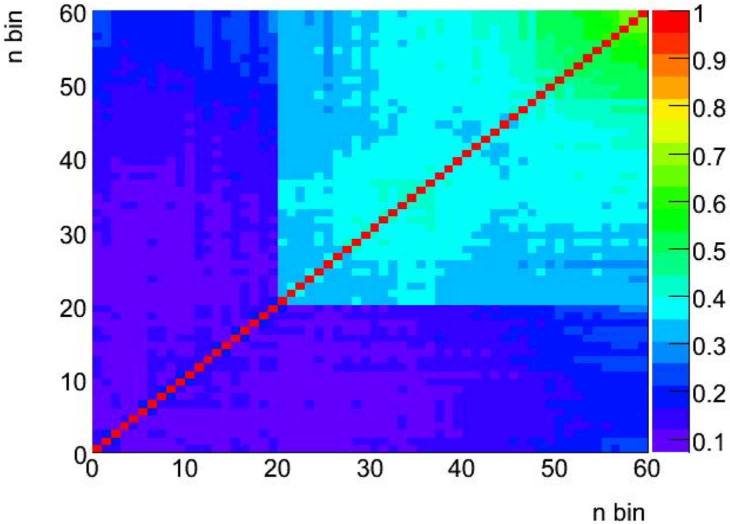

Direct comparison of the 3 KLOE measurements

→ Quantitative comparison between the ratios and unity, taking into account correlations

KLOE 10 / KLOE 08	KLOE 12 / KLOE 08
χ^2 [0.35;0.85] GeV^2 : 79.0 / 50(DOF) p-value= 0.0056	χ^2 [0.35;0.95] GeV^2 : 73.7 / 60(DOF) p-value= 0.11
χ^2 [0.35;0.58] GeV^2 : 46.2 / 23(DOF) p-value= 0.0028	χ^2 [0.35;0.58] GeV^2 : 21.8 / 23(DOF) p-value= 0.53
χ^2 [0.58;0.85] GeV^2 : 29.7 / 27(DOF) p-value= 0.33	χ^2 [0.35;0.64] GeV^2 : 27.5 / 29(DOF) p-value= 0.55
χ^2 [0.64;0.85] GeV^2 : 20.7 / 21(DOF) p-value= 0.47	χ^2 [0.64;0.95] GeV^2 : 39.4 / 31(DOF) p-value= 0.14

Quantitative comparisons of the KLOE measurements

→ Quantitative comparison between the ratios and unity, taking into account correlations

→ Fitting the ratio taking into account correlations

→ Full propagation of uncertainties and correlations – 3 methods yielding consistent results: $\pm 1\sigma$ shifts of each uncertainty, pseudo-experiments and fit uncertainties from Minuit

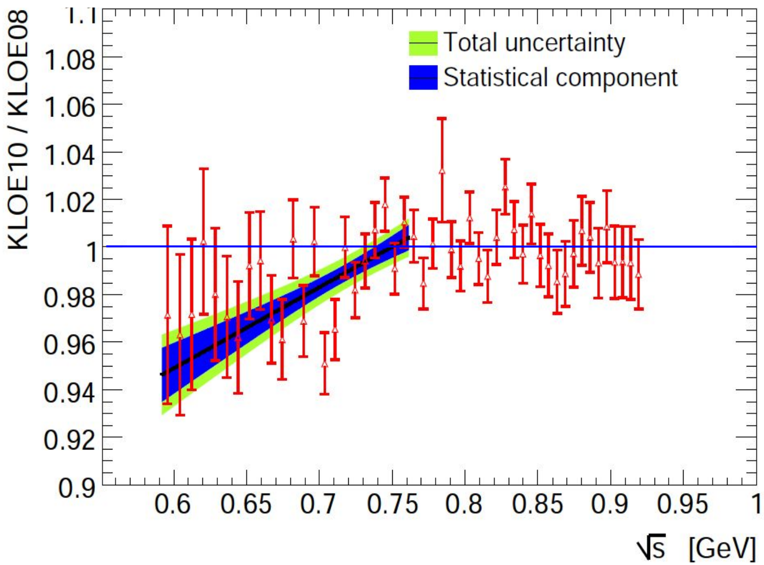

Comparison with Unity:

χ^2 [0.35;0.85] GeV^2 : 79.0 / 50(DOF)

p-value= 0.0056

χ^2 [0.35;0.58] GeV^2 : 46.2 / 23(DOF)

p-value= 0.0028

χ^2 [p0 + p1$\sqrt{s}$]: 36.1 / 21(DOF)

p-value= 0.02

p0 : 0.745 ± 0.085

p1 : 0.341 ± 0.117

→ Significant shift & slope (~2.5-3σ) at low $\sqrt{s}$, no significant shift at high $\sqrt{s}$

Similar shift & slope for KLOE 12 / KLOE 08 (*see below*)

→ Should motivate conservative treatment of uncertainties and correlations in combination

→ Fitting the ratio taking into account correlations

→ Full propagation of uncertainties and correlations – 3 methods yielding consistent results: ±1σ shifts of each uncertainty, pseudo-experiments and fit uncertainties from Minuit

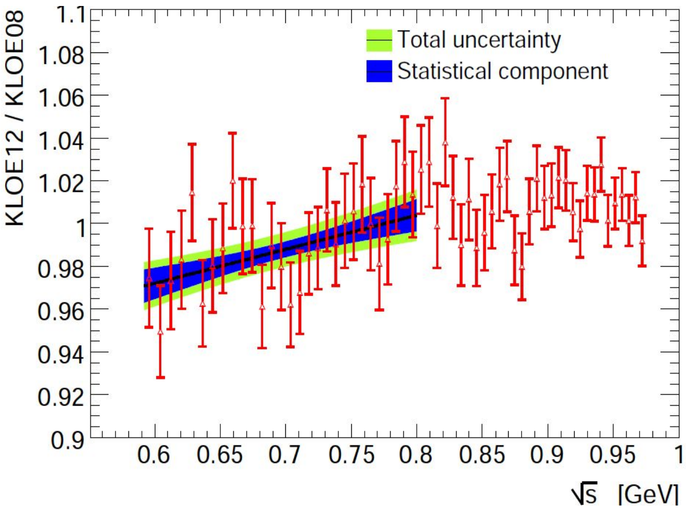

χ^2 [p0 + p1√s]: 20.7 / 27(DOF)
p-value= 0.80
p0 : 0.876 ± 0.056
p1 : 0.159 ± 0.081

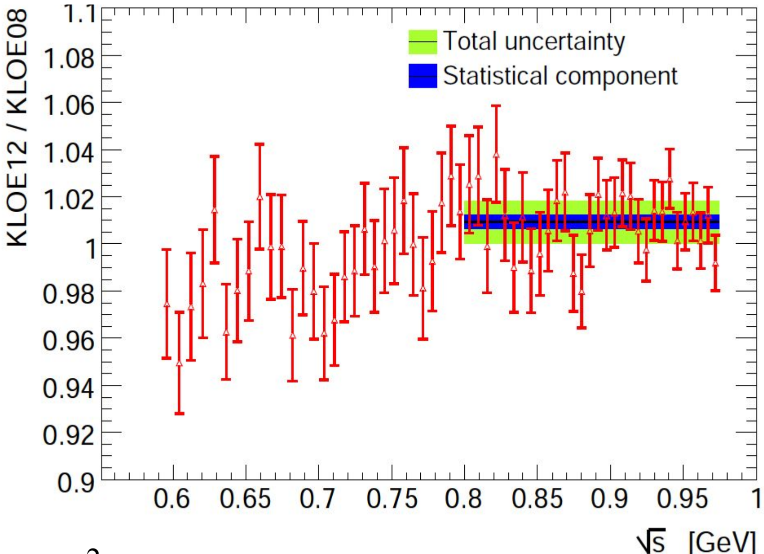

χ^2 [p0]: 38.4 / 30(DOF)
p-value= 0.14
p0 : 1.009 ± 0.009

→ Significant shift and slope (~2σ) at low √s, no significant shift at high √s

Direct comparison of the 3 KLOE measurements

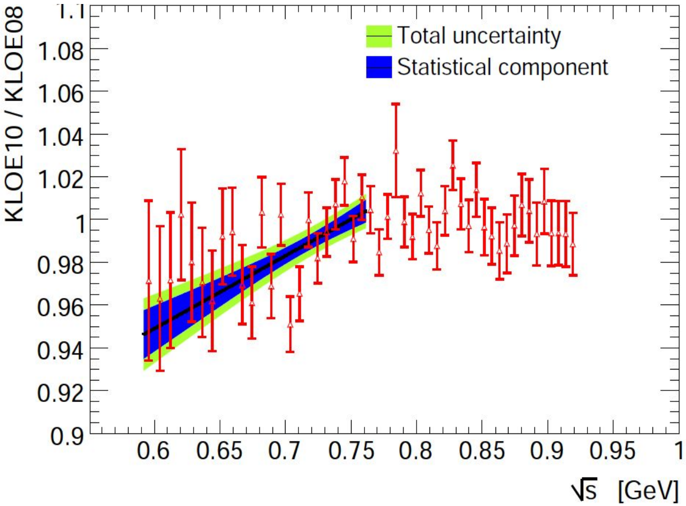

χ^2 [p0 + p1√s]: 36.1 / 21(DOF)
p-value= 0.02
p0 : 0.745 ± 0.085
p1 : 0.341 ± 0.117

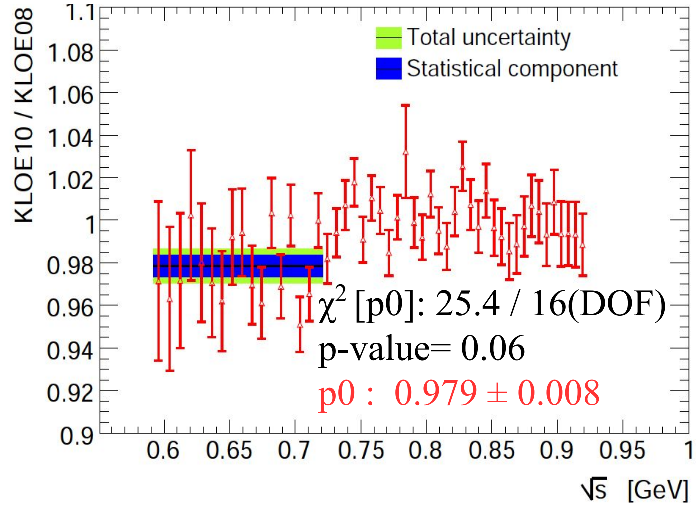

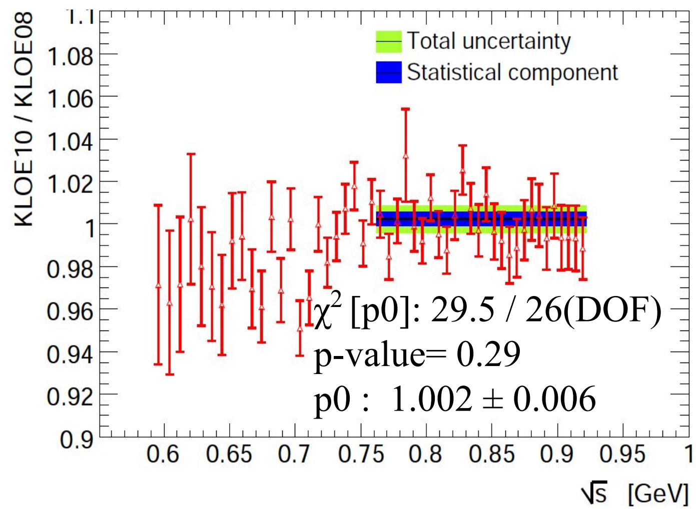

→ Significant shift and slope (~2.5-3σ) at low √s, no significant shift at high √s

Treatment of the combined KLOE data

Correlation matrix

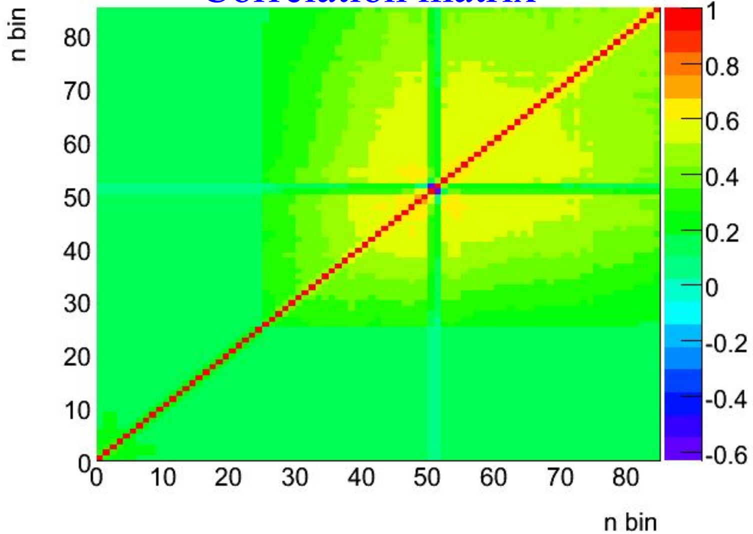

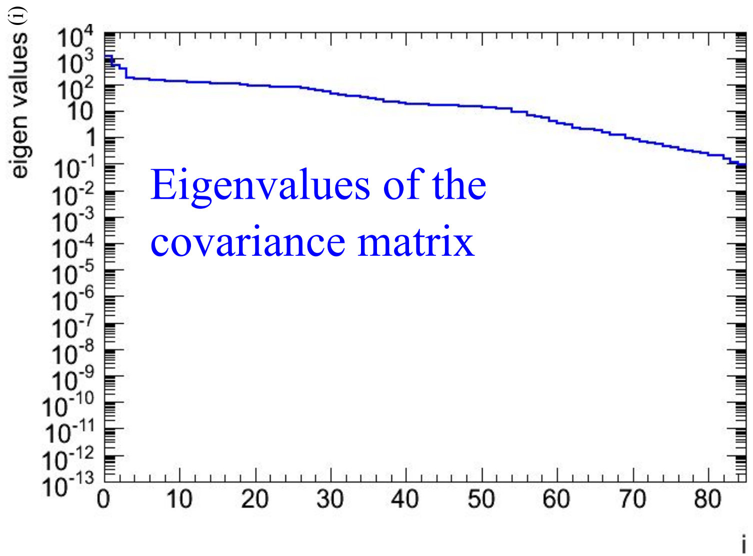

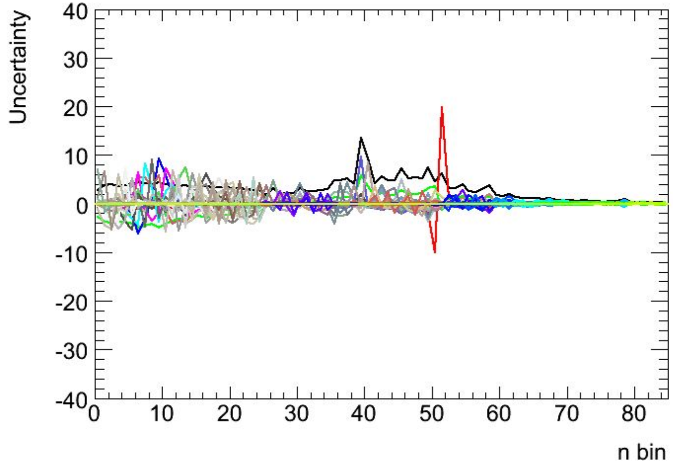

Combining the 3 KLOE measurements

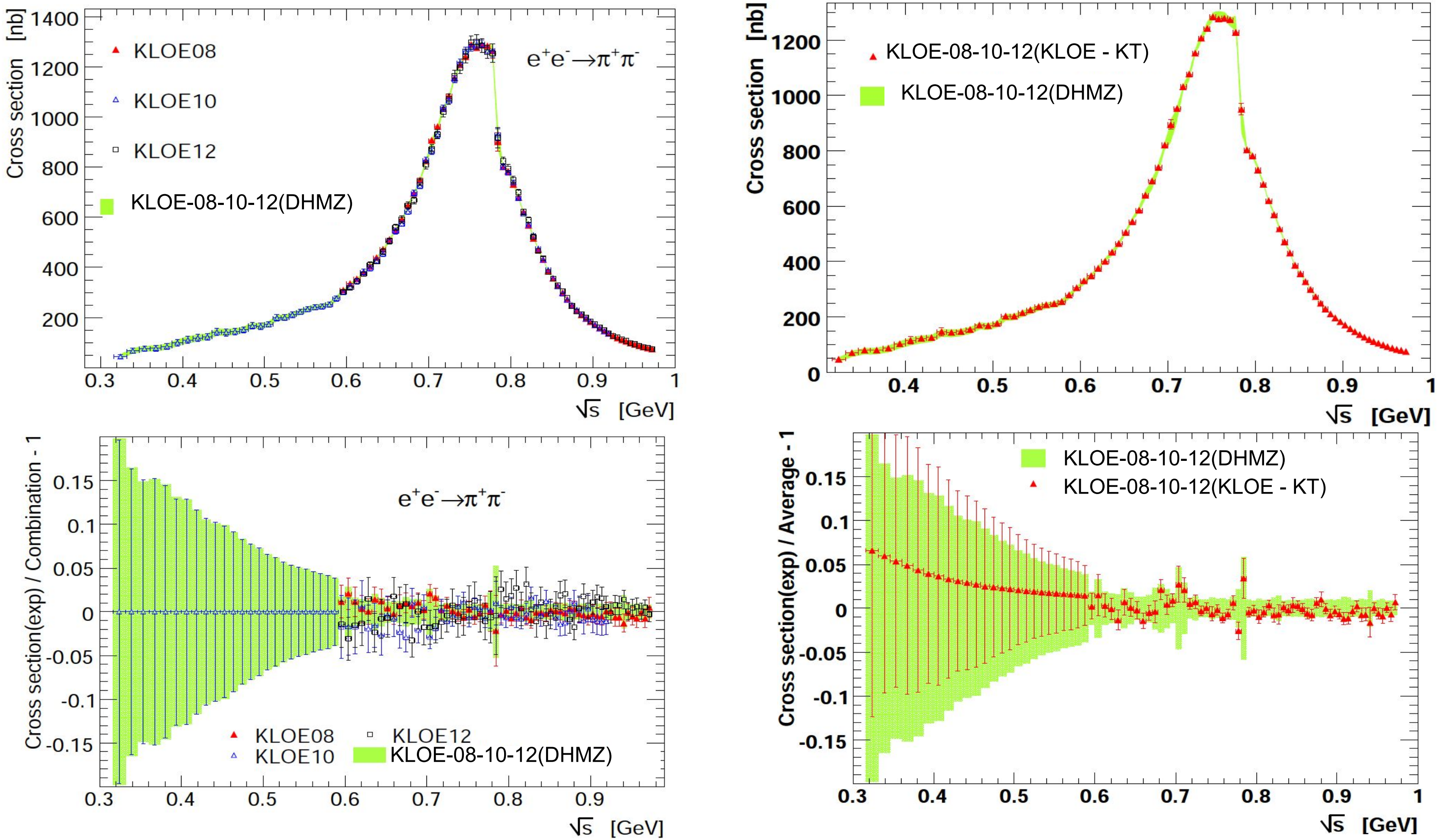

Comparison of / consequences for combination methods

Analysis aspect	DHMZ	KNT
Blinding	Not necessary (No ad-hoc choices to make)	Included for upcoming update
Binning	Fine ($\leq$ 1 MeV) final binning for average and integrals. Large (O(100 MeV) or less) common binning @ intermediate step: compare statistics of experiments coherently for deriving weights in fine bins.	Re-bin data into "clusters". Scans over cluster configurations for optimisation.
Closure test	Using model for spectrum: negligible bias. (since 2009)	Not performed
Additional constraints	Analyticity constraints for 2π channel.	None
Fitting	χ^2 minimisation with correlated uncertainties incorporated locally (in fine & large bins), for deriving weights. Full propagation of uncertainties & correlations.	χ^2 minimisation with correlated uncertainties incorporated globally.
Integration / interpolation	Av. of quadratic splines (3rd order polynomial), integral preservation in bins of measurements. Analyticity-based function for 2π (< 0.6 GeV).	Trapezoidal for continuum, quintic for resonances.
Uncertainty inflation	Local χ^2 uncertainty inflation. (since 2009) Extra BABAR-KLOE systematic. (since 2019)	Local χ^2 uncertainty inflation. (adopted since 2017)
Inter-channel correlations	Taken into account. (since 2010)	Not included.
Missing channels	Estimated based on isospin symmetry. (since 1997 - ADH)	Adopted in subsequent updates

→ Large DHMZ/KNT differences for the resulting uncertainties, as well as for the shapes of the combined spectra

WP TI	DHMZ19	KNT19
$a_\mu^{\mathrm{HVP,\,LO}} \times 10^{10}$	694.0(4.0)	692.8(2.4)

→ CHS approach for 2π and 3π: Analyticity and global χ^2 fit

$a_\mu^{\pi\pi}$ contribution [0.28; 1.8] GeV – spline-based (2018)

→ Updated result:

506.70 ± 2.32 (± 1.01 (stat.) ± 2.08 (syst.)) $[10^{-10}]$

(after uncertainty enhancement by ~14% caused by the tension between inputs, taken into account through a local rescaling)

Total uncertainty: 5.9 (2003) → 2.8 (2011) → 2.6 (2017) → 2.3 (2018)

$a_\mu^{\pi\pi}$ contribution [0.28; 1.8] GeV – spline-based (2018)

→ with KLOE-08-10-12 (KLOE-KT) used as input: 506.55 ± 2.38 [10^{-10}]
(after uncertainty enhancement by 18% caused by the tension between inputs, taken into account through a local rescaling)
→ Compensation between uncertainty reduction for KLOE-08-10-12 (KLOE-KT), inducing a change of weights in DHMZ combination, and tension enhancement

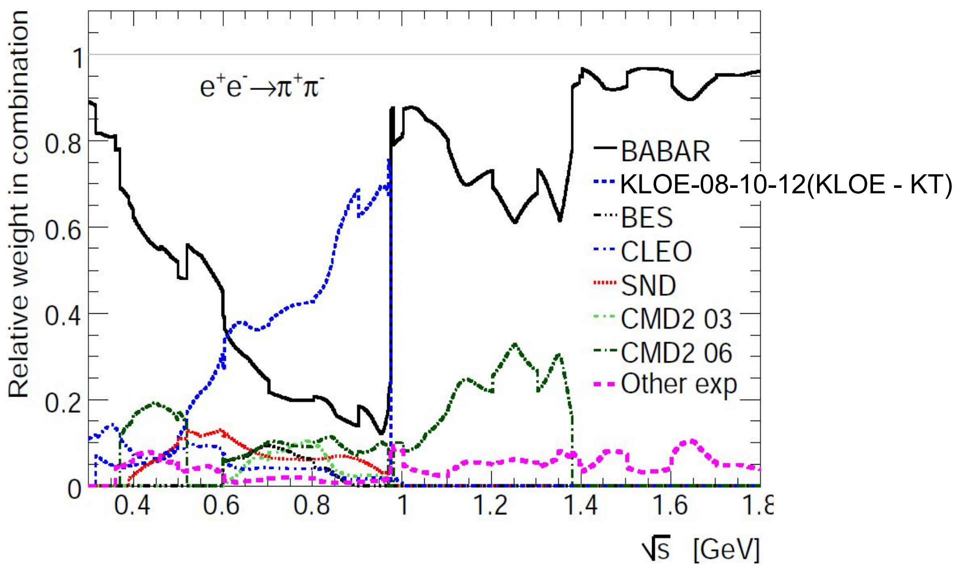

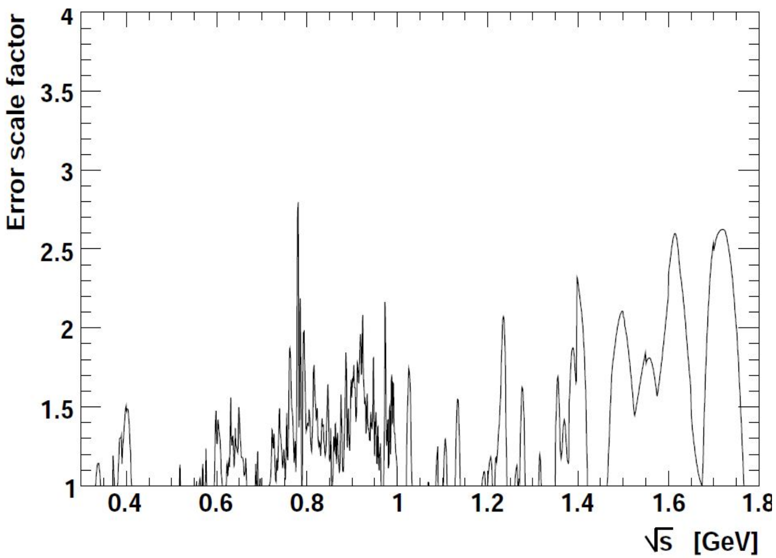

Uncertainties on uncertainties and on correlations

Topic of general interest, in other fields too

1908.00921(DHMZ), 2006.04822(WP Theory Initiative)

Back

Two different approaches for combining (e^+e^-) data

DHMZ:

→ χ^2 computed locally (in each fine bin), taking into account correlations between measurements (see previous slides)

→ Used to determine the weights on the measurements in the combination and their level of agreement

→ Uncertainties and correlations propagated using pseudo-experiments or ±1σ shifts of each uncertainty component

KNT:

→ χ^2 computed globally (for full mass range)

$$\chi^2_I = \sum_{i=1}^{N_{\rm tot}} \sum_{j=1}^{N_{\rm tot}} \left(R_i^{(m)} - \mathcal{R}_m^{i,I}\right) \mathbf{C}_I^{-1}\left(i^{(m)}, j^{(n)}\right)\left(R_j^{(n)} - \mathcal{R}_n^{j,I}\right)$$

KNT (1802.02995)

$$\chi^2 = \sum_{i=1}^{195} \sum_{j=1}^{195} \left(\sigma^0_{\pi\pi(\gamma)}(i) - \bar{\sigma}^0_{\pi\pi(\gamma)}(m)\right) \mathbf{C}^{-1}\left(i^{(m)}, j^{(n)}\right)\left(\sigma^0_{\pi\pi(\gamma)}(j) - \bar{\sigma}^0_{\pi\pi(\gamma)}(n)\right)$$

KLOE-KMT (1711.03085)

→ relies on description of correlations on long ranges

→ *One of the main sources of differences for the uncertainty on* a_μ

Evaluation of uncertainties and correlations (e^+e^-)

	$\sigma_{\pi\pi\gamma}$	$\sigma^0_{\pi\pi}$	F_π	$\Delta^{\pi\pi} a_\mu$
Reconstruction Filter	negligible			
Background subtraction	Tab. 1			0.3%
Trackmass	0.2%			
Pion cluster ID	negligible			
Tracking efficiency	0.3%			
Trigger efficiency	0.1%			
Acceptance	Tab. 2			0.2%
Unfolding	Tab. 3			negligible
L3 filter	0.1%			
$\sqrt{s}$ dependence of H	-	Tab. 4		0.2%
Luminosity	0.3%			
Experimental systematics				0.6%
FSR resummation	-	0.3%		
Radiator function H	-	0.5%		
Vacuum Polarization	-	0.1%	-	0.1%
Theory systematics				0.6%

$M^2_{\pi\pi}$ range (GeV^2)	Systematic error (%)
$0.35 \leq M^2_{\pi\pi} < 0.39$	0.6
$0.39 \leq M^2_{\pi\pi} < 0.43$	0.5
$0.43 \leq M^2_{\pi\pi} < 0.45$	0.4
$0.45 \leq M^2_{\pi\pi} < 0.49$	0.3
$0.49 \leq M^2_{\pi\pi} < 0.51$	0.2
$0.51 \leq M^2_{\pi\pi} < 0.64$	0.1
$0.64 \leq M^2_{\pi\pi} < 0.95$	-

KLOE 08 (0809.3950)

KLOE 10 (1006.5313)

	$\sigma_{\pi\pi\gamma}$	$\sigma^{bare}_{\pi\pi}$	$\vert F_\pi\vert^2$	$\Delta a^{\pi\pi}_\mu$
	threshold ; ρ-peak			(0.1 - 0.85 GeV^2)
Background Filter	0.5% ; 0.1%			negligible
Background subtraction	3.4% ; 0.1%			0.5%
$f_0 + \rho\pi$ bkg.	6.5% ; negl.			0.4%
Ω cut	1.4% ; negl.			0.2%
Trackmass cut	3.0% ; 0.2%			0.5%
π-e PID	0.3% ; negl.			negligible
Trigger	0.3% ; 0.2%			0.2%
Acceptance	1.9% ; 0.3%			0.5%
Unfolding	negl. ; 2.0%			negligible
Tracking	0.3%			
Software Trigger (L3)	0.1%			
Luminosity	0.3%			
Experimental syst.				1.0%
FSR treatment	-	7% ; negl.		0.8%
Radiator function H	-	0.5%		
Vacuum Polarization	-	Ref. [34]	-	0.1%
Theory syst.				0.9%

→ Systematics *evaluated* in ~wide mass ranges with sharp transitions

Evaluation of uncertainties and correlations (e^+e^-)

Sources	0.3-0.4	0.4-0.5	0.5-0.6	0.6-0.9	0.9-1.2	1.2-1.4	1.4-2.0	2.0-3.0
trigger/ filter	5.3	2.7	1.9	1.0	0.7	0.6	0.4	0.4
tracking	3.8	2.1	2.1	1.1	1.7	3.1	3.1	3.1
π-ID	10.1	2.5	6.2	2.4	4.2	10.1	10.1	10.1
background	3.5	4.3	5.2	1.0	3.0	7.0	12.0	50.0
acceptance	1.6	1.6	1.0	1.0	1.6	1.6	1.6	1.6
kinematic fit (χ^2)	0.9	0.9	0.3	0.3	0.9	0.9	0.9	0.9
correl $\mu\mu$ ID loss	3.0	2.0	3.0	1.3	2.0	3.0	10.0	10.0
$\pi\pi/\mu\mu$ non-cancel.	2.7	1.4	1.6	1.1	1.3	2.7	5.1	5.1
unfolding	1.0	2.7	2.7	1.0	1.3	1.0	1.0	1.0
ISR luminosity	3.4	3.4	3.4	3.4	3.4	3.4	3.4	3.4
sum (cross section)	13.8	8.1	10.2	5.0	6.5	13.9	19.8	52.4

BABAR (1205.2228)

→ Systematics *evaluated* in ~wide mass ranges with sharp transitions (statistics limitations when going to narrow ranges)

Combining the 3 KLOE measurements

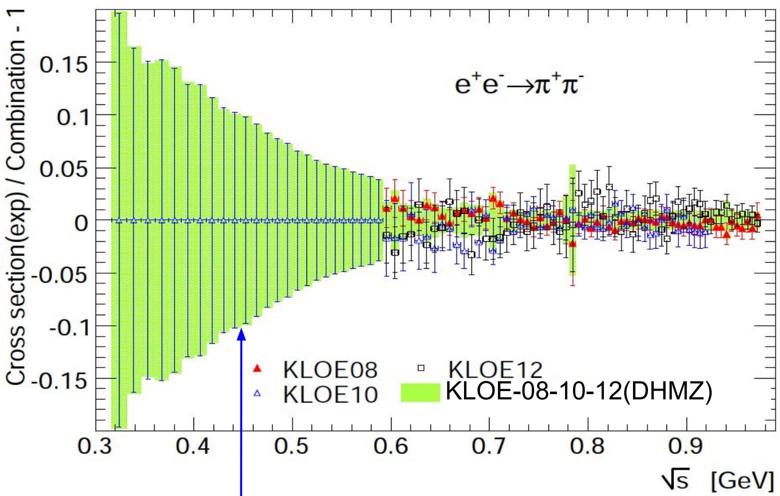

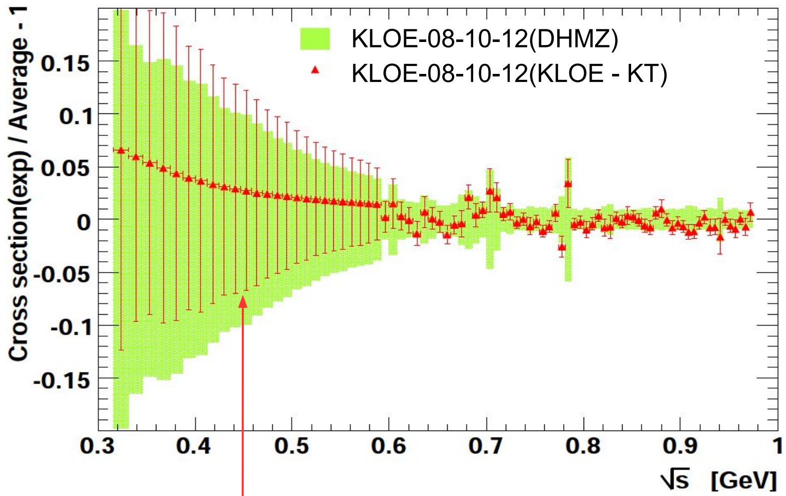

Local combination (DHMZ)

Information propagated between mass regions, through shifts of systematics - relying on correlations, amplitudes and shapes of systematics (KLOE-KT)

Combining the 3 KLOE measurements - $a_\mu^{\pi\pi}$ contribution

KLOE08 a_μ[0.6 ; 0.9] : 368.3 ± 3.2 [10^{-10}]
KLOE10 a_μ[0.6 ; 0.9] : 365.6 ± 3.3
KLOE12 a_μ[0.6 ; 0.9] : 366.8 ± 2.5
→ Correlation matrix:

	08	10	12
08	1	0.70	0.35
10	0.70	1	0.19
12	0.35	0.19	1

→ Amount of independent information provided by each measurement

→ KLOE-08-10-12(DHMZ) - a_μ[0.6 ; 0.9] : 366.5 ± 2.8 (Without χ^2 rescaling: ± 2.2)
→ Conservative treatment of uncertainties and correlations (*not perfectly known*) in weight determination

→ KLOE-08-10-12(KLOE-KT) - a_μ[0.6 ; 0.9]GeV : 366.9 ± 2.2 (Includes χ^2 rescaling)

→ Assuming perfect knowledge of the correlations to minimize average uncertainty

χ^2 definitions and properties

$$\chi^2(\mathbf{d};\mathbf{t}) = \sum_{i,j} (d_i - t_i) \cdot \left[C^{-1}(\mathbf{t})\right]_{ij} \cdot (d_j - t_j) \qquad C_{ij} = C_{ij}^{stat} + \sum_k s_i^k \cdot s_j^k$$

$$\chi^2(\mathbf{d};\mathbf{t}) = \min_{\beta_a} \left\{ \sum_{i,j} \left[d_i - \left(1 + \sum_a \beta_a \cdot \left(\boldsymbol{\epsilon}_a^{\pm}(\beta_a)\right)_i\right) t_i \right] \cdot \left[C_{\mathrm{su}}^{-1}(\mathbf{t})\right]_{ij} \cdot \left[d_j - \left(1 + \sum_a \beta_a \cdot \left(\boldsymbol{\epsilon}_a^{\pm}(\beta_a)\right)_j\right) t_j \right] + \sum_a \beta_a^2 \right\},$$

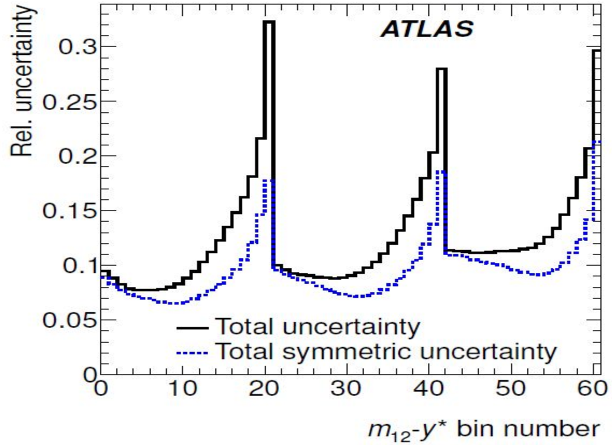

→ Two χ^2 definitions, with systematic uncertainties included in covariance matrix or treated as fitted "nuisance parameters"

→ Equivalent for symmetric Gaussian uncertainties

(1312.3524 - ATLAS)

→ *Both approaches assume the knowledge of the amplitude, shape (phase-space dependence) and correlations of systematic uncertainties*

Back

Comparing lattice QCD and data-driven results in systematically improvable ways

2308.04221 (BMW & DMZ)

Guiding ideas:

→ Need *rigorous* and *realistic* treatment of uncertainties and correlations at all levels
(Underestimated uncertainties do not bring scientific progress & can put studies on wrong path)

→ Caution about significance:
statistics-dominated measurement; prediction uncertainty limited by non-Gaussian systematic effects

→ Studies for understanding differences between data-driven and Lattice QCD approaches need to follow similar standards as the g-2 experiment: *double-blinding*

Back

Lattice calculations and comparisons w.r.t. dispersive

→ Lattice: employ simulations to compute electromagnetic-current two-point function

$$C(t) = \frac{1}{3e^2}\sum_{i=1}^{3}\int d^3x\,\langle J_i(\vec{x},t)J_i(0)\rangle \qquad C(t) = \frac{1}{24\pi^2}\int_0^\infty ds\,\sqrt{s}R(s)\,e^{-|t|\sqrt{s}}$$

$$\frac{J_\mu}{e} = \frac{2}{3}\bar{u}\gamma_\mu u - \frac{1}{3}\bar{d}\gamma_\mu d - \frac{1}{3}\bar{s}\gamma_\mu s + \frac{2}{3}\bar{c}\gamma_\mu c - \frac{1}{3}\bar{b}\gamma_\mu b + \frac{2}{3}\bar{t}\gamma_\mu t$$

$a_\mu^{\text{LO-HVP}}$, $a_{\mu,\text{win}}^{\text{LO-HVP}}$, $\delta\left(\Delta\alpha_{\text{had}}^{(5)}\right) \equiv \Delta\alpha_{\text{had}}^{(5)}(-1 \to -10\text{GeV}^2), \ldots$ are weighted sums of $C(t)$ over t

Based on BMW'20 (+) with preliminary $\delta\left(\Delta\alpha_{\text{had}}^{(5)}\right)$

→ Tensions between lattice and data-driven (DD) HVP results

$\left[\Delta a_\mu^{\text{LO-HVP}}\right]_{\text{lat-DD}} \sim 2.1\sigma \qquad \left[\Delta a_{\mu,\text{win}}^{\text{LO-HVP}}\right]_{\text{lat-DD}} \sim 4.0\sigma$

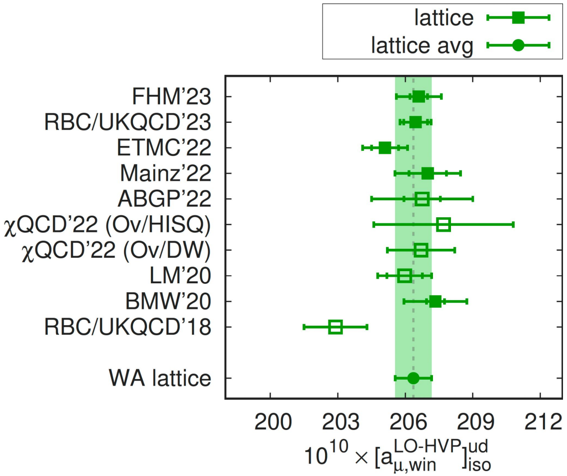

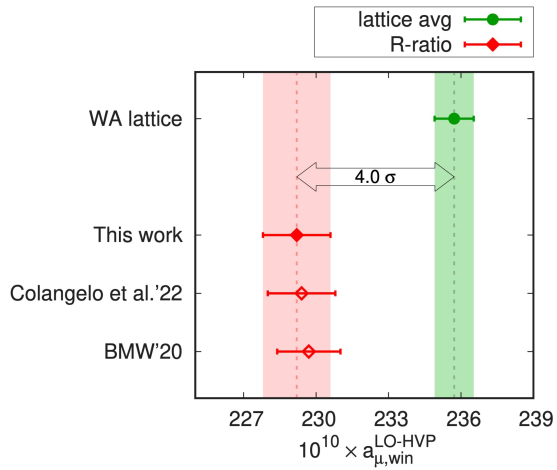

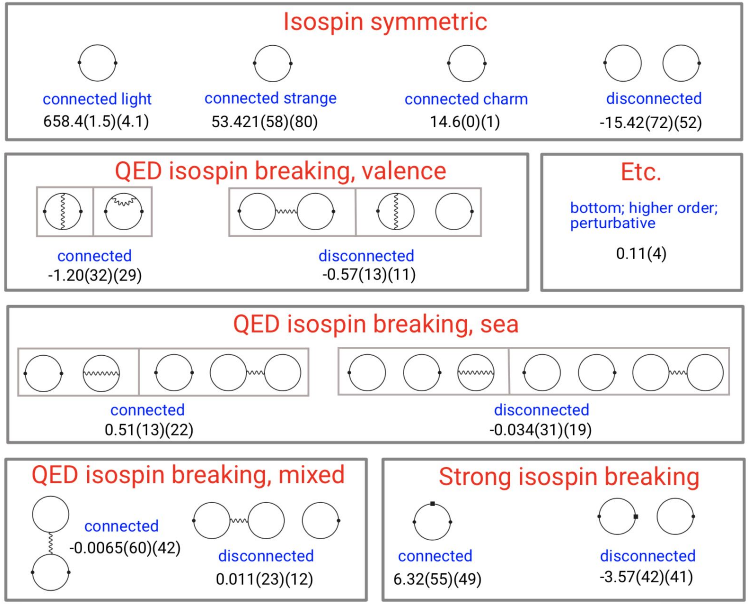

All contributions to C(t), with all limits taken: $a \to 0$, $L \to \infty$, $M_\pi \to M_\pi^\varphi$, ...

Lattice ↔ R-ratio comparison: *requirements*

$$C(t) = \frac{1}{24\pi^2}\int_0^\infty ds\,\sqrt{s}R(s)\,e^{-|t|\sqrt{s}}$$

→ R-ratio → lattice: "straightforward" (integrate R-ratio)

→ Lattice → R-ratio: inverse Laplace transform (ill-posed problem)

(Former) Status for lattice calculations:

→ Very few HVP quantities computed on lattice with:

- All contributions to C(t): flavors, various contractions, QED and SIB corrections
- All limits taken: $a \to 0$, $L \to \infty$, $M_\pi \to M_\pi^\varphi$, ...

→ None with correlations among lattice HVP observables

→ None with uncertainties on these correlations (important for checking stability of inverse problem)

→ Developed statistical approach that:

- Provides useful information with limited lattice input
- Can be systematically improved with more lattice input
- Can (eventually) incorporate physical constraints
- Includes measure of agreement of lattice & R-ratio results with comparison hypothesis
- Accounts for all correlations in lattice and R-ratio observables ...
- ... including uncertainties on these

Lattice covariances: method

→ Uncertainties and correlations critical for comparisons

→ Use extension of BMW uncertainty method with stat. resampling and syst. histogram, with flat and Akaike Information Criterion (AIC) weights

→ Applicable for observables: $\{a_j\} = \left\{a_\mu^{\text{LO-HVP}}, a_{\mu,\text{win}}^{\text{LO-HVP}}, \delta\left(\Delta\alpha_{\text{had}}^{(5)}\right), \dots\right\}$

$$H(A,B) = \sum_{\substack{\phi,\psi_A^{\text{flat}},\psi_A^{\text{AIC}}\\ \psi_B^{\text{flat}},\psi_B^{\text{AIC}}}} w_A\left(\phi,\psi_A^{\text{flat}},\psi_A^{\text{AIC}}\right) \times w_B\left(\phi,\psi_B^{\text{flat}},\psi_B^{\text{AIC}}\right) \times \mathcal{N}_2\left(A,B,\overline{A}\left(\phi,\psi_A^{\text{flat}},\psi_A^{\text{AIC}}\right),\overline{B}\left(\phi,\psi_B^{\text{flat}},\psi_B^{\text{AIC}}\right),C_{\text{stat}}^{(1)}\left(\phi,\psi_A^{\text{flat}},\psi_A^{\text{AIC}},\psi_B^{\text{flat}},\psi_B^{\text{AIC}}\right)\right)$$

with $w\left(\phi,\psi^{\text{flat}},\psi^{\text{AIC}}\right) = \frac{\text{AIC}(\phi,\psi^{\text{flat}},\psi^{\text{AIC}})}{\sum_{\psi^{\text{AIC}}}\text{AIC}(\phi,\psi^{\text{flat}},\psi^{\text{AIC}})}$

correlated / independent choices

→ Build covariance matrix from quantiles of three 1D distributions $\left(a_\mu^{\text{LO-HVP}}, a_{\mu,\text{win}}^{\text{LO-HVP}}, a_\mu^{\text{LO-HVP}} + a_{\mu,\text{win}}^{\text{LO-HVP}}\right)$

→ Separate stat. & syst. by solving (for $\lambda = 2$)

$C_{\text{stat}} + C_{\text{syst}} = C$

$\lambda C_{\text{stat}} + C_{\text{syst}} = C_\lambda$

→ $\delta\left(\Delta\alpha_{\text{had}}^{(5)}\right)$ largely uncorrelated with other two observables

→ Uncertainties and correlations of $a_\mu^{\text{LO-HVP}}$ & $a_{\mu,\text{win}}^{\text{LO-HVP}}$ contributions (units of 10^{-10})

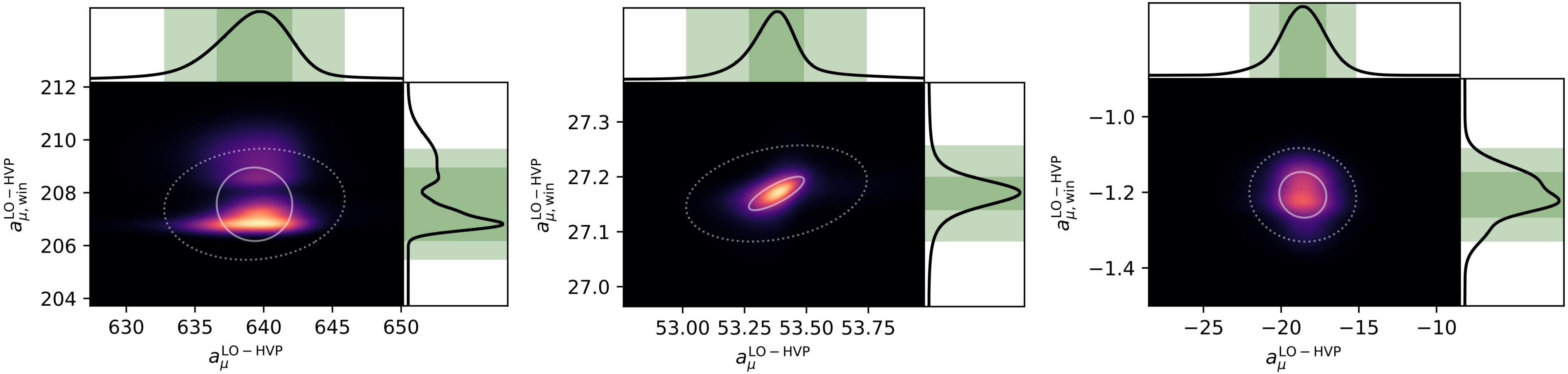

(connected *ud*) (connected *s*) (disconnected)

→ Double peak structure due to the variation $\alpha_s^{(n = 0, 3)}$ in continuum extrapolation

→ Taken into account by considering 1σ & 2σ quantiles

Uncertainties on lattice covariances

→ *Uncertainties on covariance matrix* could potentially compromise the inverse problem

→ *Stat. error on error* estimated from bootstrap on only 48 jackknife samples (sufficient for this study)

→ *Syst. error on error* from:

- For: ud, s, QED, SIB connected, and disconnected
  → Get uncertainties from 1 or 2σ quantiles
  → 0 or 100% correlations in a → 0 uncertainties of $T = a_\mu^{\text{LO-HVP}}$ and $W = a_{\mu,\text{win}}^{\text{LO-HVP}}$, with $C = T - W$

$$C_{TW} = C_{TW}^{\text{other}} + \begin{bmatrix} (dW)^2 + (dC)^2 & \{0,1\} \times (dW)^2 \\ \{0,1\} \times (dW)^2 & (dW)^2 \end{bmatrix}_{\text{cont}}$$

- Similarly for c

→ Result (in units of 10^{-20}):

$$C_{\text{lat}}^{1\sigma,0\%} = \begin{bmatrix} 30.13(4.88) & -0.05(0.03) \\ -0.05(0.03) & 1.95(0.47) \end{bmatrix} \qquad C_{\text{lat}}^{2\sigma,0\%} = \begin{bmatrix} 34.04(16.80) & 0.32(0.05) \\ 0.32(0.05) & 1.12(0.07) \end{bmatrix}$$

$$C_{\text{lat}}^{1\sigma,100\%} = \begin{bmatrix} 30.13(4.88) & 1.56(0.03) \\ 1.56(0.03) & 1.95(0.47) \end{bmatrix} \qquad C_{\text{lat}}^{2\sigma,100\%} = \begin{bmatrix} 34.04(16.80) & 1.94(0.05) \\ 1.94(0.05) & 1.12(0.07) \end{bmatrix}$$

Testing lattice

→ 1-by-1 comparison of moment integrals

Observable	lattice BMW'20	data-driven	diff.	% diff.	σ	p-value [%]
$a_\mu^{\text{LO-HVP}} \times 10^{10}$	707.5(5.5)	694.0(4.0)	13.5(6.8)	1.9(1.0)	2.0	4.7
$a_{\mu,\text{win}}^{\text{LO-HVP}} \times 10^{10}$	236.7(1.4)	229.2(1.4)	7.5(2.0)	3.2(0.8)	3.8	0.01
$\left[\Delta_{\text{had}}^{(5)}\alpha(-10\,\text{GeV}^2) - \Delta_{\text{had}}^{(5)}\alpha(-1\,\text{GeV}^2)\right] \times 10^4$	48.67(0.32)	48.02(0.32)	0.65(0.45)	1.3(0.9)	1.4	15.

→ Simultaneous comparisons with correlations

$$\chi^2(a_j) = \sum_{j,k} \left[a_j^{\text{lat}} - a_j\right] \left[C_{\text{lat}}^{-1}\right]_{jk} \left[a_k^{\text{lat}} - a_k\right] + \sum_{j,k} \left[a_j^{\text{R}} - a_j\right] \left[C_{\text{R}}^{-1}\right]_{jk} \left[a_k^{\text{R}} - a_k\right]$$

$$\chi^2_{\min} = \sum_{j,k} \left[a_j^{\text{lat}} - a_j^{\text{R}}\right] \left[(C_{\text{lat}} + C_{\text{R}})^{-1}\right]_{jk} \left[a_k^{\text{lat}} - a_k^{\text{R}}\right]$$

# observ.	χ^2/dof	p-value [%]
2	14.4/2 – 18.8/2	0.002 – 0.017
3	14.4/3 – 18.8/3	0.009 – 0.63

→ Some dilution compared to $a_{\mu,\text{win}}^{\text{LO-HVP}}$ alone, but still significant tension

→ (Taking into account the shapes of integral kernels) Differences could be explained by: a *C(t)* that is enhanced in $t \sim [0.4, 1.5]$ fm, also probably for $t \gtrsim 1.5$ fm, with possible suppression for $t \lesssim 0.4$ fm

Consequences of direct lattice / dispersive moments comparison for *C(t)*

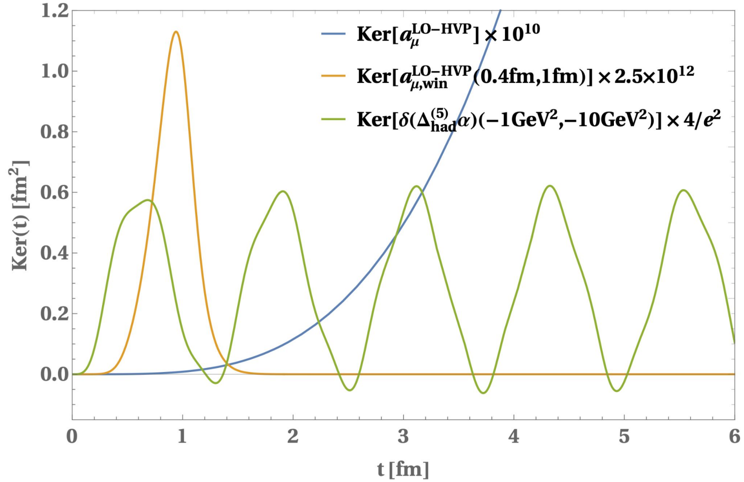

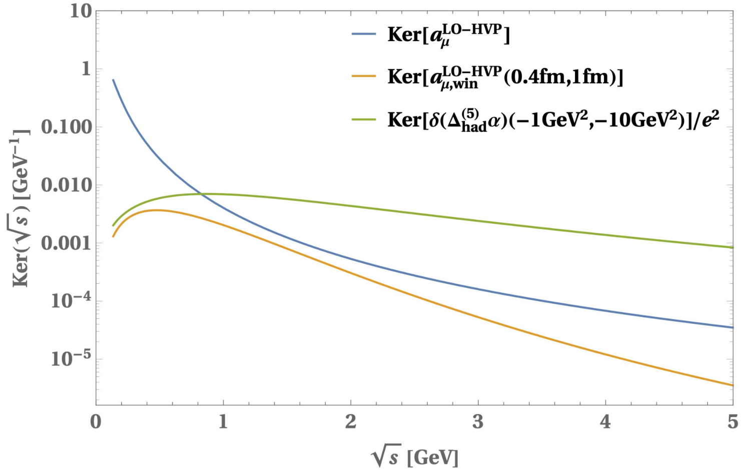

→ SD:ID:LD windows

- 10%:33%:57% for $a_\mu^{\text{LO-HVP}}$
- 70%:29%:1% for $\delta\left(\Delta\alpha_{\text{had}}^{(5)}\right)$

\+ Taking into account the tensions and agreements above:

→ Excess in *C(t)* for t ~ [0.4, 1.5] fm

→ Probably for $t \gtrsim 1.5$ fm

→ Possible suppression for $t \lesssim 0.4$ fm (mainly based on preliminary$\delta\left(\Delta\alpha_{\text{had}}^{(5)}\right)$)

Testing R-ratio: methodology

→ Chop a_j^{R} into contributions $a_{j,b}^{\mathrm{R}}$ from same $\sqrt{s}$-intervals I_b for all j :

$$a_j^{\mathrm{R}} = \sum_b a_{j,b}^{\mathrm{R}}$$

→ To accommodate lattice results a_j^{lat}, allow common rescaling of $a_{j,b}^{\mathrm{R}}$, for all j, in certain I_b :

$$a_j^{\mathrm{lat}} = \sum_b \gamma_b \cdot a_{j,b}^{\mathrm{R}}$$

- Simplest interpretation: R-ratio rescaled in I_b
- However, constrains shape of R-ratio modification in limited way: *physical deformation may be allowed*

→ If $N_j \geq N_b$, system (over-)constrained: solved here for one γ via weighted average and/or χ^2 minimization, while avoiding too strong assumptions about the knowledge of uncertainties and correlations

$$a_j^{\mathrm{lat}} = \sum_{b\,\in A} \gamma \cdot a_{j,b}^{\mathrm{R}} + \sum_{b\,\in B} a_{j,b}^{\mathrm{R}} \qquad \to \gamma = \frac{a_j^{\mathrm{lat}} - \sum_{b\,\in B} a_{j,b}^{\mathrm{R}}}{\sum_{b\,\in A} a_{j,b}^{\mathrm{R}}} \equiv \tilde{\gamma}_j\,;$$

$$\chi^2(\gamma) = \sum_{j,k} [\gamma - \tilde{\gamma}_j] \left[\left(C_{\mathrm{lat}}^{\tilde{\gamma}} + C_{\mathrm{R}}^{\tilde{\gamma}} \right)^{-1} \right]_{jk} [\gamma - \tilde{\gamma}_k]$$

$$\chi^2(\gamma) = \sum_{j,k} \left[a_j^{\mathrm{lat}} - \sum_{b\,\in A} \gamma \cdot a_{jb} - \sum_{b\,\in B} a_{jb} \right] [C_{\mathrm{lat}}^{-1}]_{jk} \left[a_k^{\mathrm{lat}} - \sum_{c\,\in A} \gamma \cdot a_{kc} - \sum_{c\,\in B} a_{kc} \right]$$
$$+ \sum_{(jb),(kc)} \left[a_{jb}^{\mathrm{R}} - a_{jb} \right] [C_{\mathrm{R}}^{-1}]_{(jb)(kc)} \left[a_{kc}^{\mathrm{R}} - a_{kc} \right]$$

→ Somewhat different interpretation, still compatible results

Sensitivity to the lattice statistical uncertainties on covariance matrix

→ Employ 2nd order sampling (bootstraps on jackknife samples) to build distributions for the quantities of interest: re-run procedure with fluctuated lattice covariance matrix

→ Quantiles of these distributions to quantitatively evaluate the impact

→ Normalisation factor and its uncertainty from fit precisely determined

→ Conclusions about χ^2 and p-values stable within lattice statistical uncertainties on covariance matrix

2 input moment integrals; Normalisation fit < 0.96 GeV;
Lattice covariance matrix "0"

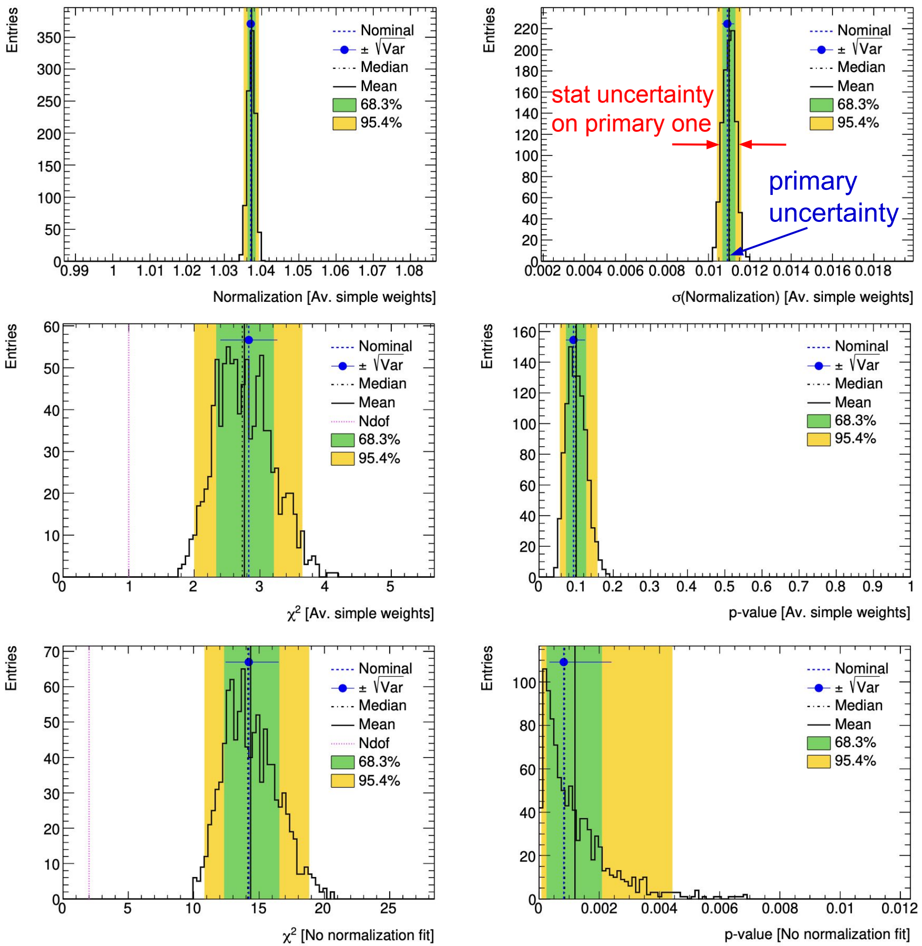

Testing R-ratio: results

→ Lattice → R-ratio: inverse Laplace transform (ill-posed problem)

→ *New in this study*: Correlations among lattice HVP observables and uncertainties on these correlations

Consider $a_j = a_\mu^{\text{LO-HVP}}, a_{\mu,\text{win}}^{\text{LO-HVP}}$ (2 observables) with $a_j = \delta\left(\Delta\alpha_{\text{had}}^{(5)}\right)$ (3 observables)

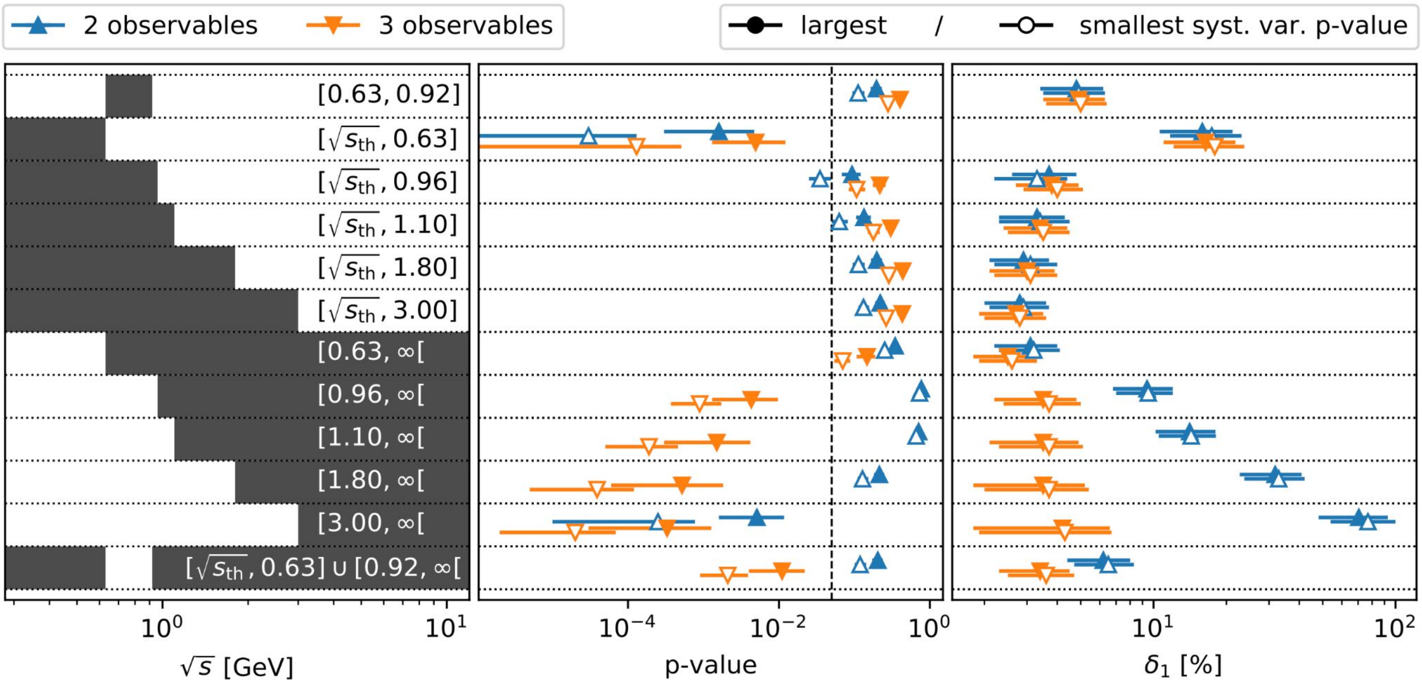

→ Differences could be explained by enhancing measured R-ratio around (/any larger interval including) ρ-peak

→ Outcome of the studies stable within stat. and syst. uncertainties on lattice covariance matrices

→ Rescalings beyond the uncertainties of Re^+e^- → No problems for EW fits in case of 3-observable

Testing R-ratio: summary of results

Modifications to measured R-ratio that could explain lattice results are:

→ Possible in ρ-peak interval [0.63, 0.92] GeV for 2 & 3 observables

- Requires rescaling of observables in that interval by ~ (5.0 ± 1.5)%

→ Disfavored in interval below ρ-peak, [$\sqrt{s_{th}}$, 0.63 GeV]

→ Possible in [$\sqrt{s_{th}}$, $\sqrt{s_{max}}$] with $\sqrt{s_{max}}$: 0.96 → 3.0GeV that include ρ-peak, for 2 & 3 observables

- Rescalings ~(4±1)% → (3±1)% for $\sqrt{s_{max}}$ ↗

→ Possible in [$\sqrt{s_{min}}$, ∞[with $\sqrt{s_{min}}$: 0.63 → 1.8 GeV, for 2 observables

- Rescalings ~(3±1)% → (32±9)% for $\sqrt{s_{min}}$ ↗

→ Disfavored in [3.0 GeV, ∞[, for 2 & 3 observables

→ Adding $\delta\left(\Delta\alpha_{had}^{(5)}\right)$ constraint eliminates the possibility of rescalings in [$\sqrt{s_{min}}$, ∞[with $\sqrt{s_{min}}$: 0.96 → 3.0 GeV that do not include ρ-peak

Results - Normalisation < 0.96 GeV; lattice covariance matrix "0"

2 input moment integrals

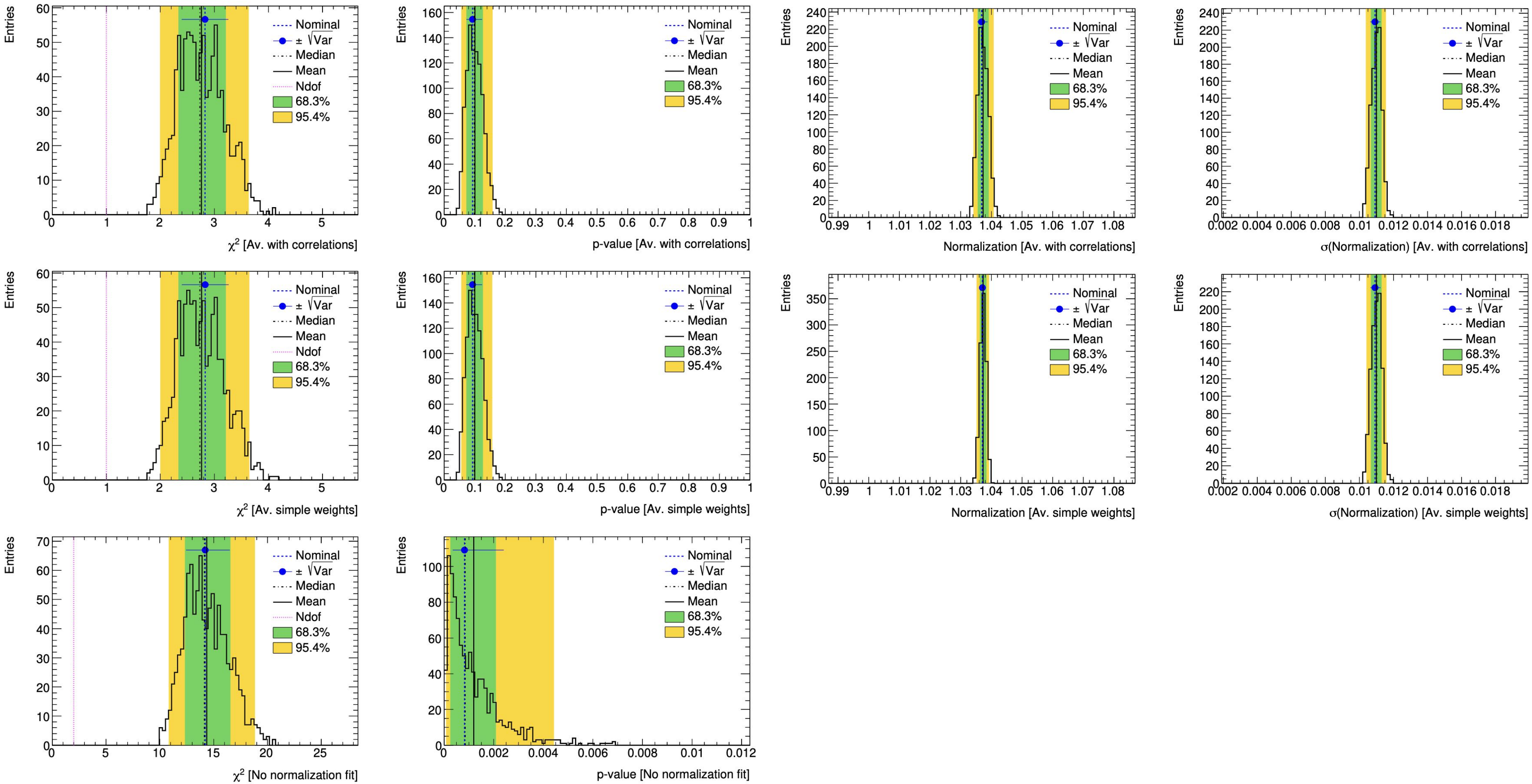

2 input moment integrals

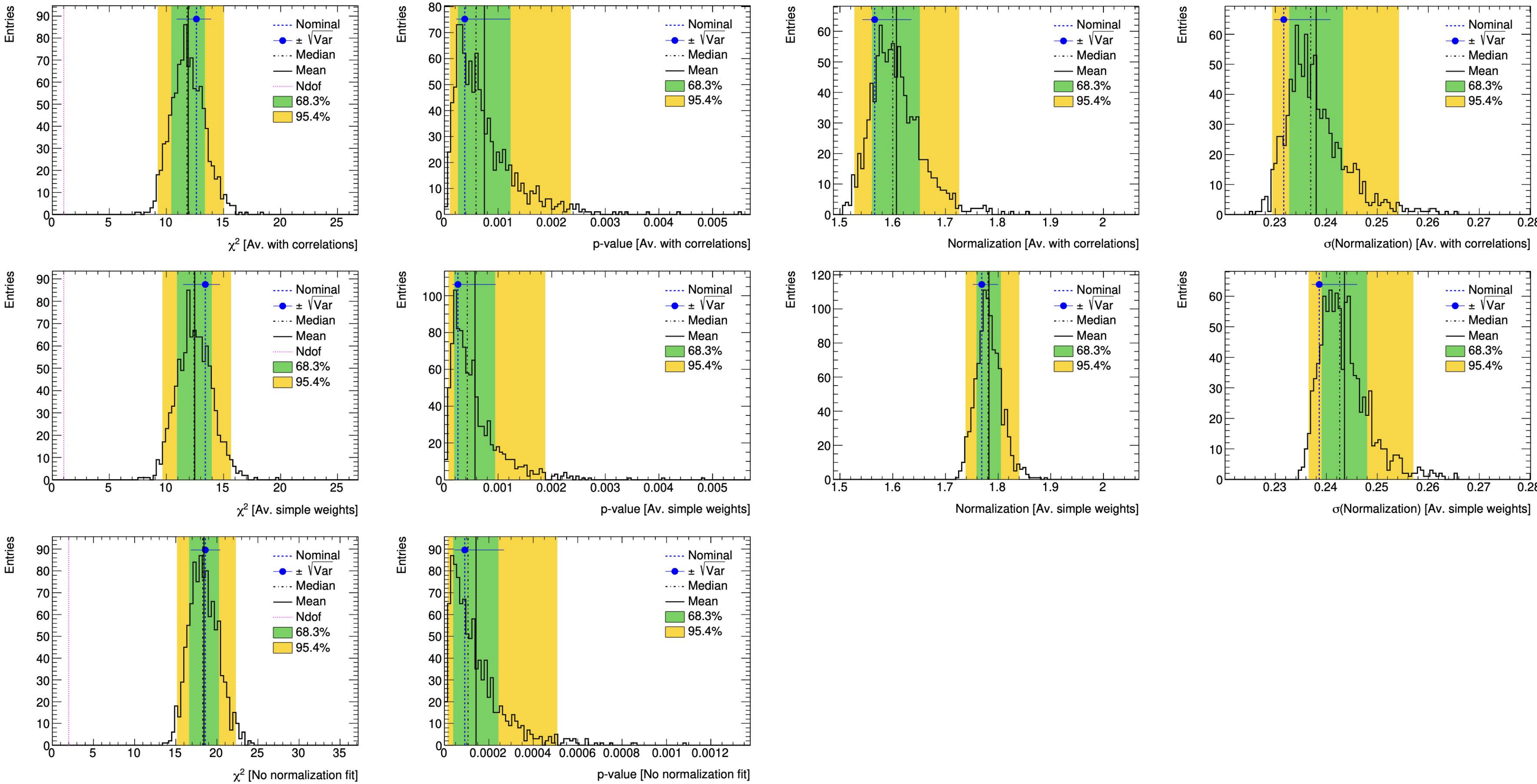

Testing R-ratio: results

Number of observables	I_1 [GeV]	Lat.cov.	$\delta_1 \equiv (\gamma_1 - 1)$	$\chi^2/ndof$	p-value	$\delta_1 \times \Delta\alpha_{\rm had}^{(5)}(M_Z^2)[I_1] \times 10^4$
2	$[\sqrt{s_{\rm th}}, 0.63]$	0	$15.9(5.3)[^{+0.9}_{-0.8}]\%$	$10.0[^{+2.4}_{-1.9}]/1$	$0.16[^{+0.31}_{-0.13}]\%$	0.80
2	$[\sqrt{s_{\rm th}}, 0.63]$	3	$17.4(5.7)[^{+0.6}_{-0.5}]\%$	$17.4[^{+2.2}_{-1.9}]/1$	$0.003[^{+0.010}_{-0.004}]\%$	0.88
2	$[0.63, \infty[$	0	$3.1(0.9)[^{+0.05}_{-0.05}]\%$	$0.9[^{+0.1}_{-0.1}]/1$	$34.6[^{+3.2}_{-3.2}]\%$	8.49
2	$[0.63, \infty[$	3	$3.2(0.9)[^{+0.02}_{-0.02}]\%$	$1.3[^{+0.1}_{-0.1}]/1$	$25.2[^{+2.8}_{-2.2}]\%$	8.71
3	$[\sqrt{s_{\rm th}}, 0.63]$	0	$16.4(5.4)[^{+0.9}_{-0.7}]\%$	$10.6[^{+2.2}_{-1.7}]/2$	$0.49[^{+0.73}_{-0.36}]\%$	0.83
3	$[\sqrt{s_{\rm th}}, 0.63]$	3	$17.9(5.8)[^{+0.6}_{-0.5}]\%$	$17.8[^{+2.1}_{-1.9}]/2$	$0.013[^{+0.038}_{-0.016}]\%$	0.91
3	$[0.63, \infty[$	0	$2.5(0.7)[^{+0.08}_{-0.07}]\%$	$3.8[^{+0.6}_{-0.5}]/2$	$14.7[^{+4.2}_{-4.0}]\%$	6.68
3	$[0.63, \infty[$	3	$2.6(0.7)[^{+0.04}_{-0.04}]\%$	$5.3[^{+0.5}_{-0.4}]/2$	$7.0[^{+1.8}_{-1.6}]\%$	6.96
2	$[\sqrt{s_{\rm th}}, 0.96]$	0	$3.7(1.1)[^{+0.1}_{-0.1}]\%$	$2.8[^{+0.5}_{-0.4}]/1$	$9.3[^{+2.8}_{-2.5}]\%$	1.32
2	$[\sqrt{s_{\rm th}}, 0.96]$	3	$3.9(1.1)[^{+0.06}_{-0.06}]\%$	$4.4[^{+0.4}_{-0.5}]/1$	$3.5[^{+1.4}_{-1.0}]\%$	1.39
2	$[0.96, \infty[$	0	$9.4(2.6)[^{+0.04}_{-0.04}]\%$	$0.09[^{+0.01}_{-0.009}]/1$	$77.0[^{+1.2}_{-1.3}]\%$	22.59
2	$[0.96, \infty[$	3	$9.5(2.5)[^{+0.02}_{-0.02}]\%$	$0.12[^{+0.01}_{-0.01}]/1$	$72.9[^{+1.5}_{-1.1}]\%$	22.75
3	$[\sqrt{s_{\rm th}}, 0.96]$	0	$3.8(1.1)[^{+0.09}_{-0.09}]\%$	$3.1[^{+0.4}_{-0.3}]/2$	$21.7[^{+4.3}_{-4.2}]\%$	1.36
3	$[\sqrt{s_{\rm th}}, 0.96]$	3	$4.0(1.1)[^{+0.06}_{-0.05}]\%$	$4.5[^{+0.4}_{-0.4}]/2$	$10.7[^{+3.2}_{-2.3}]\%$	1.42
3	$[0.96, \infty[$	2	$3.5(1.3)[^{+0.2}_{-0.2}]\%$	$10.9[^{+2.2}_{-1.6}]/2$	$0.43[^{+0.54}_{-0.30}]\%$	8.35
3	$[0.96, \infty[$	3	$3.7(1.3)[^{+0.1}_{-0.1}]\%$	$14.1[^{+1.5}_{-1.2}]/2$	$0.089[^{+0.083}_{-0.052}]\%$	8.91
2	$[\sqrt{s_{\rm th}}, 1.1]$	0	$3.3(1.0)[^{+0.1}_{-0.1}]\%$	$2.2[^{+0.4}_{-0.3}]/1$	$13.4[^{+3.2}_{-2.9}]\%$	1.40
2	$[\sqrt{s_{\rm th}}, 1.1]$	3	$3.4(1.0)[^{+0.05}_{-0.04}]\%$	$3.5[^{+0.3}_{-0.4}]/1$	$6.3[^{+1.9}_{-1.3}]\%$	1.46
2	$[1.1, \infty[$	0	$14.1(3.9)[^{+0.07}_{-0.08}]\%$	$0.1[^{+0.02}_{-0.02}]/1$	$70.9[^{+1.6}_{-1.6}]\%$	33.01
2	$[1.1, \infty[$	3	$14.3(3.8)[^{+0.04}_{-0.04}]\%$	$0.2[^{+0.02}_{-0.02}]/1$	$65.8[^{+1.8}_{-1.4}]\%$	33.31
3	$[\sqrt{s_{\rm th}}, 1.1]$	0	$3.4(1.0)[^{+0.07}_{-0.07}]\%$	$2.4[^{+0.3}_{-0.3}]/2$	$30.3[^{+4.5}_{-4.4}]\%$	1.44
3	$[\sqrt{s_{\rm th}}, 1.1]$	3	$3.5(1.0)[^{+0.04}_{-0.04}]\%$	$3.5[^{+0.3}_{-0.3}]/2$	$17.8[^{+3.8}_{-2.8}]\%$	1.49
3	$[1.1, \infty[$	2	$3.5(1.4)[^{+0.2}_{-0.2}]\%$	$13.0[^{+2.9}_{-2.0}]/2$	$0.15[^{+0.27}_{-0.12}]\%$	8.14
3	$[1.1, \infty[$	3	$3.7(1.4)[^{+0.1}_{-0.1}]\%$	$17.1[^{+1.9}_{-1.6}]/2$	$0.019[^{+0.027}_{-0.014}]\%$	8.70
2	$[\sqrt{s_{\rm th}}, 1.8]$	0	$2.9(0.8)[^{+0.1}_{-0.1}]\%$	$1.7[^{+0.3}_{-0.2}]/1$	$19.8[^{+3.4}_{-3.2}]\%$	1.63
2	$[\sqrt{s_{\rm th}}, 1.8]$	3	$3.1(0.9)[^{+0.03}_{-0.03}]\%$	$2.5[^{+0.2}_{-0.3}]/1$	$11.3[^{+2.4}_{-1.8}]\%$	1.69
2	$[1.8, \infty[$	0	$31.8(9.1)[^{+0.6}_{-0.6}]\%$	$1.5[^{+0.2}_{-0.2}]/1$	$21.4[^{+3.4}_{-3.2}]\%$	70.17
2	$[1.8, \infty[$	3	$32.9(9.2)[^{+0.4}_{-0.3}]\%$	$2.3[^{+0.2}_{-0.2}]/1$	$12.8[^{+2.5}_{-1.8}]\%$	72.62
3	$[\sqrt{s_{\rm th}}, 1.8]$	0	$3.0(0.9)[^{+0.05}_{-0.05}]\%$	$1.7[^{+0.2}_{-0.2}]/2$	$43.7[^{+4.9}_{-5.2}]\%$	1.65
3	$[\sqrt{s_{\rm th}}, 1.8]$	3	$3.1(0.9)[^{+0.03}_{-0.03}]\%$	$2.5[^{+0.2}_{-0.3}]/2$	$28.6[^{+4.5}_{-3.5}]\%$	1.70
3	$[1.8, \infty[$	2	$3.5(1.7)[^{+0.2}_{-0.1}]\%$	$15.1[^{+3.6}_{-2.4}]/2$	$0.052[^{+0.130}_{-0.046}]\%$	7.79
3	$[1.8, \infty[$	3	$3.7(1.7)[^{+0.08}_{-0.08}]\%$	$20.3[^{+2.4}_{-2.0}]/2$	$0.0039[^{+0.0081}_{-0.0034}]\%$	8.18
2	$[\sqrt{s_{\rm th}}, 3.0]$	0	$2.8(0.8)[^{+0.06}_{-0.06}]\%$	$1.5[^{+0.2}_{-0.2}]/1$	$22.0[^{+3.4}_{-3.2}]\%$	2.03
2	$[\sqrt{s_{\rm th}}, 3.0]$	3	$2.9(0.8)[^{+0.03}_{-0.03}]\%$	$2.3[^{+0.2}_{-0.2}]/1$	$13.2[^{+2.5}_{-1.9}]\%$	2.10
2	$[3.0, \infty[$	0	$70.5(22.4)[^{+3.6}_{-3.2}]\%$	$7.8[^{+1.7}_{-1.4}]/1$	$0.51[^{+0.66}_{-0.35}]\%$	143.42
2	$[3.0, \infty[$	3	$76.9(23.9)[^{+2.4}_{-2.2}]\%$	$13.4[^{+1.6}_{-1.5}]/1$	$0.025[^{+0.052}_{-0.024}]\%$	156.38
3	$[\sqrt{s_{\rm th}}, 3.0]$	0	$2.7(0.8)[^{+0.05}_{-0.05}]\%$	$1.7[^{+0.3}_{-0.2}]/2$	$43.1[^{+5.8}_{-6.1}]\%$	1.97
3	$[\sqrt{s_{\rm th}}, 3.0]$	3	$2.8(0.8)[^{+0.03}_{-0.03}]\%$	$2.7[^{+0.3}_{-0.3}]/2$	$26.3[^{+4.3}_{-3.7}]\%$	2.04
3	$[3.0, \infty[$	2	$4.2(2.4)[^{+0.09}_{-0.08}]\%$	$16.0[^{+3.9}_{-2.6}]/2$	$0.033[^{+0.094}_{-0.030}]\%$	8.59
3	$[3.0, \infty[$	3	$4.3(2.4)[^{+0.06}_{-0.05}]\%$	$21.7[^{+2.7}_{-2.2}]/2$	$0.0020[^{+0.0049}_{-0.0018}]\%$	8.80
2	$[0.63, 0.92]$	0	$4.8(1.4)[^{+0.1}_{-0.1}]\%$	$1.7[^{+0.3}_{-0.2}]/1$	$19.6[^{+3.4}_{-3.2}]\%$	1.42
2	$[0.63, 0.92]$	3	$4.9(1.4)[^{+0.06}_{-0.05}]\%$	$2.5[^{+0.2}_{-0.3}]/1$	$11.2[^{+2.4}_{-1.8}]\%$	1.47
2	$[\sqrt{s_{\rm th}}, 0.63] \cup [0.92, \infty[$	0	$6.2(1.8)[^{+0.1}_{-0.1}]\%$	$1.6[^{+0.2}_{-0.2}]/1$	$20.4[^{+3.4}_{-3.2}]\%$	15.33
2	$[\sqrt{s_{\rm th}}, 0.63] \cup [0.92, \infty[$	3	$6.5(1.8)[^{+0.07}_{-0.07}]\%$	$2.4[^{+0.2}_{-0.2}]/1$	$11.9[^{+2.4}_{-1.8}]\%$	15.88
3	$[0.63, 0.92]$	0	$4.9(1.4)[^{+0.08}_{-0.08}]\%$	$1.8[^{+0.2}_{-0.2}]/2$	$40.2[^{+4.0}_{-4.1}]\%$	1.45
3	$[0.63, 0.92]$	3	$5.0(1.4)[^{+0.05}_{-0.05}]\%$	$2.6[^{+0.2}_{-0.2}]/2$	$27.9[^{+4.0}_{-3.1}]\%$	1.50
3	$[\sqrt{s_{\rm th}}, 0.63] \cup [0.92, \infty[$	0	$3.4(1.1)[^{+0.2}_{-0.1}]\%$	$9.0[^{+1.8}_{-1.3}]/2$	$1.1[^{+1.1}_{-0.7}]\%$	8.30
3	$[\sqrt{s_{\rm th}}, 0.63] \cup [0.92, \infty[$	3	$3.6(1.1)[^{+0.08}_{-0.08}]\%$	$12.4[^{+1.3}_{-1.1}]/2$	$0.21[^{+0.18}_{-0.12}]\%$	8.80

Considering more observables in the data-driven approach

→ Enhancement of available information limited by the (anti-)correlations among the moment integrals

Moment integral	Correlation coefficients																		
$\Delta\alpha^{(5)}_{\rm had}(-10\ {\rm GeV}^2)$	1																		
$\Delta\alpha^{(5)}_{\rm had}(-9\ {\rm GeV}^2)$	0.999	1																	
$\Delta\alpha^{(5)}_{\rm had}(-8\ {\rm GeV}^2)$	0.999	0.999	1																
$\Delta\alpha^{(5)}_{\rm had}(-7\ {\rm GeV}^2)$	0.996	0.998	0.999	1															
$\Delta\alpha^{(5)}_{\rm had}(-6\ {\rm GeV}^2)$	0.993	0.995	0.998	0.999	1														
$\Delta\alpha^{(5)}_{\rm had}(-5\ {\rm GeV}^2)$	0.986	0.990	0.994	0.997	0.999	1													
$\Delta\alpha^{(5)}_{\rm had}(-4\ {\rm GeV}^2)$	0.976	0.981	0.986	0.991	0.995	0.999	1												
$\Delta\alpha^{(5)}_{\rm had}(-3\ {\rm GeV}^2)$	0.960	0.966	0.973	0.980	0.986	0.993	0.998	1											
$\Delta\alpha^{(5)}_{\rm had}(-2\ {\rm GeV}^2)$	0.931	0.939	0.948	0.957	0.967	0.977	0.987	0.996	1										
$\Delta\alpha^{(5)}_{\rm had}(-1\ {\rm GeV}^2)$	0.874	0.885	0.896	0.909	0.923	0.938	0.955	0.973	0.990	1									
$a_{\mu,\rm win}^{\rm LO\text{-}HVP}$ $[0, 0.1]$ fm	0.806	0.791	0.774	0.753	0.728	0.698	0.660	0.611	0.543	0.442	1								
$a_{\mu,\rm win}^{\rm LO\text{-}HVP}$ $[0.1, 0.4]$ fm	0.959	0.955	0.949	0.942	0.931	0.916	0.895	0.864	0.813	0.723	0.864	1							
$a_{\mu,\rm win}^{\rm LO\text{-}HVP}$ $[0.4, 0.7]$ fm	0.876	0.887	0.899	0.912	0.926	0.940	0.954	0.966	0.972	0.958	0.428	0.786	1						
$a_{\mu,\rm win}^{\rm LO\text{-}HVP}$ $[0.7, 1]$ fm	0.711	0.726	0.743	0.762	0.784	0.809	0.838	0.873	0.91	0.961	0.206	0.509	0.893	1					
$a_{\mu,\rm win}^{\rm LO\text{-}HVP}$ $[1, 1.3]$ fm	0.604	0.619	0.636	0.656	0.678	0.705	0.738	0.778	0.831	0.901	0.123	0.365	0.775	0.973	1				
$a_{\mu,\rm win}^{\rm LO\text{-}HVP}$ $[1.3, 1.6]$ fm	0.553	0.568	0.584	0.604	0.626	0.653	0.686	0.728	0.783	0.861	0.093	0.305	0.710	0.941	0.993	1			
$a_{\mu,\rm win}^{\rm LO\text{-}HVP}$ $[1.6, 2.6]$ fm	0.508	0.522	0.537	0.556	0.577	0.604	0.636	0.677	0.733	0.814	0.074	0.260	0.647	0.891	0.963	0.987	1		
$a_{\mu,\rm win}^{\rm LO\text{-}HVP}$ $[2.6, 4]$ fm	0.419	0.431	0.445	0.461	0.479	0.502	0.530	0.567	0.617	0.694	0.052	0.197	0.523	0.753	0.840	0.885	0.944	1	
$a_{\mu,\rm win}^{\rm LO\text{-}HVP}$ $[4, \infty[$ fm	0.312	0.321	0.332	0.344	0.358	0.375	0.397	0.426	0.466	0.528	0.034	0.137	0.381	0.565	0.646	0.698	0.787	0.942	1

→ Employing blinding approach in BMW - DHMZ collaboration: here sharing only uncertainties and correlations for dispersive result while pending lattice-based calculations of new moments

Considering more observables in the data-driven approach

→ Quantify available information through the distribution of eigenvalues for covariance, correlation and normalized covariance matrices (complementary information): strong correlations yield small eigenvalues

Moment integral		Eigenvalues		
$a_{\mu,\mathrm{win}}^{\mathrm{LO\text{-}HVP}}$ $[t_{\min}, t_{\max}]$	Total uncertainty	Covariance	Correlation	Normalized covariance
$[0, 0.1]$ fm	$8.18 \cdot 10^{-12}$	$3.12 \cdot 10^{-20}$	4.85	$2.04 \cdot 10^{-4}$
$[0.1, 0.4]$ fm	$3.86 \cdot 10^{-11}$	$3.52 \cdot 10^{-21}$	1.76	$8.39 \cdot 10^{-5}$
$[0.4, 0.7]$ fm	$6.43 \cdot 10^{-11}$	$6.38 \cdot 10^{-22}$	$3.32 \cdot 10^{-1}$	$1.45 \cdot 10^{-5}$
$[0.7, 1]$ fm	$8.00 \cdot 10^{-11}$	$1.53 \cdot 10^{-22}$	$4.88 \cdot 10^{-2}$	$2.06 \cdot 10^{-6}$
$[1, 1.3]$ fm	$7.90 \cdot 10^{-11}$	$8.77 \cdot 10^{-24}$	$4.27 \cdot 10^{-3}$	$1.87 \cdot 10^{-7}$
$[1.3, 1.6]$ fm	$6.32 \cdot 10^{-11}$	$4.64 \cdot 10^{-25}$	$4.47 \cdot 10^{-4}$	$1.88 \cdot 10^{-8}$
$[1.6, \infty[$ fm	$1.15 \cdot 10^{-10}$	$7.89 \cdot 10^{-26}$	$1.51 \cdot 10^{-5}$	$6.34 \cdot 10^{-10}$

Normalized covariance ← $[C_{\mathrm{R}}]_{ij} / \left(a_i^{\mathrm{R}} \cdot a_j^{\mathrm{R}}\right)$

Moment integral		Eigenvalues		
$a_{\mu,\mathrm{win}}^{\mathrm{LO\text{-}HVP}}$ $[t_{\min}, t_{\max}]$	Total uncertainty	Covariance	Correlation	Normalized covariance
$[0, 0.1]$ fm	$8.18 \cdot 10^{-12}$	$2.76 \cdot 10^{-20}$	6.07	$2.49 \cdot 10^{-4}$
$[0.1, 0.4]$ fm	$3.86 \cdot 10^{-11}$	$3.17 \cdot 10^{-21}$	1.99	$9.28 \cdot 10^{-5}$
$[0.4, 0.7]$ fm	$6.43 \cdot 10^{-11}$	$5.11 \cdot 10^{-22}$	$6.86 \cdot 10^{-1}$	$2.72 \cdot 10^{-5}$
$[0.7, 1]$ fm	$8.00 \cdot 10^{-11}$	$1.33 \cdot 10^{-22}$	$2.29 \cdot 10^{-1}$	$9.71 \cdot 10^{-6}$
$[1, 1.3]$ fm	$7.90 \cdot 10^{-11}$	$1.52 \cdot 10^{-23}$	$2.12 \cdot 10^{-2}$	$8.76 \cdot 10^{-7}$
$[1.3, 1.6]$ fm	$6.32 \cdot 10^{-11}$	$1.20 \cdot 10^{-24}$	$2.36 \cdot 10^{-3}$	$9.89 \cdot 10^{-8}$
$[1.6, 2.6]$ fm	$9.32 \cdot 10^{-11}$	$2.91 \cdot 10^{-25}$	$3.90 \cdot 10^{-4}$	$1.59 \cdot 10^{-8}$
$[2.6, 4]$ fm	$2.01 \cdot 10^{-11}$	$2.15 \cdot 10^{-26}$	$3.43 \cdot 10^{-5}$	$1.41 \cdot 10^{-9}$
$[4, \infty[$ fm	$2.64 \cdot 10^{-12}$	$1.78 \cdot 10^{-27}$	$5.83 \cdot 10^{-7}$	$2.50 \cdot 10^{-11}$

→ 2 extra moment integrals add ~1 d.o.f.

Considering more observables in the data-driven approach

Moment integral	Total uncertainty	Eigenvalues Covariance	Eigenvalues Correlation	Eigenvalues Normalized covariance
$\Delta\alpha_{\rm had}^{(5)}(-10\ {\rm GeV}^2)$	$4.80 \cdot 10^{-5}$	$1.48 \cdot 10^{-8}$	14.74	$5.21 \cdot 10^{-4}$
$\Delta\alpha_{\rm had}^{(5)}(-9\ {\rm GeV}^2)$	$4.64 \cdot 10^{-5}$	$2.17 \cdot 10^{-10}$	3.26	$1.34 \cdot 10^{-4}$
$\Delta\alpha_{\rm had}^{(5)}(-8\ {\rm GeV}^2)$	$4.48 \cdot 10^{-5}$	$4.09 \cdot 10^{-12}$	$7.36 \cdot 10^{-1}$	$2.92 \cdot 10^{-5}$
$\Delta\alpha_{\rm had}^{(5)}(-7\ {\rm GeV}^2)$	$4.29 \cdot 10^{-5}$	$1.94 \cdot 10^{-14}$	$2.40 \cdot 10^{-1}$	$1.02 \cdot 10^{-5}$
$\Delta\alpha_{\rm had}^{(5)}(-6\ {\rm GeV}^2)$	$4.09 \cdot 10^{-5}$	$2.22 \cdot 10^{-16}$	$2.16 \cdot 10^{-2}$	$8.90 \cdot 10^{-7}$
$\Delta\alpha_{\rm had}^{(5)}(-5\ {\rm GeV}^2)$	$3.85 \cdot 10^{-5}$	$3.40 \cdot 10^{-18}$	$2.45 \cdot 10^{-3}$	$1.02 \cdot 10^{-7}$
$\Delta\alpha_{\rm had}^{(5)}(-4\ {\rm GeV}^2)$	$3.57 \cdot 10^{-5}$	$1.99 \cdot 10^{-20}$	$4.17 \cdot 10^{-4}$	$1.68 \cdot 10^{-8}$
$\Delta\alpha_{\rm had}^{(5)}(-3\ {\rm GeV}^2)$	$3.23 \cdot 10^{-5}$	$9.27 \cdot 10^{-23}$	$3.92 \cdot 10^{-5}$	$1.59 \cdot 10^{-9}$
$\Delta\alpha_{\rm had}^{(5)}(-2\ {\rm GeV}^2)$	$2.78 \cdot 10^{-5}$	$1.40 \cdot 10^{-23}$	$2.33 \cdot 10^{-6}$	$8.94 \cdot 10^{-11}$
$\Delta\alpha_{\rm had}^{(5)}(-1\ {\rm GeV}^2)$	$2.07 \cdot 10^{-5}$	$7.03 \cdot 10^{-25}$	$1.15 \cdot 10^{-7}$	$4.78 \cdot 10^{-12}$
$a_{\mu,\rm win}^{\rm LO\text{-}HVP}$ $[0, 0.1]$ fm	$8.18 \cdot 10^{-12}$	$1.47 \cdot 10^{-25}$	$3.46 \cdot 10^{-10}$	$1.22 \cdot 10^{-14}$
$a_{\mu,\rm win}^{\rm LO\text{-}HVP}$ $[0.1, 0.4]$ fm	$3.86 \cdot 10^{-11}$	$7.96 \cdot 10^{-28}$	$3.76 \cdot 10^{-13}$	$1.19 \cdot 10^{-17}$
$a_{\mu,\rm win}^{\rm LO\text{-}HVP}$ $[0.4, 0.7]$ fm	$6.43 \cdot 10^{-11}$	$1.66 \cdot 10^{-28}$	$2.28 \cdot 10^{-13}$	$7.40 \cdot 10^{-18}$
$a_{\mu,\rm win}^{\rm LO\text{-}HVP}$ $[0.7, 1]$ fm	$8.00 \cdot 10^{-11}$	$4.50 \cdot 10^{-30}$	$9.74 \cdot 10^{-14}$	$3.10 \cdot 10^{-18}$
$a_{\mu,\rm win}^{\rm LO\text{-}HVP}$ $[1, 1.3]$ fm	$7.90 \cdot 10^{-11}$	$5.25 \cdot 10^{-31}$	$3.07 \cdot 10^{-14}$	$9.72 \cdot 10^{-19}$
$a_{\mu,\rm win}^{\rm LO\text{-}HVP}$ $[1.3, 1.6]$ fm	$6.32 \cdot 10^{-11}$	$8.57 \cdot 10^{-32}$	$1.40 \cdot 10^{-14}$	$4.38 \cdot 10^{-19}$
$a_{\mu,\rm win}^{\rm LO\text{-}HVP}$ $[1.6, 2.6]$ fm	$9.32 \cdot 10^{-11}$	$-4.56 \cdot 10^{-27}$	$-2.24 \cdot 10^{-14}$	$-7.06 \cdot 10^{-19}$
$a_{\mu,\rm win}^{\rm LO\text{-}HVP}$ $[2.6, 4]$ fm	$2.01 \cdot 10^{-11}$	$-2.01 \cdot 10^{-23}$	$-3.79 \cdot 10^{-14}$	$-1.19 \cdot 10^{-18}$
$a_{\mu,\rm win}^{\rm LO\text{-}HVP}$ $[4, \infty[$ fm	$2.64 \cdot 10^{-12}$	$-1.12 \cdot 10^{-22}$	$-1.22 \cdot 10^{-13}$	$-3.83 \cdot 10^{-18}$

$[C_{\rm R}]_{ij} / \left(a_i^{\rm R} \cdot a_j^{\rm R}\right)$

→ 10 extra moment integrals, but no additional independent d.o.f.

Detailed conclusions for lattice / dispersive comparisons

→ Presented flexible method for comparing lattice QCD and data-driven HVP results

→ Find that discrepancies/agreements between lattice and data-driven results for

$a_\mu^{\text{LO-HVP}}$, $a_{\mu,\text{win}}^{\text{LO-HVP}}$, $\delta\left(\Delta\alpha_{\text{had}}^{(5)}\right)$

On lattice side, result from:

- a $C(t)$ that is enhanced in $t \sim [0.4, 1.5]$ fm
- also probably for $t \gtrsim 1.5$ fm
- with possible suppression for $t \lesssim 0.4$ fm (mainly based on preliminary $\delta\left(\Delta\alpha_{\text{had}}^{(5)}\right)$)

On data-driven side, could be explained by:

- enhancing measured R-ratio around ρ-peak
- or in any larger interval including ρ-peak

→ Lattice and measured R-ratio correlations of uncertainties critical for drawing such conclusions

Detailed conclusions for lattice / dispersive comparisons

→ Important to check that uncertainties on uncertainties and correlations do not spoil picture, especially for inverse problem

- checked here for lattice stat and syst uncertainties
- must do so for measured R-ratio uncertainties

→ Also important not to share results between 2 approaches before they are final (mutual blinding)

→ With more HVP observables, many generalizations possible, also including physics-driven constraints

→ However, limit on independent HVP observables in data-driven and lattice approaches

→ Same methods can be used to combine determinations of lattice and data-driven results for HVP observables, once differences are understood

→ No problems with EW fits in case of 3-observable comparisons (not shown)

Some references to related work on HVP

→ Windows proposed in RBC/UKQCD arXiv:1801.07224

→ Discussed in context of detailed comparison in Colangelo et al arXiv:2205.12963

→ Consequences of rescaling of measured R-ratio studied in Crivellin et al arXiv:2003.04886, Keshavarzi et al arXiv:2006.12666, de Rafael arXiv:2006.13880, Malaescu et al arXiv:2008.08107

→ Consequences of lattice $\Delta a_\mu^{\text{LO-HVP}}$ on $\pi^+\pi^-$ contributions to R-ratio with physical constraints in Colangelo et al arXiv:2010.07943

→ Use of Backus-Gilbert method for reconstruction of smeared R-ratio from lattice C(t) in Hansen et al arXiv:1903.06476, Alexandrou et al arXiv:2212.08467

→ Proposal for comparing measured R-ratio and lattice C(t) via spectral-width sumrules in Boito et al arXiv:2210.13677

… (many other references for reconstructing spectral functions from lattice correlators)

Merging dispersive and lattice HVP calculations

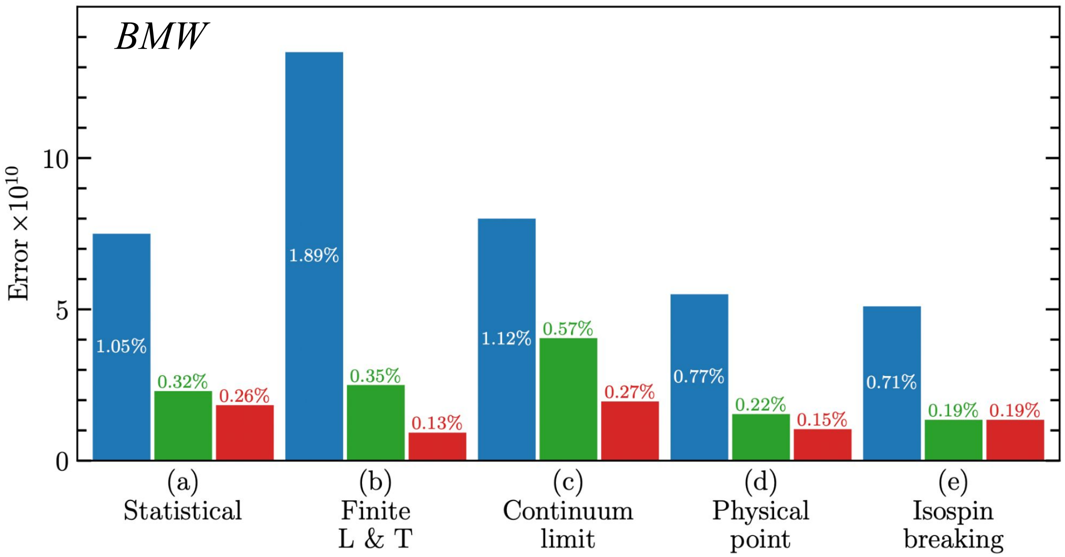

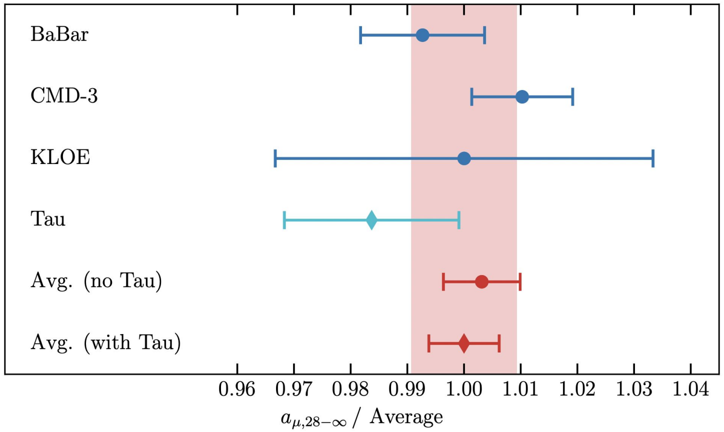

2407.10913

→ *Currently most precise prediction, based on improved lattice QCD (BMW) + data-driven inputs (DMZ) at large-t (input data in good agreement at low energy)*

Back

Merging dispersive and lattice HVP calculations

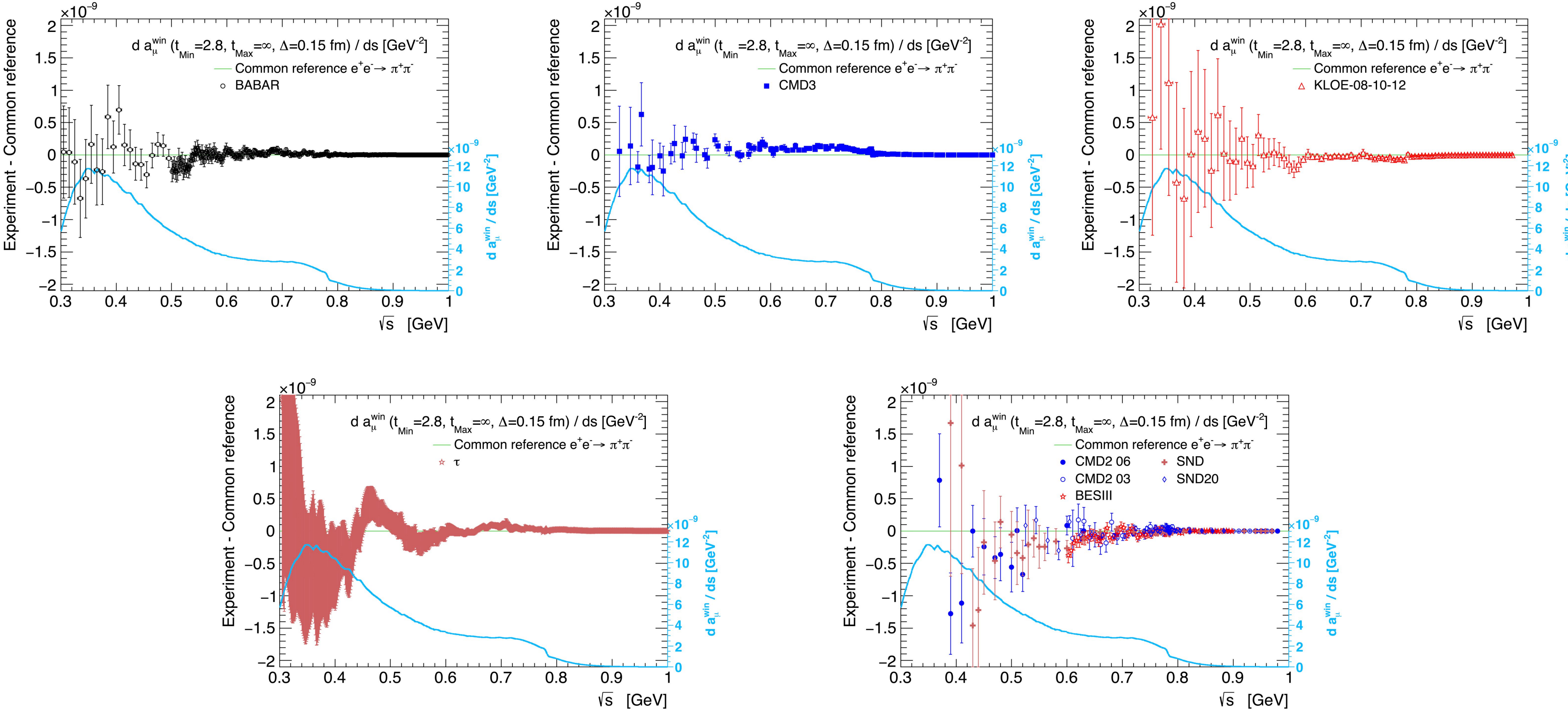

2407.10913

Comparisons of lattice HVP calculations

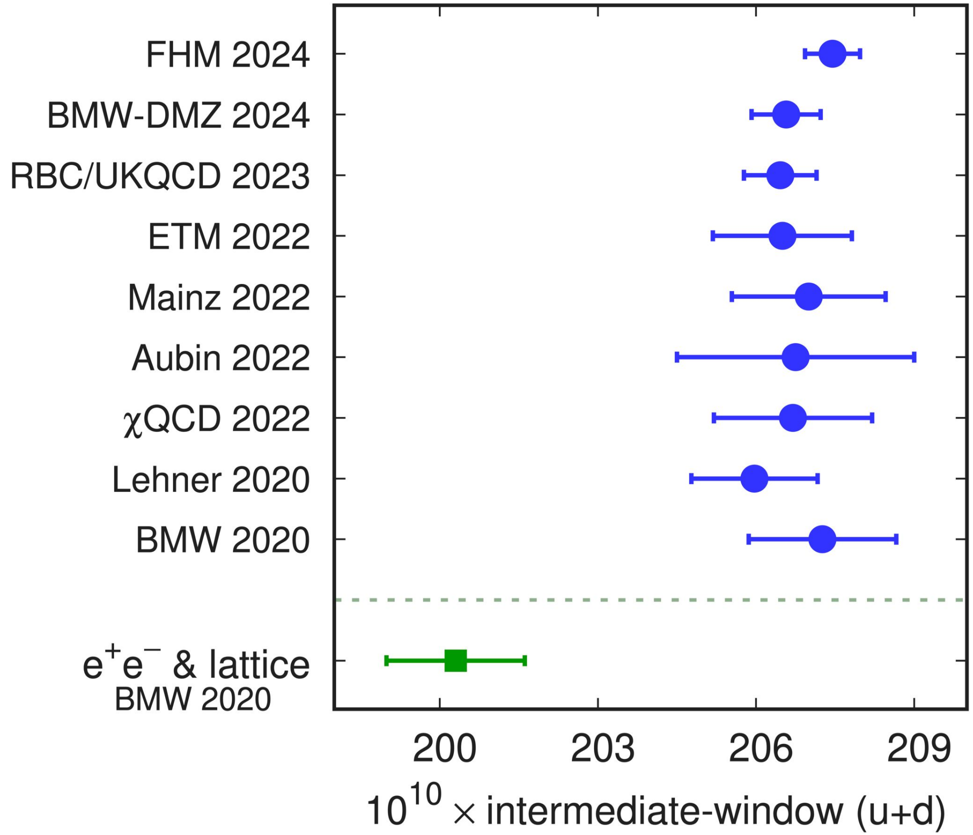

CERN Courier March-April '25

Impact of correlations between a_μ and α_{QED} on the EW fit

2008.08107(BM, Matthias Schott)

See also: Crivellin et al, 2003.04886; Keshavarzi et al., 2006.12666 ;de Rafael, 2006.13880; Colangelo et al, 2010.07943

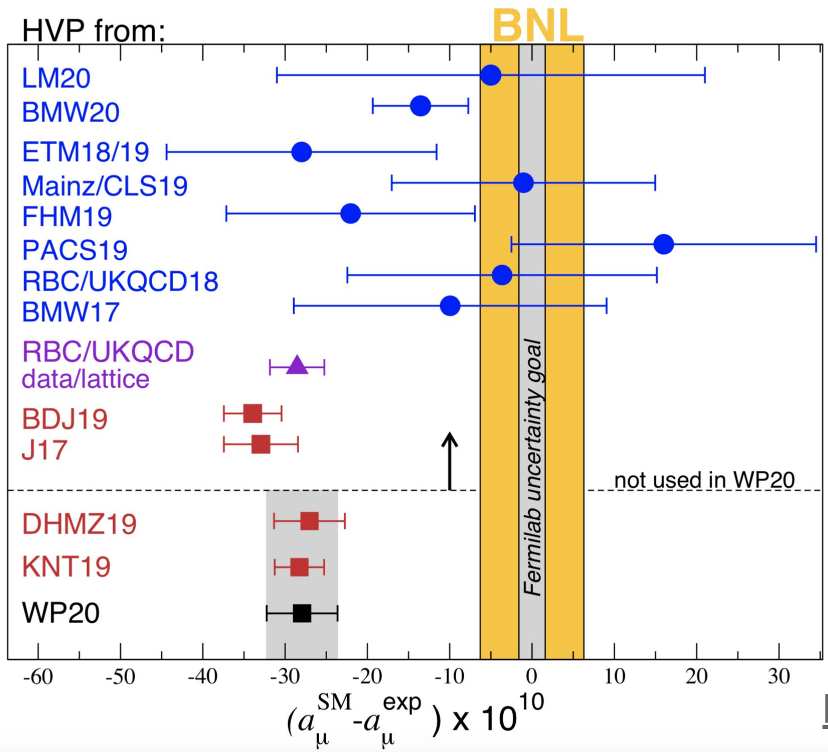

Back

Approaches considered for treating the a_μ - α_{QED} correlations

Studied approaches probing different hypotheses concerning the possible source(s) of the a_μ tension(s) :

(0) Scaling factor applied to the HVP contribution from some energy range of the hadronic spectrum

→ Approaches taking into account (*for the first time*) the full correlations between the uncertainties of the HVP contributions to a_μ and α_{QED} , based on input from DHMZ 19 (arXiv:1908.00921): correlations between points/bins of a measurement in a given channel, between different measurements in the same channel, between different channels; full treatment of the BABAR-KLOE tension in the $\pi^+\pi^-$ channel

Computation (Energy range)	$a_\mu^{\text{HVP, LO}}$ $[10^{-10}]$	$\Delta\alpha_{\text{had}}(M_Z^2)$ $[10^{-4}]$	ρ
Phenomenology (Full HVP)	694.0 ± 4.0	275.3 ± 1.0	44%
Phenomenology ([Th.; 1.8 GeV])	635.5 ± 3.9	55.4 ± 0.4	86%
Phenomenology ([Th.; 1 GeV])	539.8 ± 3.8	36.3 ± 0.3	99.5%
Lattice (Full HVP)BMW 20 (v1)	712.4 ± 4.5	-	-

(1) Cov. matrix of a_μ and α_{QED} (Pheno) described by a nuisance parameter (NP_1) impacting both quantities (used to shift a_μ to some "target" value - coherent shift applied to α_{QED}) and another one (NP_2) impacting only α_{QED} (used in the EW fit)
Note: "target" values chosen in order to reach agreement with the BMW 20 prediction / Experimental a_μ ($\pm 1\sigma$)

Uncertainty components	$a_\mu^{\text{HVP, LO}}$	$\Delta\alpha_{\text{had}}(M_Z^2)$
NP_1	$\sigma(a_\mu^{\text{HVP, LO}})$	$\sigma(\Delta\alpha_{\text{had}}(M_Z^2)) \cdot \rho$
NP_2	0	$\sigma(\Delta\alpha_{\text{had}}(M_Z^2)) \cdot \sqrt{1-\rho^2}$

(2) Include the HVP contribution to a_μ as extra parameter in the EW fit, constrained by the Pheno & BMW 20 values
Note: Also accounted for the coherent impact of α_S on the HVP contribution and on the EW fit

Results: comparing the Phenomenology & BMW 20 values

$a_\mu^{\text{HVP, LO}}$ shift (Energy range)	*Approach 0* Scaling factor	*Approach 0* $\Delta'\alpha_{\text{had}}(M_Z^2)$	*Approach 1* Shift NP_1	*Approach 1* $\sigma'\left(\Delta\alpha_{\text{had}}(M_Z^2)\right)$	*Approach 1* $\Delta'\alpha_{\text{had}}(M_Z^2)$
$a_{\mu\,(\text{Lattice})}^{\text{HVP, LO}} - a_{\mu\,(\text{Pheno})}^{\text{HVP, LO}}$ (Full HVP)	1.027	0.02826	4.6	$9.0 \cdot 10^{-5}$	0.02774
$(a_{\mu\,(\text{Lattice})}^{\text{HVP, LO}} - 1\sigma) - a_{\mu\,(\text{Pheno})}^{\text{HVP, LO}}$ (Full HVP)	1.020	0.02808	3.5	$9.0 \cdot 10^{-5}$	0.02769
$a_{\mu\,(\text{Lattice})}^{\text{HVP, LO}} - a_{\mu\,(\text{Pheno})}^{\text{HVP, LO}}$ ([Th.; 1.8 GeV])	1.029	0.02769	4.7	$9.5 \cdot 10^{-5}$	0.02768
$(a_{\mu\,(\text{Lattice})}^{\text{HVP, LO}} - 1\sigma) - a_{\mu\,(\text{Pheno})}^{\text{HVP, LO}}$ ([Th.; 1.8 GeV])	1.022	0.02765	3.5	$9.5 \cdot 10^{-5}$	0.02764
$a_{\mu\,(\text{Lattice})}^{\text{HVP, LO}} - a_{\mu\,(\text{Pheno})}^{\text{HVP, LO}}$ ([Th.; 1 GeV])	1.034	0.02765	-	-	-
$(a_{\mu\,(\text{Lattice})}^{\text{HVP, LO}} - 1\sigma) - a_{\mu\,(\text{Pheno})}^{\text{HVP, LO}}$ ([Th.; 1 GeV])	1.026	0.02762	-	-	-

→ Large scaling factors (w.r.t. exp. uncertainties) & significant shifts of NP_1

$a_\mu^{\text{HVP, LO}}$ shift (Energy range)	Nominal $\Delta'\alpha_{\text{had}}(M_Z^2)$	Nominal χ^2/ndf	*Approach 0* $\Delta'\alpha_{\text{had}}(M_Z^2)$	*Approach 0* χ^2/ndf	*Approach 1* $\Delta'\alpha_{\text{had}}(M_Z^2)$	*Approach 1* χ^2/ndf	*Approach 2* $\Delta'\alpha_{\text{had}}(M_Z^2)$	*Approach 2* χ^2/ndf
	0.02753	18.6/16 (p=0.29)	-	-	-	-	0.02753	28.1/17 (p=0.04)
$a_{\mu\,(\text{Lattice})}^{\text{HVP, LO}} - a_{\mu\,(\text{Pheno})}^{\text{HVP, LO}}$ (Full HVP)	-	-	0.02826	27.6/16 (p=0.04)	0.02774	20.3/16 (p=0.21)	-	χ^2(BMW20-Pheno): 9.3
$a_{\mu\,(\text{Lattice})}^{\text{HVP, LO}} - a_{\mu\,(\text{Pheno})}^{\text{HVP, LO}}$ ([Th.; 1.8 GeV])	-	-	0.02769	19.9/16 (p=0.22)	0.02768	19.8/16 (p=0.23)	-	-
$a_{\mu\,(\text{Lattice})}^{\text{HVP, LO}} - a_{\mu\,(\text{Pheno})}^{\text{HVP, LO}}$ ([Th.; 1.0 GeV])	-	-	0.02765	19.6/16 (p=0.24)	-	-	-	-

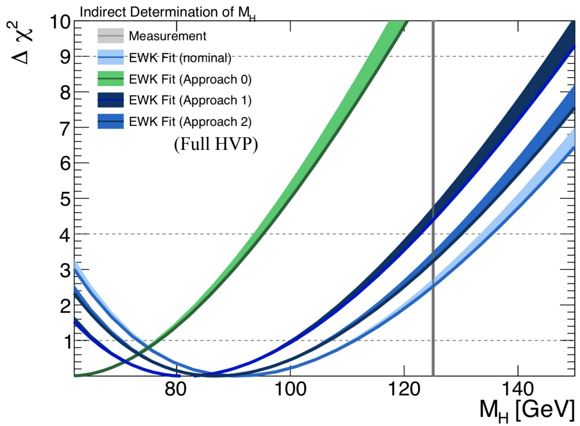

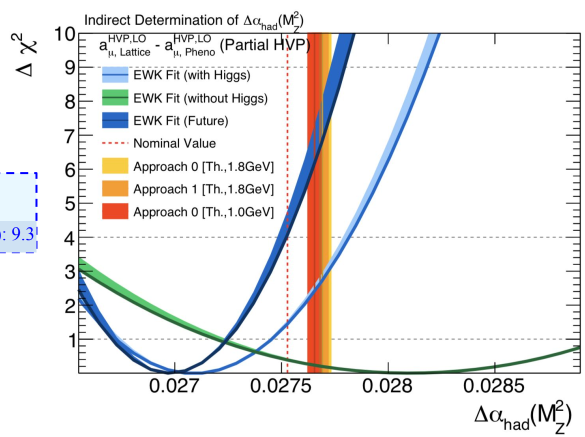

→ Addressing the BMW 20 - Pheno difference for a_μ has little impact on the EW fit, except for the unrealistic scenario rescaling the full HVP contribution

Note: Similar conclusions for the comparison with the Experimental a_μ value (see next slides)

Scaling factors and NP shifts

$a_\mu^{\text{HVP, LO}}$ shift (Energy range)	*Approach 0*		*Approach 1*		
	Scaling factor	$\Delta'\alpha_{\text{had}}(M_Z^2)$	Shift NP$_1$	$\sigma'\left(\Delta\alpha_{\text{had}}(M_Z^2)\right)$	$\Delta'\alpha_{\text{had}}(M_Z^2)$
$a_{\mu\,(\text{Lattice})}^{\text{HVP, LO}} - a_{\mu\,(\text{Pheno})}^{\text{HVP, LO}}$ (Full HVP)	1.027	0.02826	4.6	$9.0 \cdot 10^{-5}$	0.02774
$(a_{\mu\,(\text{Lattice})}^{\text{HVP, LO}} - 1\sigma) - a_{\mu\,(\text{Pheno})}^{\text{HVP, LO}}$ (Full HVP)	1.020	0.02808	3.5	$9.0 \cdot 10^{-5}$	0.02769
$a_{\mu\,(\text{Lattice})}^{\text{HVP, LO}} - a_{\mu\,(\text{Pheno})}^{\text{HVP, LO}}$ ([Th.; 1.8 GeV])	1.029	0.02769	4.7	$9.5 \cdot 10^{-5}$	0.02768
$(a_{\mu\,(\text{Lattice})}^{\text{HVP, LO}} - 1\sigma) - a_{\mu\,(\text{Pheno})}^{\text{HVP, LO}}$ ([Th.; 1.8 GeV])	1.022	0.02765	3.5	$9.5 \cdot 10^{-5}$	0.02764
$a_{\mu\,(\text{Lattice})}^{\text{HVP, LO}} - a_{\mu\,(\text{Pheno})}^{\text{HVP, LO}}$ ([Th.; 1 GeV])	1.034	0.02765	-	-	-
$(a_{\mu\,(\text{Lattice})}^{\text{HVP, LO}} - 1\sigma) - a_{\mu\,(\text{Pheno})}^{\text{HVP, LO}}$ ([Th.; 1 GeV])	1.026	0.02762	-	-	-
$a_\mu^{\text{Exp}} - a_\mu^{\text{SM (Pheno)}}$ (Full HVP)	1.037	0.02856	6.6	$9.0 \cdot 10^{-5}$	0.02782
$(a_\mu^{\text{Exp}} - 1\sigma) - a_\mu^{\text{SM (Pheno)}}$ (Full HVP)	1.028	0.02831	5.0	$9.0 \cdot 10^{-5}$	0.02775
$a_\mu^{\text{Exp}} - a_\mu^{\text{SM (Pheno)}}$ ([Th.; 1.8 GeV])	1.041	0.02776	6.6	$9.5 \cdot 10^{-5}$	0.02774
$(a_\mu^{\text{Exp}} - 1\sigma) - a_\mu^{\text{SM (Pheno)}}$ ([Th.; 1.8 GeV])	1.031	0.02770	5.0	$9.5 \cdot 10^{-5}$	0.02769
$a_\mu^{\text{Exp}} - a_\mu^{\text{SM (Pheno)}}$ ([Th.; 1 GeV])	1.048	0.02771	-	-	-
$(a_\mu^{\text{Exp}} - 1\sigma) - a_\mu^{\text{SM (Pheno)}}$ ([Th.; 1 GeV])	1.036	0.02766	-	-	-

→ Large scaling factors (w.r.t. uncertainties) & significant shifts of NP$_1$

LEP/LHC/Tevatron					
M_Z [GeV]	91.188 ± 0.002	R_c^0	0.1721 ± 0.003	M_H [GeV]	125.09 ± 0.15
$\sigma_{\rm had}^0$ [nb]	41.54 ± 0.037	R_b^0	0.21629 ± 0.00066	M_W [GeV]	80.380 ± 0.013
Γ_Z [GeV]	2.495 ± 0.002	A_c	0.67 ± 0.027	m_t [GeV]	172.9 ± 0.5
A_l (SLD)	0.1513 ± 0.00207	A_l (LEP)	0.1465 ± 0.0033	$\sin^2\theta_{\rm eff}^l$	0.2314 ± 0.00023
$A_{\rm FB}^l$	0.0171 ± 0.001	m_c [GeV]	$1.27^{+0.07}_{-0.11}$ GeV	**After HL-LHC**	
$A_{\rm FB}^c$	0.0707 ± 0.0035	m_b [GeV]	$4.20^{+0.17}_{-0.07}$ GeV	M_W [GeV]	80.380 ± 0.008
$A_{\rm FB}^b$	0.0992 ± 0.0016	$\alpha_s(M_Z)$	0.1198 ± 0.003	$\sin^2\theta_{\rm eff}^l$	0.2314 ± 0.00012
R_l^0	20.767 ± 0.025	$\Delta\alpha_{\rm had}^{(5)}(M_Z^2)$ $[10^{-5}]$	2760 ± 9	m_t [GeV]	172.9 ± 0.3

$a_\mu^{\rm HVP,\,LO}$ shift	Nominal		*Approach* 0		*Approach* 1		*Approach* 2	
(Energy range)	$\Delta'\alpha_{\rm had}(M_Z^2)$	χ^2/ndf	$\Delta'\alpha_{\rm had}(M_Z^2)$	χ^2/ndf	$\Delta'\alpha_{\rm had}(M_Z^2)$	χ^2/ndf	$\Delta'\alpha_{\rm had}(M_Z^2)$	χ^2/ndf
	0.02753	18.6/16 (p=0.29)	-	-	-	-	0.02753	28.1/17 (p=0.04) χ^2(BMW20-Pheno): 9.3
$a_\mu^{\rm HVP,\,LO}$ (Lattice) $- a_\mu^{\rm HVP,\,LO}$ (Pheno) (Full HVP)	-	-	0.02826	27.6/16 (p=0.04)	0.02774	20.3/16 (p=0.21)	-	
$a_\mu^{\rm HVP,\,LO}$ (Lattice) $- a_\mu^{\rm HVP,\,LO}$ (Pheno) ([Th.; 1.8 GeV])	-	-	0.02769	19.9/16 (p=0.22)	0.02768	19.8/16 (p=0.23)	-	-
$a_\mu^{\rm HVP,\,LO}$ (Lattice) $- a_\mu^{\rm HVP,\,LO}$ (Pheno) ([Th.; 1.0 GeV])	-	-	0.02765	19.6/16 (p=0.24)	-	-	-	-
$a_\mu^{\rm Exp} - a_\mu^{\rm SM}$ (Pheno) (Full HVP)	-	-	0.02856	33.6/16 (p=0.01)	0.02782	21.2/16 (p=0.17)	-	-
$a_\mu^{\rm Exp} - a_\mu^{\rm SM}$ (Pheno) ([Th.; 1.8 GeV])	-	-	0.02776	20.6/16 (p=0.19)	0.02774	20.4/16 (p=0.20)	-	-
$a_\mu^{\rm Exp} - a_\mu^{\rm SM}$ (Pheno) ([Th.; 1.0 GeV])	-	-	0.02771	20.1/16 (p=0.22)	-	-	-	-

EW fit results: χ^2 scans

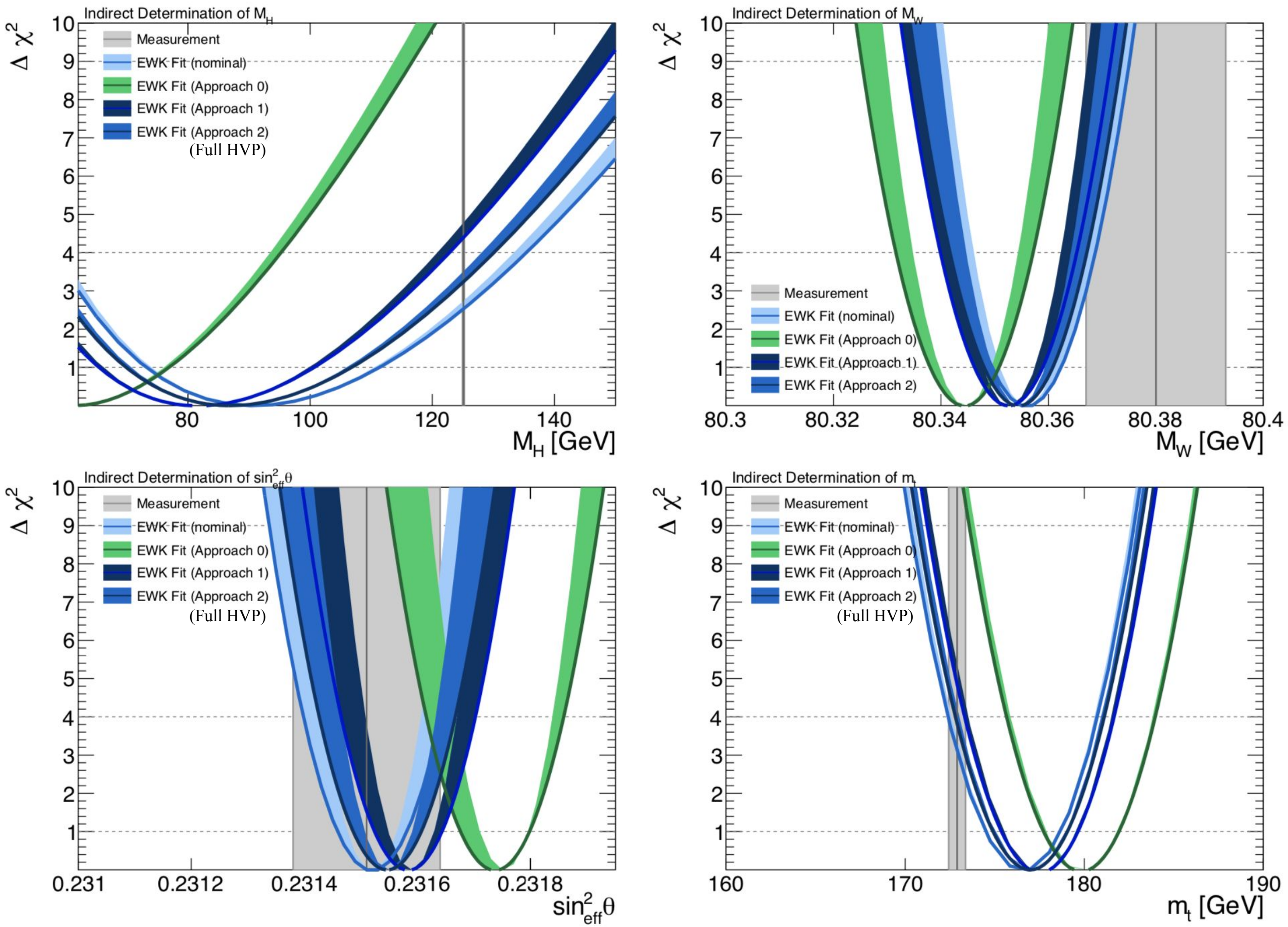

EW fit results: parameter scans for varying $\Delta\alpha_{had}(M_Z^2)$

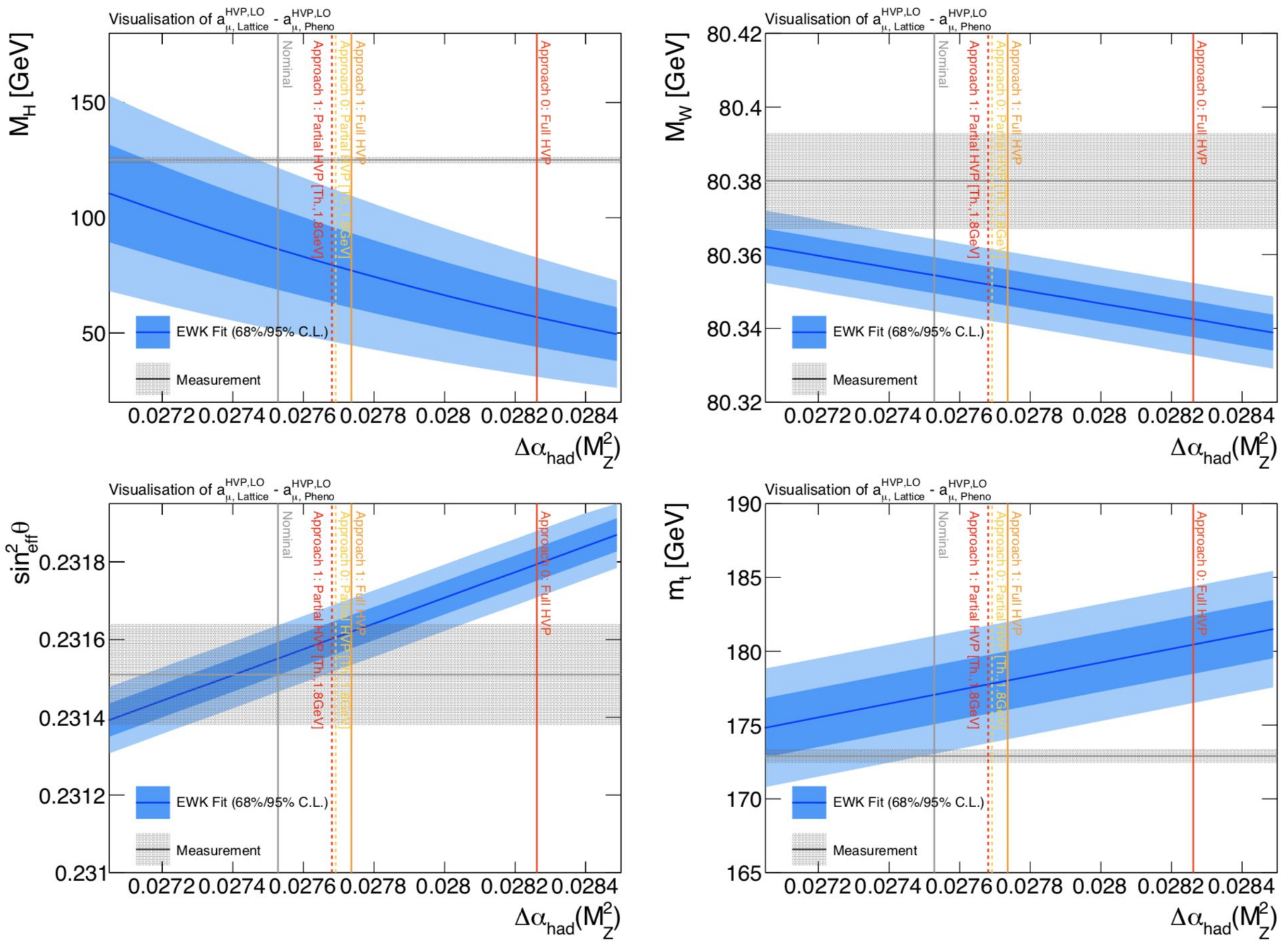

EW fit results: indirect determination of $\Delta\alpha_{had}(M_Z^2)$

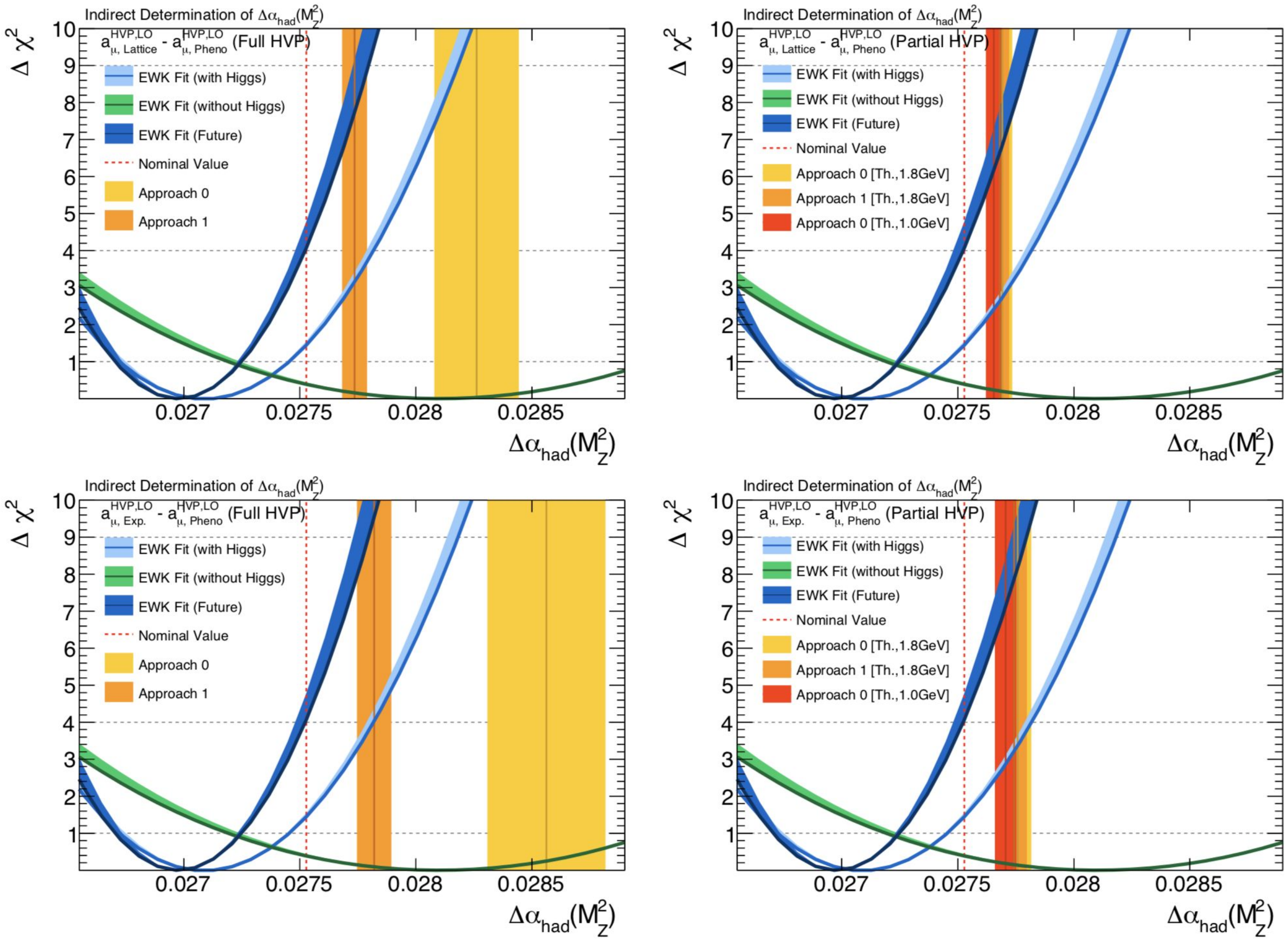

Backup jet studies

Jet definitions

- Main guidelines: infrared and collinear safety

  (guaranteed in data, but important for the theoretical interpretation at all orders)

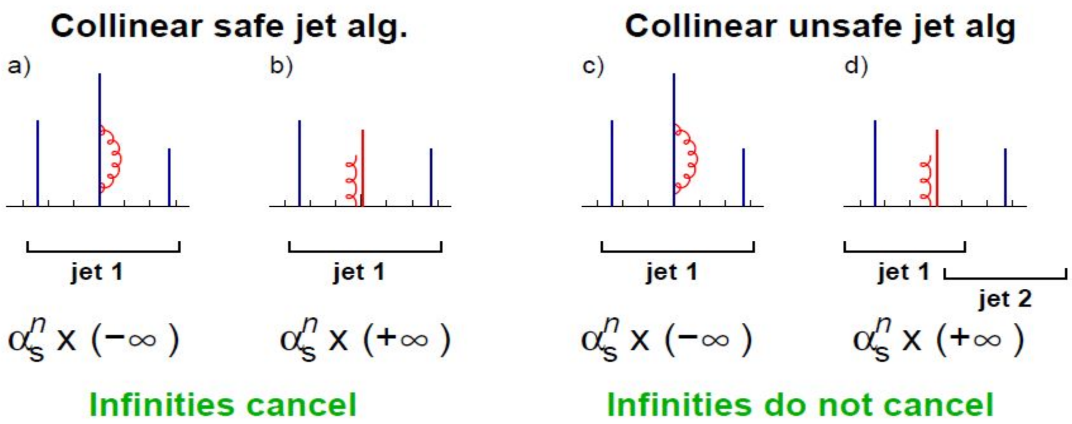

G. Salam 0906.1833

- Most used algorithms:

→ Sequential recombination, using distance between objects: anti-k_t, k_t, Cambrige/Aachen

$$d_{ij} = \min(p_{ti}^{2p}, p_{tj}^{2p}) \frac{\Delta R_{ij}^2}{R^2}, \qquad \Delta R_{ij}^2 = (y_i - y_j)^2 + (\phi_i - \phi_j)^2$$

$$d_{iB} = p_{ti}^{2p},$$

→ Algorithms applicable coherently at the "truth" and reconstructed level

Back

Jet definitions

G. Salam
0906.1833

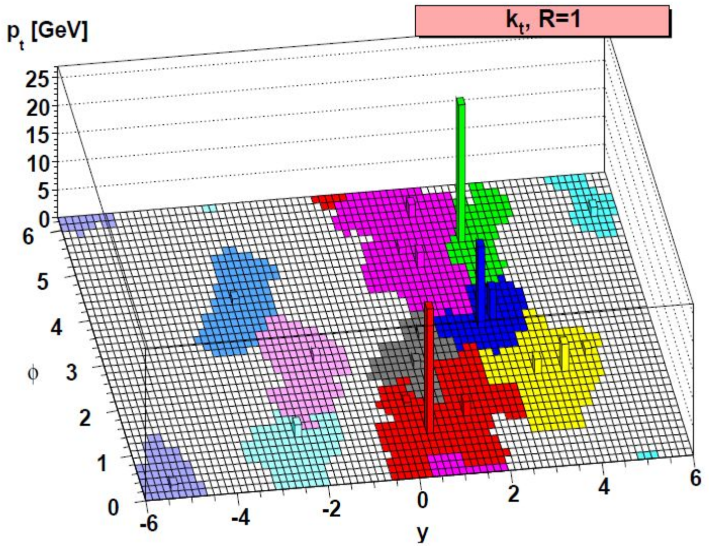

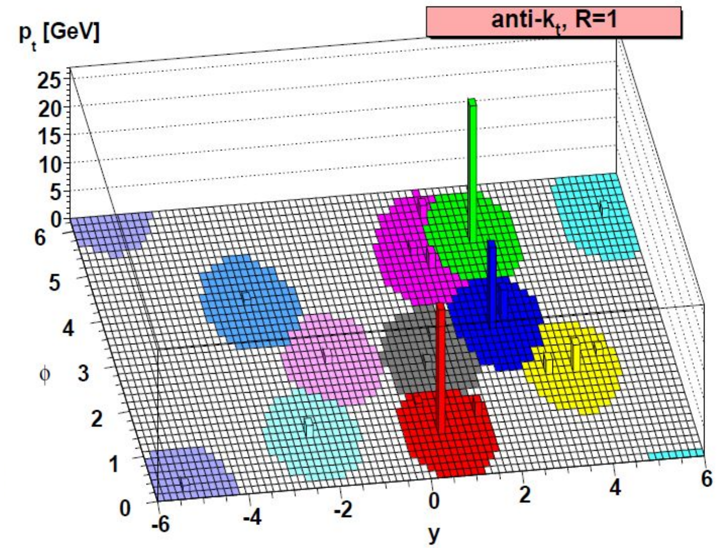

→ anti-k_t jets have more circular shapes compared to k_t

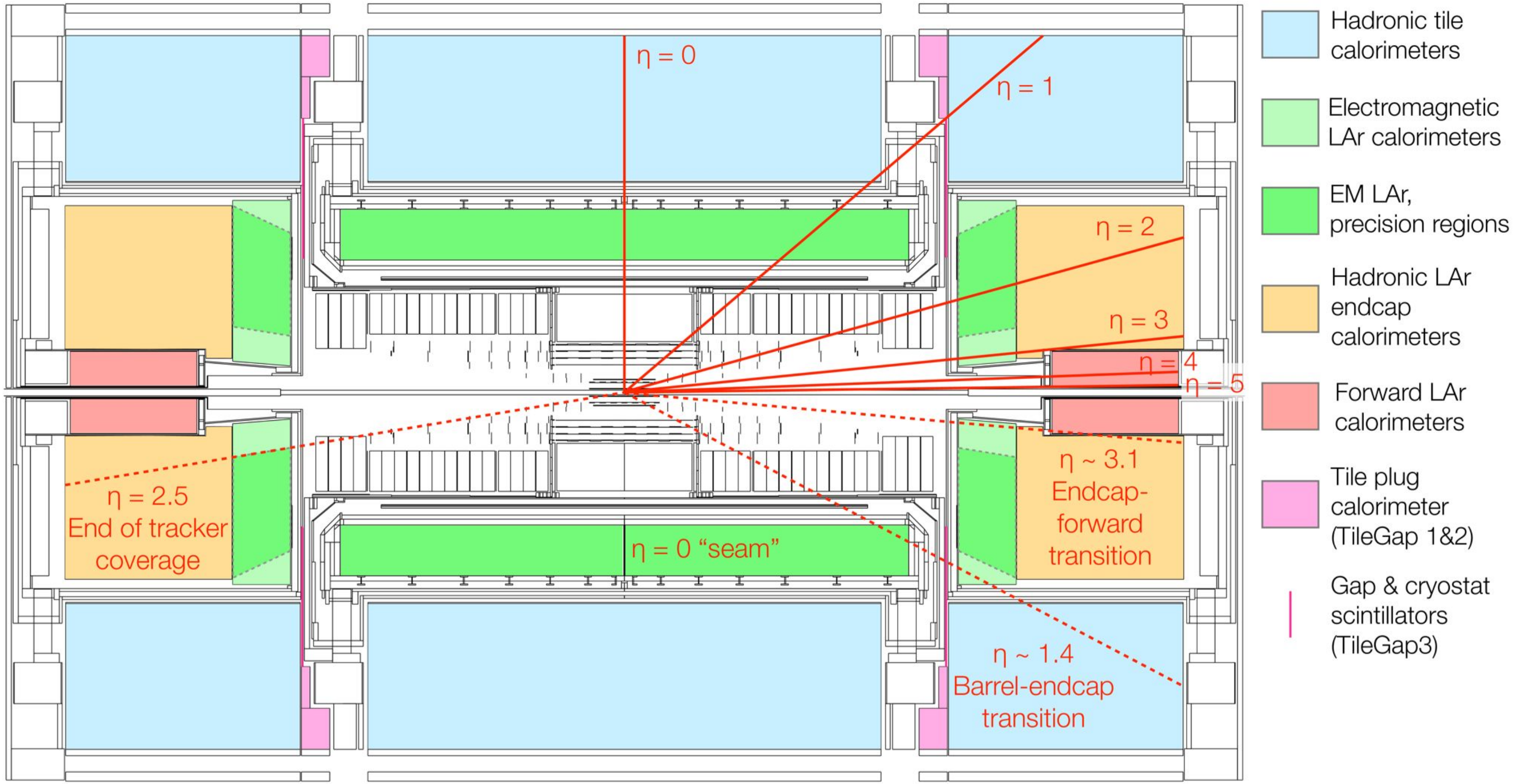

η = 0
η = 1
η = 2
η = 3
η = 4
η = 5
η ~ 3.1
Endcap-
forward
transition
η = 2.5
End of tracker
coverage
η = 0 “seam”
η ~ 1.4
Barrel-endcap
transition
Hadronic tile
calorimeters
Electromagnetic
LAr calorimeters
EM LAr,
precision regions
Hadronic LAr
endcap
calorimeters
Forward LAr
calorimeters
Tile plug
calorimeter
(TileGap 1&2)
Gap & cryostat
scintillators
(TileGap3)

Pile-up correction(s)

$$p_T \mapsto p_T - \rho A_T - \alpha (N_{PV} - 1) - \beta \mu$$

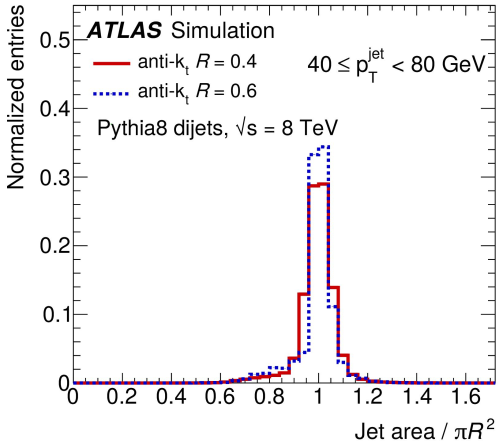

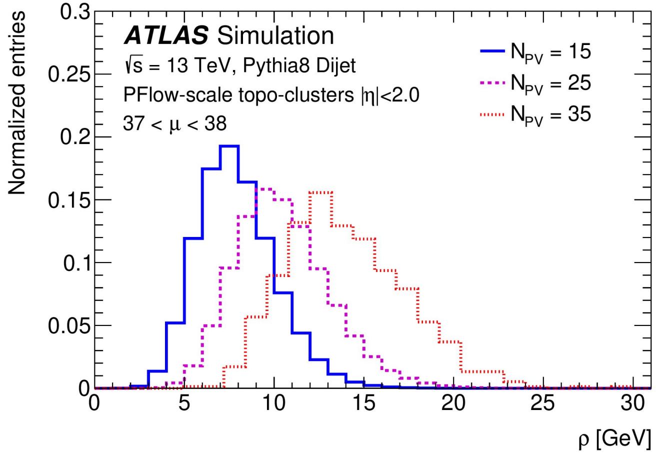

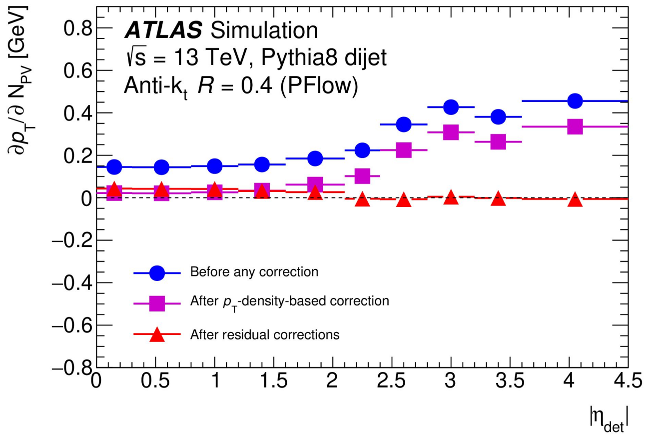

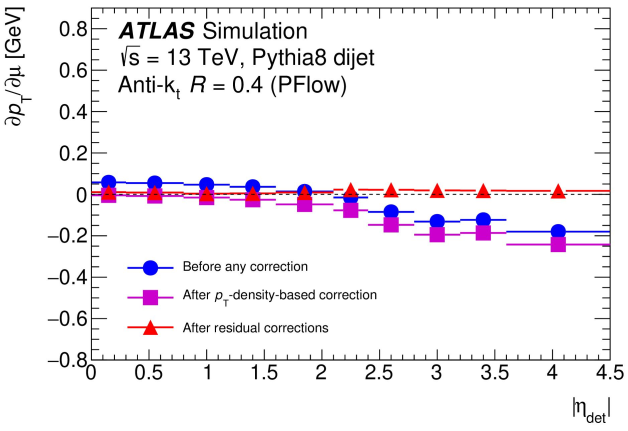

Back

MC-based jet energy and mass scales

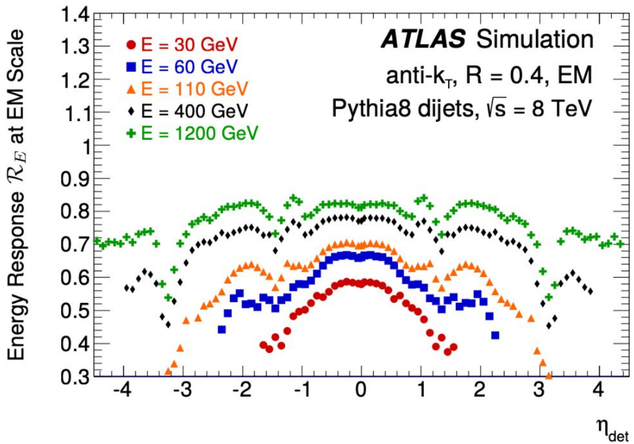

(a) Jet energy response $\mathcal{R}_E$, EM scale, $R = 0.4$

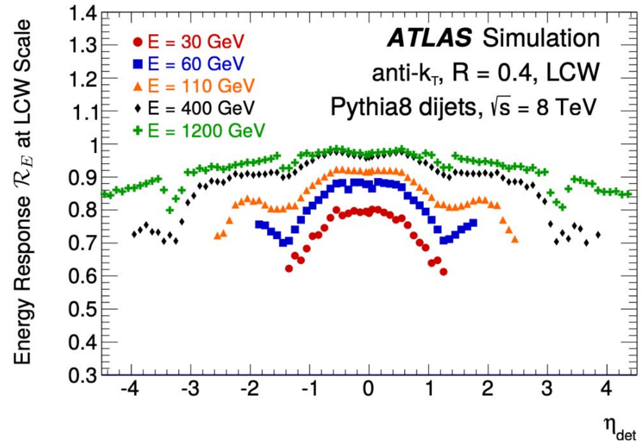

(b) Jet energy response $\mathcal{R}_E$, LCW scale, $R = 0.4$

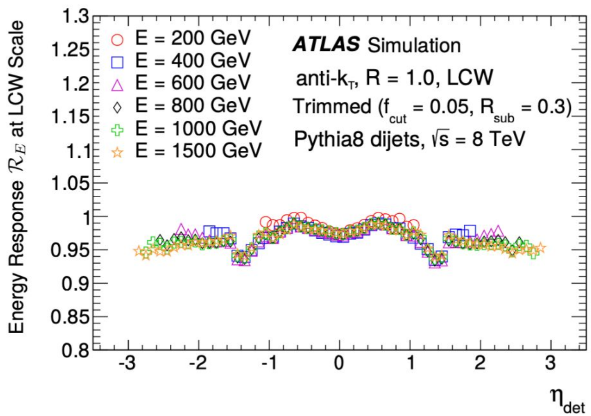

(c) Jet energy response $\mathcal{R}_E$, LCW scale, $R = 1.0$

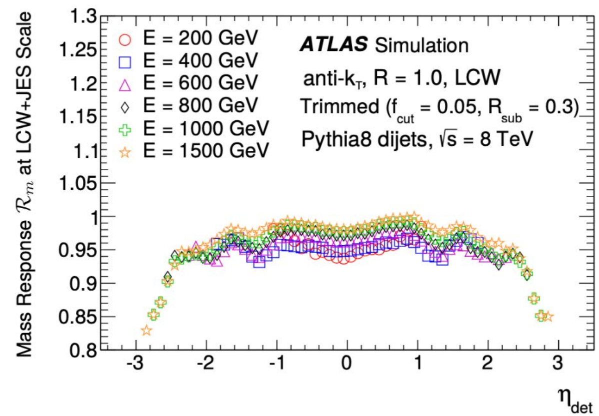

(d) Jet mass response $\mathcal{R}_m$, LCW scale, $R = 1.0$

GSC & GNNC – variables & sensitivity

Calorimeter	$f_{\mathrm{LAr},0-3}$	the E_{frac} measured in the 0th-3rd layer of the EM LAr calorimeter
	$f_{\mathrm{TILE}0-2}$*	the E_{frac} measured in the 0th-2nd layer of the hadronic tile calorimeter
	$f_{\mathrm{HEC},0-3}$	the E_{frac} measured in the 0th-3rd layer of the hadronic end cap calorimeter
	$f_{\mathrm{FCAL},0-2}$	the E_{frac} measured in the 0th-2nd layer of the forward calorimeter
	$N_{90\%}$	The minimum number of clusters containing 90% of the jet energy.
Jet kinematics	$p_{\mathrm{T}}^{\mathrm{JES}}$ *	The jet p_{T} after the MCJES calibration
	η_{det}	The detector η
Tracking	w_{track}*	the average p_{T}-weighted transverse distance in the η-ϕ plane between the jet axis and all tracks of $p_{\mathrm{T}} > 1$ GeV ghost-associated with the jet
	N_{track}*	the number of tracks with $p_{\mathrm{T}} > 1$ GeV ghost-associated with the jet
	f_{charged}*	the fraction of the jet p_{T} measured from ghost-associated tracks
Muon segments	N_{segments}*	the number of muon track segments ghost-associated with the jet
Pileup	μ	The average number of interactions per bunch crossing
	N_{PV}	The number of reconstructed primary vertices

Table 1: List of variables used as input to the GNNC. Variables with a * correspond to variables that are also used by the GSC.

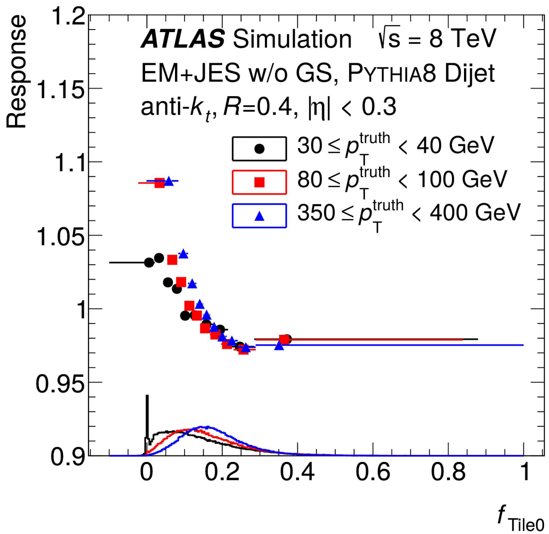

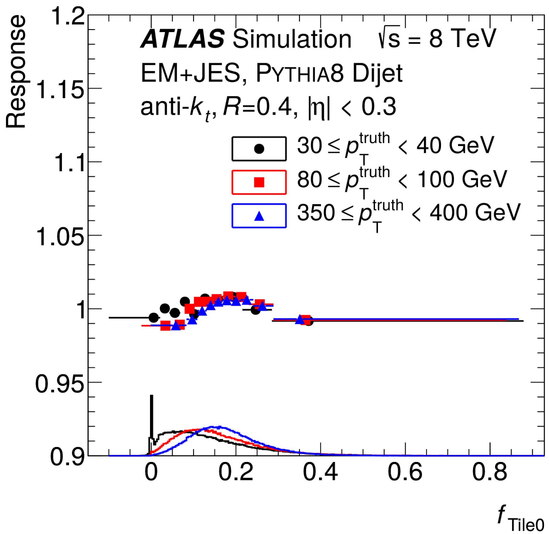

→ Little / no dependence left for the response after having applied the corrections

GSC & GNNC – performance

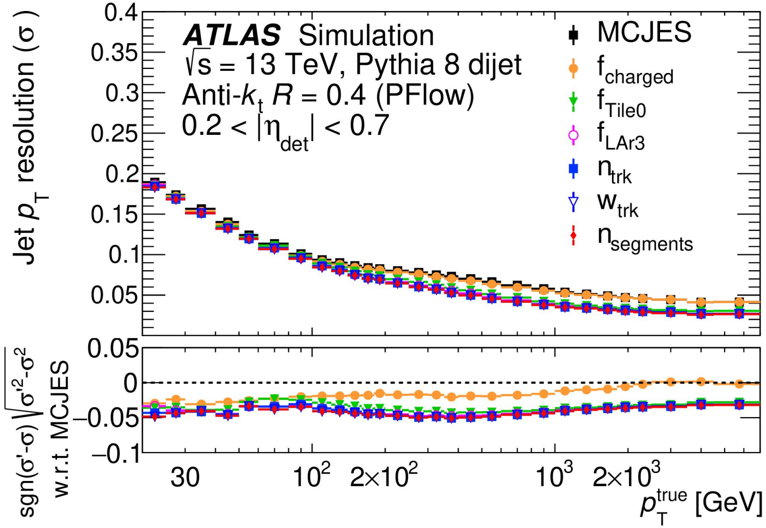

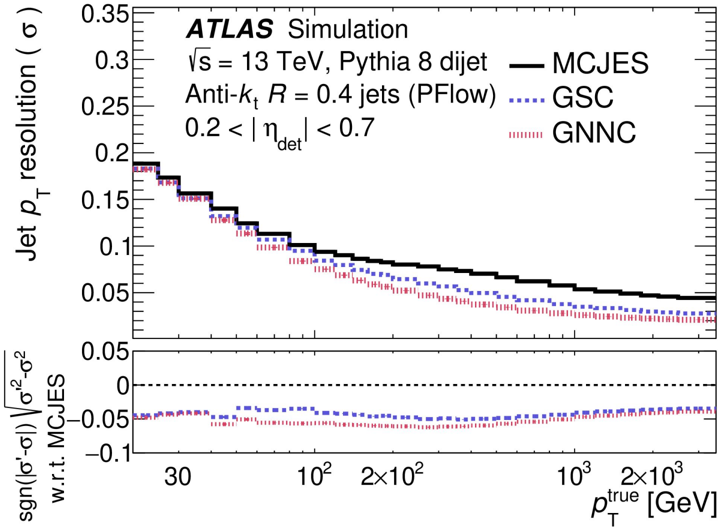

→ Improvement of the JER with the GSC and some further improvement using GNNC

→ Work during Laura Boggia's QT, aiming to merge GNNC and the in-situ step

→ *Potential to eventually merge all the MC-based and in-situ steps*

→ Central reference method / matrix method (using more combinations of central-forward bins, obtaining hence a better statistical precision)

→ Deriving calibration factors in bins of p_T, η

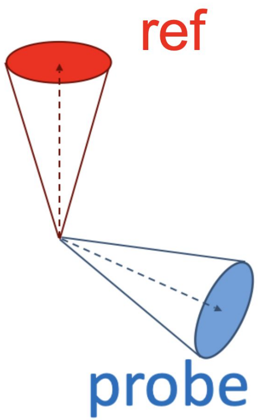

$$S(c_{1x},\ldots,c_{Nx}) = \sum_{j=2}^{N}\sum_{i=1}^{j-1}\left(\frac{1}{\Delta\langle\mathcal{R}_{ijx}\rangle}(c_{ix}\langle\mathcal{R}_{ijx}\rangle - c_{jx})\right)^2 + X(c_{ix})$$

$$X(c_i) = \lambda\left(\tfrac{1}{N}\textstyle\sum_{i=1}^{N} c_i - 1\right)^2$$

$$\sum_{i=1}^{\alpha-1}\left(\left(\frac{-\langle\mathcal{R}_{i\alpha}\rangle}{\Delta^2\langle\mathcal{R}_{i\alpha}\rangle}+\frac{\lambda}{N^2}\right)c_i\right) + \left(\sum_{i=1}^{\alpha-1}\frac{1}{\Delta^2\langle\mathcal{R}_{i\alpha}\rangle}+\sum_{i=\alpha+1}^{N}\frac{\langle\mathcal{R}_{\alpha i}\rangle^2}{\Delta^2\langle\mathcal{R}_{\alpha i}\rangle}+\frac{\lambda}{N^2}\right)c_\alpha + \sum_{i=\alpha+1}^{N}\left(\left(\frac{-\langle\mathcal{R}_{\alpha i}\rangle}{\Delta^2\langle\mathcal{R}_{\alpha i}\rangle}+\frac{\lambda}{N^2}\right)c_i\right) - \frac{\lambda}{N} = 0$$

Back

In-situ η – intercalibration calibration method

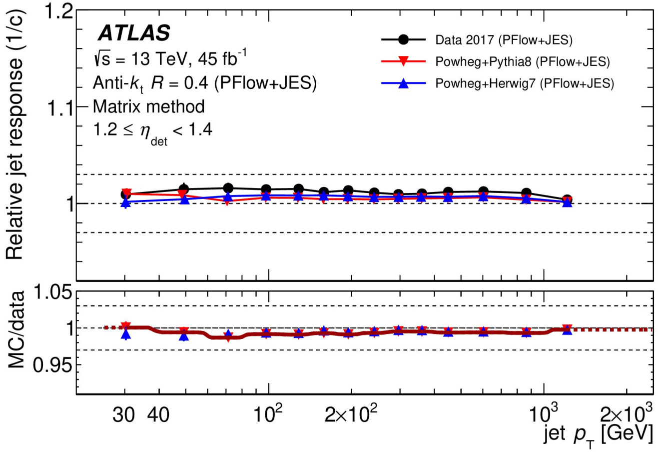

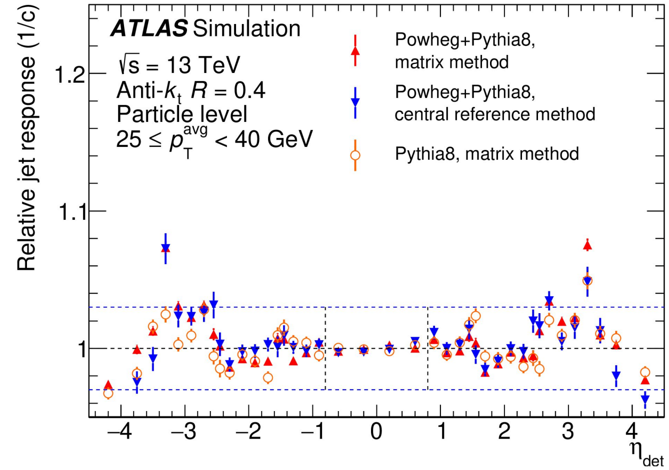

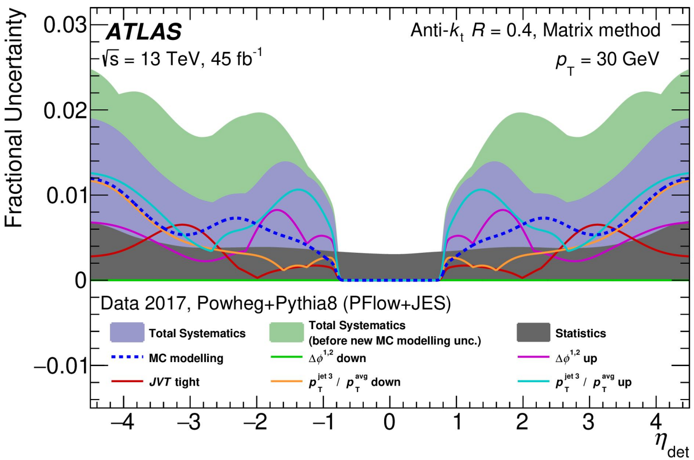

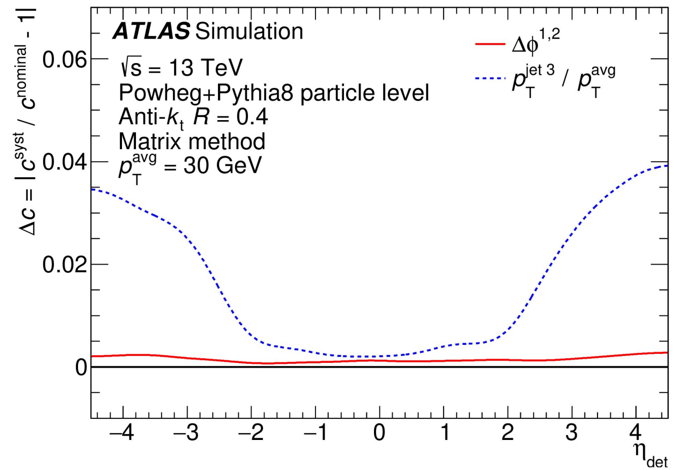

E/p method

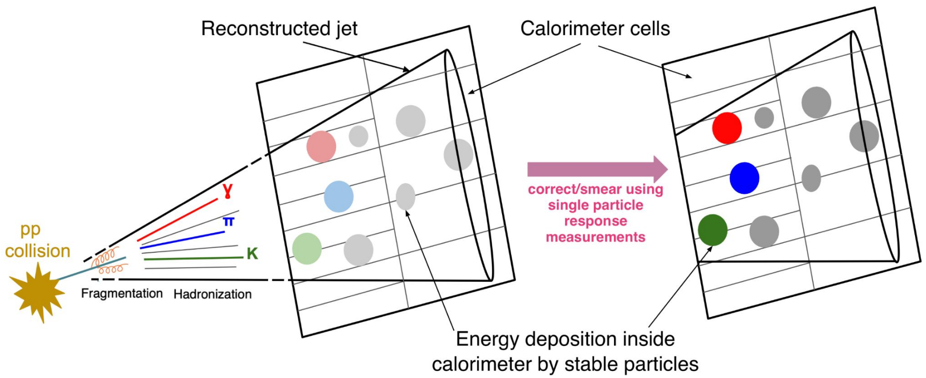

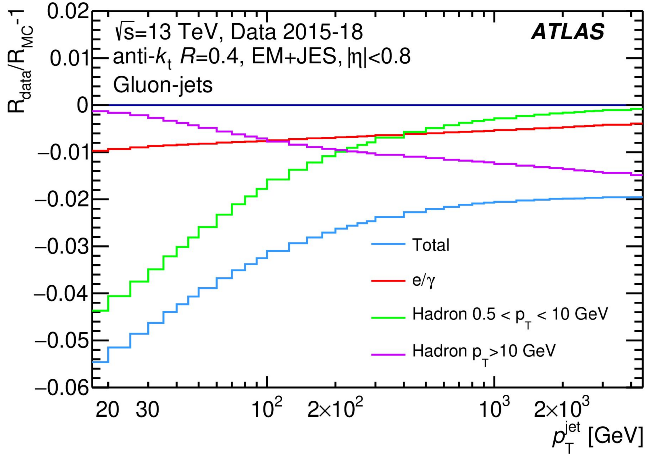

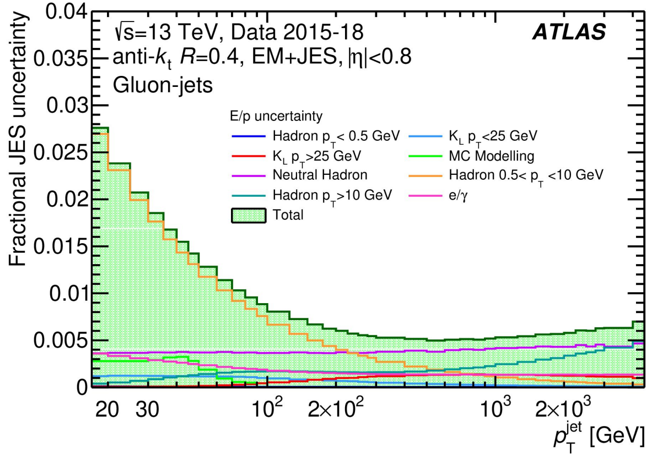

→ Important improvement of the E/p method

(Lata Panwar's PostDoc)

Back

→ Constraint using random cones in zero-bias data and from distribution of soft jet momenta

→ Closure test for random cone method in MC

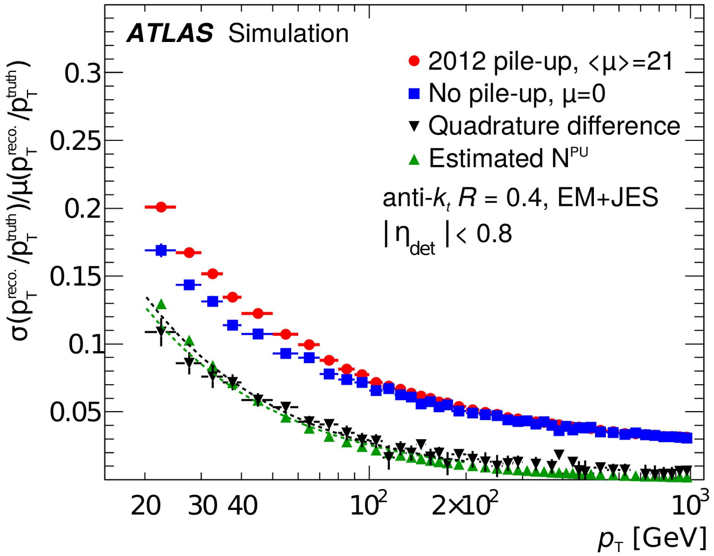

	EM $R = 0.4$	LCW $R = 0.4$	EM $R = 0.6$	LCW $R = 0.6$
$\langle\sigma_\rho\rangle$ ($Z \to \mu\mu$, data) [GeV]	1.81	3.25	1.81	3.25
$\langle\sigma_\rho\rangle$ ($Z \to \mu\mu$, MC) [GeV]	2.09	3.72	2.09	3.72
$\langle\sigma_\rho\rangle\sqrt{A}$ ($Z \to \mu\mu$, data) [GeV]	1.28	2.30	1.92	3.46
Random cone, data [GeV]	1.52	2.61	2.42	4.19
Difference [%]	16	12	21	17
$\langle\sigma_\rho\rangle\sqrt{A}$ ($Z \to \mu\mu$, MC) [GeV]	1.48	2.64	2.22	3.96
Random cone, MC [GeV]	1.60	2.73	2.61	4.49
Difference [%]	7.5	4.4	15	12

Back

Resolution measurement from dijet balance

Dijet balance

$$\mathcal{A} = \frac{p_{\mathrm{T}}^{\mathrm{probe}} - p_{\mathrm{T}}^{\mathrm{ref}}}{p_{\mathrm{T}}^{\mathrm{avg}}}$$

$$\sigma_{\mathcal{A}}^{\mathrm{probe}} = \frac{\sigma_{p_{\mathrm{T}}}^{\mathrm{probe}} \oplus \sigma_{p_{\mathrm{T}}}^{\mathrm{ref}}}{p_{\mathrm{T}}^{\mathrm{avg}}} = \left\langle \frac{\sigma_{p_{\mathrm{T}}}}{p_{\mathrm{T}}} \right\rangle_{\mathrm{probe}} \oplus \left\langle \frac{\sigma_{p_{\mathrm{T}}}}{p_{\mathrm{T}}} \right\rangle_{\mathrm{ref}}$$

→ MC-based subtraction of truth-level smearing

→ Closure test in MC

Bisector

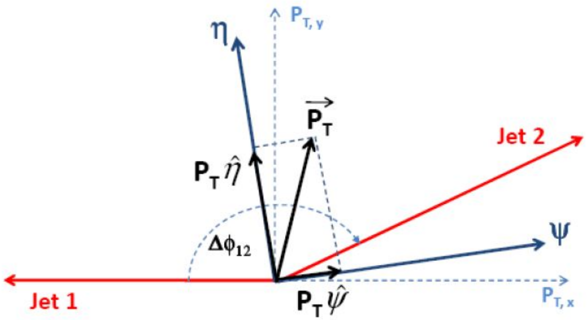

→ Attempt to distinguish physics and detector effects

$$\frac{\sigma_{p_{\mathrm{T}}}}{p_{\mathrm{T}}} = \frac{\sigma_{\Psi} \ominus \sigma_{\eta}}{p_{\mathrm{T}} \sqrt{2 \langle |\cos \Delta\phi_{12}| \rangle}}$$

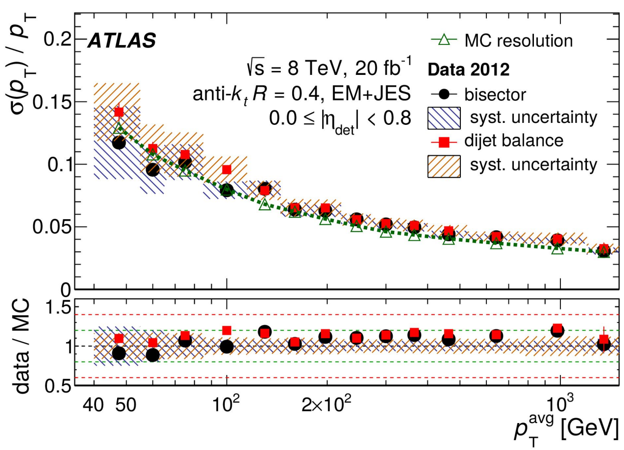

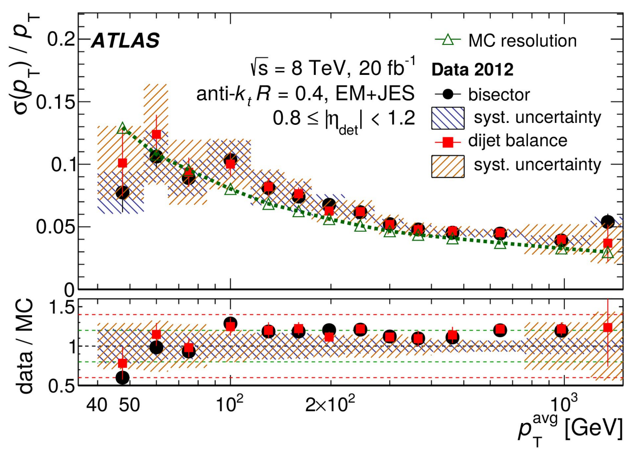

V + jet: Evaluating the JER

→ MC-based subtraction of truth-level smearing
→ Closure test in MC

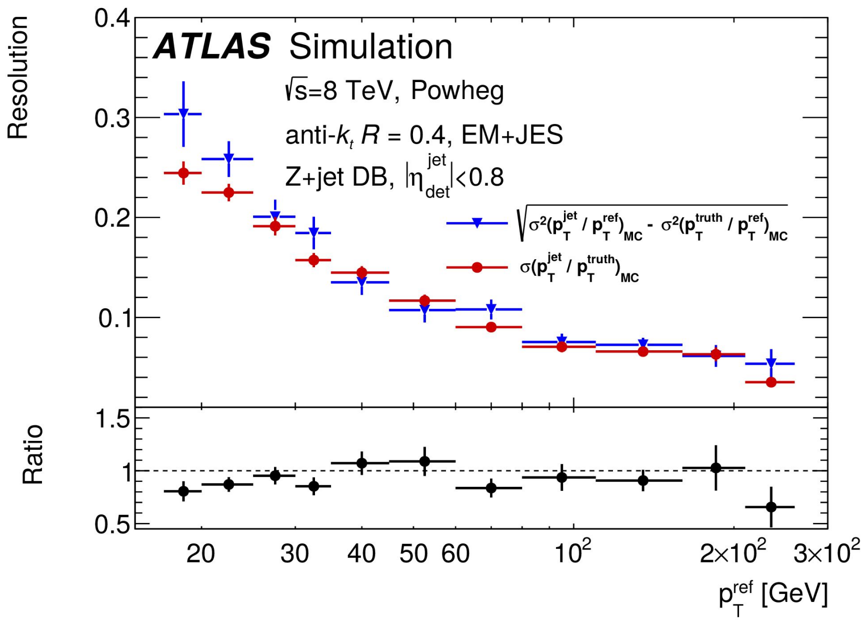

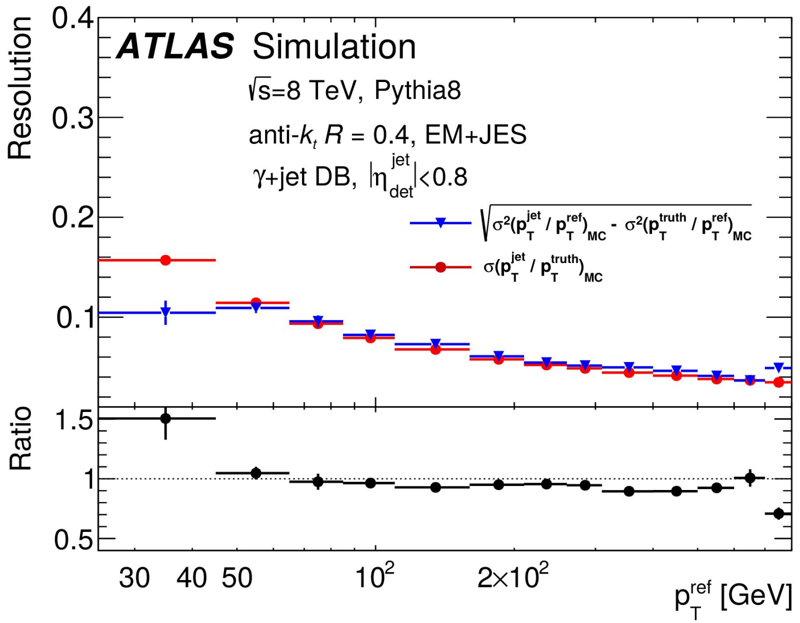

γ-jet + Z-jet + Dijets + Zero Bias JER fit (η<0.8)

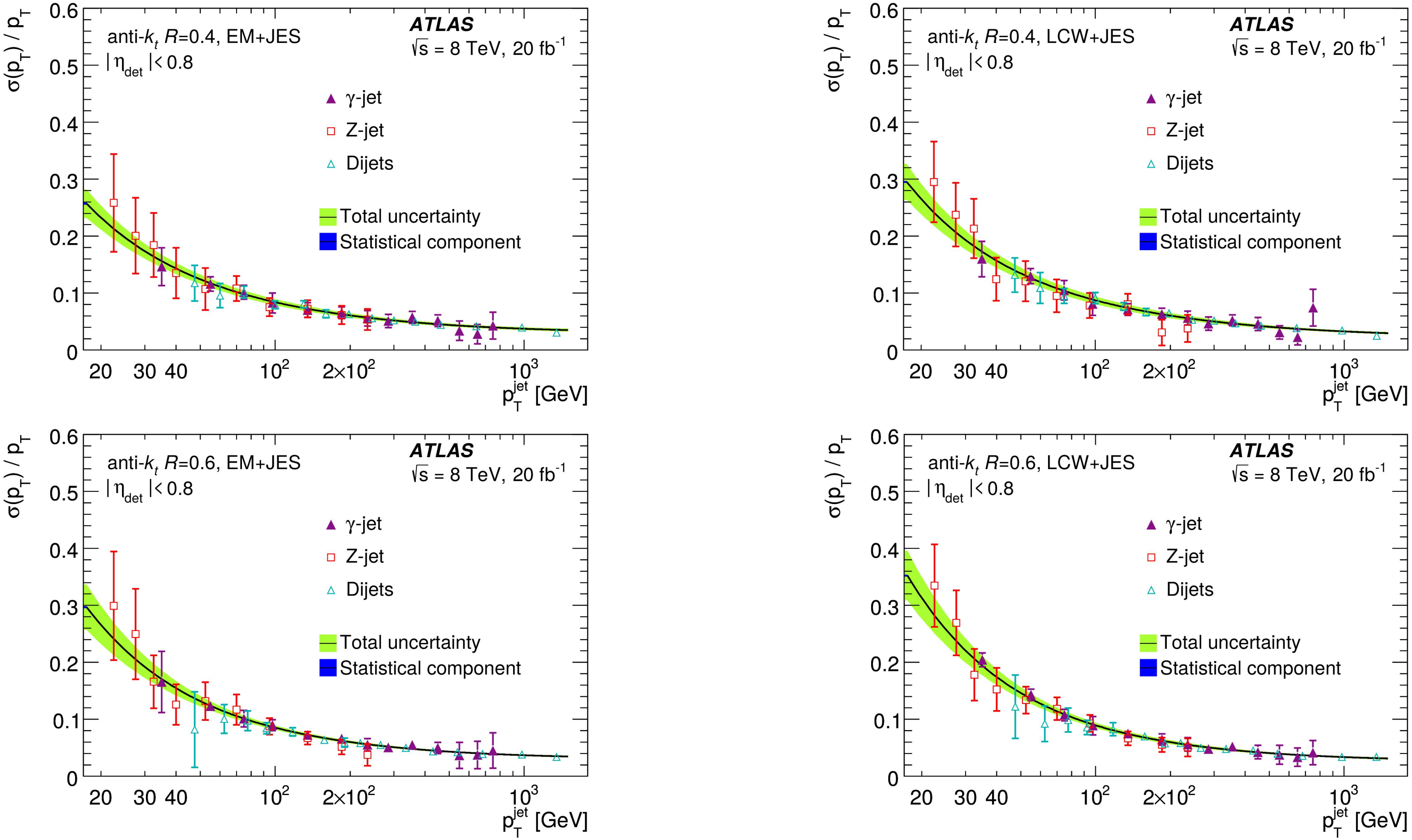

JER in-situ combination

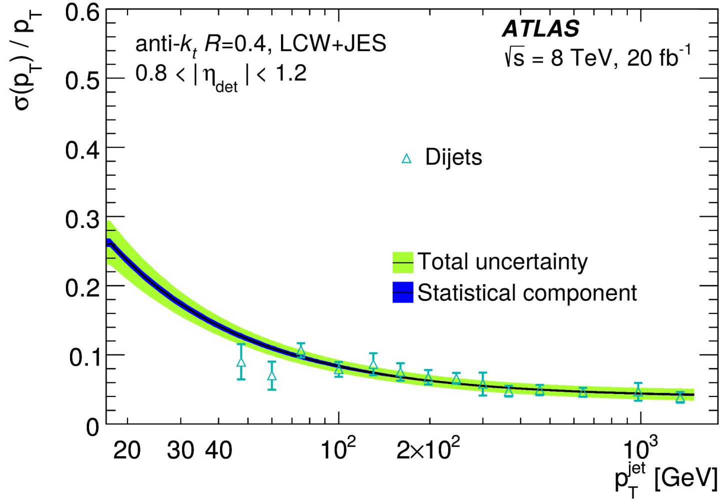

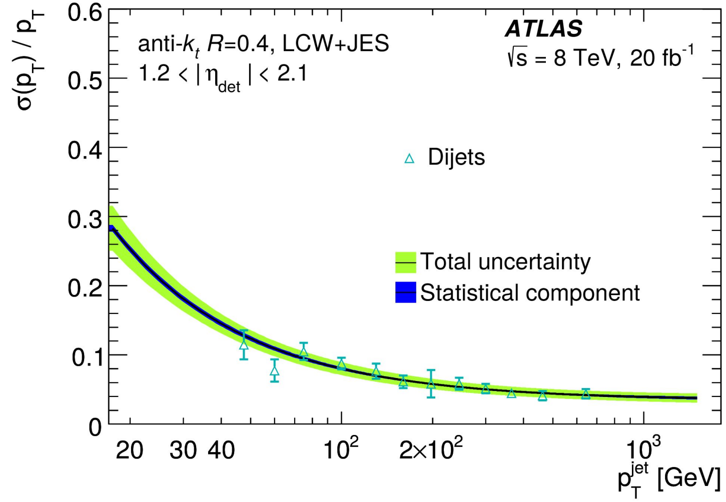

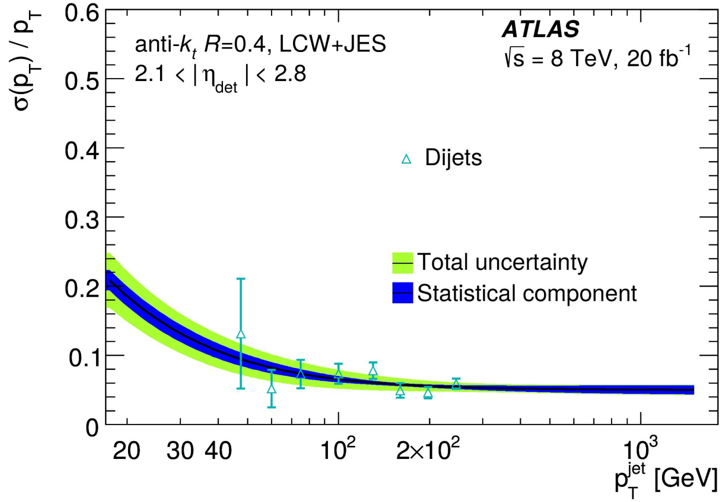

γ-jet + Z-jet + Dijets + Zero Bias JER fit (EM JES, R=0.4, η<0.8)

→ Propagation of in-situ uncertainties with toys and $\pm 1\sigma$ shifts: good agreement between the two methods (except for two fits at large η - poor constraint on S & non-Gaussian distribution)

→ χ^2 definition does not include uncertainty on N (only uncertainties on data points are included)
Small (~1-2 units) changes in χ^2 value for N $\pm$ 0.632 GeV

→ Uncertainty band not rescaled by global χ^2/ndof (recall: local rescaling for JES)

In-situ uncertainties (N fixed) :

S = 0.713 $\pm$ 0.067 $\sqrt{\text{GeV}}$

C = 0.030 $\pm$ 0.003

Corr(S; C) = -0.25 (in-situ)

Zero-bias:

N = 3.325 $\pm$ 0.632 GeV

N : 0.632 ; S : -0.038 ; C: 0.001

N : -0.632 ; S : 0.030 ; C:-0.001

χ^2_{diag}/ndof = 8 /35

χ^2_{corr}/ndof = 71 /35

→ Some indication of higher order contributions to JER function

Propagation of JER uncertainties and correlations

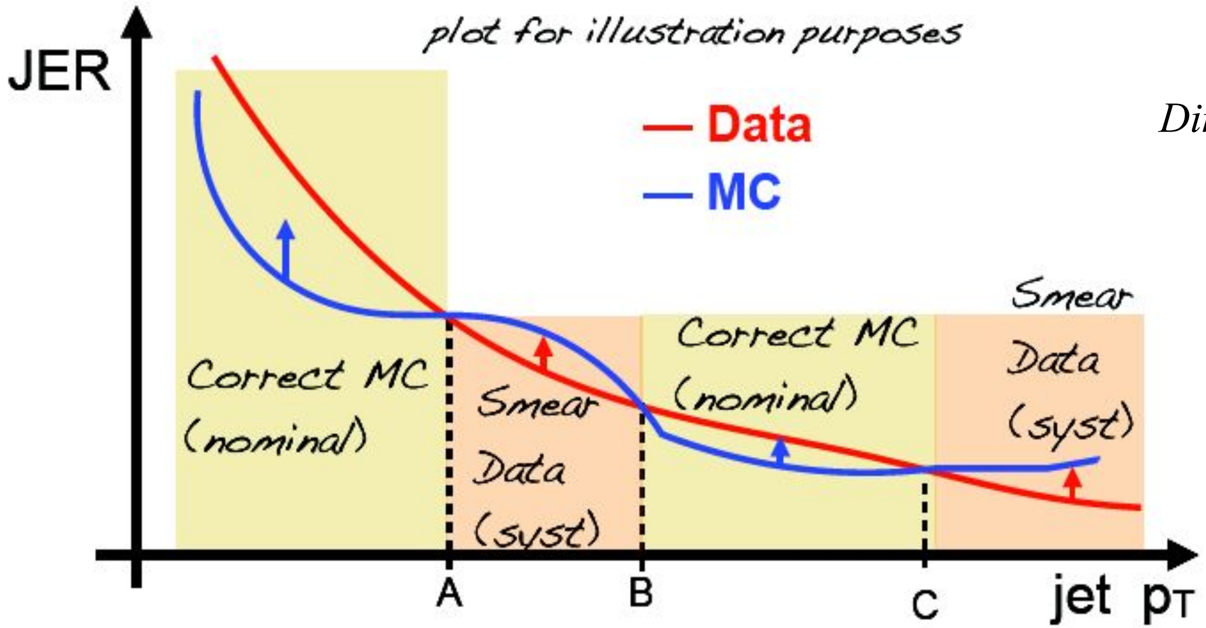

Dimitris Varouchas - PostDoc

- **Nominal** value
  - **Correct MC**, if $JER_{Data} > JER_{MC}$
- **Systematic variation** (for the **uncertainty propagation** only)
  - **Smear Data**, if $JER_{Data} < JER_{MC}$

→ $p_T(W)$: large resolution effects for MET reconstruction & need relatively fine binning in order to discriminate among theoretical predictions

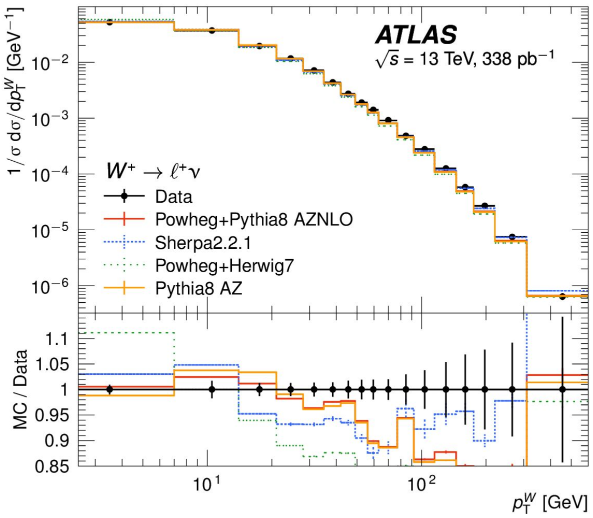

2404.06204

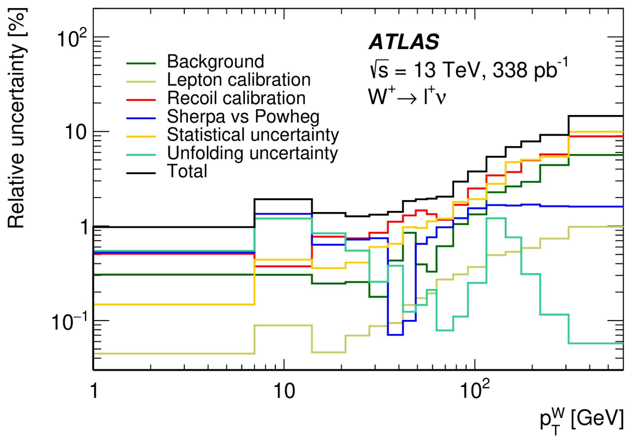

→ Unfolding in a different context:

inverse Laplace transform to convert spacelike lattice QCD results into timelike quantities

Back

An Iterative, Bayes-inspired Unfolding Method

$$P_{ij} = \frac{A_{ij}}{\sum_{k=1}^{n_d} A_{kj}}$$

$$\tilde{P}_{ij} = \frac{A_{ij}}{\sum_{k=1}^{n_u} A_{ik}} \; ; \boldsymbol{u} = \widetilde{\boldsymbol{P}} \cdot \boldsymbol{d}$$

→ Note: $\tilde{P}_{ij}$ depends on the shape of the truth distribution in MC

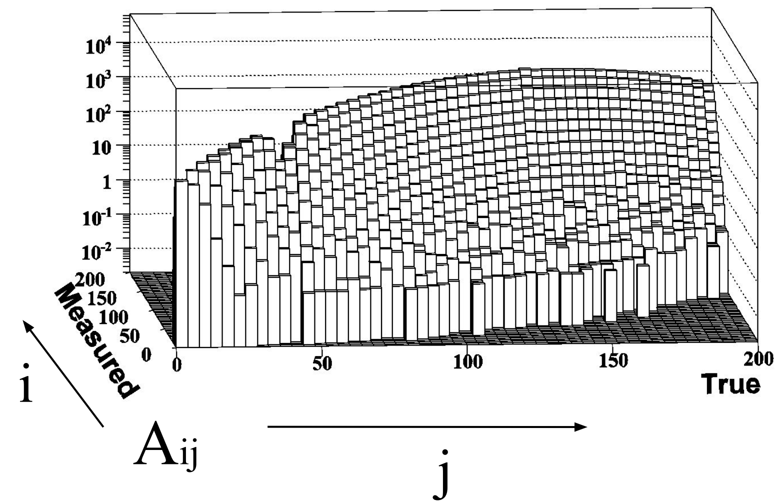

- 1st unfolding, where the original transfer matrix is used

1) Transfer matrix improvement (hence of the unfolding probability matrix)

Reweight the truth MC distribution based on previous unfolding result.

2) Improved unfolding

→ Choice on number of iterations = regularization

→ Other methods exist, like e.g. dynamical local regularization in IDS (treatment of fluctuations in each bin, at each step of the procedure)

Data-driven closure test: motivation, procedure, example

→ In-situ determination of the unfolding uncertainty related to the data/MC shape difference and to the regularization : - reweight true MC by smooth function: improved data/recoMC agreement
- unfold the reweighted reconstructed MC
- compare with reweighted true MC

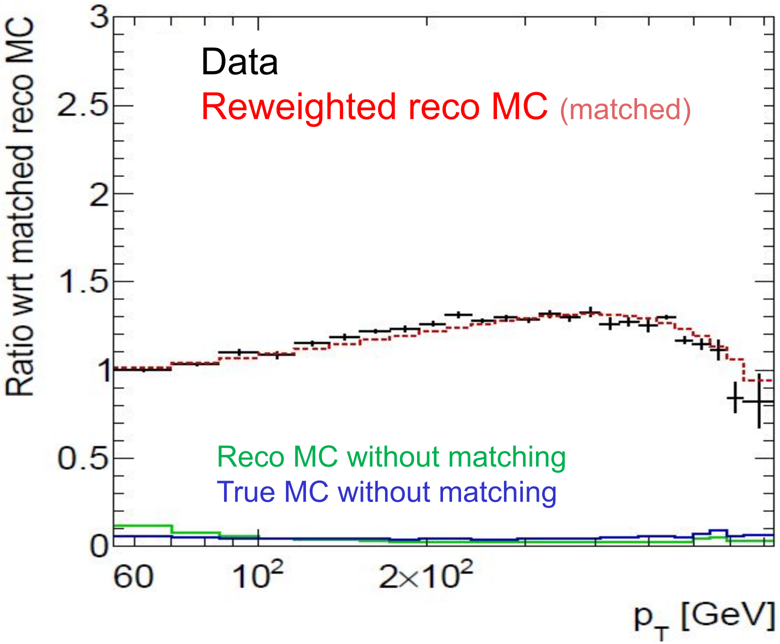

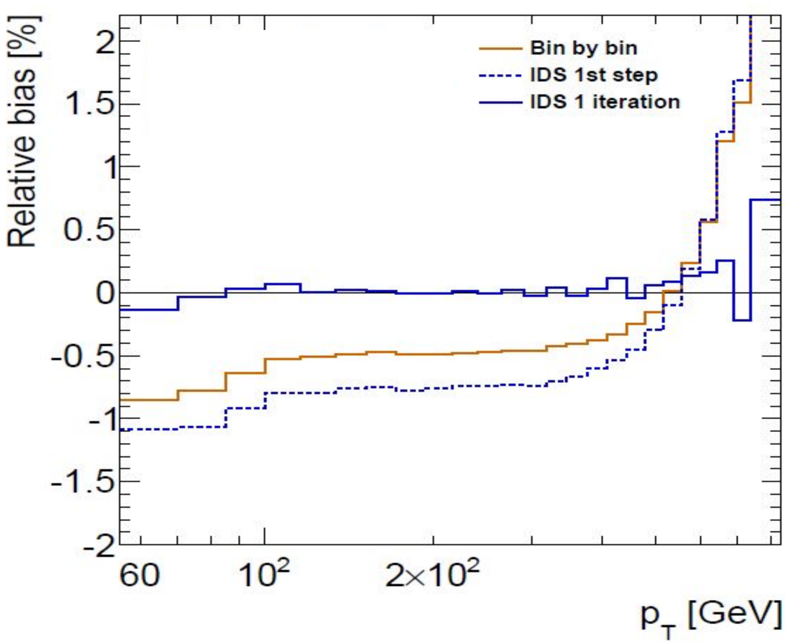

→ Applicable in cases without very different degenerated solutions (see eigenvalues of folding matrix, quality of the data/reweighted MC etc.). In other cases allows to learn about the ill-posedness of the problem

→ Method introduced in arXiv:0907.3791, used in arXiv:1112.6297 etc. … arXiv:2405.20041 (Omnifold 24-d) …

Choice of the phase-space

- Selection defining phase-space at “truth” level – as close as possible to the reconstructed-level selection: *minimize extrapolation to reduce model dependence*

- Include over-/under-flow bins when migrations to the region of interest are relevant

  → These extra bins are generally not published

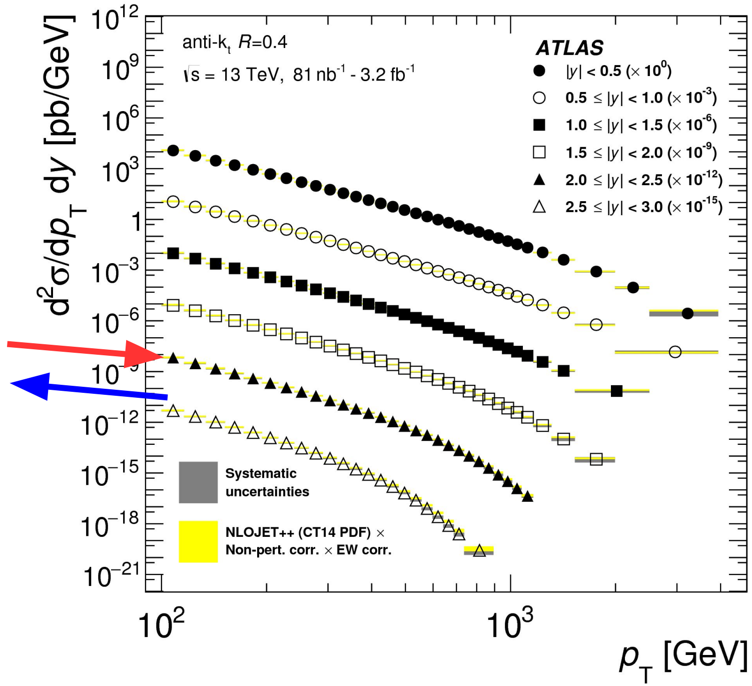

Iterative methods: choice of the number of iterations

- Number of iterations = regularization parameter: optimising variance / bias

→ Take into account: *systematic uncertainty related to the unfolding method (bias due to MC/data shape difference & regularization)*; impact on statistical uncertainties & correlations; constraints induced on binning choice

- Compare data and the modified reconstructed MC: see how much information is left to be propagated from the data shape to the truth MC shape

  → bin-by-bin comparison or using a χ^2 (see e.g. arxiv:0907.3791, arXiv:2404.06204)

- Suggestion in IBU publication: compare results from consecutive steps (NIM A 362, 487 (1995))

→ risk of ~small changes between consecutive steps, while having a significant bias

Tests of the unfolding

- "Technical closure test" → same MC for the transfer matrix and input distribution (pseudo-data) - expect perfect agreement between unfolding result and truth MC
- "Data-driven closure test" → allows to evaluate a systematic related to the unfolding method and the choice of regularization (see next slides)

- "Linearity test" → MC samples with various truth inputs; check linear dependence between unfolded and truth values of a quantity of interest
- "Pull test" → relevant only for unfolding methods providing an estimate of the statistical uncertainties (i.e. not from pseudo-experiments) - tests their reliability

- ML-based methods allow to enhance the dimensionality & obtain results event-by-event: enables computing secondary quantities arXiv:2109.13243
- IcINN: iteratively improve (reweight) MC simulation; publish unfolded distributions for each data event

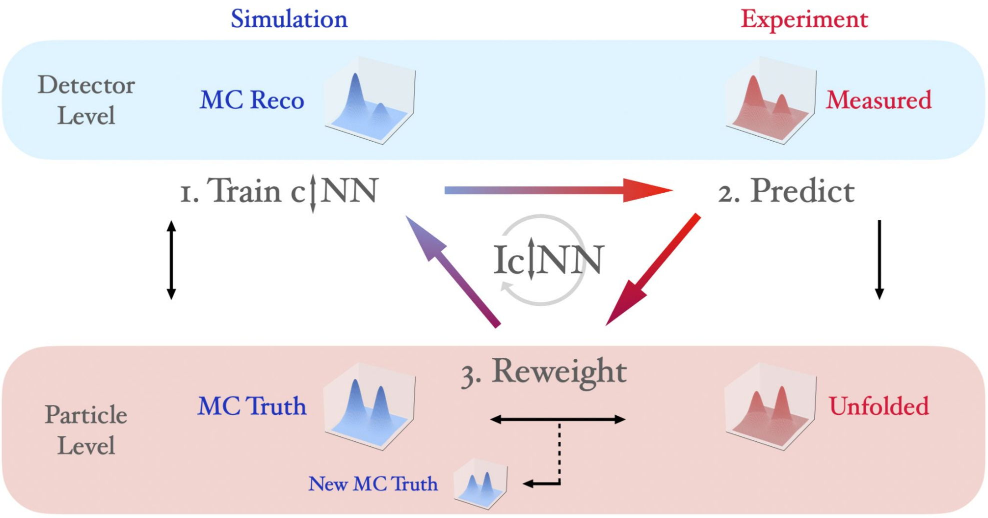

arXiv:2212.08674

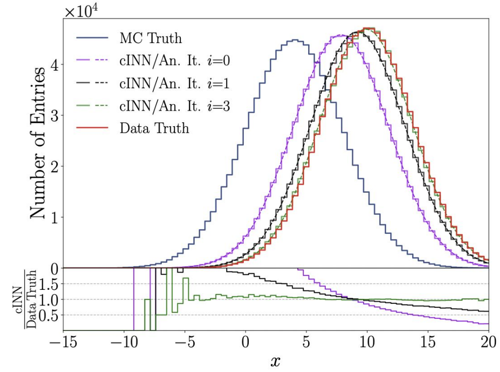

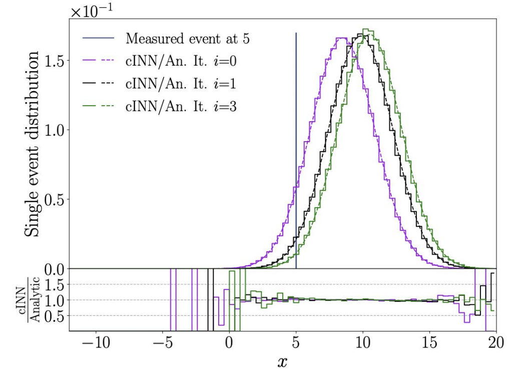

Back

Comparison of Transfer Matrix- / ML-based unfolding

→ Comparison typically performed for the full unfolded distributions

→ *New*: even-by-event comparison arXiv:2310.17037

$pp \to Z\gamma\gamma,\ Z \to \mu^-\mu^+$

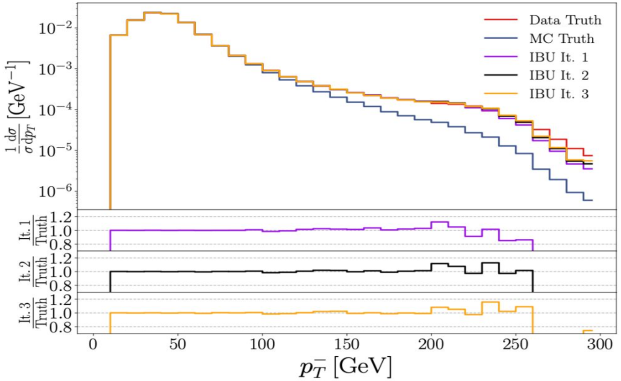

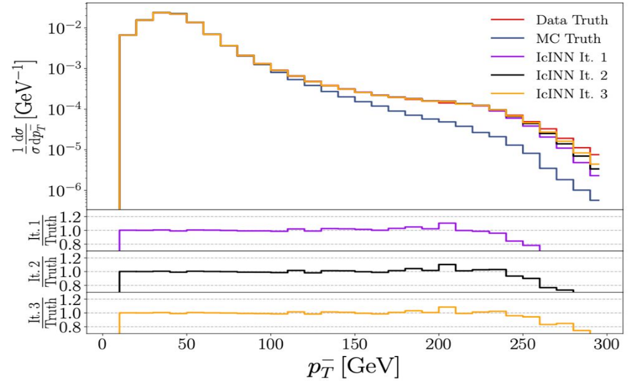

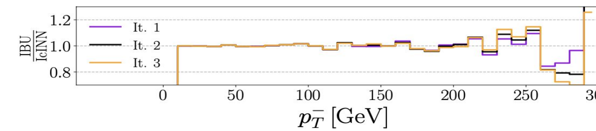

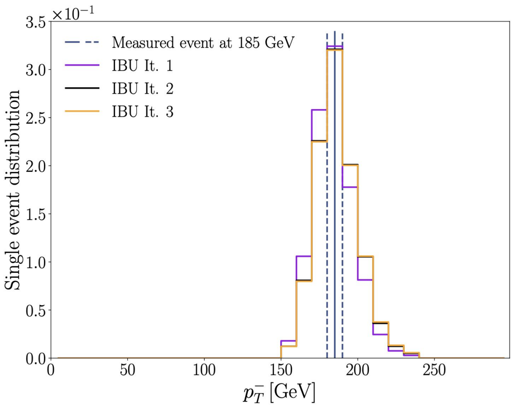

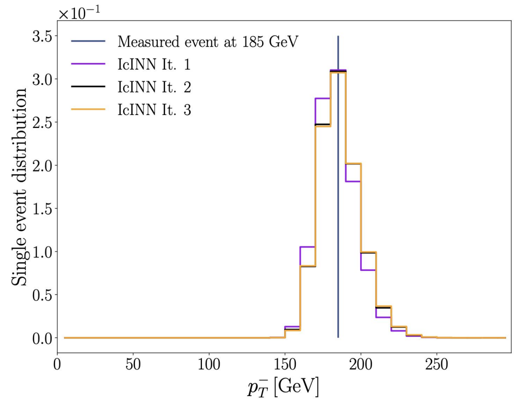

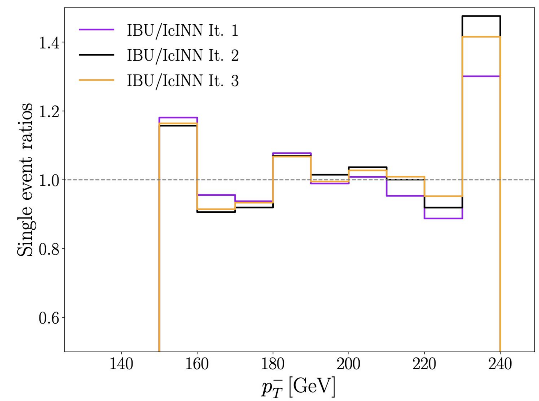

Comparison of Transfer Matrix- / ML-based unfolding

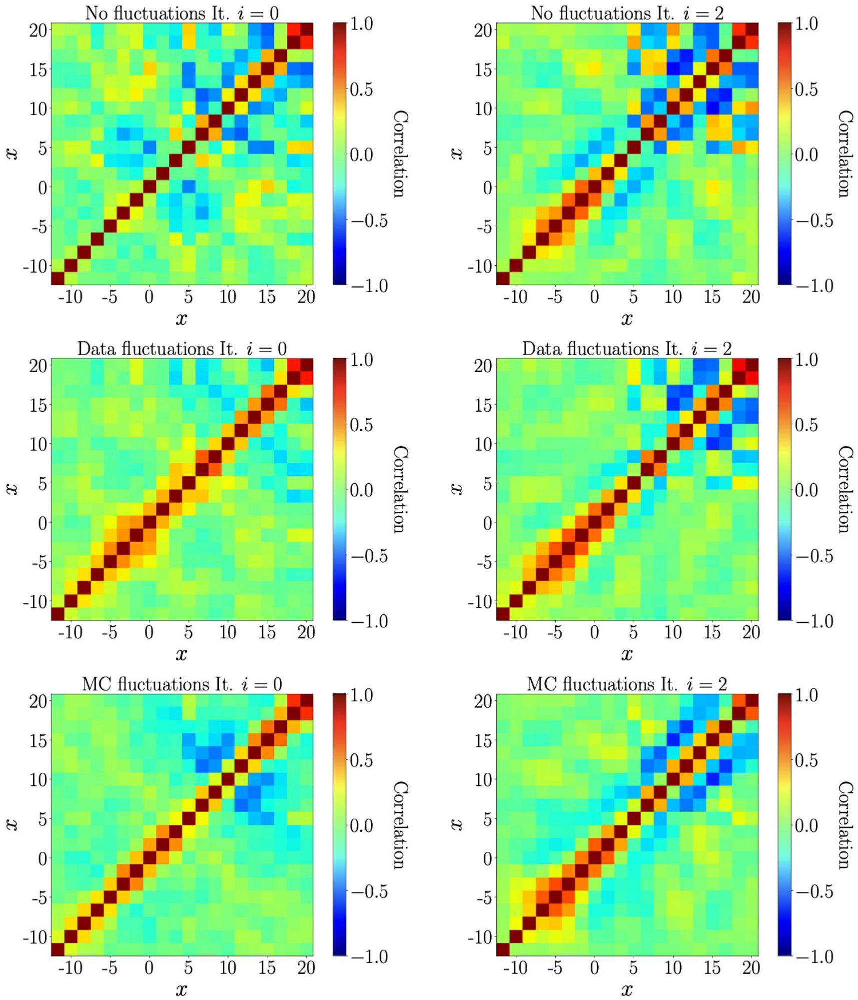

→ Bootstrap method implemented for IcINN, for small number of observables (GPU challenge for training):

Evaluate statistical uncertainties and correlations

arXiv:2212.08674

Trigger and pile-up

- Trigger prescales and pile-up treatment take into account variations in data-taking conditions
- Jet trigger efficiencies determined in-situ using unbiased samples
- Each trigger used in the region where it is fully efficient

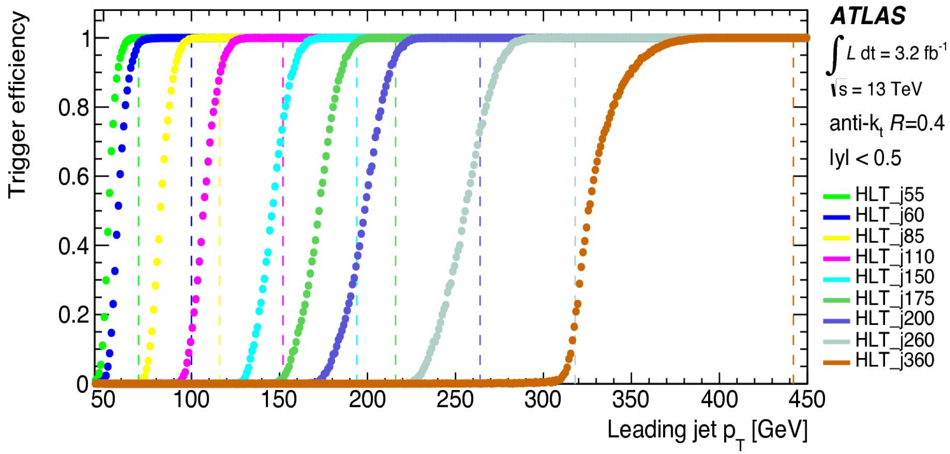

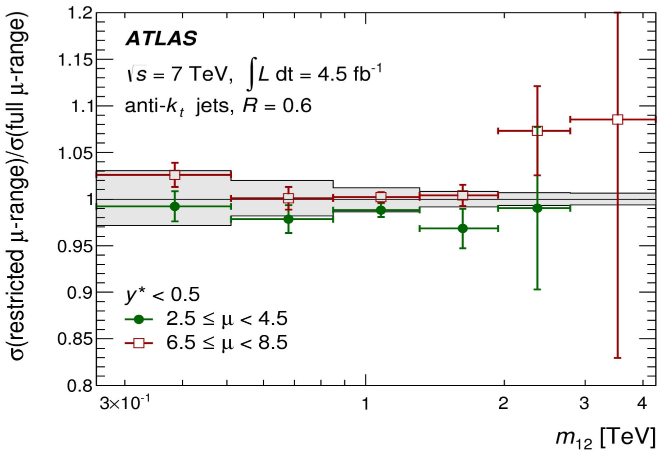

Back

Dijet 3D measurement - CMS

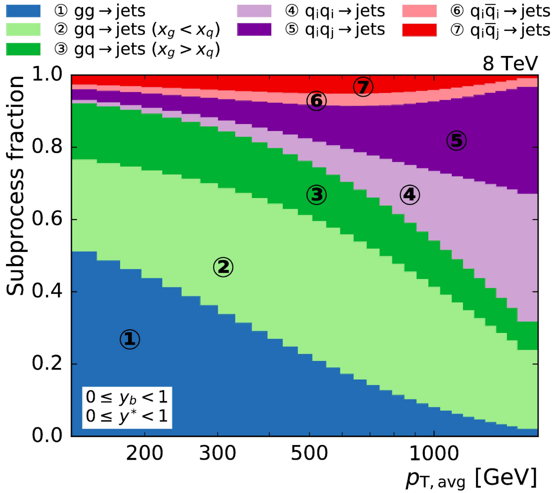

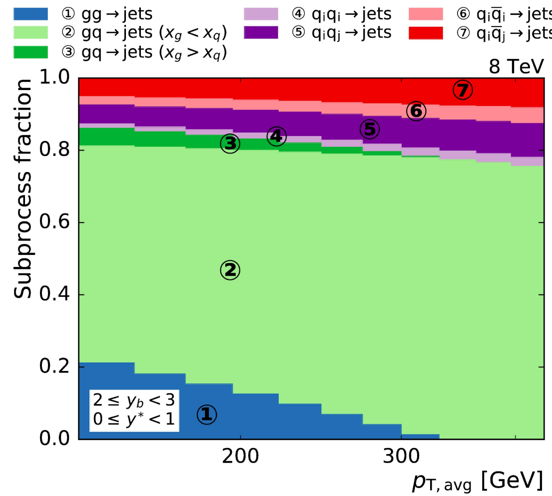

→ Contributions of various processes in different phase-space regions: sensitivity to PDFs

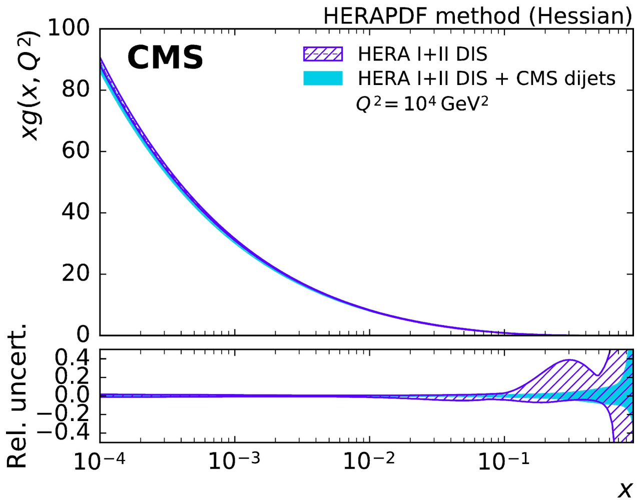

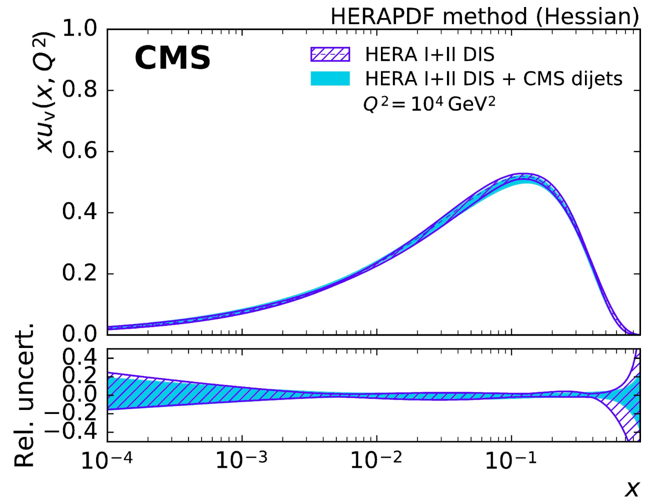

→ Good data/theory agreement within uncertainties observed for most PDF sets: CT14, MMHT 2014, NNPDF 3.0, HERAPDF 2.0, ABMP16

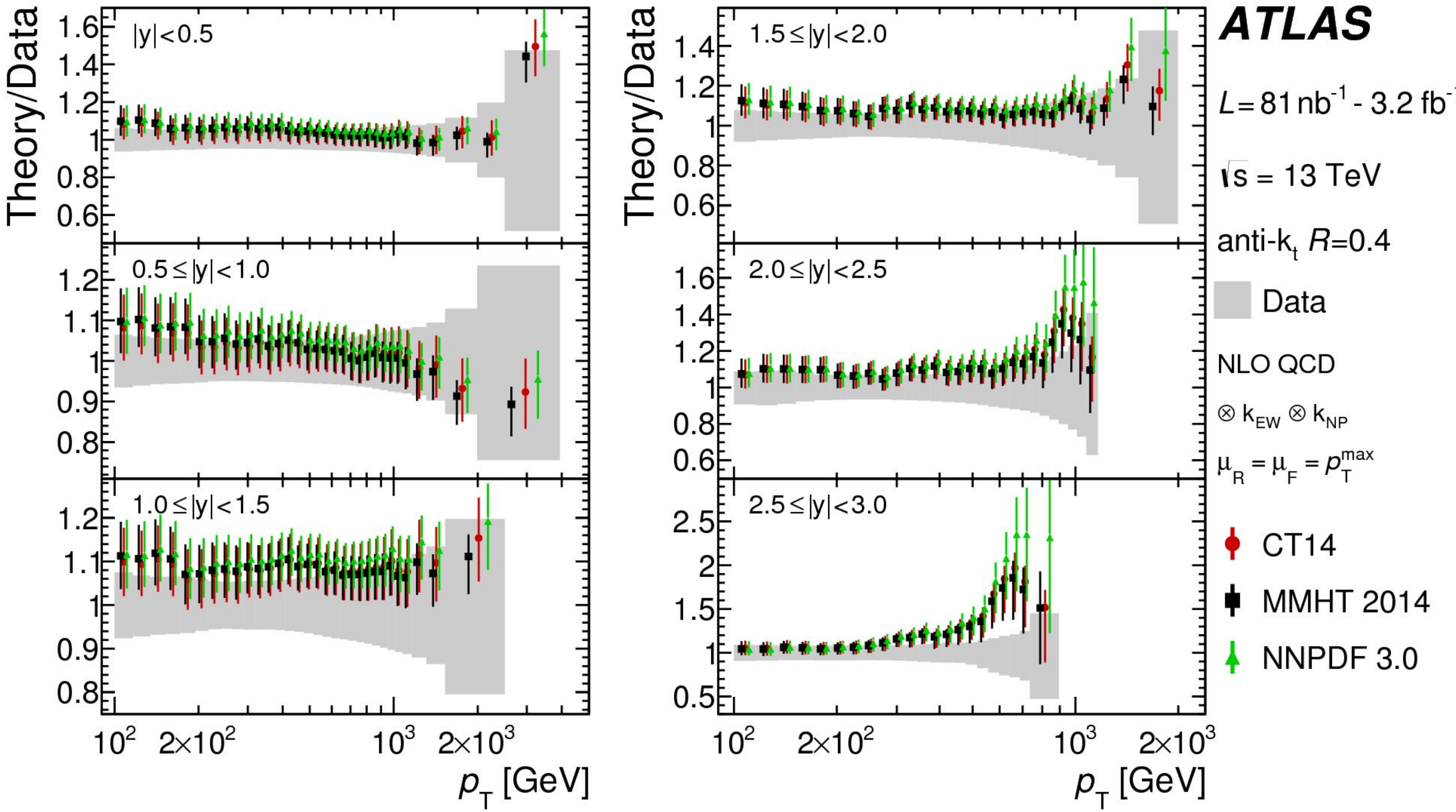

Back

→ Good data/theory agreement within uncertainties observed for most PDF sets: CT14, MMHT 2014, NNPDF 3.0, HERAPDF 2.0, ABMP16

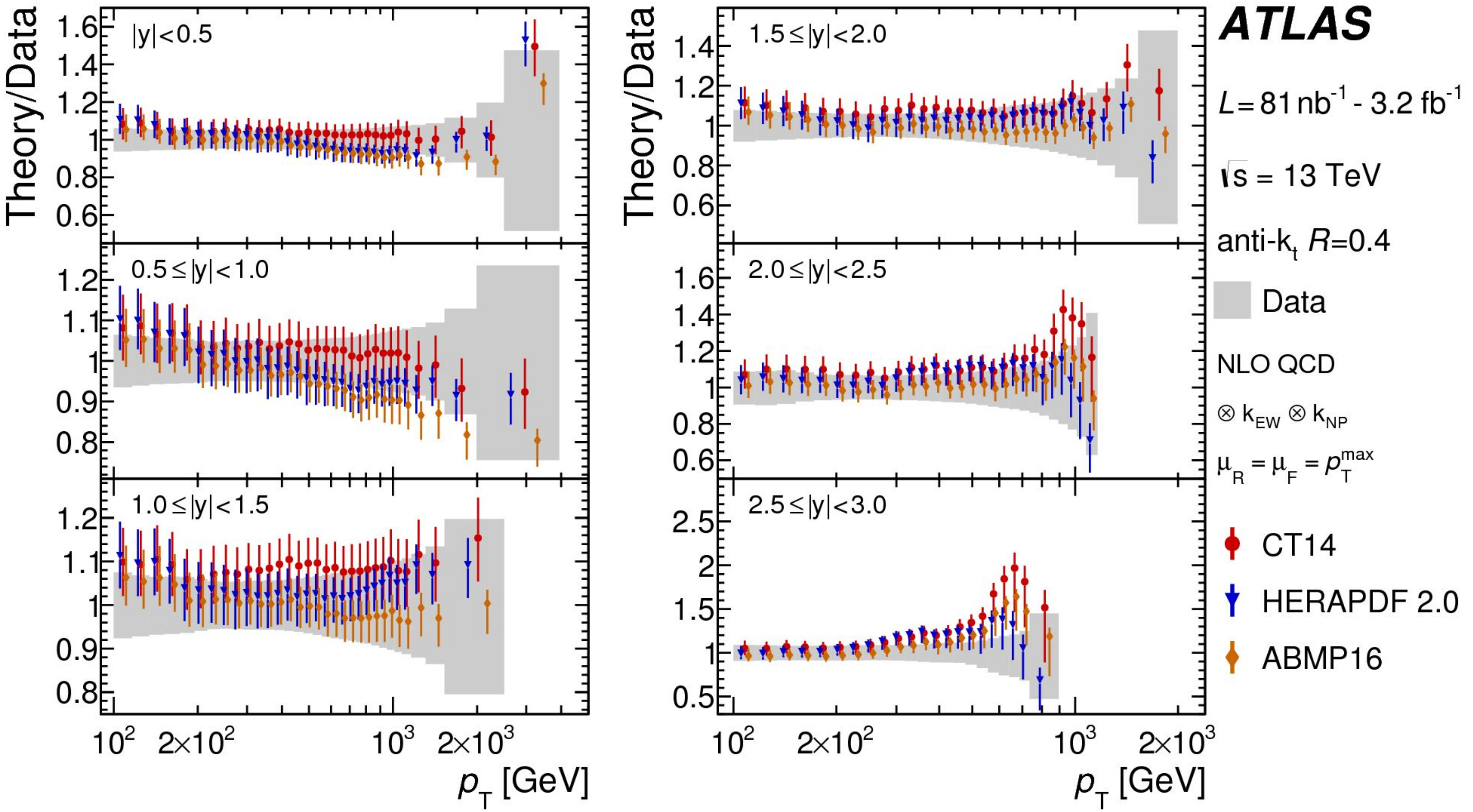

Inclusive jet cross sections: NLO/NNLO

→ Better data/theory agreement for NNLO, when using the p_T^{jet} scale choice

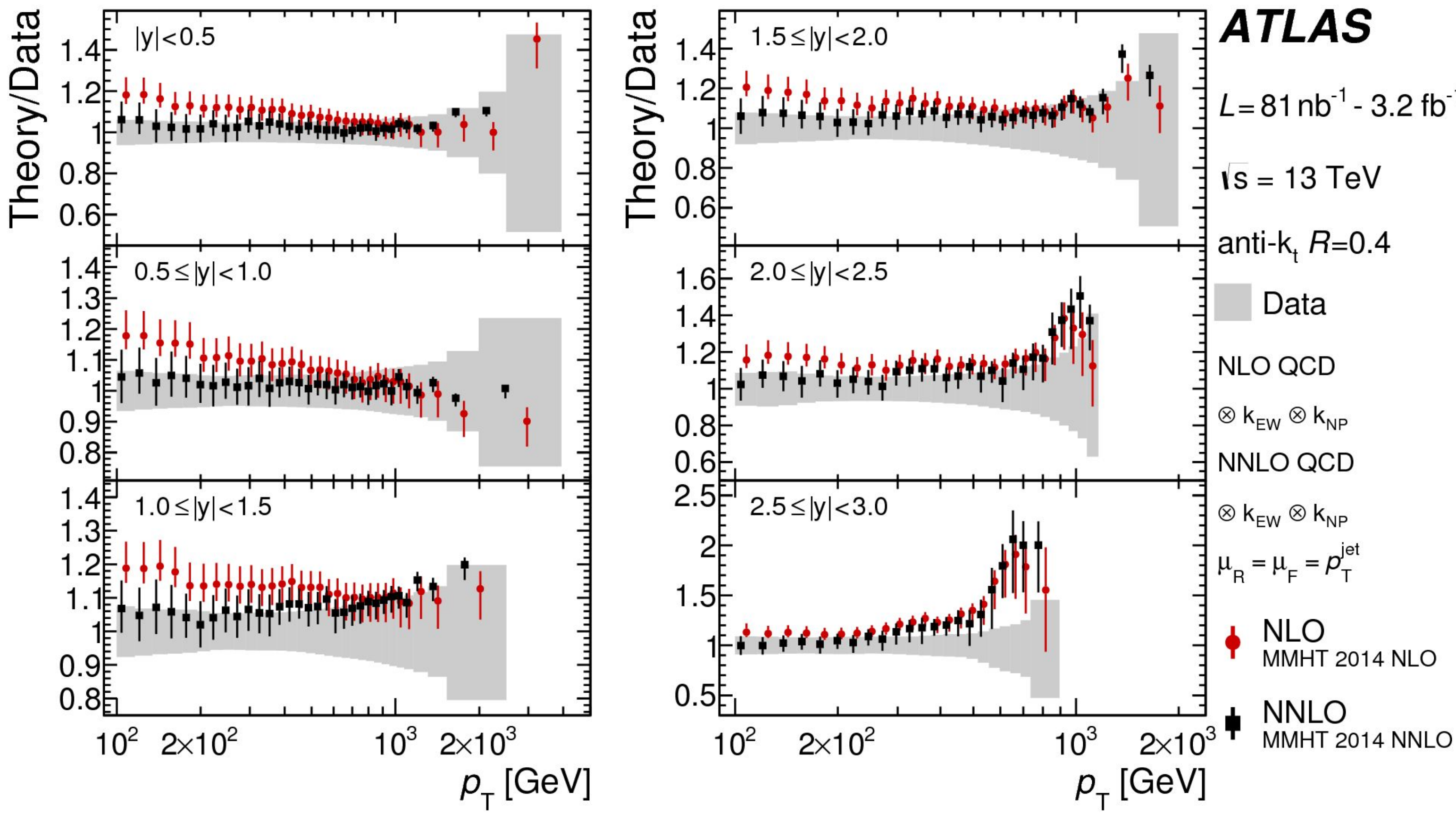

Inclusive jet cross sections: NLO/NNLO

→ Better data/theory agreement for NLO, when using the p_T^{max} scale choice

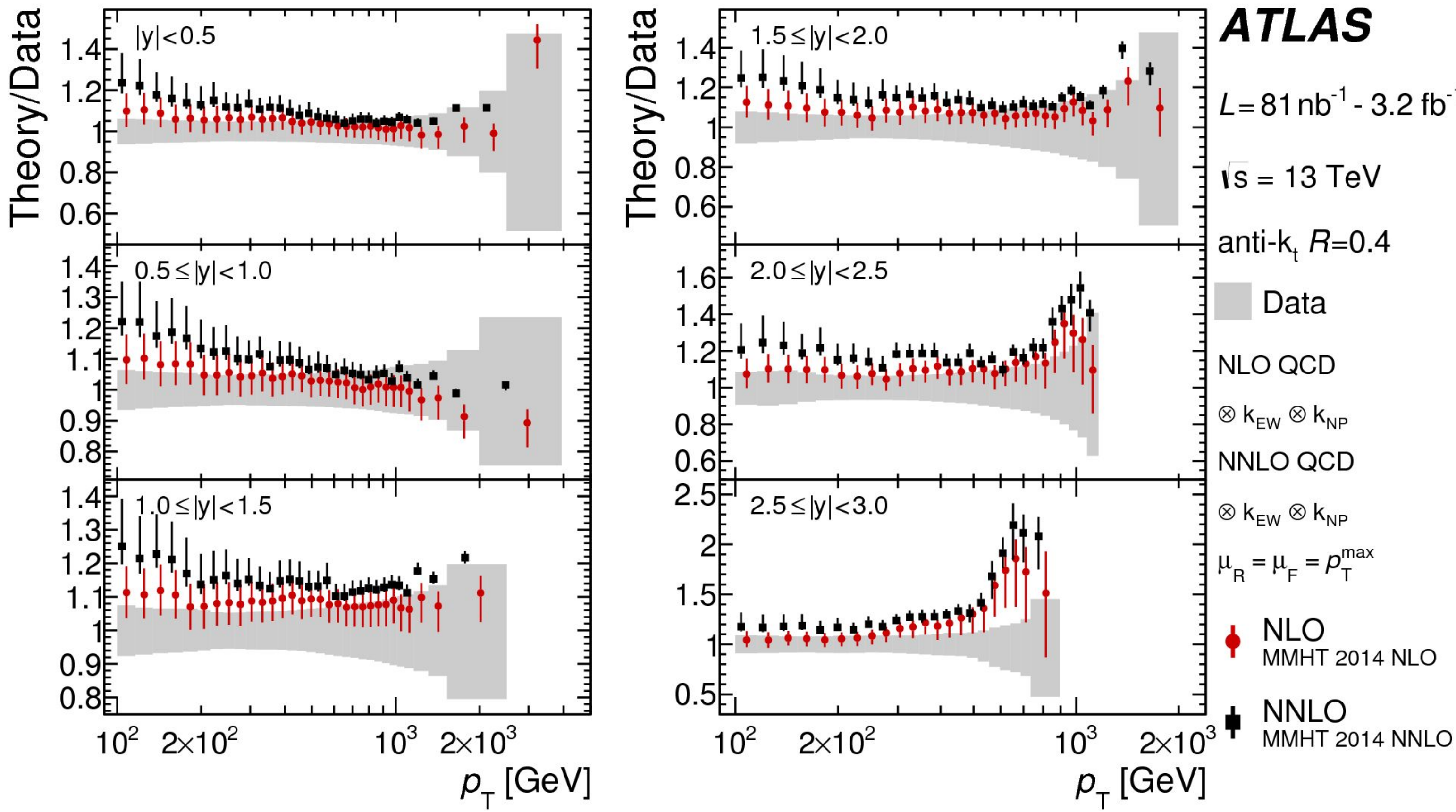

Dijet cross sections: theory/data

→ Good data/theory agreement within uncertainties observed for most PDF sets: CT14, MMHT 2014, NNPDF 3.0, HERAPDF 2.0, ABMP16

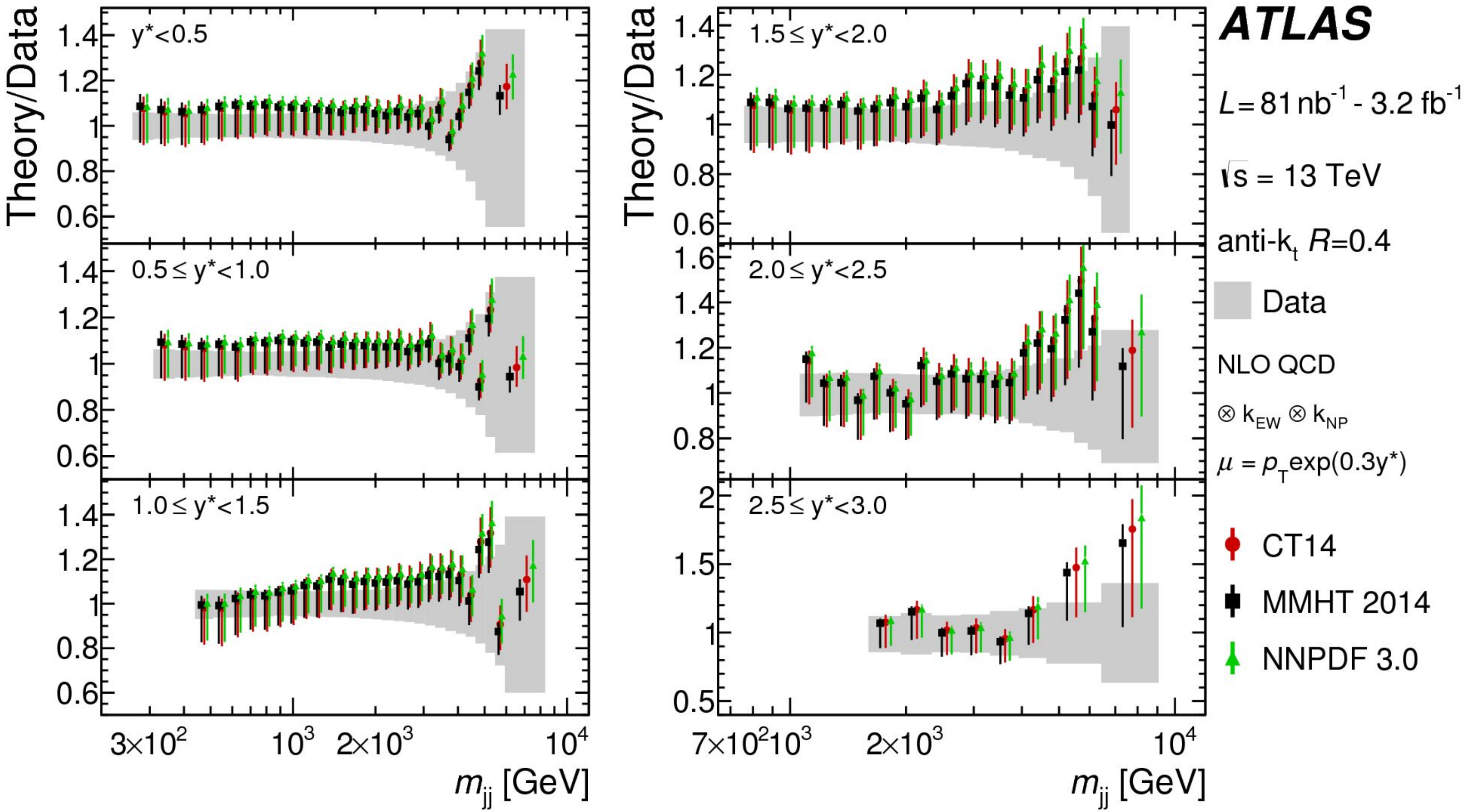

Dijet cross sections: theory/data

→ Good data/theory agreement within uncertainties observed for most PDF sets:
CT14, MMHT 2014, NNPDF 3.0, HERAPDF 2.0, ABMP16

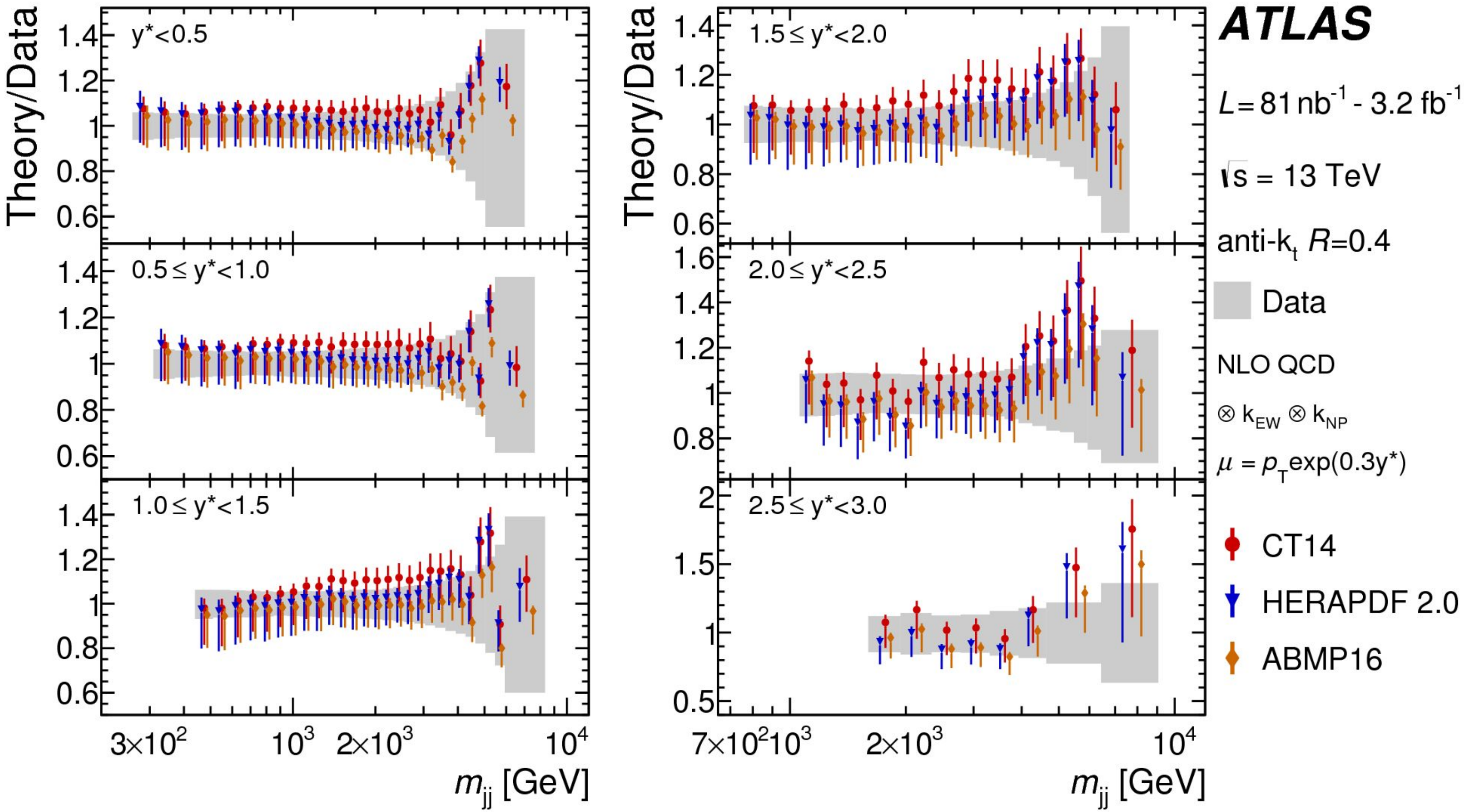

Inclusive jet cross sections at √s=8 TeV: Theory/Data

→ Good data/theory agreement within uncertainties observed for most PDF sets

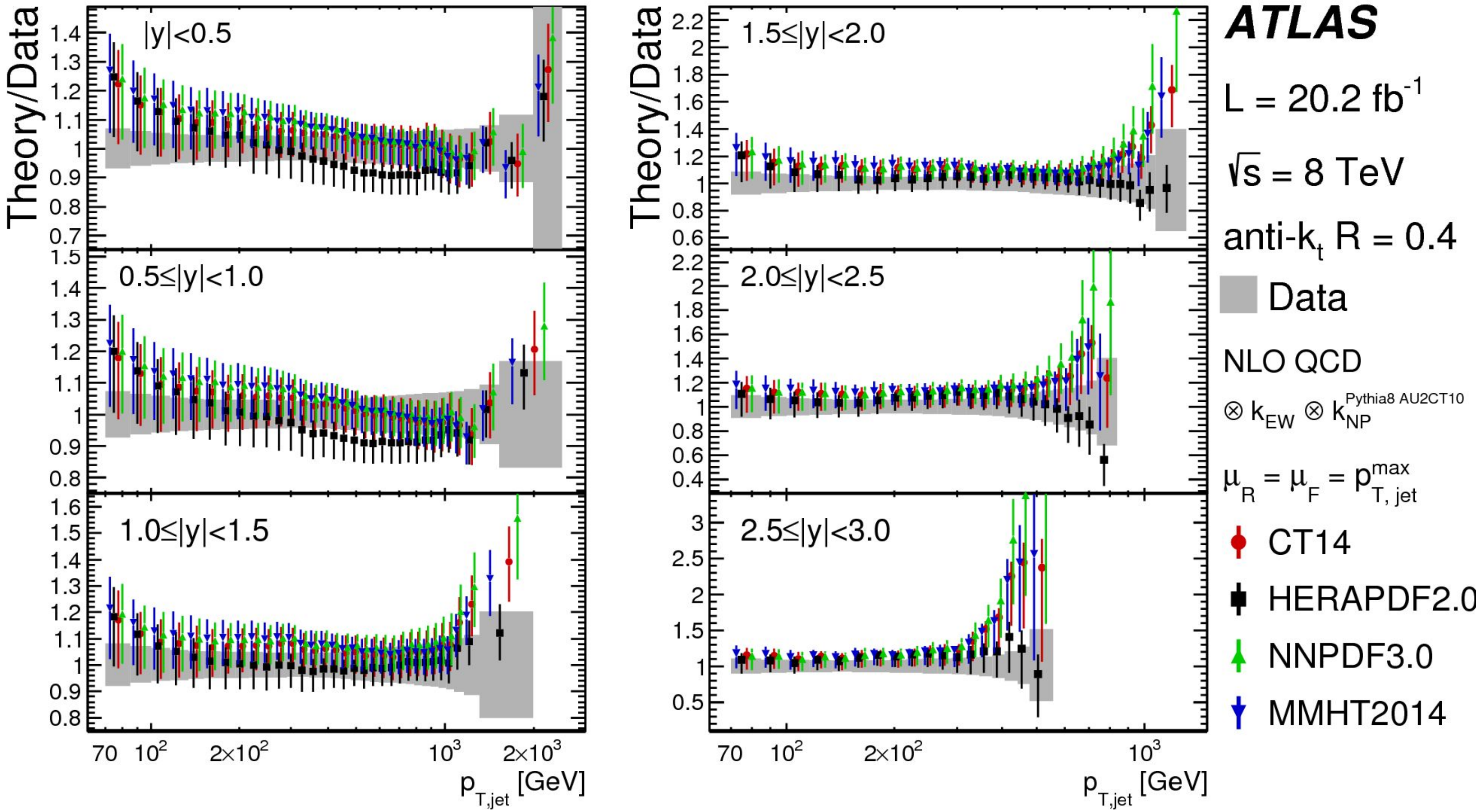

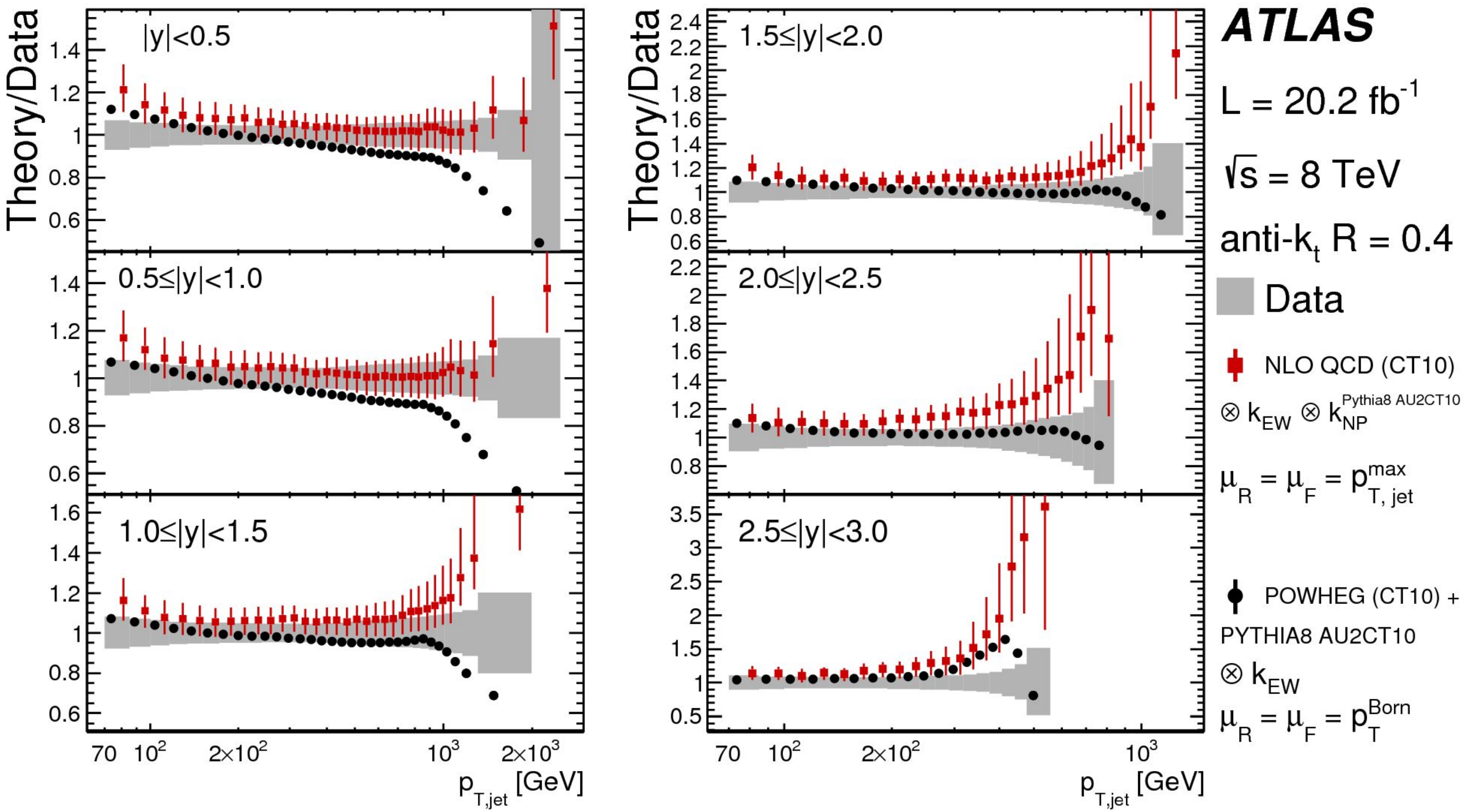
Theory/Data
|y|<0.5
0.5≤|y|<1.0
1.0≤|y|<1.5
1.5≤|y|<2.0
2.0≤|y|<2.5
2.5≤|y|<3.0
p_T,jet [GeV]
ATLAS
L = 20.2 fb^-1
√s = 8 TeV
anti-k_t R = 0.4
Data
NLO QCD (CT10)
⊗ k_EW ⊗ k_NP^Pythia8 AU2CT10
μ_R = μ_F = p_T, jet^max
POWHEG (CT10) +
PYTHIA8 AU2CT10
⊗ k_EW
μ_R = μ_F = p_T^Born

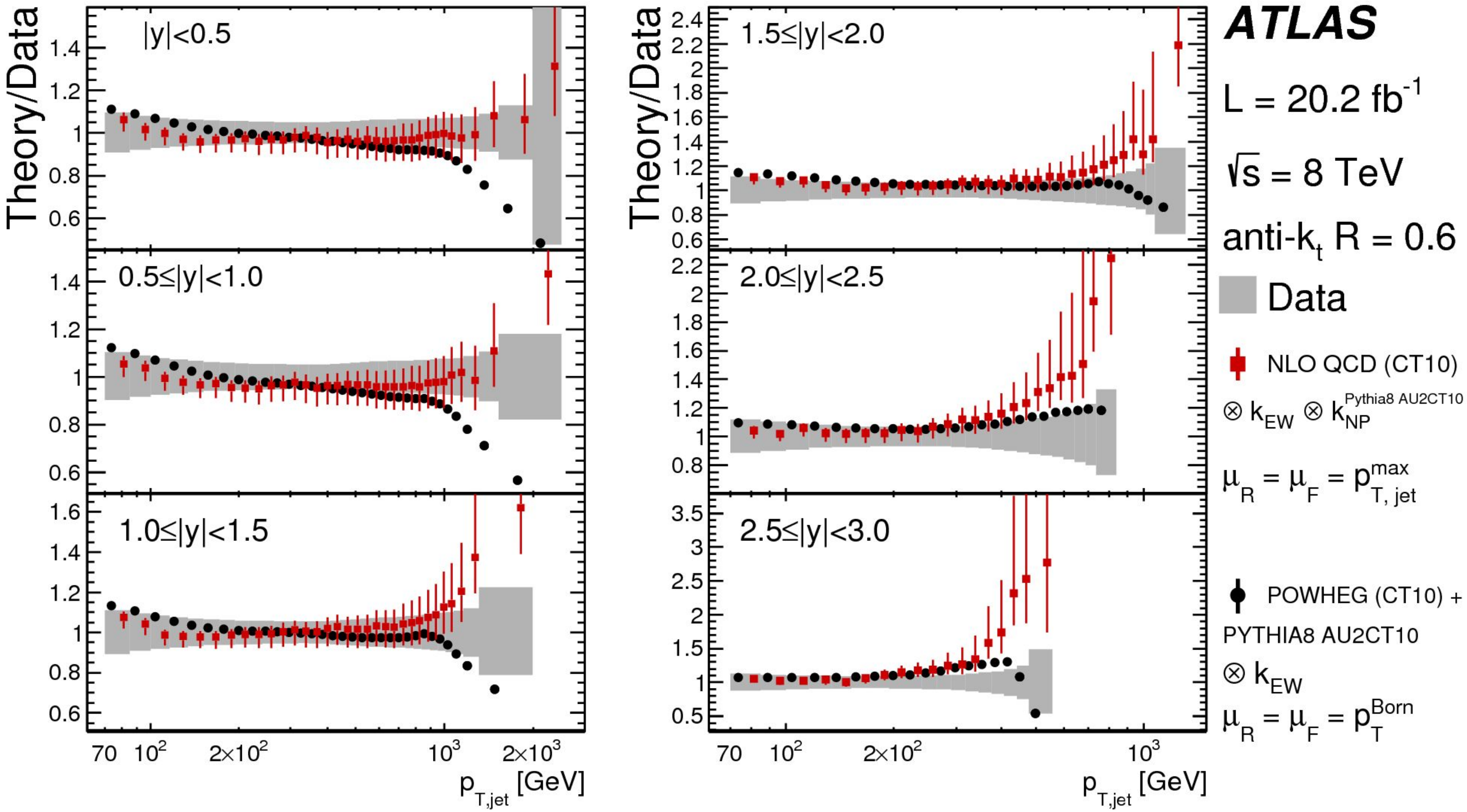

ATLAS
L = 20.2 fb-1
√s = 8 TeV
anti-kt R = 0.6
Data
NLO QCD (CT10)
⊗ kEW ⊗ kNP Pythia8 AU2CT10
μR = μF = pT, jet max
POWHEG (CT10) +
PYTHIA8 AU2CT10
⊗ kEW
μR = μF = pT Born
Theory/Data
|y|<0.5
0.5≤|y|<1.0
1.0≤|y|<1.5
1.5≤|y|<2.0
2.0≤|y|<2.5
2.5≤|y|<3.0
pT,jet [GeV]

α_s determination in a given (p_T ; $|y|$) bin

→ Theory prediction: $\sigma(\alpha_s)$ using NLOJET++(CT10) with NP corrections

→ Computed for the α_s values that were used in the PDF fits: interpolation between these values and extrapolation outside the covered range

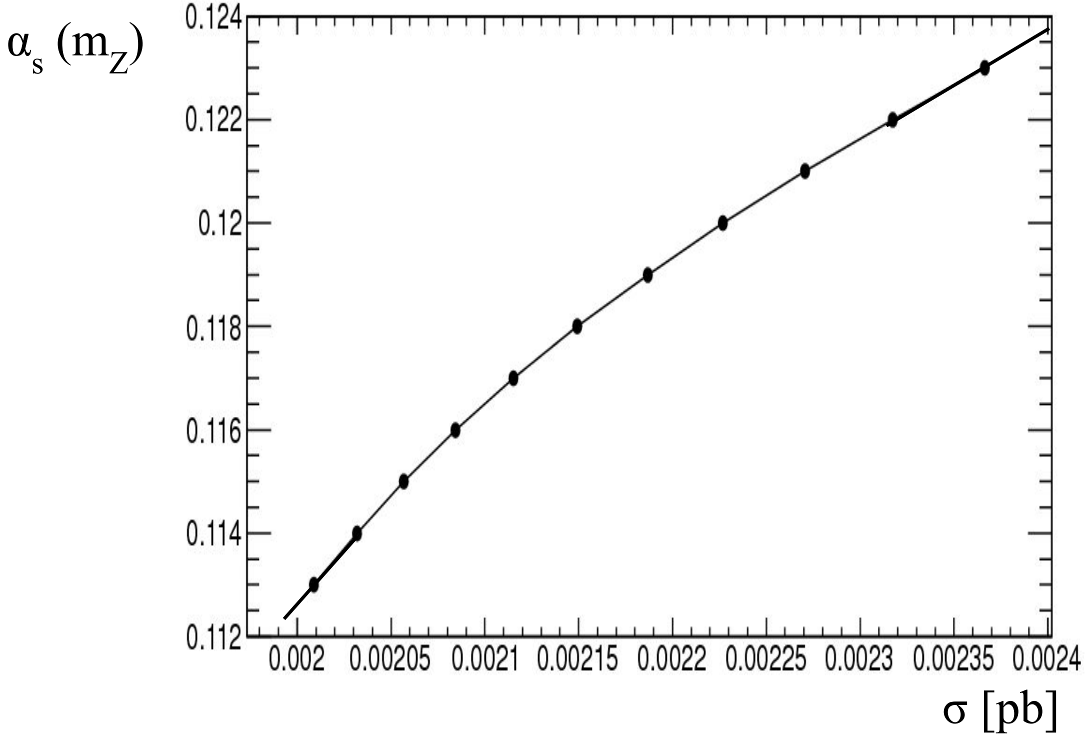

Back

Covariance & correlation matrices - α_s - all |y| bins

→ Using toys: both statistical and systematic uncertainties are fluctuated, taking into account correlations; $\alpha_s(\sigma_{toy})$ determined for each toy

Correlation matrix

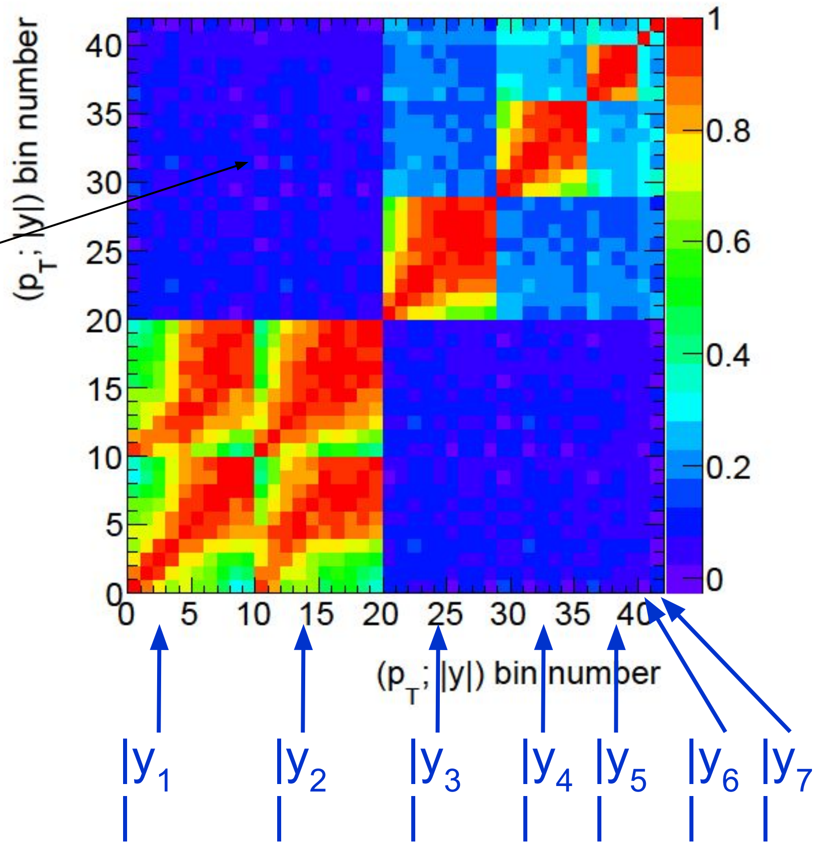

Small correlations of systematic uncertainties between central and forward regions

Theoretical uncertainties & full result for α_s from inclusive jets

1) Scale uncertainty:
tested $(\mu_r; \mu_f) \in \{(1;1), (0.5;1), (2;1), (1;0.5), (1;2), (0.5;0.5), (2;2)\}$

2) PDF(CT10) uncertainties propagated using 26 (positive and negative) nuisance parameters

3) Uncertainty due to the PDF choice

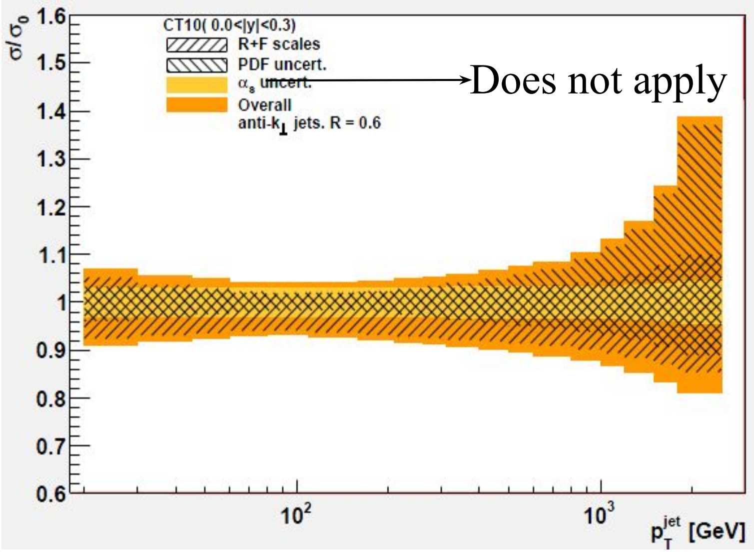

$$\alpha_s = 0.1151 \pm 0.0001(\text{stat}) \pm 0.0047(\text{exp syst}) \pm 0.0060(\text{jet size}) \pm 0.0014(p_T \text{ range})$$
$$^{+0.0044}_{-0.0011}(\text{scale}) \pm 0.0010(\text{PDF e. v.}) \, ^{+0.0022}_{-0.0015}(\text{PDF choice}) \pm \, ^{+0.0009}_{-0.0034}(\text{NP corr.})$$

→ Good agreement with world average

→ Largest systematic uncertainty from choice of the jet size (R)

→ *Scale choice effectively different for jets with R=0.4 / R=0.6*
Is this well motivated for a given type of events for which we just consider various observables?
(i.e. jet cross-sections with various jet sizes)

1) Simple average - central |y| bin

→ In each toy make simple average (weight=$1/N_{bins}$) of the α_s values in 10 bins (45−600GeV) where the α_s scan in PDF fits "covers" well the distribution: discard few low precision bins at low and high p_T

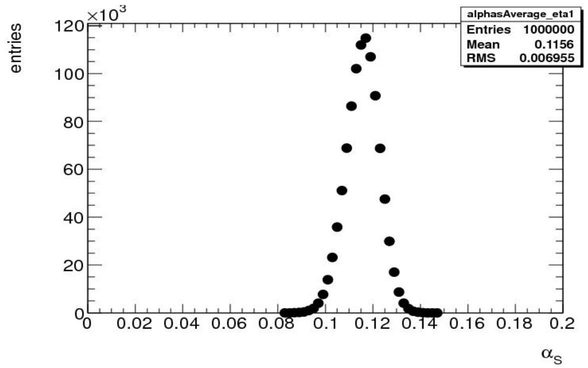

→ α_s = 0.1156 +0.0067 −0.0072 (exp.)

2) Weighted average - central |y| bin

→ In each toy make weighted average (weight=$1/\sigma_i^2$) of the α_s values in 10 bins (45−600GeV)

→ α_s = 0.1155 +0.0067 −0.0069 (exp.)

→ Small uncertainty reduction /simple average

→ χ^2_{diag}/dof = 0.049 (9 dof)
Correlations important to evaluate fit quality

→ Weights ∈ [0;1]

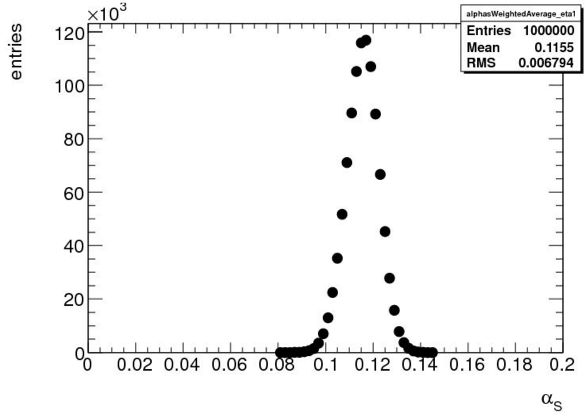

3) Average using χ^2 minimization - central |y| bin

$$\chi^2 = (\alpha_s - \alpha_s^{av}) C^{-1} (\alpha_s - \alpha_s^{av})^T$$

→ Covariance and correlation matrices computed after symmetrization of α_s uncertainties

(compensation of asymmetries in data uncertainties and non-linear effects in $\sigma(\alpha_s)$)

Covariance matrix

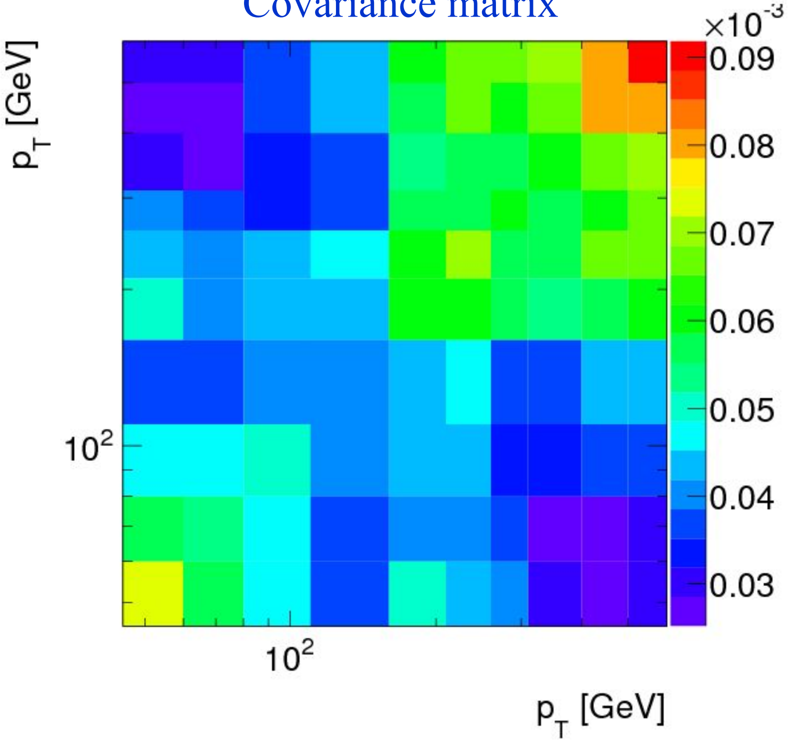

Correlation matrix

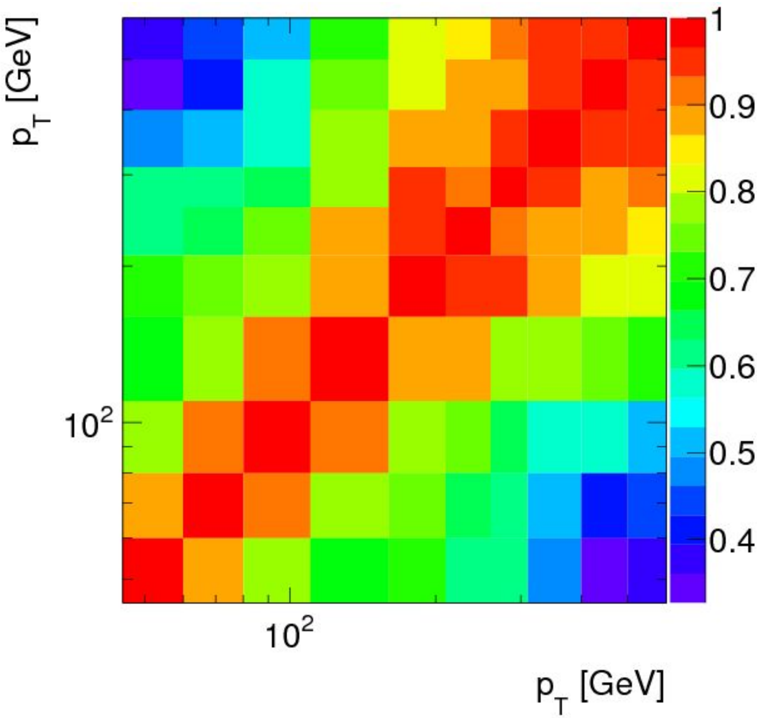

3) Average using χ^2 minimization - central |y| bin

$\longrightarrow$ In each toy compute α_s average by minimizing

$\chi^2 = (\alpha_s - \alpha_s^{av})C^{-1}(\alpha_s - \alpha_s^{av})^T$

$\longrightarrow$ $\alpha_s = 0.1160 \pm 0.0051$ (exp.)

$\longrightarrow$ χ^2_{correl}/dof = 0.39 (9 dof)

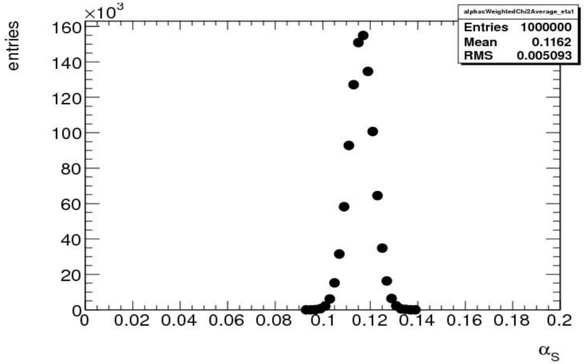

$\longrightarrow$ Problem in the weights:

{0.019; 0.646; -0.785; 1.576; -1.262; -0.157; 0.576; 0.991; -0.116; -0.488}

"Standard" problem of χ^2 in presence of strong correlations

$\longrightarrow$ Important reduction of the uncertainty/weighted av.

χ^2 minimization ~ uncertainty minimization, but fully relies on the correlations of uncertainties for determining the nominal value and the final (smallest) uncertainty: ignores uncertainties on correlations ! (which do exist for <u>any data set</u> !)

$\longrightarrow$ The weighted average uses correlations only in the uncertainty propagation

α_s from inclusive jets: weighted averages - all |y| bins

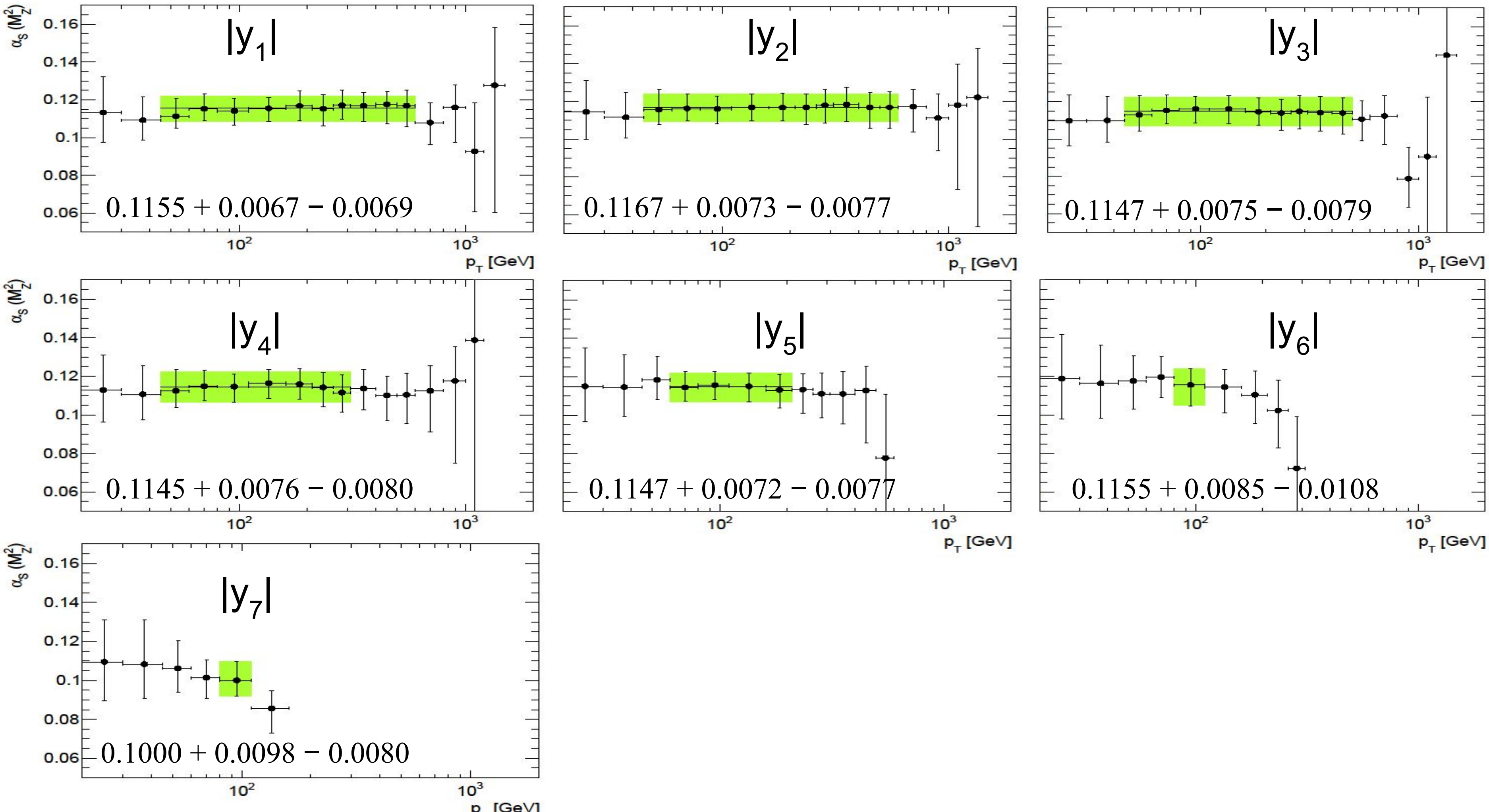

α_s from inclusive jets: weighted average & running

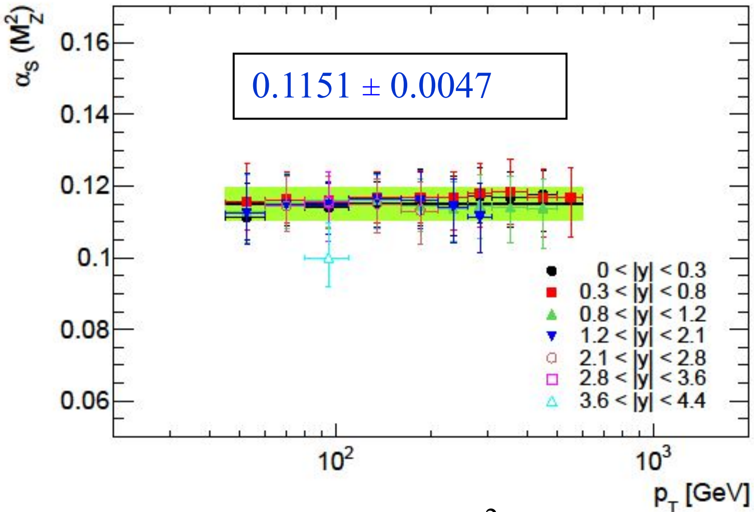

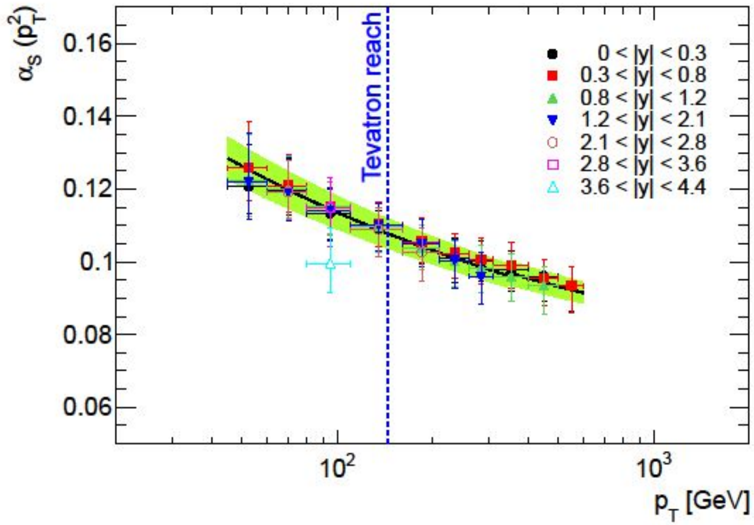

→ Weighted average ($\sim 1/\sigma_i^2$) for nominal result:
- avoid biases in the weights due to uncertainties on correlations
- full propagation of correlations for the evaluation of uncertainties

→ Reduction of the uncertainty for the average when including all |y| bins:
small correlations of the systematic uncertainties between different |y| bins

→ $\chi^2_{correl}/\mathrm{dof} = 0.54$ (41 dof)

→ Test of RGE for $p_T \in [45;600]$GeV

→ Shift of central value & error reduction minimizing χ^2_{correl}: (0.1165 ± 0.0033);
negative weights present here too

$\langle Q \rangle$ (GeV)	TEEC $\alpha_s(Q^2)$ value (NNPDF 3.0)
412	0.0966 ± 0.0014 (exp.) $^{+0.0054}_{-0.0015}$ (scale) ± 0.0009 (PDF) ± 0.0001 (NP)
437	0.0964 ± 0.0012 (exp.) $^{+0.0048}_{-0.0011}$ (scale) ± 0.0009 (PDF) ± 0.0002 (NP)
472	0.0955 ± 0.0011 (exp.) $^{+0.0051}_{-0.0015}$ (scale) ± 0.0009 (PDF) ± 0.0001 (NP)
522	0.0936 ± 0.0011 (exp.) $^{+0.0043}_{-0.0010}$ (scale) ± 0.0010 (PDF) ± 0.0001 (NP)
604	0.0933 ± 0.0011 (exp.) $^{+0.0050}_{-0.0014}$ (scale) ± 0.0011 (PDF) ± 0.0003 (NP)
810	0.0907 ± 0.0013 (exp.) $^{+0.0049}_{-0.0020}$ (scale) ± 0.0011 (PDF) ± 0.0002 (NP)

$\langle p_{T3} \rangle$ (GeV)	$\alpha_s(\langle p_{T3} \rangle)$ value (TEEC, NNPDF 3.0)
169	0.1072 ± 0.0017 (exp.) $^{+0.0067}_{-0.0019}$ (scale) ± 0.0011 (PDF) ± 0.0001 (NP)
174	0.1074 ± 0.0014 (exp.) $^{+0.0060}_{-0.0014}$ (scale) ± 0.0012 (PDF) ± 0.0002 (NP)
179	0.1068 ± 0.0014 (exp.) $^{+0.0064}_{-0.0019}$ (scale) ± 0.0012 (PDF) ± 0.0001 (NP)
186	0.1052 ± 0.0014 (exp.) $^{+0.0054}_{-0.0013}$ (scale) ± 0.0013 (PDF) ± 0.0001 (NP)
197	0.1060 ± 0.0014 (exp.) $^{+0.0065}_{-0.0018}$ (scale) ± 0.0014 (PDF) ± 0.0004 (NP)
215	0.1052 ± 0.0018 (exp.) $^{+0.0066}_{-0.0027}$ (scale) ± 0.0015 (PDF) ± 0.0003 (NP)

→ *For observables like $R_{3/2}$, $N_{3/2}$, $R_{\Delta\Phi}$ and (A)TEEC, sensitivity to α_s originates from probability of emission of extra radiation (3^{rd} jet etc.)*

→ Effect acknowledged by evolving α_s to $<p_{T3}>$ (significantly lower than $<H_{T2}>$)

Back

Thoughts on RGE tests through jet measurements

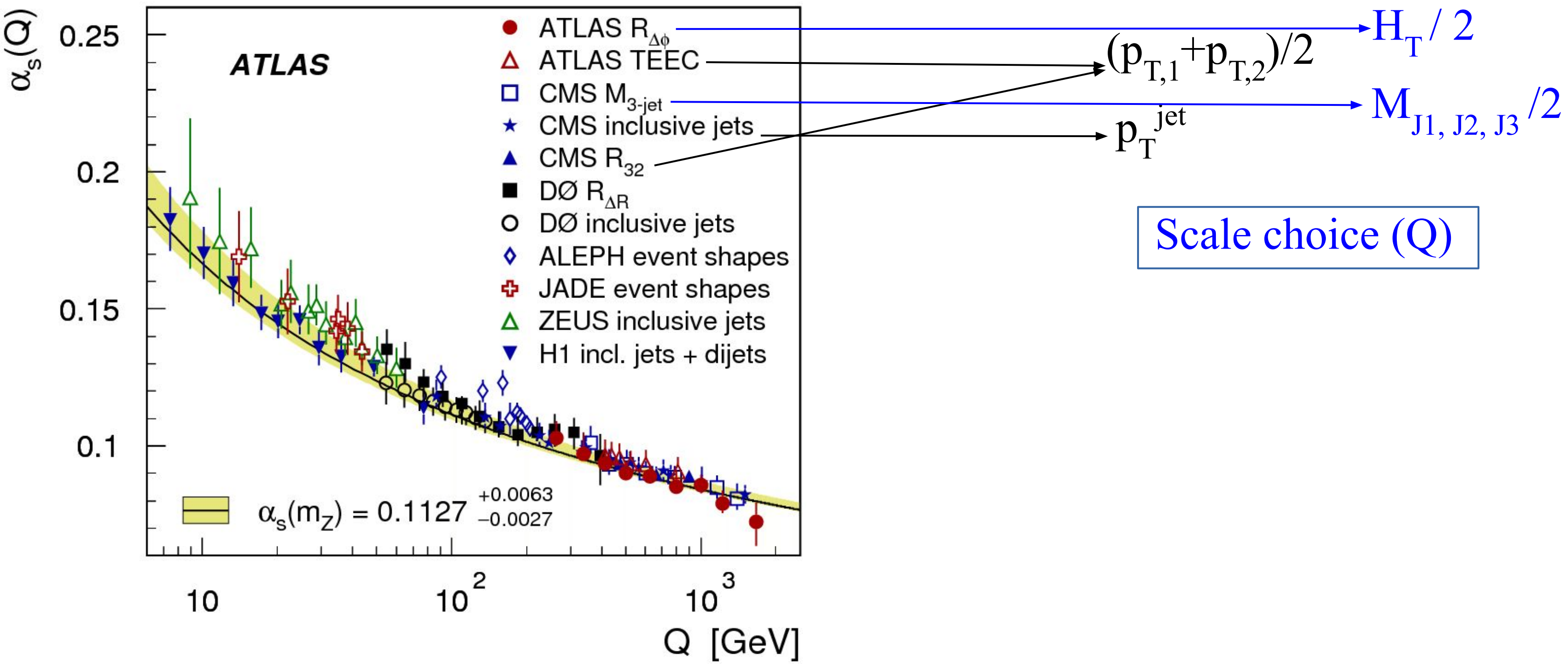

Scale choice (Q)

→ *Can one really claim tests of RGE at scales from event-level observables ???*

e.g. $p_T^{\text{lead. jet}}(R_{3/2})$, $p_T^{\text{(all jets)}}(N_{3/2})$, $(p_{T,1}+p_{T,2})/2$, $H_T/2$, $M_{J1,J2,J3}/2$ (large even for low $p_{T,1\text{-}3}$)

→ *"Traditional criteria" of minimizing uncertainties/k-factors is not relevant here*

→ *Relevant scale for RGE test using $R_{3/2}$, $N_{3/2}$, $R_{\Delta\Phi}$ and (A)TEEC related to $p_{T,3}$ (low)*

Need consistency between scale for theory calculation and RGE test claim; MiNLO procedure may provide a way forward.

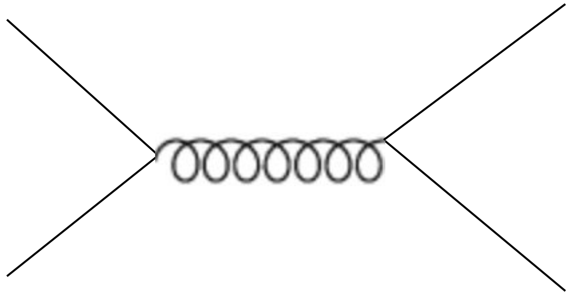

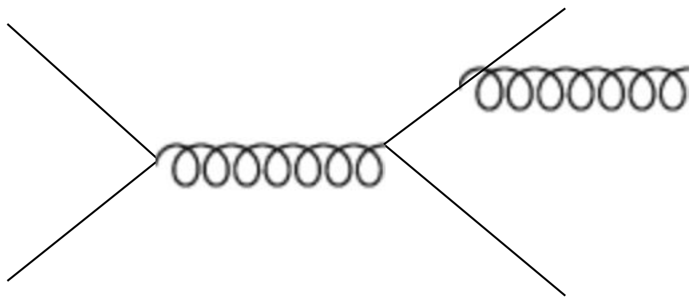

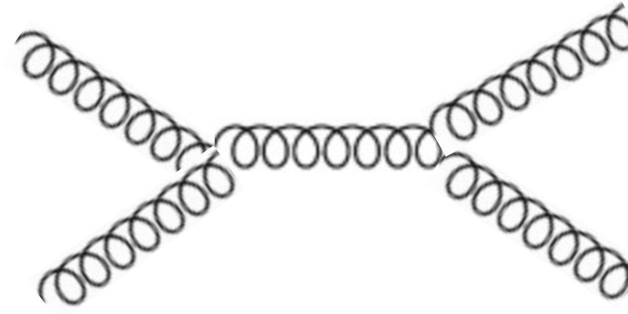

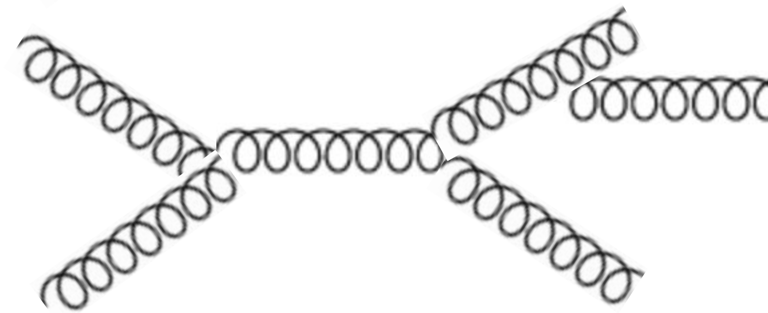

→ *PDF uncertainties non-negligible* (typically between total experimental and NLO scale uncertainty) *for cross-section ratio measurements & (A)TEEC:*

- probability of extra radiation (which makes these observables non-trivial) sensitive to the type of partons in the initial state
- both α_s & PDF sensitivities of the observables are reduced when taking ratios and they are both relevant for the α_s evaluation

Result quantitative comparisons for "all" PDFs

- Individual |y| bins, wide p_T ranges: p-values generally > 4% (~1% or lower for R=0.6, 0.5 < |y| < 1 at 8 TeV, 1.5 < |y| < 2 at 13 TeV), decreasing when considering wider phase-space regions

- Full |y| range, wide p_T ranges: p-values << 10^{-3}
  (p_T > 100 GeV) χ^2/ndf: ~ 313-385/159 (8 TeV); 384-475/177 (13 TeV)
- Data/theory tension also seen initially by CMS in arXiv:1410.6765 when using the original data, uncertainties and correlations from arXiv:1212.6660
- CMS noticed that "Changing the correlation in the JES uncertainty from 0% to 100% produces a steep rise in χ^2/ndf " and modified the correlation model

- Good data/theory agreement on full phase-space for ATLAS dijets (13 TeV)

- Full |y| range, narrow p_T ranges: good data/theory agreement for 70 < p_T < 100 GeV;
  p-values are often below 10^{-3} for the other narrow p_T ranges

- Pairs of |y| bins(consecutive / central-forward), narrow p_T ranges at >100 GeV:
  Good data/theory agreement → *source of low p-values not in a single |y| bin, nor due to some possible central/forward tension*

- Little sensitivity to choice of non-perturbative correction and to scale choice

Back

Role of uncertainty correlations

→ Correlations of uncertainties between various phase-space regions have a key role in χ^2 evaluation (e.g. ignoring correlations yields a very small χ^2/ndf)

→ Experimental uncertainties (examples for ATLAS measurements):

- JES in-situ statistical uncertainties: correlations well known (e.g. > 240 components for calibration using dijet balance reduce χ^2 by more than 200 units)
- JES Flavour Response, JES MJB Fragmentation, JES Pile-up Rho Topology:
  "2-point systematics" from comparison of various MC generators – unknown correlations

→ Theoretical uncertainties:

- α_S , PDFs: correlations (generally) well known
- Scale variations, alternative scale choice, non-perturbative corrections:
  "2-point systematics" – unknown correlations

→ *Good understanding of the sources of systematic uncertainties required in order to evaluate uncertainties on correlations: performed detailed tests using realistic alternative correlation scenarios*

Testing realistic alternative correlation assumptions

→18 options for splitting the systematics with unknown correlations in
2 or 3 sub-components with smooth p_T and/or $|y|$ dependence

Splitting option	Sub-component(s) definition(s), completed by complementary
1	$L(\ln(p_{\mathrm{T}}[\mathrm{TeV}]), \ln(0.1), \ln(2.5))\cdot$ uncertainty
2	$L(\ln(p_{\mathrm{T}}[\mathrm{TeV}]), \ln(0.1), \ln(2.5)) \cdot 0.5\cdot$ uncertainty
3	$L(p_{\mathrm{T}}[\mathrm{TeV}], 0.1, 2.5)\cdot$ uncertainty
4	$L(p_{\mathrm{T}}[\mathrm{TeV}], 0.1, 2.5) \cdot 0.5\cdot$ uncertainty
5	$L((\ln(p_{\mathrm{T}}[\mathrm{TeV}]))^2, (\ln(0.1))^2, (\ln(2.5))^2)\cdot$ uncertainty
6	$L((\ln(p_{\mathrm{T}}[\mathrm{TeV}]))^2, (\ln(0.1))^2, (\ln(2.5))^2) \cdot 0.5\cdot$ uncertainty
7	$L(\|y\|, 0, 3)\cdot$ uncertainty
8	$L(\|y\|, 0, 3) \cdot 0.5\cdot$ uncertainty
9	$L(\ln(p_{\mathrm{T}}[\mathrm{TeV}]), \ln(0.1), \ln(2.5)) \cdot L(\|y\|, 0, 3)\cdot$ uncertainty
10	$L(\ln(p_{\mathrm{T}}[\mathrm{TeV}]), \ln(0.1), \ln(2.5)) \cdot \sqrt{1 - L(\|y\|, 0, 3)^2}\cdot$ uncertainty
11	$L(\ln(p_{\mathrm{T}}[\mathrm{TeV}]), \ln(0.1), \ln(2.5)) \cdot L(\|y\|, 0, 3) \cdot 0.5\cdot$ uncertainty
12	$L(\ln(p_{\mathrm{T}}[\mathrm{TeV}]), \ln(0.1), \ln(2.5)) \cdot \sqrt{1 - L(\|y\|, 0, 3)^2} \cdot 0.5\cdot$ uncertainty
13	$L(\ln(p_{\mathrm{T}}[\mathrm{TeV}]), \ln(0.1), \ln(2.5)) \cdot \sqrt{1 - L(\|y\|, 0, 1.5)^2}\cdot$ uncertainty $L(\ln(p_{\mathrm{T}}[\mathrm{TeV}]), \ln(0.1), \ln(2.5)) \cdot L(\|y\|, 1.5, 3)\cdot$ uncertainty
14	$L(\ln(p_{\mathrm{T}}[\mathrm{TeV}]), \ln(0.1), \ln(2.5)) \cdot \sqrt{1 - L(\|y\|, 0, 1)^2}\cdot$ uncertainty $L(\ln(p_{\mathrm{T}}[\mathrm{TeV}]), \ln(0.1), \ln(2.5)) \cdot L(\|y\|, 1, 3)\cdot$ uncertainty
15	$L(\ln(p_{\mathrm{T}}[\mathrm{TeV}]), \ln(0.1), \ln(2.5)) \cdot \sqrt{1 - L(\|y\|, 0, 2)^2}\cdot$ uncertainty $L(\ln(p_{\mathrm{T}}[\mathrm{TeV}]), \ln(0.1), \ln(2.5)) \cdot L(\|y\|, 2, 3)\cdot$ uncertainty
16	$\sqrt{1 - L(\ln(p_{\mathrm{T}}[\mathrm{TeV}]), \ln(0.1), \ln(2.5))^2} \cdot \sqrt{1 - L(\|y\|, 0, 1.5)^2}\cdot$ uncertainty $\sqrt{1 - L(\ln(p_{\mathrm{T}}[\mathrm{TeV}]), \ln(0.1), \ln(2.5))^2} \cdot L(\|y\|, 1.5, 3)\cdot$ uncertainty
17	$\sqrt{1 - L(\ln(p_{\mathrm{T}}[\mathrm{TeV}]), \ln(0.1), \ln(2.5))^2} \cdot \sqrt{1 - L(\|y\|, 0, 1)^2}\cdot$ uncertainty $\sqrt{1 - L(\ln(p_{\mathrm{T}}[\mathrm{TeV}]), \ln(0.1), \ln(2.5))^2} \cdot L(\|y\|, 1, 3)\cdot$ uncertainty
18	$\sqrt{1 - L(\ln(p_{\mathrm{T}}[\mathrm{TeV}]), \ln(0.1), \ln(2.5))^2} \cdot \sqrt{1 - L(\|y\|, 0, 2)^2}\cdot$ uncertainty $\sqrt{1 - L(\ln(p_{\mathrm{T}}[\mathrm{TeV}]), \ln(0.1), \ln(2.5))^2} \cdot L(\|y\|, 2, 3)\cdot$ uncertainty

L(x, min, max) = (x-min)/(max-min)

→ Tested for *experimental and theoretical systematic uncertainties*

Changed theorists' view on how to interpret our measurements

→ One component added to the ones listed for each option in the table, to keep total uncertainty unchanged

Testing realistic alternative correlation assumptions

→ Splitting the *theory systematic uncertainties* with unknown correlations in *6 sub-components with smooth p_T and $|y|$ dependence*

$$f_1(p_\mathrm{T}, y) = C(p_\mathrm{T}, y) \cdot c_1 / \log\left(M(y)/p_\mathrm{T}\right),$$
$$f_2(p_\mathrm{T}, y) = C(p_\mathrm{T}, y) \cdot c_2 \cdot y^2 / \log\left(M(y)/p_\mathrm{T}\right),$$
$$f_3(p_\mathrm{T}, y) = C(p_\mathrm{T}, y) \cdot c_3,$$
$$f_4(p_\mathrm{T}, y) = C(p_\mathrm{T}, y) \cdot c_4 \cdot y^2,$$
$$f_5(p_\mathrm{T}, y) = C(p_\mathrm{T}, y) \cdot c_5 \cdot \log\left(15 p_\mathrm{T}/M(y)\right),$$
$$f_6(p_\mathrm{T}, y) = C(p_\mathrm{T}, y) \cdot c_6 \cdot y^2 \cdot \log\left(15 p_\mathrm{T}/M(y)\right)$$

$$M(y) = \sqrt{s} \cdot exp(-y)$$

Based on:
Phys. Rev. D81 (2010) 035018
arXiv:0907.5052 [hep-ph]

→ 3 options for various values of the coefficients ($c_1 - c_6$)

Quantitative comparison between data and NLO theory prediction

8 TeV – ATLAS inclusive jets (arXiv:1706.03192)

Rapidity ranges	P_{obs} CT14	MMHT2014	NNPDF3.0	HERAPDF2.0
Anti-k_t jets $R = 0.4$				
$\lvert y\rvert < 0.5$	44%	28%	25%	16%
$0.5 \leq \lvert y\rvert < 1.0$	43%	29%	18%	18%
$1.0 \leq \lvert y\rvert < 1.5$	44%	47%	46%	69%
$1.5 \leq \lvert y\rvert < 2.0$	3.7%	4.6%	7.7%	7.0%
$2.0 \leq \lvert y\rvert < 2.5$	92%	89%	89%	35%
$2.5 \leq \lvert y\rvert < 3.0$	4.5%	6.2%	16%	9.6%
Anti-k_t jets $R = 0.6$				
$\lvert y\rvert < 0.5$	6.7%	4.9%	4.6%	1.1%
$0.5 \leq \lvert y\rvert < 1.0$	1.3%	0.7%	0.4%	0.2%
$1.0 \leq \lvert y\rvert < 1.5$	30%	33%	47%	67%
$1.5 \leq \lvert y\rvert < 2.0$	12%	16%	15%	3.1%
$2.0 \leq \lvert y\rvert < 2.5$	94%	94%	91%	38%
$2.5 \leq \lvert y\rvert < 3.0$	13%	15%	20%	8.6%

→Generally good agreement for individual |y| bins

Splitting options for $R = 0.4$	CT14	NNPDF3.0
JES Flavour Response Opt 7		
JES MJB Fragmentation Opt 17		
JES Pile-up Rho topology Opt 18		
Scale variations Opt 17		
Alternative scale choice Opt 7		
Non-perturbative corrections Opt 7	268/159	257/159
JES Flavour Response Opt 7		
JES MJB Fragmentation Opt 17		
JES Pile-up Rho topology Opt 18		
Scale variations Opt 20		
Alternative scale choice Opt 17		
Non-perturbative corrections Opt 7	261/159	260/159

χ^2/ndf	$p_T^{jet,max}$ $R = 0.4$	$R = 0.6$	p_T^{jet} $R = 0.4$	$R = 0.6$
$p_T > 70$ GeV				
CT14	349/171	398/171	340/171	392/171
HERAPDF2.0	415/171	424/171	405/171	418/171
NNPDF3.0	351/171	393/171	350/171	393/171
MMHT2014	356/171	400/171	354/171	399/171
$p_T > 100$ GeV				
CT14	321/159	360/159	313/159	356/159
HERAPDF2.0	385/159	374/159	377/159	370/159
NNPDF3.0	333/159	356/159	331/159	356/159
MMHT2014	335/159	364/159	333/159	362/159
$100 < p_T < 900$ GeV				
CT14	272/134	306/134	262/134	301/134
HERAPDF2.0	350/134	331/134	340/134	326/134
NNPDF3.0	289/134	300/134	285/134	299/134
MMHT2014	292/134	311/134	284/134	308/134
$100 < p_T < 400$ GeV				
CT14	128/72	149/72	118/72	145/72
HERAPDF2.0	148/72	175/72	141/72	170/72
NNPDF3.0	119/72	141/72	115/72	139/72
MMHT2014	132/72	143/72	122/72	140/72

→Tension when including all |y| bins

Quantitative comparison between data and NLO theory prediction

13 TeV – ATLAS inclusive jets and dijets (arXiv:1711.02692)

Rapidity ranges	P_{obs} CT14	MMHT 2014	NNPDF 3.0	HERAPDF 2.0	ABMP16
$p_{\mathrm{T}}^{\mathrm{max}}$					
$\|y\| < 0.5$	67%	65%	62%	31%	50%
$0.5 \leq \|y\| < 1.0$	5.8%	6.3%	6.0%	3.0%	2.0%
$1.0 \leq \|y\| < 1.5$	65%	61%	67%	50%	55%
$1.5 \leq \|y\| < 2.0$	0.7%	0.8%	0.8%	0.1%	0.4%
$2.0 \leq \|y\| < 2.5$	2.3%	2.3%	2.8%	0.7%	1.5%
$2.5 \leq \|y\| < 3.0$	62%	71%	69%	25%	55%
$p_{\mathrm{T}}^{\mathrm{jet}}$					
$\|y\| < 0.5$	69%	67%	66%	30%	46%
$0.5 \leq \|y\| < 1.0$	7.4%	8.9%	8.6%	3.4%	2.0%
$1.0 \leq \|y\| < 1.5$	69%	62%	68%	45%	54%
$1.5 \leq \|y\| < 2.0$	1.3%	1.6%	1.4%	0.1%	0.5%
$2.0 \leq \|y\| < 2.5$	8.7%	6.6%	7.4%	1.0%	3.6%
$2.5 \leq \|y\| < 3.0$	65%	72%	72%	28%	59%

→Generally good agreement for inclusive jets for individual |y| bins

χ^2/dof all $\|y\|$ bins	CT14	MMHT 2014	NNPDF 3.0	HERAPDF 2.0	ABMP16
$p_{\mathrm{T}}^{\mathrm{max}}$	419/177	431/177	404/177	432/177	475/177
$p_{\mathrm{T}}^{\mathrm{jet}}$	399/177	405/177	384/177	428/177	455/177

→Tension when including all |y| bins for inclusive jets

y^* ranges	P_{obs} CT14	MMHT 2014	NNPDF 3.0	HERAPDF 2.0	ABMP16
$y^* < 0.5$	79%	59%	50%	71%	71%
$0.5 \leq y^* < 1.0$	27%	23%	19%	32%	31%
$1.0 \leq y^* < 1.5$	66%	55%	48%	66%	69%
$1.5 \leq y^* < 2.0$	26%	26%	28%	9.9%	25%
$2.0 \leq y^* < 2.5$	41%	34%	29%	3.6%	20%
$2.5 \leq y^* < 3.0$	45%	46%	40%	25%	38%
all y^* bins	9.4%	6.5%	11%	0.1%	5.1%

→Good data/theory agreement for dijets

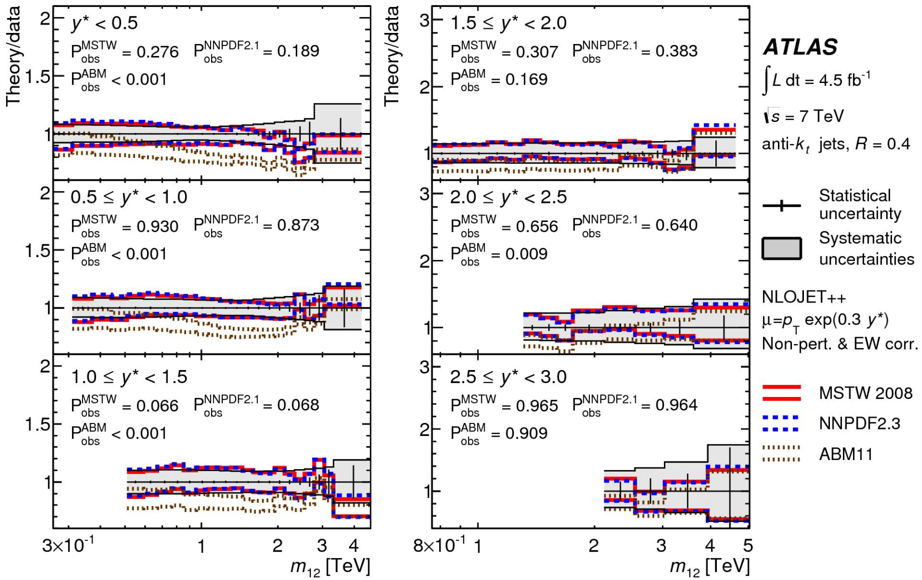

PDF set	y^* ranges	mass range (full/high)	P_{obs} $R = 0.4$	P_{obs} $R = 0.6$
CT10	$y^* < 0.5$	high	0.742	0.785
	$y^* < 1.5$	high	0.080	0.066
	$y^* < 1.5$	full	0.324	0.168
HERAPDF1.5	$y^* < 0.5$	high	0.688	0.504
	$y^* < 1.5$	high	0.025	0.007
	$y^* < 1.5$	full	0.137	0.025
MSTW 2008	$y^* < 0.5$	high	0.328	0.533
	$y^* < 1.5$	high	0.167	0.183
	$y^* < 1.5$	full	0.470	0.352
NNPDF2.1	$y^* < 0.5$	high	0.405	0.568
	$y^* < 1.5$	high	0.151	0.125
	$y^* < 1.5$	full	0.431	0.242
ABM11	$y^* < 0.5$	high	0.024	$< 10^{-3}$
	$y^* < 1.5$	high	$< 10^{-3}$	$< 10^{-3}$
	$y^* < 1.5$	full	$< 10^{-3}$	$< 10^{-3}$

→ Sensitivity to PDFs: level of agreement strongly depends on the PDF set and phase-space region

→ Valuable experimental inputs to constrain proton PDFs: Published information on cross-sections & uncertainties, with their correlations and asymmetries

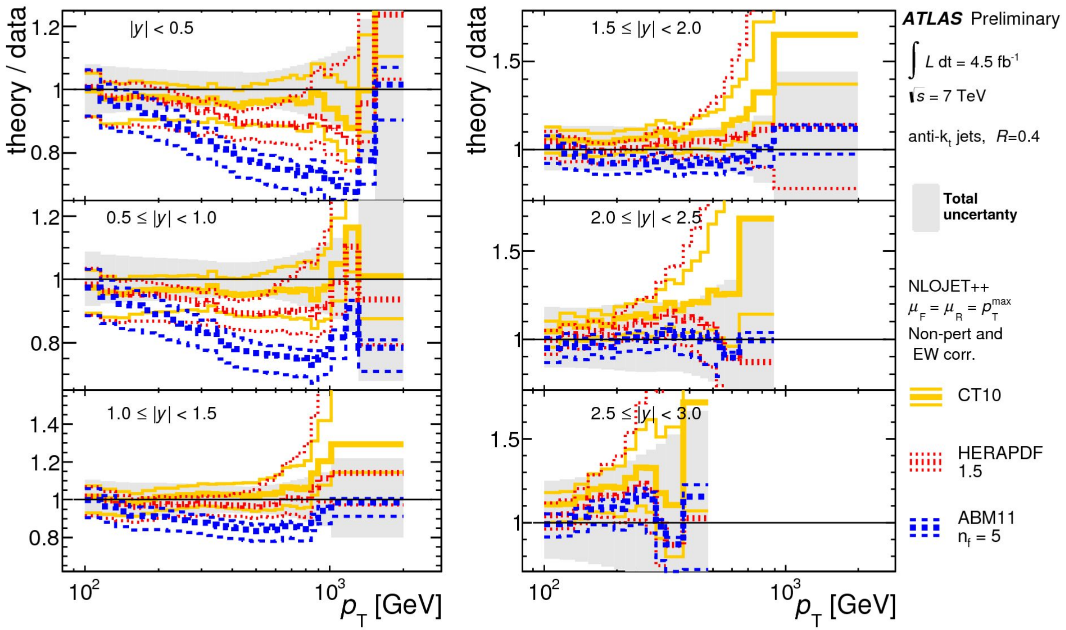

y ranges	P_{obs} (ATLAS Preliminary)					
	NLO PDF set:	CT10	MSTW2008	NNPDF2.1	HERAPDF1.5	ABM11
$\|y\| < 0.5$		84%	61%	72%	56%	$\boxed{< 0.1\%}$
$0.5 \leq \|y\| < 1.0$		91%	93%	89%	49%	$\boxed{< 0.1\%}$
$1.0 \leq \|y\| < 1.5$		89%	88%	85%	93%	$\boxed{2.7\%}$
$1.5 \leq \|y\| < 2.0$		93%	88%	91%	75%	55%
$2.0 \leq \|y\| < 2.5$		86%	82%	85%	26%	57%
$2.5 \leq \|y\| < 3.0$		95%	94%	97%	82%	85%

→ P_{obs} strongly depends on the PDF set and phase-space region

Quantitative data/theory comparison & limit setting

→ Define global test statistic (over a set of bins), at the unfolded level, using full information on correlations and uncertainty distributions

-Likelihood: can accommodate non-Gaussian distributions

-χ^2(with correlations) standard definitions require symmetrization of uncertainties but can be generalized

→ Perform scan of parameters of theory model (ex: Λ for CI) and apply test statistic to compare with unfolded data: Obtain "observed" $\chi^2(\Lambda)$

→ Generate toys with full set of uncertainties (transposed to SM+NP theory): comparison between nominal / fluctuated SM+NP : allows to reconstruct the distribution of the test statistic (important when using a χ^2 with error symmetrization).

→ p-value to test data/QCD agreement

→ CLs = $p_{s+b}/(1-p_b)$ for setting limits on New Physics

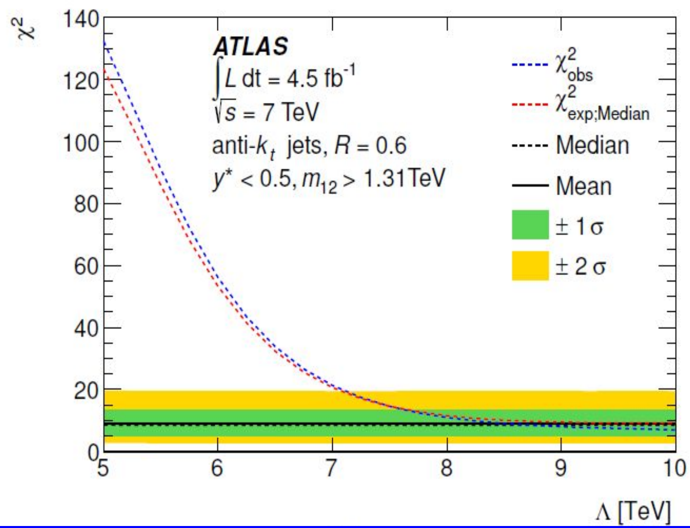

Back

Resonance and angular searches

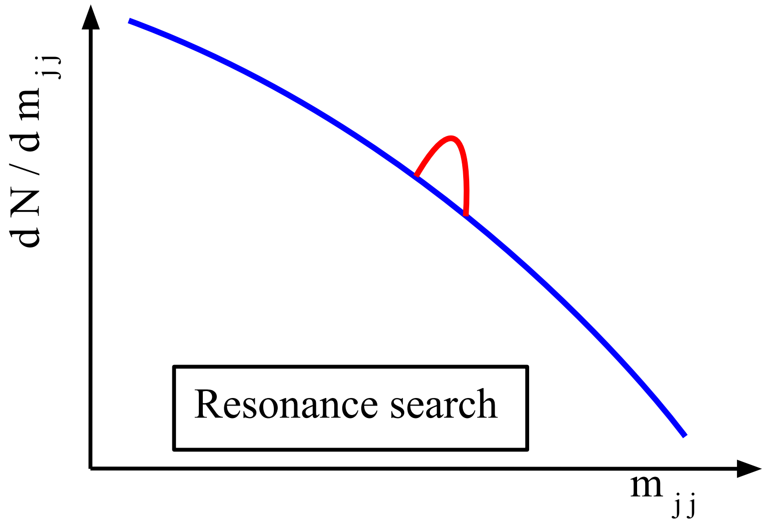

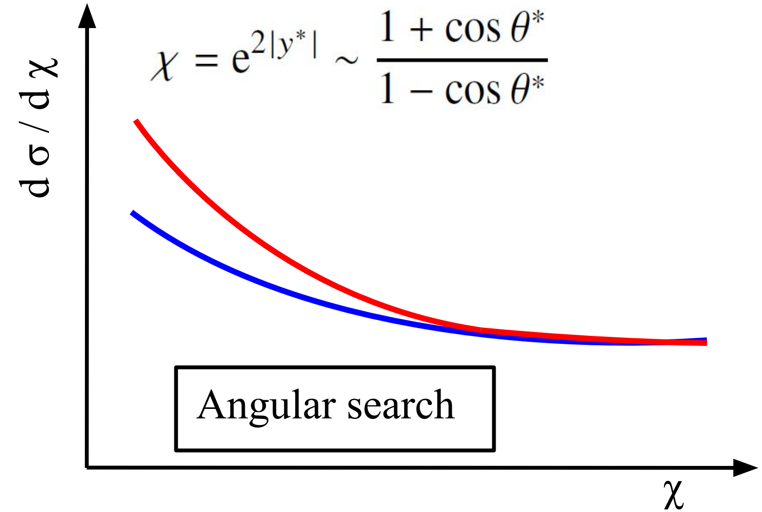

→ Sensitive to narrow resonances (QBH, q* etc.)

→ Smooth QCD background described by smooth (fitted) function

→ Sensitive to resonant and non-resonant signals (CI, QBH etc.)

→ ~Flat QCD background described by MC, normalized to data

Tests of the folding-based approach:

→ Detailed comparisons of transfer matrices for various signal models

→ Studied statistical uncertainties and correlations induced by transfer matrix – negligible impact

→ Studied possibility to use geometrical matching when building “A”

Back

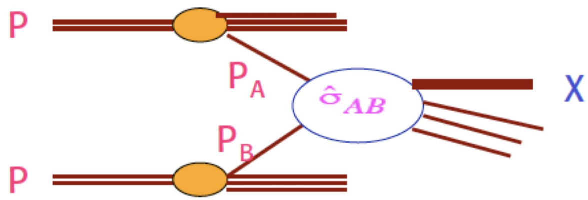

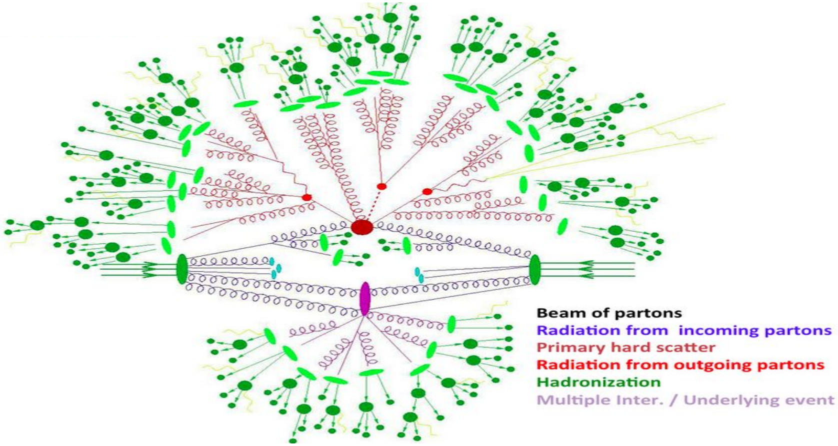

Pile-up

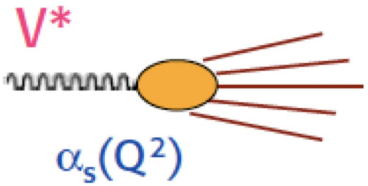

@ FCCee:

→ Short distance interaction of virtual bosons with quarks

→ No PDFs

→ No underlying event & MPI

→ No pile-up

Back

α_S evaluation from *(ISR) jet production*

N^3LO + NNLL (arXiv:1902.08158) N^2LO + NLLA (arXiv:1205.3714)

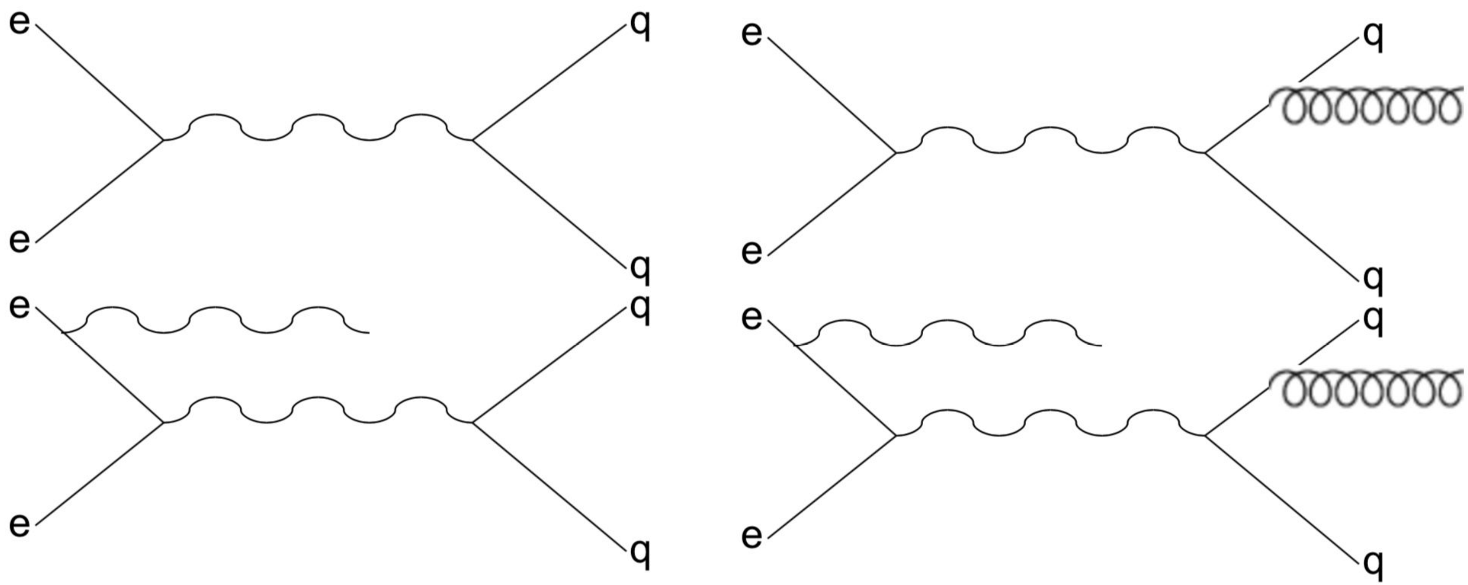

→ Sensitivity to α_S e.g. from 3/2 jet ratios (OR jet rates w.r.t. total hadronic Xsec)

→ High luminosity allows to select large samples of events with collinear / large angle ISR photons: allows to scan √s' with the same detector and collider conditions – important for RGE test

→ Need to study jet and photon energy calibration and resolution, acceptance and reconstruction efficiency etc. in view of *optimizing the detector design*
Should be able to target $\delta\alpha_S / \alpha_S < 1\%$

→ Numerous algorithms/methods developed for studying into detail the jet substructure in the LHC environment:
Important for understanding QCD effects inside jets, jet tagging (e.g. q/g, boosted top, H→bb), New Physics searches

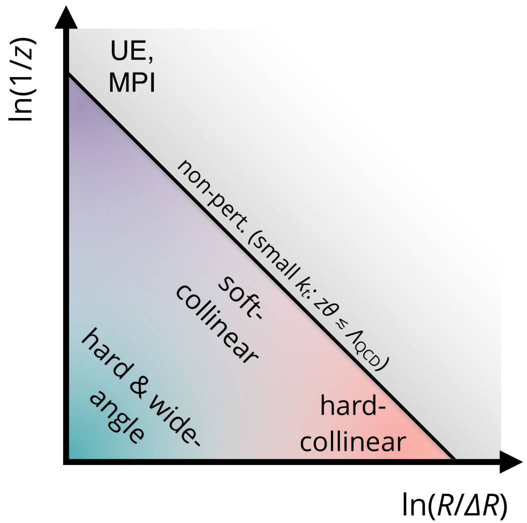

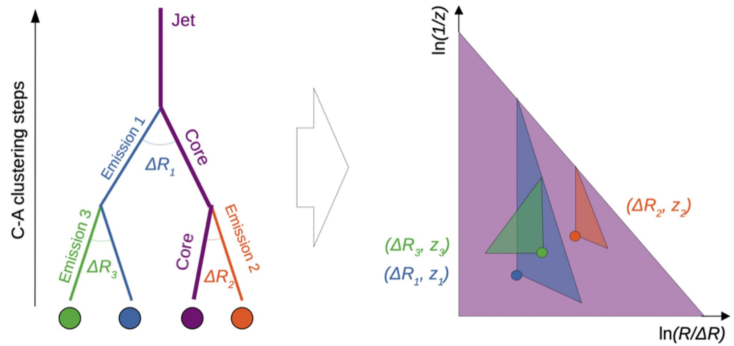

ΔR / k_T / z = angle / transverse momentum / energy fraction of emission with respect to core

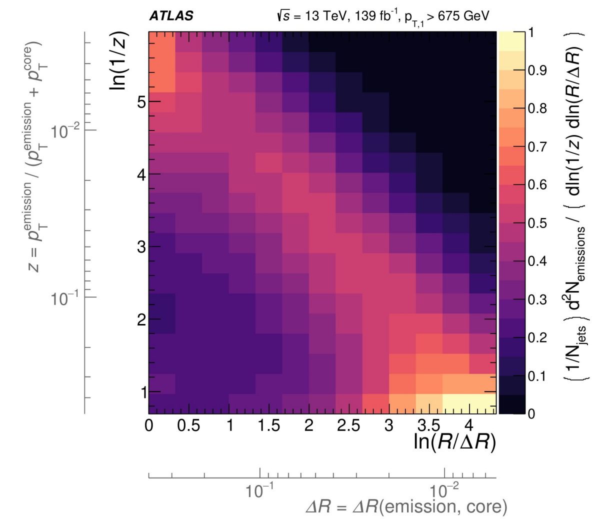

2004.03540

→ The Lund Jet Plane allows for an effective way to distinguish (non)perturbative effects

→ Huge potential for doing precision studies of jet substructure in the clean FCC-ee environment
→ Need to *perform detector optimization* in terms of granularity, energy resolution, (tracking/calorimeter) acceptance

α_S evaluation from *hadronic τ decays*

→ τ hadronic spectral functions (SFs) from ALEPH, unfolded of detector effects

→ Broadly used for $(g\text{-}2)_\mu$ predictions and other QCD studies

1312.1501

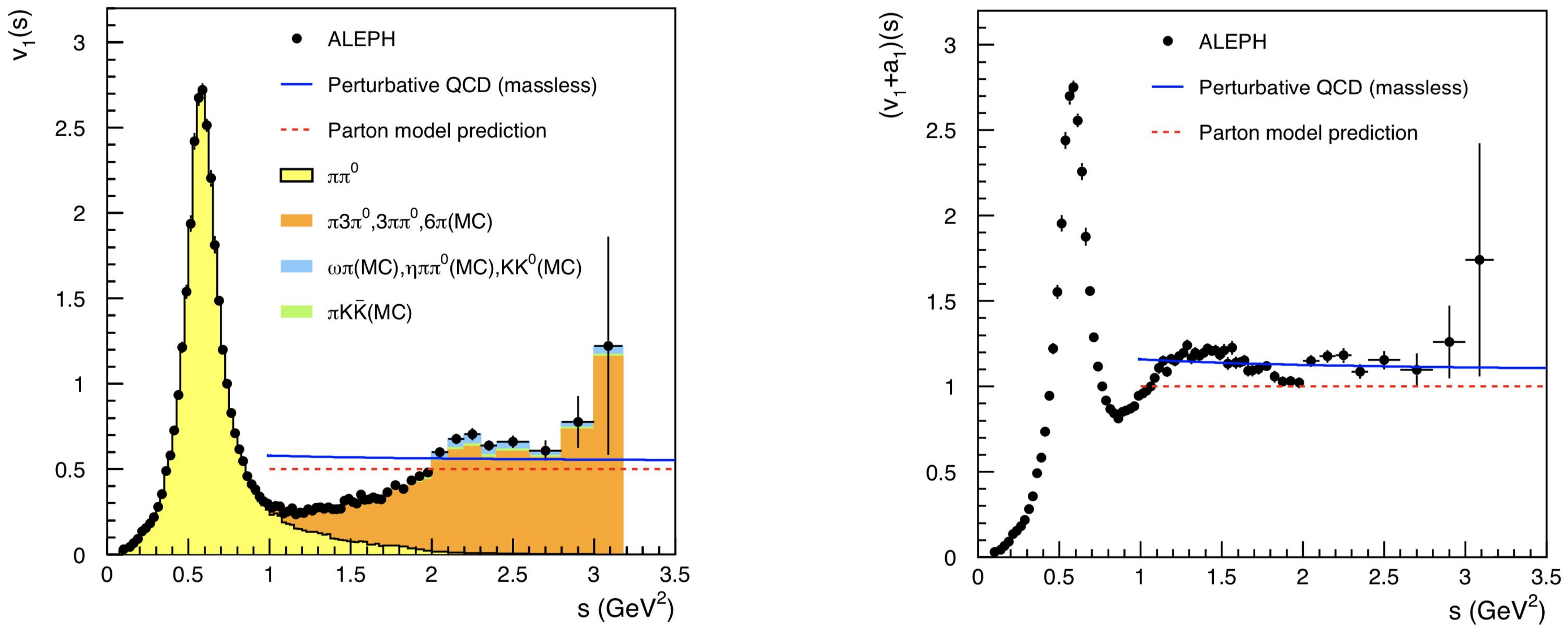

$$\upsilon_1 / a_1\left[\tau^- \to V^- / A^- \nu_\tau\right] \propto \frac{\mathrm{BR}\left[\tau^- \to V^- / A^- \nu_\tau\right]}{\mathrm{BR}\left[\tau^- \to e^- \bar{\nu}_e \nu_\tau\right]} \frac{1}{N_{V/A}} \frac{dN_{V/A}}{ds} \frac{m_\tau^2}{\left(1 - s/m_\tau^2\right)^2 \left(1 + s/m_\tau^2\right)}$$

branching fractions mass spectrum kinematic factor

α_S evaluation from *hadronic τ decays*

→ τ hadronic spectral functions ($\pi\pi^0$ channel) from various experiments

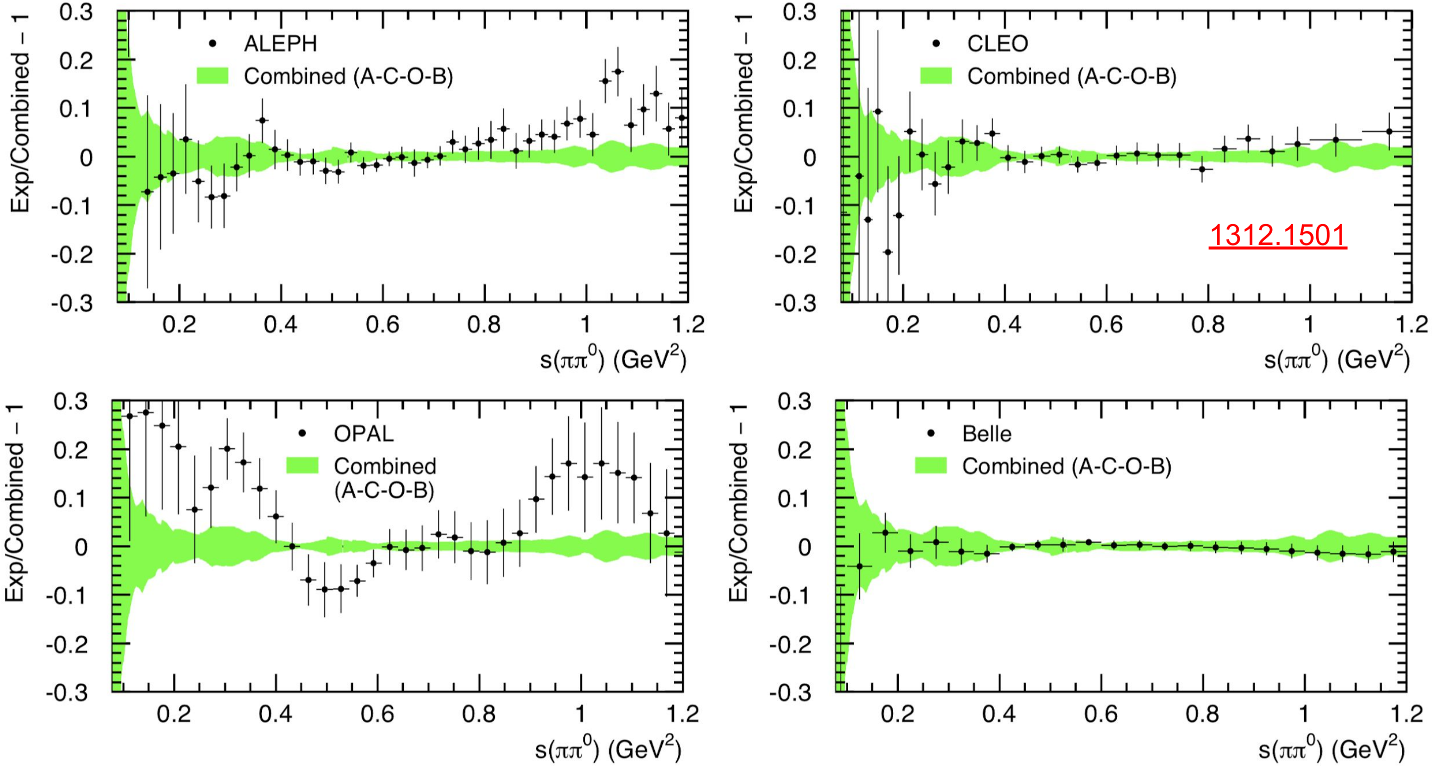

→ Normalisation: branching fractions best determined by ALEPH (large boost, high granularity)

→ Shape best determined by Belle (high statistics); improvements @ Belle II

→ What precision can one achieve at FCCee? Need to study acceptance, reconstruction efficiency, resolution etc. in view of *optimizing the detector design* for SFs measurements

α_S evaluation from *hadronic τ decays*

$$R_\tau = \frac{\Gamma(\tau^- \to \text{hadrons}\ \nu_\tau)}{\Gamma(\tau^- \to e^- \nu_e \nu_\tau)}$$

EW correction: $\simeq 0.0010$ (neglected)

Perturbative quark-mass terms:

$$\sum_{i,j=u,d,s} C_{U,ij}(s_0) \frac{m_i(s_0)\cdot m_j(s_0)}{s_0}$$

$$R_{\tau,U}(s_0) \propto |V_{\mathrm{CKM}}|^2 S_{\mathrm{EW}} \left(1 + \delta^{(0)} + \delta'_{\mathrm{EW}} + \delta_U^{(2,m_q)} + \sum_{D=4,6,\ldots} \delta_U^{(D)}\right)$$

Perturbative contribution

$$-2\pi i \oint_{|s|=s_0} \frac{ds}{s_0}\left(1-2\frac{s}{s_0}+2\left(\frac{s}{s_0}\right)^3-\left(\frac{s}{s_0}\right)^4\right)\cdot D(s)$$

where: $D(s) = \dfrac{1}{4\pi^2}\sum_{n=0}^{\infty} \tilde{K}_n(\xi) a_s^n(-\xi s)$

Adler function to avoid unphysical subtractions:

$$D(s) \equiv -s\frac{d\Pi(s)}{ds}$$

Nonperturbative contribution

$$\delta_U^{(D)} = (-1)^D \sum_{\dim O = D} C_U(\mu) \frac{\langle O(\mu)\rangle_U}{s_0^{D/2}}$$

→ Theoretical prediction available at N^{3}LO: need for even higher precision at the time of FCC-ee to reduce dominant uncertainty from perturbative series (CIPT/FOPT), to benefit from the statistical precision ($\delta\alpha_S / \alpha_S << 1\%$)

→ More precise SFs will allow to better pin down non-perturbative corrections and probe the structure of the QCD vacuum (condensates)

α_S evaluation from *hadronic Z decays*

→ Theoretical prediction available at N^3LO

→ Better convergence of the perturbative series and less non-perturbative corrections compared to precise determinations at lower scales (e.g. from τ decays)

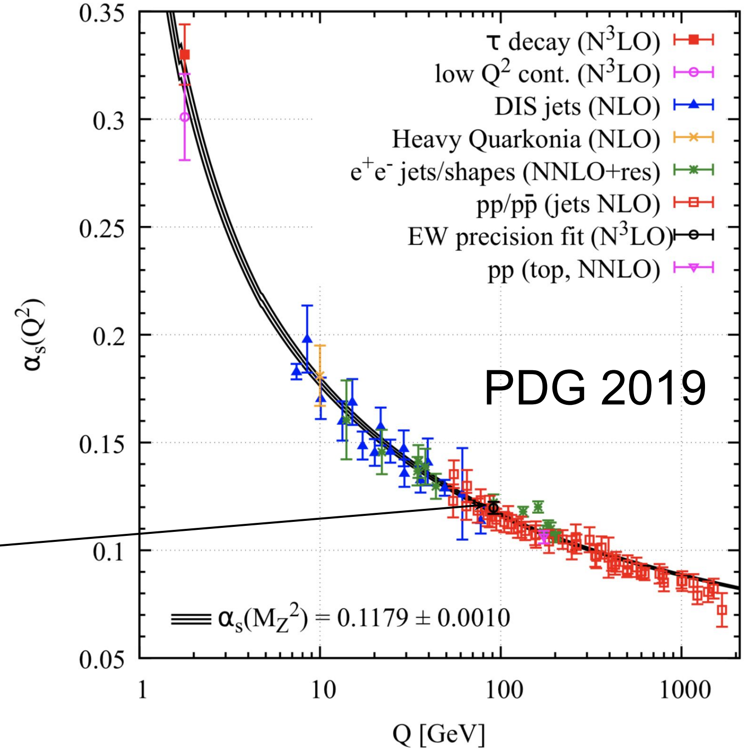

→ Used for "reference value": determinations at other energies evolved at the m_Z scale and then compared to *test the RGE from QCD*

→ Need to study acceptance and reconstruction efficiency etc. in view of *optimizing detector design*

Ultimate goal: *test RGE & unification of couplings*

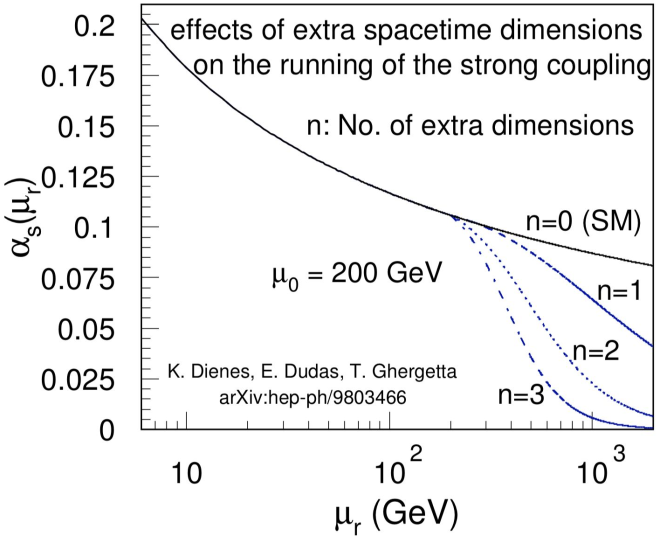

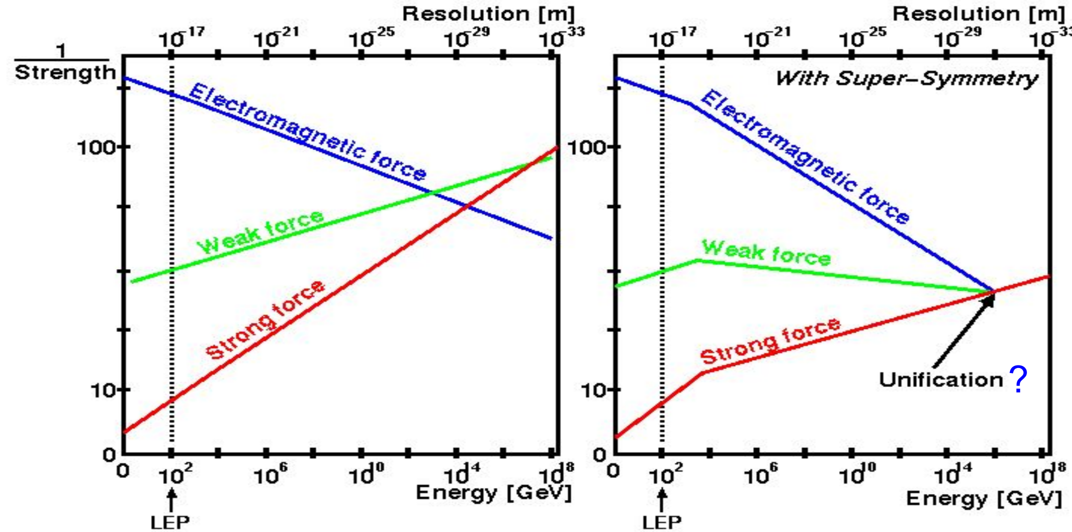

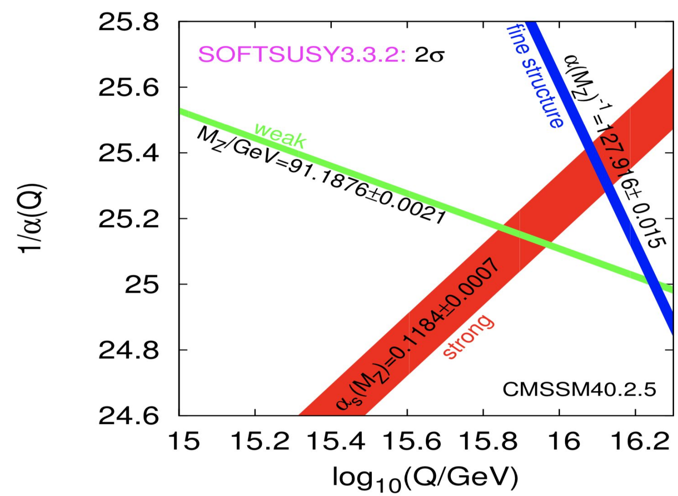

→ A deviation from the SM prediction for the RGE can be an indication of New Physics

→ Are the coupling constants unified at the Plank scale?

→ *Need to evaluate the strong coupling at multiple scales, with high precision*